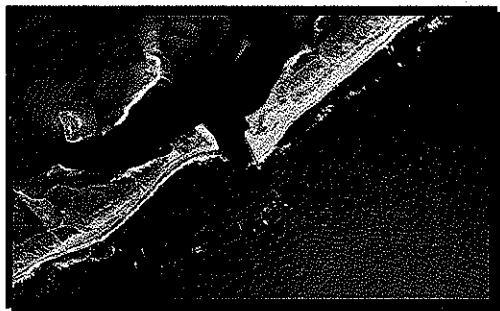
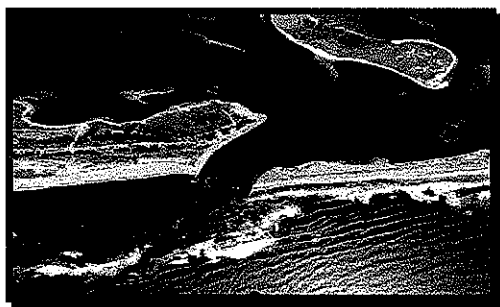


Work Order 2

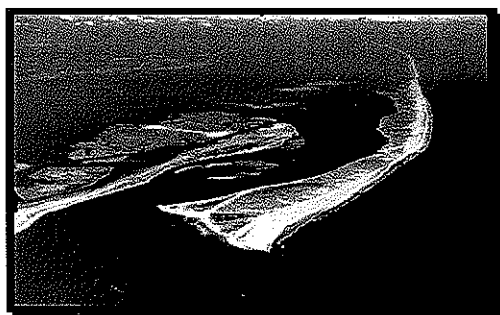
Task 2.0 - Draft



**Atlantic Coast of Long Island,
Fire Island Inlet to Montauk
Point, New York**



**Storm Damage Reduction
Reformulation Study**



Water Quality Modeling

September, 1999

A Joint Venture, URS Consultants, Inc./Moffatt & Nichol Engineers

<u>Table of Contents</u>	<u>Page</u>
1. INTRODUCTION.....	1
1.1. General.....	1
1.2. Objective.....	1
1.3. Scope of Work	2
2. BAY ENVIRONMENTAL CONDITIONS	4
2.1. General.....	4
2.2. Water Levels	6
2.3. Fresh Water Sources	6
2.4. Bay Salinity.....	7
2.5. Bay Temperature.....	12
3. SIMULATION MODELS	40
3.1. General Description	40
3.2. Hydrodynamic Model (MIKE 21 HD)	40
3.3. Advection-Dispersion Model (MIKE 21 AD)	41
3.4. Residence Time Computations	42
4. NUMERICAL MESH GENERATION	45
4.1. General.....	45
4.2. Bathymetric Data	45
4.3. Mesh Parameters.....	47
5. MODEL CALIBRATION (EXISTING CONDITIONS).....	51
5.1. General.....	51
5.2. Tidal Hydrodynamics.....	52
5.2.1. Model Parameters.....	53

5.2.2. Calibration Results	53
5.3. Advection/Dispersion	55
5.3.1. Model Parameters.....	55
5.3.2. Salinity Boundary Conditions.....	56
5.3.3. Salinity Calibration Results	57
5.3.4. Temperature Boundary Conditions.....	59
5.3.5. Temperature Calibration Results.....	61
5.3.6. Residence Time	62
6. IMPACTS OF BARRIER ISLAND BREACHING	90
6.1. General.....	90
6.2. Breach Characteristics	90
6.2.1. Breach Locations	90
6.2.2. Breach Sizes	91
6.3. Breach Case 1 (3-Month Breach)	92
6.3.1. Salinity	92
6.3.2. Temperature.....	94
6.3.3. Residence Times.....	95
6.4. Breach Case 2 (9-Month Breach)	96
6.4.1. Salinity	96
6.4.2. Temperature.....	97
6.4.3. Residence Time	98
7. FINDINGS AND CONCLUSIONS	173
7.1. General.....	173
7.2. Model Calibration	173
7.3. Future Without-Project Inlet/Bay Water Quality.....	173
7.3.1. Future Without-Project Inlet/Bay Salinity.....	174
7.3.2. Future Without-Project Inlet/Bay Temperature.....	175
7.3.3. Future Without-Project Inlet/Bay Residence Time	176

8. REFERENCES.....178

<u>List of Figures</u>	<u>Page</u>
Figure 2.1 : Project area map.	17
Figure 2.2 : Project area detail map - Western Great South Bay.....	18
Figure 2.3 : Project area detail map - Central Great South Bay, Fire Island Inlet.	19
Figure 2.4 : Project area detail map - Eastern Great South Bay.	20
Figure 2.5 : Project area detail map - Moriches Bay.	21
Figure 2.6 : Project area detail map - Shinnecock Bay.....	22
Figure 2.7 : Project area detail map - Mecox Bay to Amagansett National Wildlife Refuge.	23
Figure 2.8 : Project area detail map - Napeague State Park to Montauk Point.....	24
Figure 2.9 : Great South Bay measurement station locations.	25
Figure 2.10 : Moriches Bay measurement station locations.	26
Figure 2.11 : Shinnecock Bay measurement station locations.	27
Figure 2.12 : Great South Bay salinity data for stations 150, 230, and 250	28
Figure 2.13 : Great South Bay salinity data frequency distribution.	29
Figure 2.14 : Moriches Bay salinity data for stations 120, 140, and 180	30
Figure 2.15 : Moriches Bay salinity data frequency distribution.....	31
Figure 2.16 : Shinnecock Bay salinity data for stations 120, 140, and 180.....	32
Figure 2.17 : Shinnecock Bay salinity data frequency distribution.	33
Figure 2.18 : Great South Bay temperature data for stations 150, 230, and 250.....	34
Figure 2.19 : Great South Bay temperature data frequency distribution.	35
Figure 2.20 : Moriches Bay temperature data for stations 120, 140, and 180	36
Figure 2.21 : Moriches Bay temperature data frequency distribution.	37
Figure 2.22 : Shinnecock Bay temperature data for stations 120, 140, and 180.	38
Figure 2.23 : Shinnecock Bay temperature data frequency distribution.....	39
Figure 4.1 : Great South Bay numerical mesh grid.	48
Figure 4.2 : Moriches Bay numerical mesh grid.....	49

Figure 4.3 : Shinnecock Bay numerical mesh grid.	50
Figure 5.1 : Great South Bay Boundary Condition Locations.....	63
Figure 5.2 : Moriches Bay Boundary Condition Locations.....	64
Figure 5.3 : Shinnecock Bay Boundary Condition Locations.	65
Figure 5.4 : Great South Bay Salinity Calibration Results.	66
Figure 5.5 : Great South Bay Salinity at Peak Ebb Tide.	67
Figure 5.6 : Great South Bay Salinity at Peak Flood Tide.....	68
Figure 5.7 : Moriches Bay Salinity Calibration Results.	69
Figure 5.8 : Moriches Bay Salinity at Peak Ebb Tide.....	70
Figure 5.9 : Moriches Bay Salinity at Peak Flood Tide.....	71
Figure 5.10 : Shinnecock Bay Salinity Calibration Results.....	72
Figure 5.11 : Shinnecock Bay Salinity at Peak Ebb Tide.	73
Figure 5.12 : Shinnecock Bay Salinity at Peak Flood Tide.	74
Figure 5.13 : Great South Bay Temperature Calibration Results.	75
Figure 5.14 : Great South Bay Temperature at Peak Ebb Tide.	76
Figure 5.15 : Great South Bay Temperature at Peak Flood Tide.....	77
Figure 5.16 : Moriches Bay Temperature Calibration Results.	78
Figure 5.17 : Moriches Bay Temperature at Peak Ebb Tide.....	79
Figure 5.18 : Moriches Bay Temperature at Peak Flood Tide.....	80
Figure 5.19 : Shinnecock Bay Temperature Calibration Results.....	81
Figure 5.20 : Shinnecock Bay Temperature at Peak Ebb Tide.	82
Figure 5.21 : Shinnecock Bay Temperature at Peak Flood Tide.	83
Figure 5.22 : Great South Bay Residence Time Stability Curves.....	84
Figure 5.23 : Great South Bay Residence Time Distribution.	85
Figure 5.24 : Moriches Bay Residence Time Stability Curves.....	86
Figure 5.25 : Moriches Bay Residence Time Distribution.	87
Figure 5.26 : Shinnecock Bay Residence Time Stability Curves.	88
Figure 5.27 : Shinnecock Bay Residence Time Distribution.....	89
Figure 6.1 : Central Great South Bay - Vulnerable Breach Location Map.....	100
Figure 6.2 : Eastern Great South Bay - Vulnerable Breach Location Map.	101
Figure 6.3 : Moriches Bay - Vulnerable Breach Location Map.	102

Figure 6.4 : Shinnecock Bay - Vulnerable Breach Location Map.....	103
Figure 6.5 : Great South Bay - Breach Finite Difference Mesh.	104
Figure 6.6 : Moriches Bay - Breach Finite Difference Mesh.	105
Figure 6.7 : Shinnecock Bay - Breach Finite Difference Mesh.	106
Figure 6.8 : Great South Bay - Existing Conditions vs. With-Breach Salinity.	107
Figure 6.9 : Great South Bay - 3-Month Breach Peak Ebb Tide Salinity Contours.	108
Figure 6.10 : Great South Bay - 3-Month Breach Peak Flood Tide Salinity Contours.	109
Figure 6.11 : Great South Bay - 3-Month Breach Effect Salinity Contours at Peak Ebb Tide. .	110
Figure 6.12 : Great South Bay - 3-Month Breach Effect Salinity Contours at Peak Flood Tide.	111
Figure 6.13 : Moriches Bay - Existing Conditions vs. With-Breach Salinity.....	112
Figure 6.14 : Moriches Bay - 3-Month Breach Peak Ebb Tide Salinity Contours.	113
Figure 6.15 : Moriches Bay - 3-Month Breach Peak Flood Tide Salinity Contours.	114
Figure 6.16 : Moriches Bay - 3-Month Breach Effect Salinity Contours at Peak Ebb Tide.	115
Figure 6.17 : Moriches Bay - 3-Month Breach Effect Salinity Contours at Peak Flood Tide....	116
Figure 6.18 : Shinnecock Bay - Existing Conditions vs. With-Breach Salinity.	117
Figure 6.19 : Shinnecock Bay - 3-Month Breach Peak Ebb Tide Salinity Contours.....	118
Figure 6.20 : Shinnecock Bay - 3-Month Breach Peak Flood Tide Salinity Contours.....	119
Figure 6.21 : Shinnecock Bay - 3-Month Breach Effect Salinity Contours at Peak Ebb Tide...	120
Figure 6.22 : Shinnecock Bay - 3-Month Breach Effect Salinity Contours at Peak Flood Tide.	121
Figure 6.23 : Great South Bay - Existing Conditions vs. With-Breach Temperature.	122
Figure 6.24 : Great South Bay - 3-Month Breach Peak Ebb Tide Temperature Contours.	123
Figure 6.25 : Great South Bay - 3-Month Breach Peak Flood Tide Temperature Contours.	124
Figure 6.26 : Great South Bay - 3-Month Breach Effect Temperature Contours at Peak Ebb Tide.	125
Figure 6.27 : Great South Bay - 3-Month Breach Effect Temperature Contours at Peak Flood Tide.	126
Figure 6.28 : Moriches Bay - Existing Conditions vs. With-Breach Temperature.....	127
Figure 6.29 : Moriches Bay - 3-Month Breach Peak Ebb Tide Temperature Contours.	128
Figure 6.30 : Moriches Bay - 3-Month Breach Peak Flood Tide Temperature Contours.	129

Figure 6.31 : Moriches Bay - 3-Month Breach Effect Temperature Contours at Peak Ebb Tide.	130
Figure 6.32 : Moriches Bay - 3-Month Breach Effect Temperature Contours at Peak Flood Tide.	131
Figure 6.33 : Shinnecock Bay - Existing Conditions vs. With-Breach Temperature.	132
Figure 6.34 : Shinnecock Bay - 3-Month Breach Peak Ebb Tide Temperature Contours.	133
Figure 6.35 : Shinnecock Bay - 3-Month Breach Peak Flood Tide Temperature Contours.	134
Figure 6.36 : Shinnecock Bay - 3-Month Breach Effect Temperature Contours at Peak Ebb Tide.	135
Figure 6.37 : Shinnecock Bay - 3-Month Breach Effect Temperature Contours at Peak Flood Tide.	136
Figure 6.38 : Great South Bay - 3-Month Breach Residence Time.	137
Figure 6.39 : Great South Bay - Existing Conditions vs. 3-Month Breach Residence Time.	138
Figure 6.40 : Moriches Bay - 3-Month Breach Residence Time.	139
Figure 6.41 : Moriches Bay - Existing Conditions vs. 3-Month Breach Residence Time.	140
Figure 6.42 : Shinnecock Bay - 3-Month Breach Residence Time.	141
Figure 6.43 : Shinnecock Bay - Existing Conditions vs. 3-Month Breach Residence Time.	142
Figure 6.44 : Great South Bay - 9-Month Breach Peak Ebb Tide Salinity Contours.	143
Figure 6.45 : Great South Bay - 9-Month Breach Peak Flood Tide Salinity Contours.	144
Figure 6.46 : Great South Bay - 9-Month Breach Effect Salinity Contours at Peak Ebb Tide.	145
Figure 6.47 : Great South Bay - 9-Month Breach Effect Salinity Contours at Peak Flood Tide.	146
Figure 6.48 : Moriches Bay - 9-Month Breach Peak Ebb Tide Salinity Contours.	147
Figure 6.49 : Moriches Bay - 9-Month Breach Peak Flood Tide Salinity Contours.	148
Figure 6.50 : Moriches Bay - 9-Month Breach Effect Salinity Contours at Peak Ebb Tide.	149
Figure 6.51 : Moriches Bay - 9-Month Breach Effect Salinity Contours at Peak Flood Tide.	150
Figure 6.52 : Shinnecock Bay - 9-Month Breach Peak Ebb Tide Salinity Contours.	151
Figure 6.53 : Shinnecock Bay - 9-Month Breach Peak Flood Tide Salinity Contours.	152
Figure 6.54 : Shinnecock Bay - 9-Month Breach Effect Salinity Contours at Peak Ebb Tide.	153
Figure 6.55 : Shinnecock Bay - 9-Month Breach Effect Salinity Contours at Peak Flood Tide.	154
Figure 6.56 : Great South Bay - 9-Month Breach Peak Ebb Tide Temperature Contours.	155

Figure 6.57 : Great South Bay - 9-Month Breach Peak Flood Tide Temperature Contours.	156
Figure 6.58 : Great South Bay - 9-Month Breach Effect Temperature Contours at Peak Ebb Tide.	157
Figure 6.59 : Great South Bay - 9-Month Breach Effect Temperature Contours at Peak Flood Tide.	158
Figure 6.60 : Moriches Bay - 9-Month Breach Peak Ebb Tide Temperature Contours.	159
Figure 6.61 : Moriches Bay - 9-Month Breach Peak Flood Tide Temperature Contours.	160
Figure 6.62 : Moriches Bay - 9-Month Breach Effect Temperature Contours at Peak Ebb Tide.	161
Figure 6.63 : Moriches Bay - 9-Month Breach Effect Temperature Contours at Peak Flood Tide.	162
Figure 6.64 : Shinnecock Bay - 9-Month Breach Peak Ebb Tide Temperature Contours.....	163
Figure 6.65 : Shinnecock Bay - 9-Month Breach Peak Flood Tide Temperature Contours.....	164
Figure 6.66 : Shinnecock Bay - 9-Month Breach Effect Temperature Contours at Peak Ebb Tide.	165
Figure 6.67 : Shinnecock Bay - 9-Month Breach Effect Temperature Contours at Peak Flood Tide.	166
Figure 6.68 : Great South Bay - 9-Month Breach Residence Time.....	167
Figure 6.69 : Great South Bay - Existing Conditions vs. 9-Month Breach Residence Time.	168
Figure 6.70 : Moriches Bay - 9-Month Breach Residence Time.	169
Figure 6.71 : Moriches Bay - Existing Conditions vs. 9-Month Breach Residence Time.	170
Figure 6.72 : Shinnecock Bay - 9-Month Breach Residence Time.	171
Figure 6.73 : Shinnecock Bay - Existing Conditions vs. 9-Month Breach Residence Time.....	172

List of Tables

Page

Table 2.1 – Tide Range and Tidal Prism Range.....	6
Table 2.2 – Study Area Fresh Water Sources.....	7
Table 2.3 – Great South Bay (East of Inlet) Salinity.....	9
Table 2.4 – Great South Bay (West of and Inlet) Salinity.....	9
Table 2.5 – Moriches Bay Salinity.....	11

VIII

Table 2.6 – Shinnecock Bay Salinity	12
Table 2.7 – Great South Bay Temperature	13
Table 2.8 – Moriches Bay Temperature	15
Table 2.9 – Shinnecock Bay Temperature	15
Table 5.1 – Dispersion Coefficients	55
Table 5.2 – Great South Bay Source Temperature	60
Table 6.1 – Barrier Island Breach Characteristics	92

1. INTRODUCTION

1.1. General

The US Army Corps of Engineers, New York District (CENAN) is conducting a comprehensive feasibility-level reformulation of the shore protection and storm damage reduction project for the south shore of Long Island, New York, from Fire Island Inlet to Montauk Point. The Reformulation Study is a multi-year effort, involving project planning and engineering, economic analyses, and environmental studies. Numerous study tasks are involved in the planning of storm damage reduction projects for the approximately 83-mile study area length.

The project area is located entirely in Suffolk County, Long Island, New York, along the Atlantic and bay shores of the towns of Babylon, Islip, Brookhaven, Southampton and East Hampton. The study area encompasses Great South Bay, Moriches Bay and Shinnecock Bay which interact with the Atlantic Ocean through Fire Island Inlet, Moriches Inlet and Shinnecock Inlet, respectively. The project area includes the ocean and bay shorelines, Fire Island, Moriches and Shinnecock Inlets, barrier island beaches, the mainland, as well as the borrow areas for beach construction and replenishment.

1.2. Objective

This submission presents work performed as part of the **Inlet Dynamics Study** for the Reformulation study. The present submission presents the results of numerical models for each of the study area inlets and bays to identify impacts associated with barrier island breaches on bay physical properties including salinity, temperature, and residence time. Model calibration for existing conditions is presented along with results for breached, i.e. future without-project, conditions.

Note that the present submission is closely associated with the inlet dynamics study performed for historic and existing conditions described in *Interim Submission No. 9A, Inlet Dynamics - Existing Conditions* (February, 1999) and future-without project conditions described in *Interim Submission No. 9B, Inlet Dynamics - Without-Project Future Conditions* (March, 1999).

1.3. Scope of Work

The scope of work for the modeling study is summarized below.

Task 1 – Data Collection. The availability of data for the performance of this study will be ascertained. Data requirements include:

- Previous numerical modeling studies performed for the bays
- Bay bathymetry records
- Field measured current and tide data sets (circulation patterns)
- Existing temperature and salinity data
- Freshwater inputs from previous studies or reports; potential data to include rivers, creeks, surface runoff, groundwater, sewerage and other effluents)

Task 2 – Mesh Preparation. A numerical computation mesh will be created to represent the geometry and bathymetry of Shinnecock, Moriches, and Great South Bay, Fire Island Inlet and adjoining water bodies. This mesh will be created through use of existing conditions bathymetry records.

Task 3 – Model Calibration. Available data sources will be examined to determine data that are applicable to the calibration of the numerical flow model to ensure that estuary circulation patterns are well represented. All numerical modeling will be performed through use of the MIKE 21 software suite.

Task 4 – Model Application. The model will be applied to estimate the impacts on water quality parameters (i.e. residence times, circulation, salinity, and temperature) of a barrier island breach along Fire Island. Model applications will be performed for a combination of breach scenarios for normal tide conditions, where these scenarios are defined by breach location and geometry (i.e. cross-sectional area). One existing condition will be simulated for normal tide conditions.

Task 5 – Recommendation for Additional Analyses. Recommendations for future analyses will be performed based on results of the proposed modeling study and based on coordination with CENAN personnel.

2. BAY ENVIRONMENTAL CONDITIONS

2.1. General

The Federally authorized project area extends east from Fire Island Inlet to Montauk Point along the Atlantic Coast of Suffolk County, Long Island, New York, as shown in Figure 2.1. The study area includes the barrier islands, the Atlantic Ocean shorelines and adjacent back-bay areas along Great South, Moriches and Shinnecock Bays. The total study length encompasses approximately 83 miles along the Atlantic Ocean and comprises approximately 70 percent of the total ocean frontage of Long Island, as well as several hundred miles of bay shoreline. Locations and features pertinent to the project area and referenced below are depicted in Figures 2.2 to 2.8.

A series of barrier islands characterize the western portion of the study area extending approximately 50 miles from Fire Island Inlet to Southampton. The barrier island chain includes the 30 mile segment extending east from Fire Island Inlet to Moriches Inlet; the 16-mile barrier island segment between Moriches Inlet and Shinnecock Inlet which contains Westhampton and Tiana Beaches; and the 4-mile long barrier island extending from Shinnecock Inlet to Southampton.

The study area estuarial system, which separates the barrier island chain from the Long Island mainland, is comprised of Great South, Moriches, and Shinnecock Bays. These bays have connections with the Atlantic Ocean through Fire Island, Moriches, and Shinnecock Inlets, respectively. These inlets account for three of the six openings in the barrier island chain along the south shore of Long Island. Federal navigation projects have been established at each project inlet. Fire Island, Moriches, and Shinnecock Inlets, as well as adjacent barrier island beaches and bay areas (i.e. those areas directly impacted by inlet processes), comprise the elements of the inlet dynamics study area.

Great South Bay. Great South Bay is the largest of the project area estuaries with a total water surface area of about 110 square miles. The bay extends about 33 miles from Massapequa in the

west along South Oyster Bay to Smith Point in the east near Bellport Bay. Numerous tidal rivers and creeks, as well as several significant embayments, including Patchogue and Nicoll Bays and Great Cove, characterize the northern shore of Great South Bay. The larger tidal rivers include the Connetquot River and Champlin Creek. Great South Bay may generally be separated into two distinct basins relative to the location of Fire Island Inlet. East of the inlet, bay widths vary from between 2 to 5 miles with water depths averaging roughly 6 to 8 feet. Maximum bay water depths reach about 15 feet. West of the inlet, Great South Bay and South Oyster Bay are characterized by widths which are generally less than 1.5 miles. Water depths to the west of the inlet are shallow, averaging approximately 2 feet.

Moriches Bay. Moriches Bay is a relatively small estuary with a number of tidal rivers and creeks and is connected to the ocean via Moriches Inlet. Moriches Bay is separated from the Atlantic Ocean by Westhampton Beach and Fire Island and has a surface area of roughly 16 square miles. The Bay consists of two basins with average water depths of 6 to 7 feet. Moriches Bay extends to Smith Point (inclusive of Narrow Bay) in the western basin where it adjoins Great South Bay and to Potunk Point in the eastern basin where it meets Shinnecock Bay through the Quantuck and Quogue Canals. Moriches Bay is about 14 miles long (East-West) and has widths (North-South) which range from 0.75 to 2.5 miles. Widths in Narrow Bay range from approximately 0.2 to 0.4 miles. Connections to Great South and Shinnecock Bays are greatly constricted by landmasses as evident in Figures 2.2 to 2.8. The northern side of the bay features numerous streams and tidal creeks, the largest of which are the Forge River and Seatuck Creek.

Shinnecock Bay. Shinnecock Bay, similar to Moriches Bay to the west, is a relatively small estuary comprised of an ocean entrance, a western connection to Moriches Bay, and several tidal rivers and creeks. The bay covers a total water surface area of approximately 15 square miles and extends from the Village of Southampton to the east to the Village of Quogue to the west where it connects with Moriches Bay through the Quantuck and Quogue Canals. These canals, which are about 200 feet in width, are connected by Quantuck Bay which has a surface area of about 2 square miles, and allow the exchange of water between Moriches and Shinnecock Bays. Shinnecock Bay is about 9 miles in length and has widths that range from about 0.4 to 2.8 miles. Average water depths in the bay are about 6 feet with maximum depths of 10 feet. Of the

tributaries on the north shore of Shinnecock Bay, Tiana Bay and Weesuck Creek are the largest and are located within the bay's western basin.

2.2. Water Levels

Water levels in Great South, Moriches, and Shinnecock Bays are dominated by astronomical tides under normal conditions and by storm tides during northeasters and hurricanes. Astronomical tides in the bays are semi-diurnal and controlled by tidal elevations at Fire Island, Moriches, and Shinnecock Inlets. Bay tides are somewhat smaller than and lag the ocean tide. Variations in tidal ranges throughout the estuaries are relatively small. The uniformity of tide ranges throughout Great South, Moriches, and Shinnecock Bays is a characteristic of the so-called "pumping mode" of inlet-bay hydraulics where water levels within an embayment remain nearly horizontal during filling and emptying. Table 2.1 shows the mean tide range and tidal prism at each inlet (NOAA, 1996).

TABLE 2.1 MEAN TIDE RANGE AND TIDAL PRISM RANGE		
Inlet	Tide Range (at Inlet) (feet)	Tidal Prism Range (ft ³ x 10 ⁶)
Fire Island	Democrat Point = 2.6 Fire Island Breakwater = 4.1	1,840 to 3,380
Moriches	2.9	230 to 990
Shinnecock	2.9	960 to 1,120

2.3. Fresh Water Sources

Fresh water enters the study area primarily through tributaries and groundwater seepage. However, little information is available for fresh water sources. The U.S. Geological Survey (USGS) monitors several tributaries in the Great South Bay watershed at locations significantly

upstream from the bays. Table 2.2 shows the average daily flow rates into the study area for the USGS monitored tributaries (see Figures 2.2 to 2.8 for locations).

TABLE 2.2 STUDY AREA FRESH WATER SOURCES	
Source	Flow (ft ³ /s)
Carlls River	26.4
Carmans River	25.3
Champlin Creek	7.1
Connetquot River	39.2
Massapequa Creek	8.2
Patchogue River	20.5
Penataquit Creek	6.3
Sampawams Creek	10.0
Santapogue River	4.2
Swan River	12.3

The cumulative fresh water flow from these stations averages approximately 160 ft³/s. CENAN (1975) estimated that these 10 gauging stations accounted for 62% of the drainage area for the Great South Bay watershed indicating that the total fresh water flow into Great South Bay is on the order of 260 ft³/s.

2.4. Bay Salinity

Pritchard (1983) indicates that spatial and temporal salinity distributions in the bays along the south shore of Long Island depend on two major factors: (1) freshwater inflow rates which vary both yearly and seasonally, and (2) exchange rate of sea and bay waters through tidal inlets. Therefore, salinity levels are dictated by the balance between: (1) saltwater inflow through bay inlets, (2) flow exchanges between bays and (3) freshwater flow entering the bay via major rivers and creeks (see Figures 2.2 to 2.8) and other sources (i.e. groundwater, sewage, etc.).

Salinity data for the present study were obtained from the Department of Health Services, Office of Ecology, Suffolk County, New York. The data consist of salinity and temperature measurements for 31 stations throughout Great South Bay shown in Figure 2.9, 10 stations located in Moriches Bay shown in Figure 2.10, and 10 stations located in Shinnecock Bay shown in Figure 2.11 for the period from March 1977 through December 1997. Measurements were taken on a monthly to annual basis.

Great South Bay. Spatial and temporal salinity values in Great South Bay varied significantly during the March 1977 to December 1997 data collection period. Average salinity, salinity ranges, and standard deviations of the salinity values at each measurement station during the 20-year measurement period are listed in Tables 2.3 and 2.4 for stations east and west of Fire Island Inlet (including the inlet), respectively. Stations 280, 290, and 300 will not be considered in this study due to the lack of synoptic data at these stations.

Figure 2.12 depicts salinity values at measurement stations 150, 230, and 250 shown in Figure 2.8 located in eastern Great South Bay, Fire Island Inlet, and South Oyster Bay (west of Great South Bay), respectively. Frequency distributions of the salinity values in Figure 2.12 are shown in Figure 2.13. Salinity ranged from 20 to 30 parts per thousand (ppt) in the eastern basin 21 to 32 ppt in the western basin, and 28 to 34 ppt in the inlet.

TABLE 2.3
GREAT SOUTH BAY (EAST OF INLET) SALINITY

Station	Average (ppt)	Range (ppt)	Std. Dev. (ppt)
100	25.5	21.8 - 30.5	2.3
110	24.3	18.9 - 29.2	2.5
120	25.2	17.4 - 28.3	2.5
130	25.2	21.2 - 27.9	2.0
140	26.4	22.2 - 29.3	2.3
150	26.2	22.5 - 29.4	2.1
160	25.6	22.1 - 29.1	2.2
170	27.6	24.8 - 31.1	1.9
180	28.6	25.7 - 30.9	1.4
190	27.0	24.5 - 30.8	1.6

TABLE 2.4
GREAT SOUTH BAY (WEST OF AND INLET) SALINITY

Station	Average (ppt)	Range (ppt)	Std. Dev. (ppt)
200	29.6	27.2 - 32.2	1.5
210	29.2	26.2 - 31.2	1.4
220	31.4	29.5 - 32.9	0.9
230	30.9	28.2 - 33.2	1.2
240	27.8	23.8 - 30.5	1.7
250	28.9	24.6 - 30.7	1.6
260	30.6	25.6 - 32.3	1.6
270	29.6	25.1 - 31.7	1.5

The high salinity variations experienced in Great South Bay are judged to result from the influx of fresh water from the many tributaries supplying Great South Bay. Pritchard and Gomes-Reyes (1986) determined that nearly 25% of all surface freshwater influx to Great South Bay enters via Carman's River in eastern Great South Bay, corresponding approximately to measurement station 110 in Figure 2.9. The high volume of freshwater influx into eastern Great

South Bay is not evident from the freshwater inflow data as Carman's river does not appear to be a large source. This freshwater influx is, however, reflected in salinity values throughout the bay. Average salinity is lowest at the mouth of Carman's River and increases with distance from the river with the highest average bay salinities occurring in South Oyster Bay west of Great South Bay. Furthermore, flow exchanges between Great South Bay and Moriches Bay may exhibit additional influence on salinity levels within the eastern basin of Great South Bay.

Moriches Bay. As in Great South Bay, salinity values within Moriches Bay varied during the March 1977 to December 1997 data collection period. Average salinity, salinity ranges, and standard deviations of the salinity values at each measurement station during the 20-year measurement period are listed in Table 2.5.

Historical salinity variations are presented in Figure 2.14 for Stations 120, 140, and 180 (see Figure 2.10) located in the western basin of Moriches Bay, at Moriches Inlet, and in the eastern basin of Moriches Bay, respectively. Frequency distributions for the salinity values in Figure 2.14 are shown in Figure 2.15.

Salinity variations in the eastern basin and Moriches Inlet have ranged from 28 to 33 ppt. Large variations have occurred in the western basin where salinity has ranged from a low of 21 ppt to approximately 33 ppt. The relatively high salinity variations experienced in the western basin are expected since most of the rivers and creeks discharging freshwater into Moriches Bay are located within the western basin. Furthermore, flow exchanges between Great South Bay and the western basin may influence salinity levels within the western basin whereas there is little flow exchange between the eastern basin and Shinnecock Bay. Average salinities in the inlet, the eastern basin and the western basin during the 20-year measurement period were 31.0 , 29.9 and 28.6 ppt, respectively.

TABLE 2.5
MORICHES BAY SALINITY

Station	Average (ppt)	Range (ppt)	Std. Dev. (ppt)
100	27.0	20.8 - 31.7	2.6
110	26.5	20.2 - 30.9	2.4
120	28.6	21.9 - 32.3	2.6
130	30.2	24.6 - 32.7	2.0
140	31.0	27.3 - 33.0	1.2
150	30.4	24.5 - 32.7	1.4
160	29.6	27.4 - 31.6	0.9
170	28.4	19.5 - 31.5	1.9
180	29.9	26.9 - 31.8	1.0
190	28.8	26.0 - 31.1	1.2
200	27.4	23.6 - 30.4	1.4

Shinnecock Bay. The average values, salinity ranges, and standard deviations of the salinity measured at each station during the 20-year collection period in Shinnecock Bay are listed in Table 2.6.

Historical salinity variations are depicted in Figure 2.16 for Stations 120, 140, and 180 (see Figure 2.10) located in the eastern basin of Shinnecock Bay, at Shinnecock Inlet, and in the western basin of Shinnecock Bay, respectively. Frequency distributions for the salinity values in Figure 2.16 are shown in Figure 2.17.

TABLE 2.6
SHINNECOCK BAY SALINITY

Station	Average (ppt)	Range (ppt)	Std. Dev. (ppt)
100	27.9	25.7 - 31.1	1.1
110	30.1	27.1 - 32.3	1.1
120	29.7	27.2 - 32.4	1.2
130	30.4	27.3 - 34.1	1.2
140	31.1	28.7 - 32.6	0.9
150	30.2	28.0 - 32.1	1.0
160	31.0	28.9 - 32.9	0.9
170	30.7	27.9 - 32.8	1.1
180	29.4	26.1 - 32.6	1.2
190	28.0	23.8 - 30.9	1.2

Salinity variations throughout Shinnecock Bay have been moderate and have ranged from 26 to 33 ppt. The relatively uniform salinity variations in Shinnecock Bay reflect the uniform distribution of freshwater sources between the eastern and western basin. Furthermore, there is little flow exchange between Moriches Bay and Shinnecock Bay, reducing the effects of Moriches Bay on Shinnecock Bay salinity. Average salinities in the inlet, the eastern basin and the western basin during the 20-year measurement period were 31.1 , 29.7 and 29.4 ppt, respectively.

2.5. Bay Temperature

Spatial and temporal temperature distributions in the bays along the south shore of Long Island are dependent upon: (1) season, and (2) exchange rate of sea and bay waters through tidal inlets. Temperature levels are dictated by the balance between: (1) ocean water temperatures through bay inlets, (2) freshwater flow entering the bay via major rivers and creeks (see Figures 2.2 to 2.8) and (3) solar radiation.

Temperature data for the present study were obtained from the Department of Health Services, Office of Ecology, Suffolk County, New York data set.

Great South Bay. Temporal temperature values in Great South Bay vary significantly during the March 1977 to December 1997 data collection period due to change in season. Average temperatures, temperature ranges, and standard deviations of the temperature values at each measurement station during the 20-year measurement period are listed in Table 2.7. Stations 280, 290, and 300 will not be considered in this discussion due to the paucity of data measurements taken at these stations.

Figure 2.18 depicts temperature values at measurement stations 150, 230, and 250 located in eastern Great South Bay, Fire Island Inlet, and South Oyster Bay (west of Great South Bay), respectively. Frequency distributions of the temperature values in Figure 2.18 are shown in Figure 2.19. Temperature values ranged from 0 to 30 °C in the eastern and western basins and 3 to 27 °C in the inlet. Average temperatures in Great South Bay varied spatially only ± 1.2 °C from the median temperature. These results indicate that bay water temperature is similar to the ocean water temperature and that bay temperatures are more sensitive to differences in solar heating due to water depth variations.

TABLE 2.7 GREAT SOUTH BAY TEMPERATURE			
Station	Average (°C)	Range (°C)	Std. Dev. (°C)
100	15.6	1.4 - 25.2	7.1
110	15.8	1.2 - 25.4	7.2
120	15.6	1.0 - 25.4	7.3
130	15.7	1.7 - 25.6	7.1
140	15.6	0.6 - 25.2	7.2
150	16.1	0.1 - 25.7	7.5
160	16.3	0.9 - 25.5	7.4

170	16.1	0.4 - 26.3	7.5
180	15.8	2.6 - 25.8	7.3
190	16.3	1.1 - 26.8	7.5
200	15.1	2.4 - 25.4	7.0
210	16.3	3.8 - 24.8	7.0
220	14.1	1.6 - 22.1	6.3
230	14.5	1.6 - 24.4	6.3
240	16.5	2.9 - 25.3	7.1
250	16.5	4.5 - 25.4	7.0
260	16.0	3.5 - 25.0	6.8
270	16.3	4.3 - 25.1	6.7

Moriches Bay. Time-averaged temperatures throughout Moriches Bay fall within a 1.4°C range from 11.9 to 13.3 °C with the spatial mean of the bay temperature 1.1°C higher than the ocean temperature at the inlet. This indicates that the bay is heated relatively evenly and temperatures in the bay are similar to the ocean temperatures. However, temperature values varied drastically through time during the March 1977 to December 1997 data collection period. Time-averaged temperatures, temperature ranges, and standard deviations of the temperature values at each measurement station during the 20-year measurement period are listed in Table 2.8.

Historical temperature variations are depicted in Figure 2.20 for Stations 120, 140, and 180 (see Figure 2.10) located in the western basin of Moriches Bay, at Moriches Inlet, and in the eastern basin of Moriches Bay, respectively. Frequency distributions for the temperature values in Figure 2.20 are shown in Figure 2.21.

Average temperatures tend increase with distance inland from the inlet. This temperature gradient can be attributed to the majority of the temperature measurements occurring during the late spring, summer, and early fall months at which point the bay is warmed slightly more than the ocean due to solar radiation.

TABLE 2.8
MORICHES BAY TEMPERATURE

Station	Average (°C)	Range (°C)	Std. Dev. (°C)
100	13.1	0.0 - 26.8	7.6
110	13.2	0.7 - 26.3	7.5
120	12.6	1.3 - 26.6	7.0
130	11.9	1.7 - 25.8	6.4
140	11.6	1.9 - 24.6	6.1
150	12.2	2.2 - 24.4	6.4
160	12.8	1.2 - 25.1	6.9
170	13.2	1.5 - 25.6	7.0
180	12.6	2.0 - 25.5	6.8
190	13.1	0.6 - 25.8	7.3
200	13.3	0.7 - 26.8	7.7

Shinnecock Bay. As in Moriches Bay, time-averaged temperatures throughout Shinnecock Bay range from 11.6 to 12.6°C with the spatial mean of temperatures 0.6°C higher than the ocean temperature at the inlet, indicating that the bay is heated relatively evenly and temperatures in the bay are similar to the ocean temperatures. Temperature values varied drastically temporally during the March 1977 to December 1997 data collection period, due to seasonal changes. Time-averaged temperatures, temperature ranges, and standard deviations of the temperature values at each measurement station during the 20-year measurement period are listed in Table 2.9.

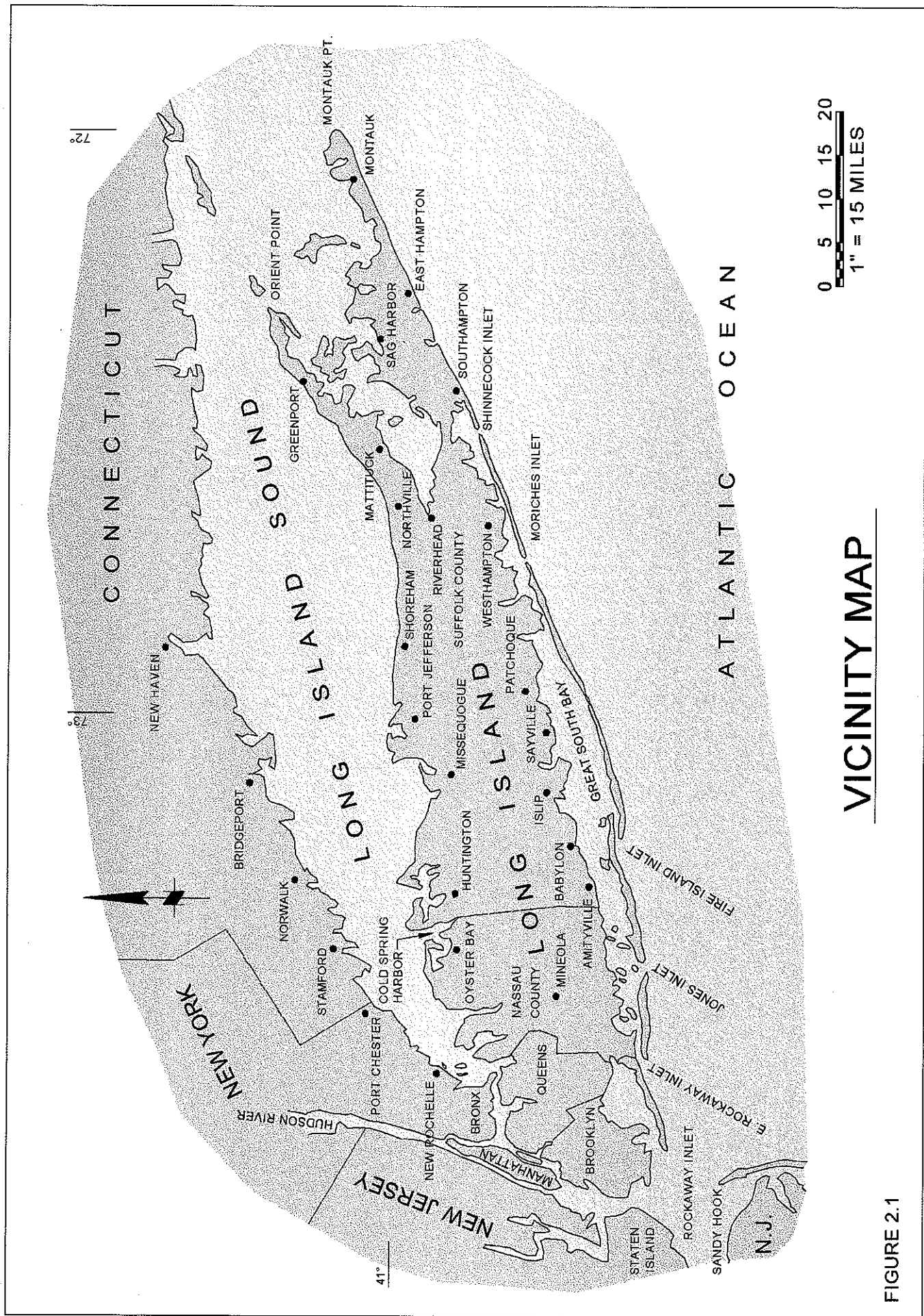
TABLE 2.9
SHINNECOCK BAY TEMPERATURE

Station	Average (°C)	Range (°C)	Std. Dev. (°C)
100	12.2	0.0 - 25.5	7.3
110	12.0	0.0 - 25.9	6.8
120	11.8	0.0 - 24.4	6.6

130	11.6	0.1 - 23.9	6.2
140	11.3	1.6 - 21.8	5.7
150	11.8	0.5 - 23.6	6.4
160	11.6	1.5 - 22.9	5.9
170	11.8	0.6 - 24.8	6.1
180	12.1	0.1 - 26.0	6.7
190	12.6	0.0 - 27.7	7.3

Historical temperature variations are depicted in Figure 2.22 for Stations 120, 140, and 180 (see Figure 2.11) located in the eastern basin of Shinnecock Bay, at Shinnecock Inlet, and in the western basin of Shinnecock Bay, respectively. Frequency distributions for the temperature values in Figure 2.22 are shown in Figure 2.23.

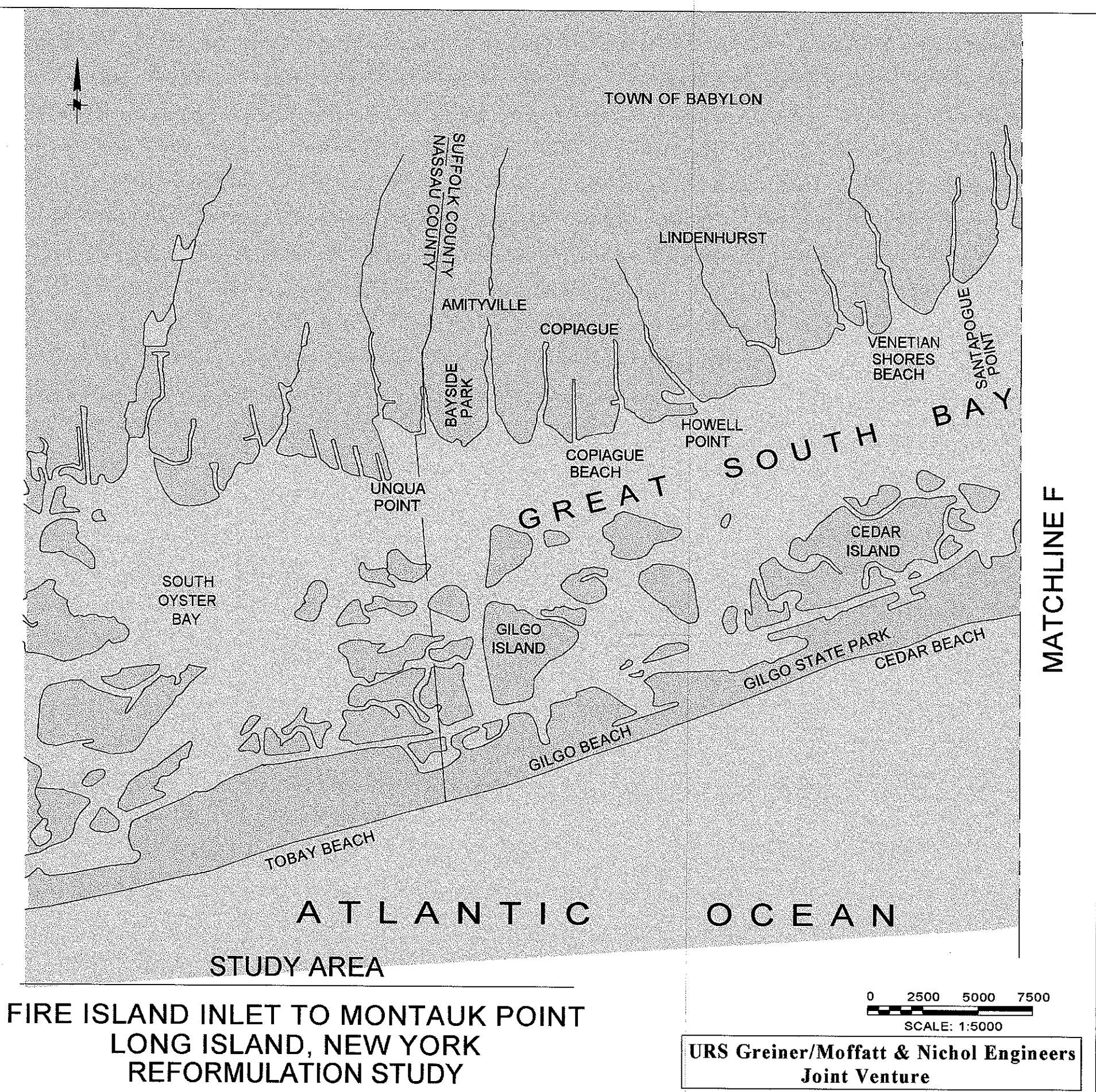
Average temperatures tend to be higher at stations further inland from the inlet. As in Moriches Bay, this temperature gradient can be attributed to the majority of the temperature measurements occurring during the late spring, summer, and early fall months at which point the ocean is slightly cooler than the bay.



VICINITY MAP

FIGURE 2.1

\\3982-07\\DWG\\IMP-2-2.DWG

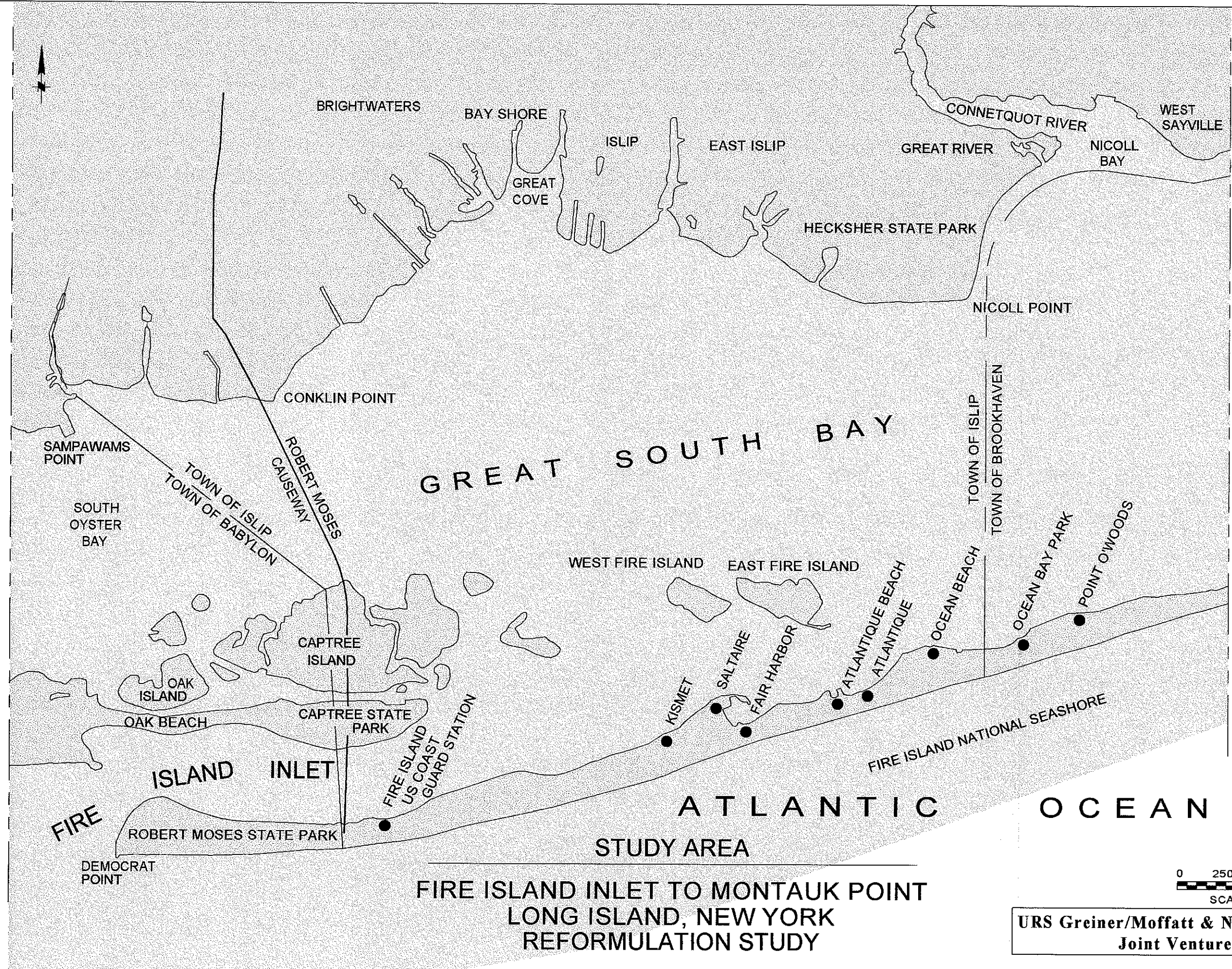


FIRE ISLAND INLET TO MONTAUK POINT
LONG ISLAND, NEW YORK
REFORMULATION STUDY

FIGURE 2.2

13892-071DWG\FIMP-2-3.DWG

MATCHLINE F



MATCHLINE E

FIRE ISLAND INLET TO MONTAUK POINT
LONG ISLAND, NEW YORK
REFORMULATION STUDY

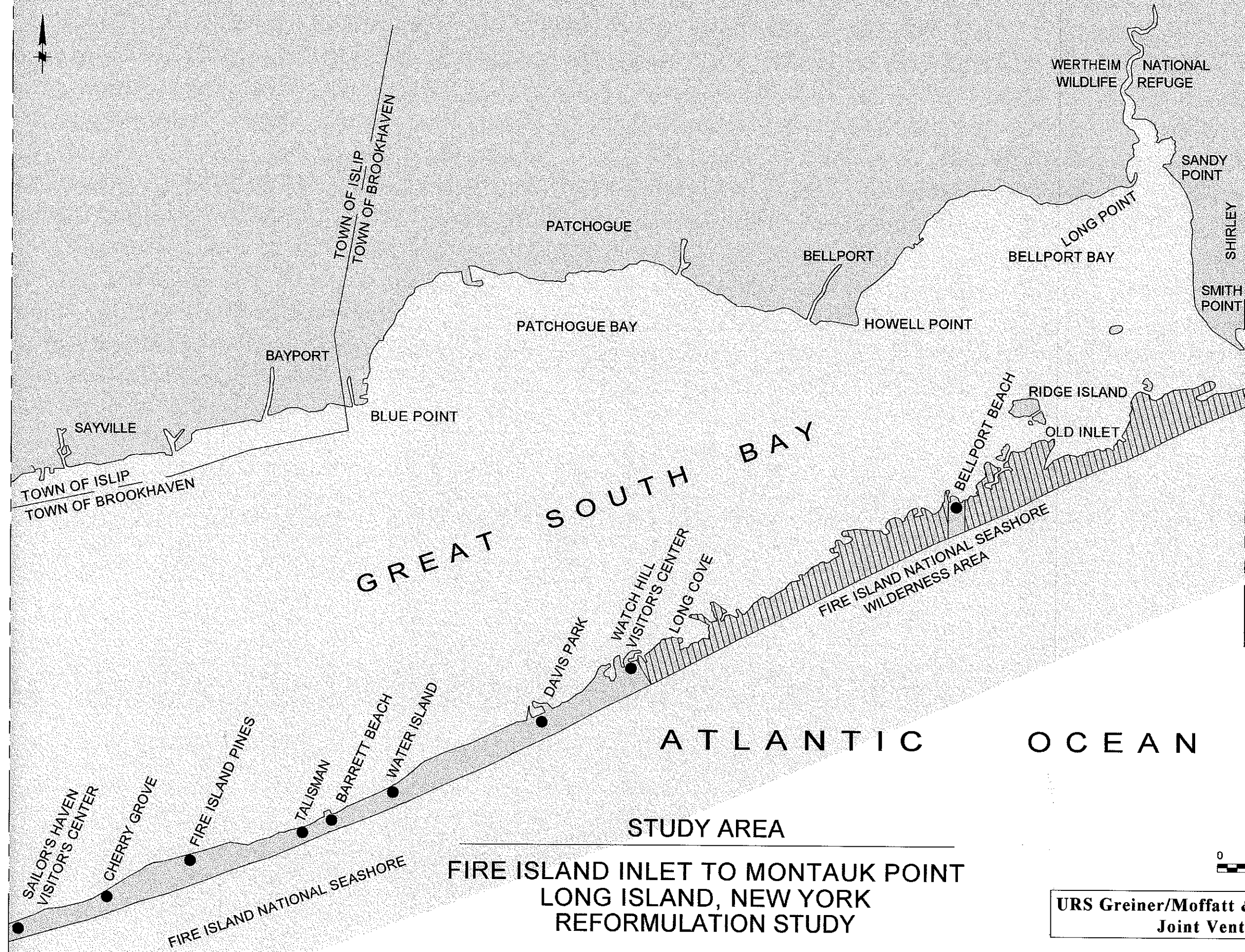
0 2500 5000 7500
SCALE: 1:5000

URS Greiner/Moffatt & Nichol Engineers
Joint Venture

FIGURE 2.3

\\3892-07\DWG\FIMP-2-4.DWG

MATCHLINE E



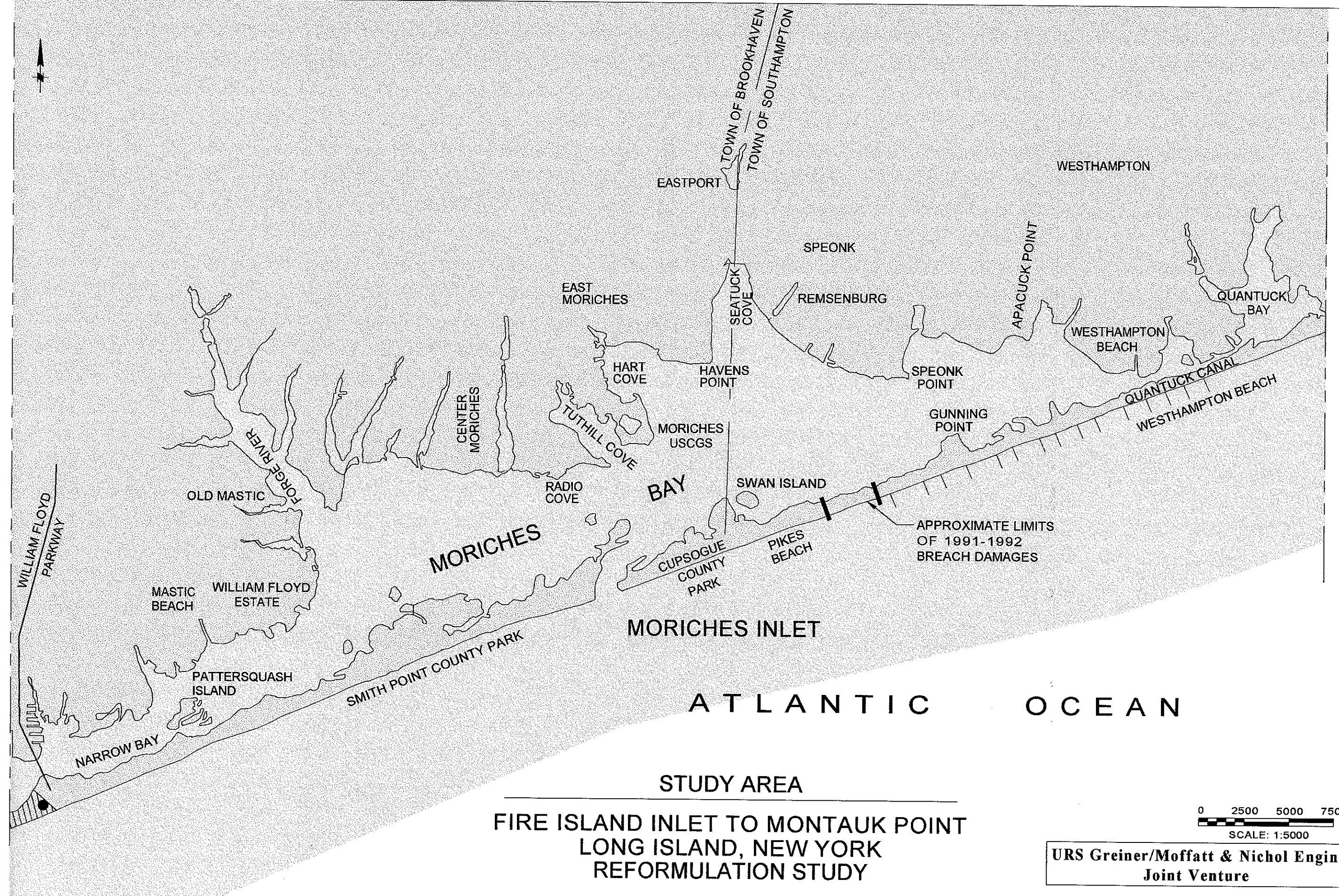
MATCHLINE D

URS Greiner/Moffatt & Nichol Engineers
Joint Venture

FIGURE 2.4

13892-07DWG\FIMP-2-5.DWG

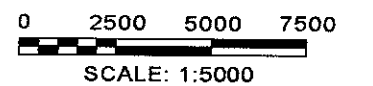
MATCHLINE D



MATCHLINE C

STUDY AREA

FIRE ISLAND INLET TO MONTAUK POINT
LONG ISLAND, NEW YORK
REFORMULATION STUDY

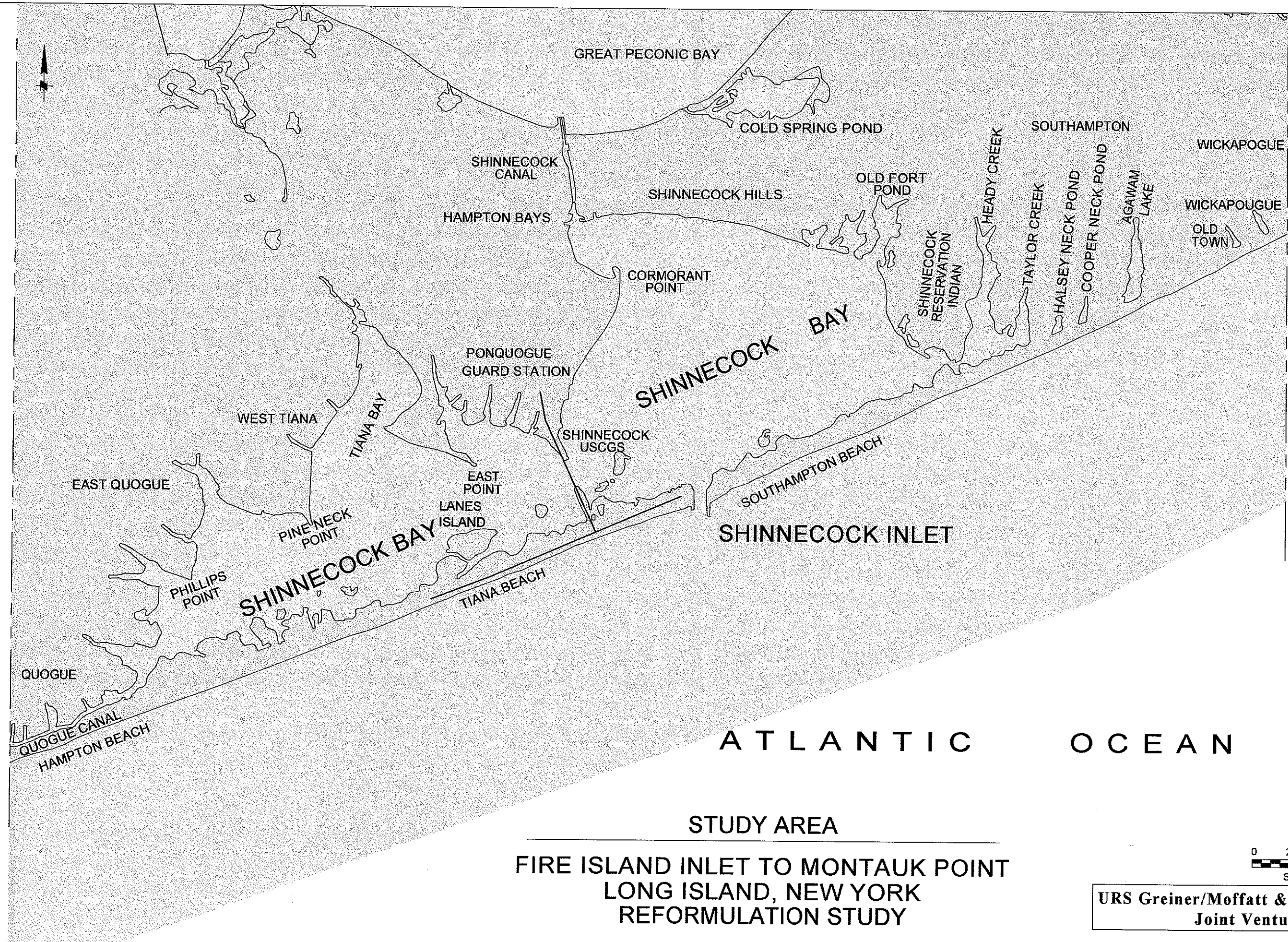


URS Greiner/Moffatt & Nichol Engineers
Joint Venture

FIGURE 2.5

13982-07\DWG\FIMP-2-6.DWG

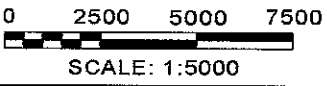
MATCHLINE C



MATCHLINE B

STUDY AREA

FIRE ISLAND INLET TO MONTAUK POINT
LONG ISLAND, NEW YORK
REFORMULATION STUDY

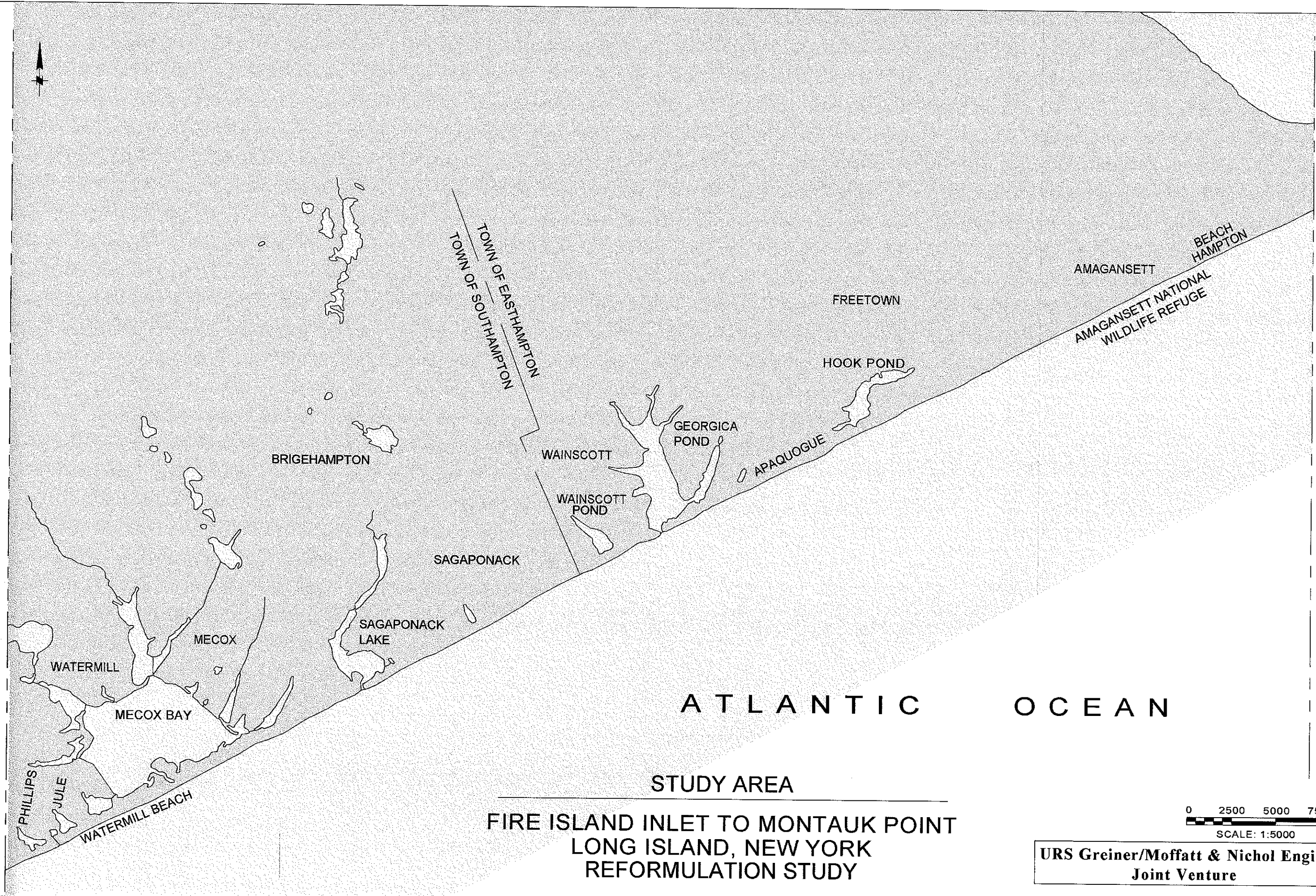


URS Greiner/Moffatt & Nichol Engineers
Joint Venture

FIGURE 2.6

13882-0710 WGA-TMP-2-7.DWG

MATCHLINE B



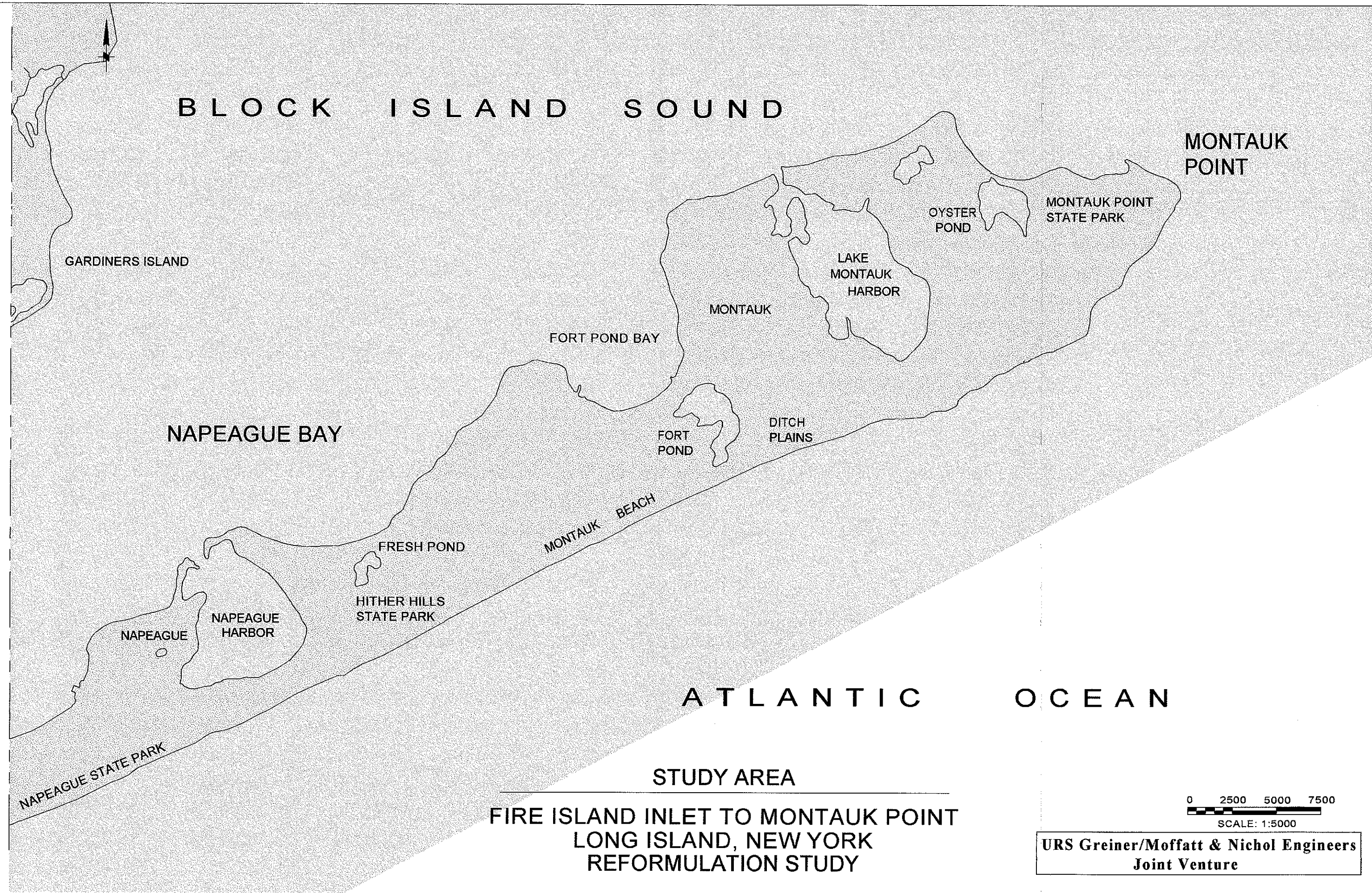
MATCHLINE A

STUDY AREA
FIRE ISLAND INLET TO MONTAUK POINT
LONG ISLAND, NEW YORK
REFORMULATION STUDY

URS Greiner/Moffatt & Nichol Engineers
Joint Venture

FIGURE 2.7

MATCHLINE A

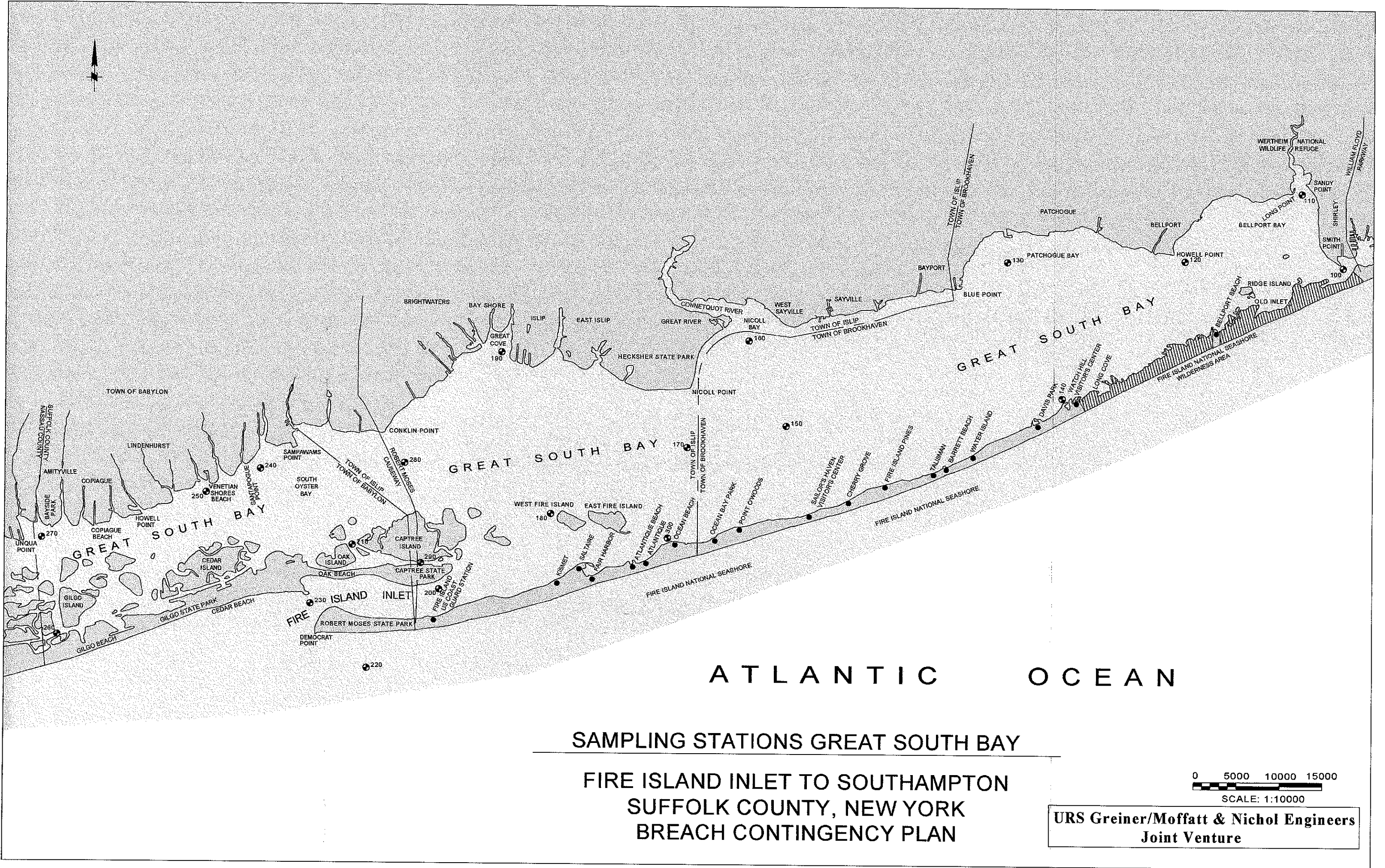


0 2500 5000 7500
SCALE: 1:5000

URS Greiner/Moffatt & Nichol Engineers
Joint Venture

FIGURE 2.8

13982-071DWGIMP-2-09.DWG



SAMPLING STATIONS GREAT SOUTH BAY

FIRE ISLAND INLET TO SOUTHAMPTON

SUFFOLK COUNTY, NEW YORK

BREACH CONTINGENCY PLAN

0 5000 10000 15000

SCALE: 1:10000

URS Greiner/Moffatt & Nichol Engineers

Joint Venture

FIGURE 2.9

13892-07\DWG\FIMP-2-10.DWG

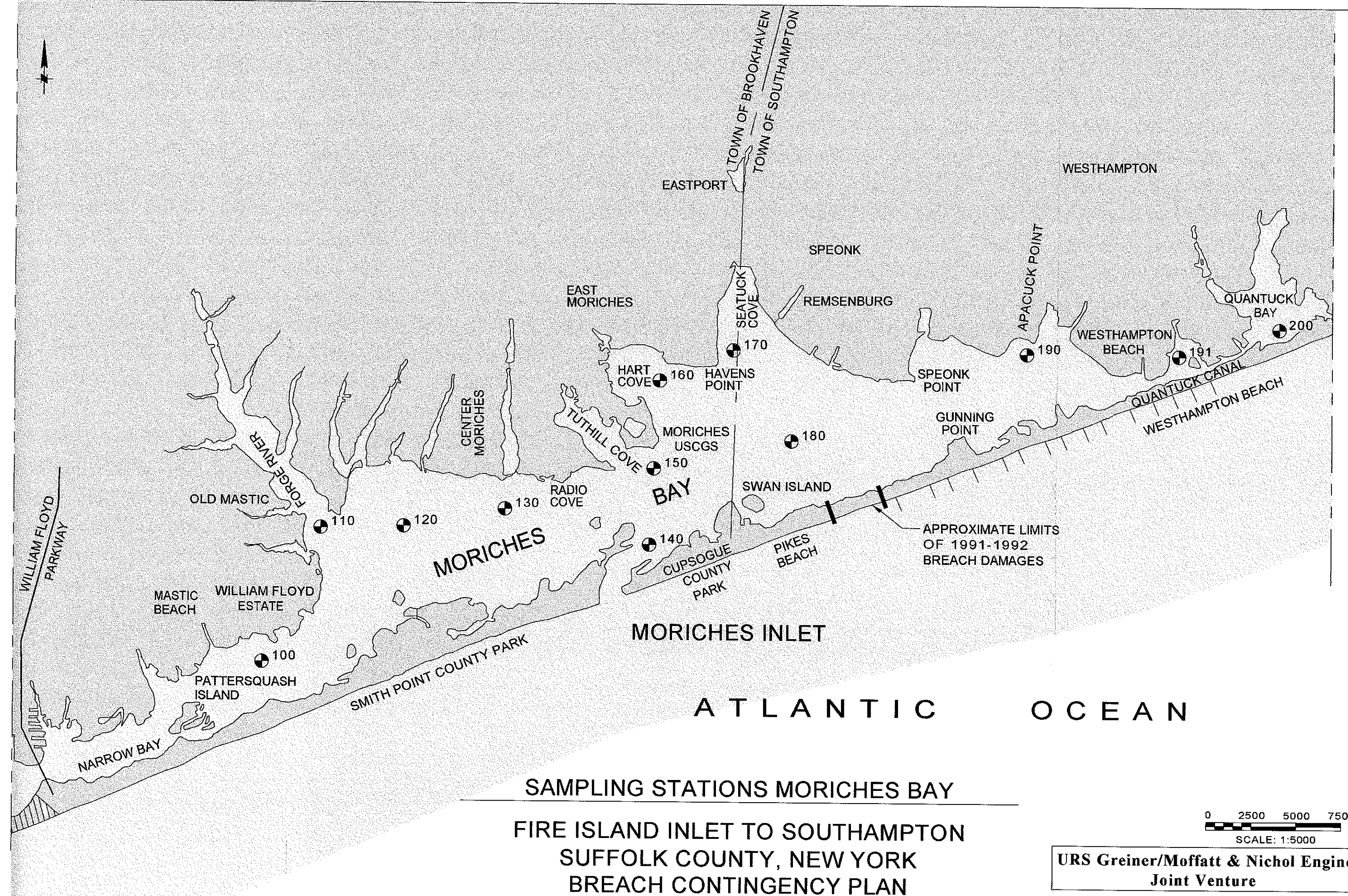
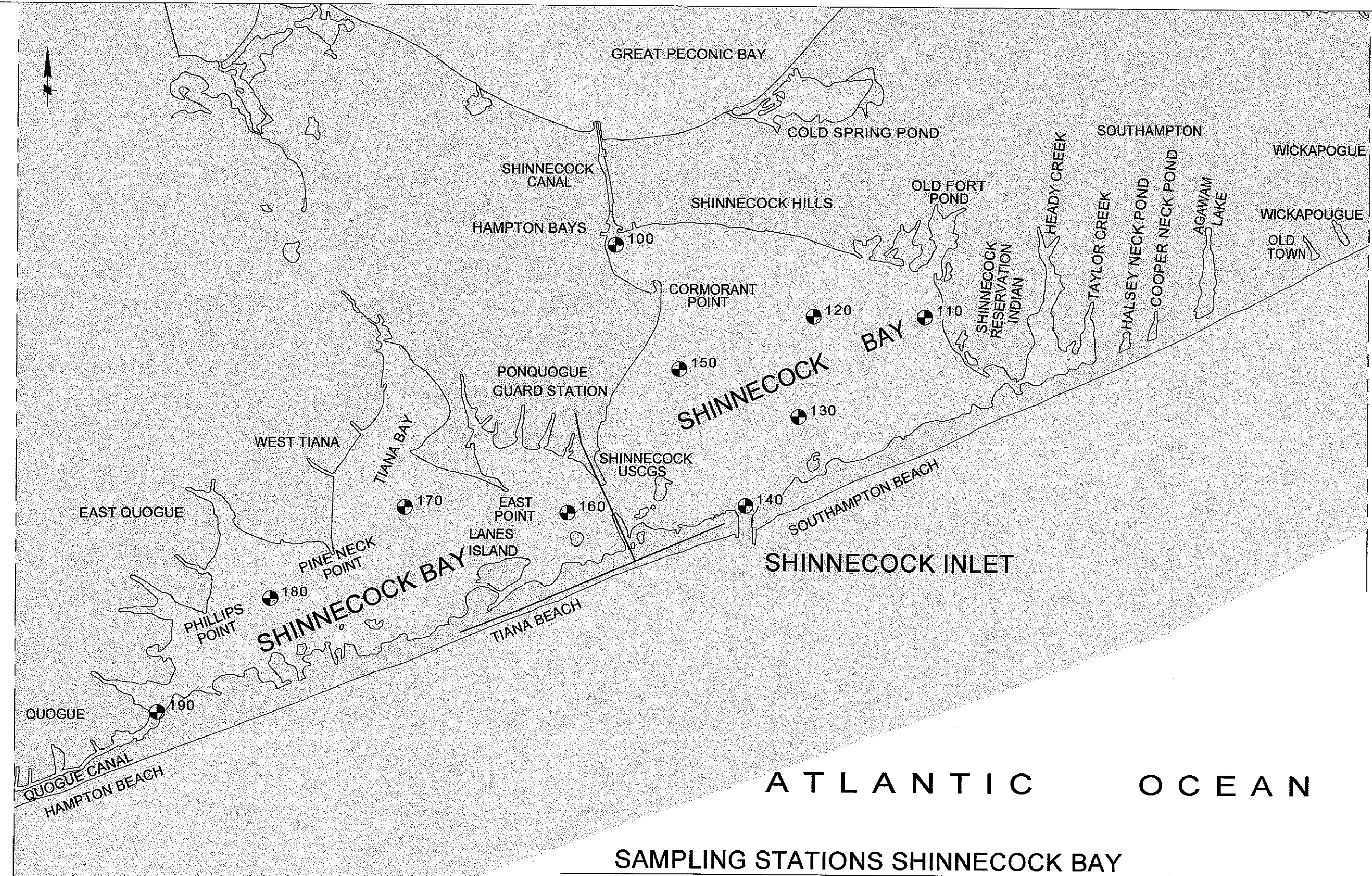


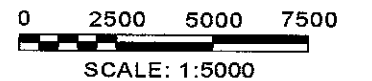
FIGURE 2.10

MATCHLINE C



SAMPLING STATIONS SHINNECOCK BAY

FIRE ISLAND INLET TO SOUTHAMPTON
SUFFOLK COUNTY, NEW YORK
BREACH CONTINGENCY PLAN



URS Greiner/Moffatt & Nichol Engineers
Joint Venture

FIGURE 2.11

Great South Bay
Measured Salinity Data

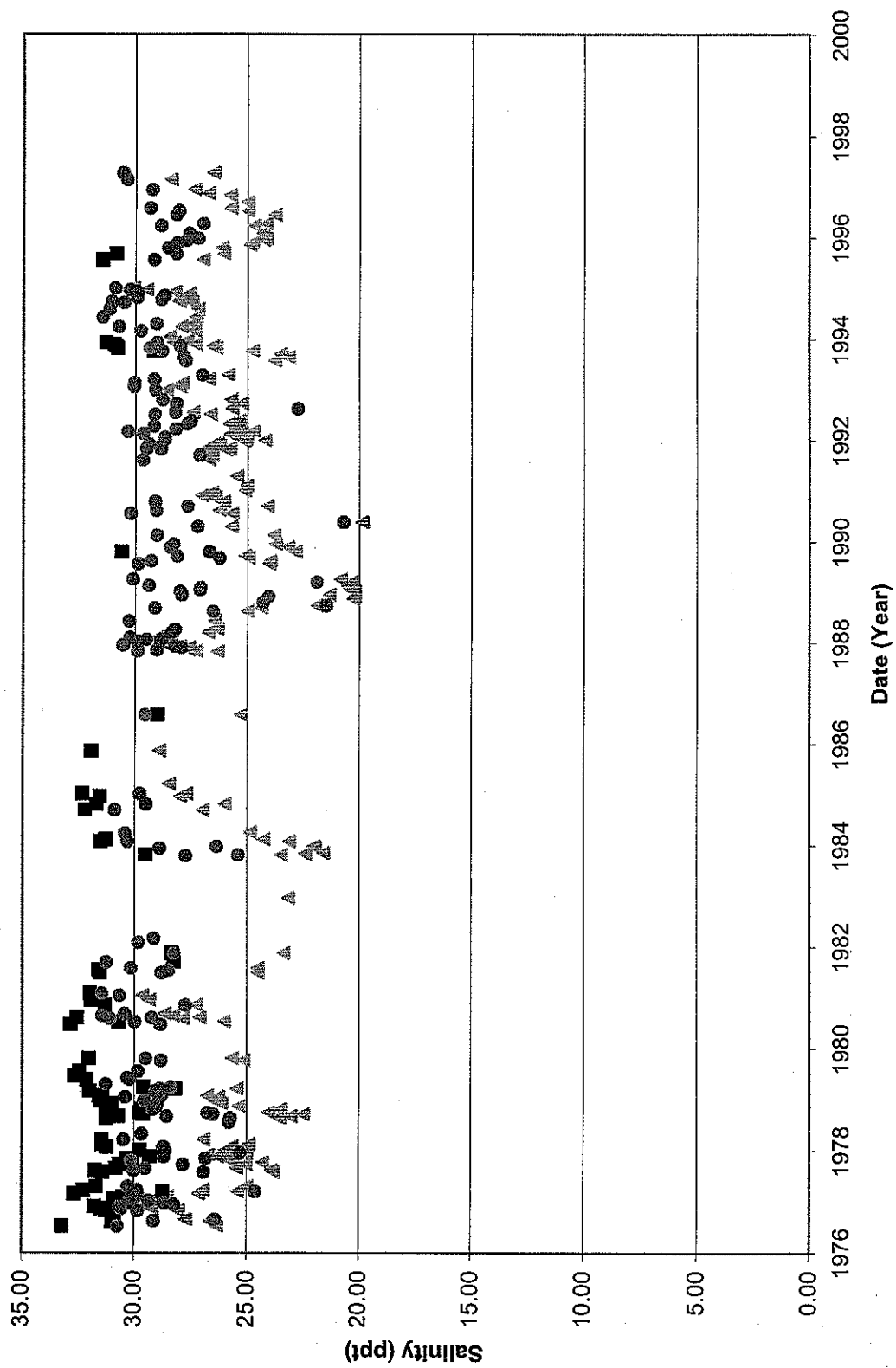


FIGURE 2.12

Great South Bay Measured Salinity Distributions

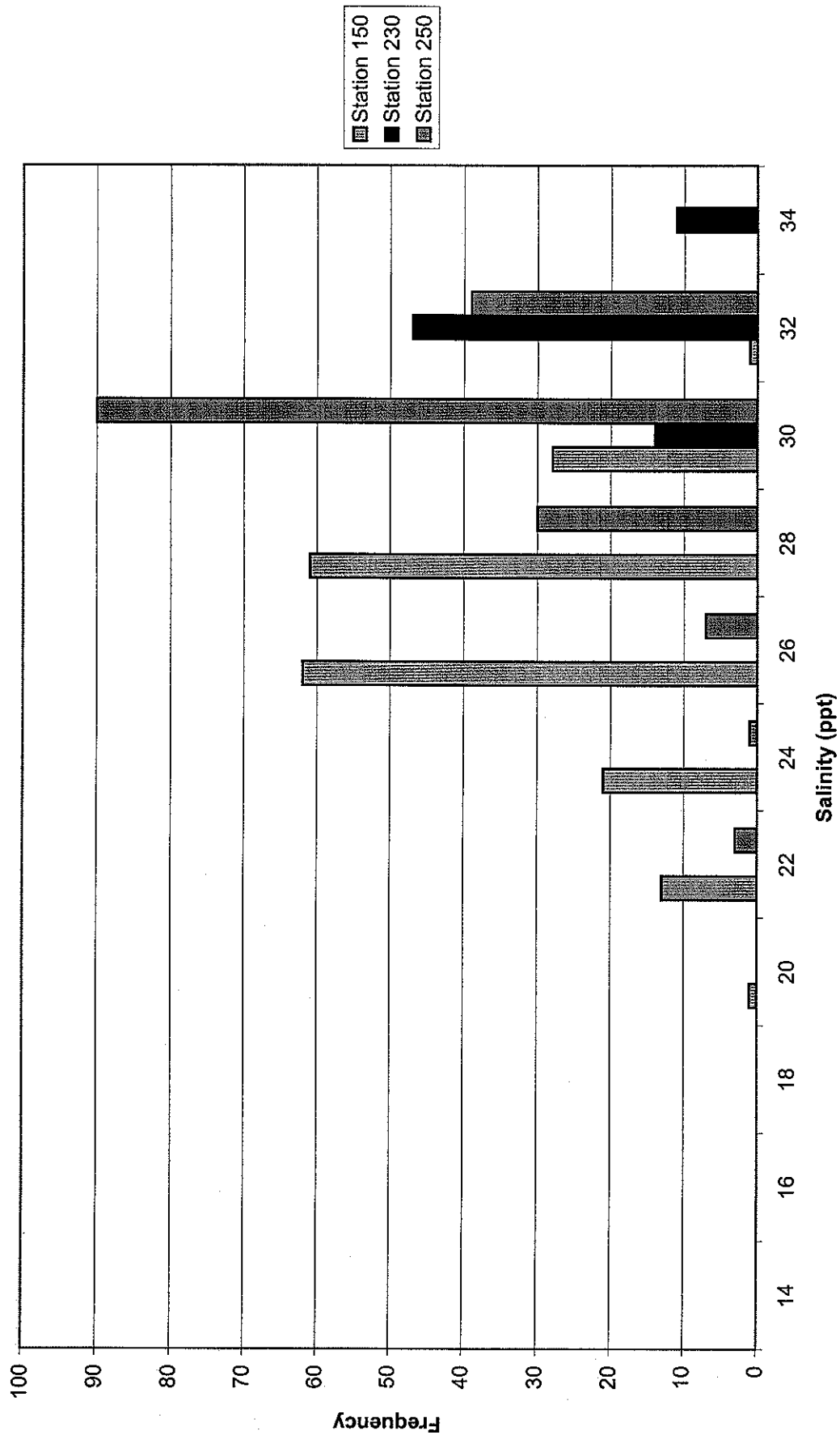


FIGURE 2.13

**Moriches Bay
Measured Salinity Data**

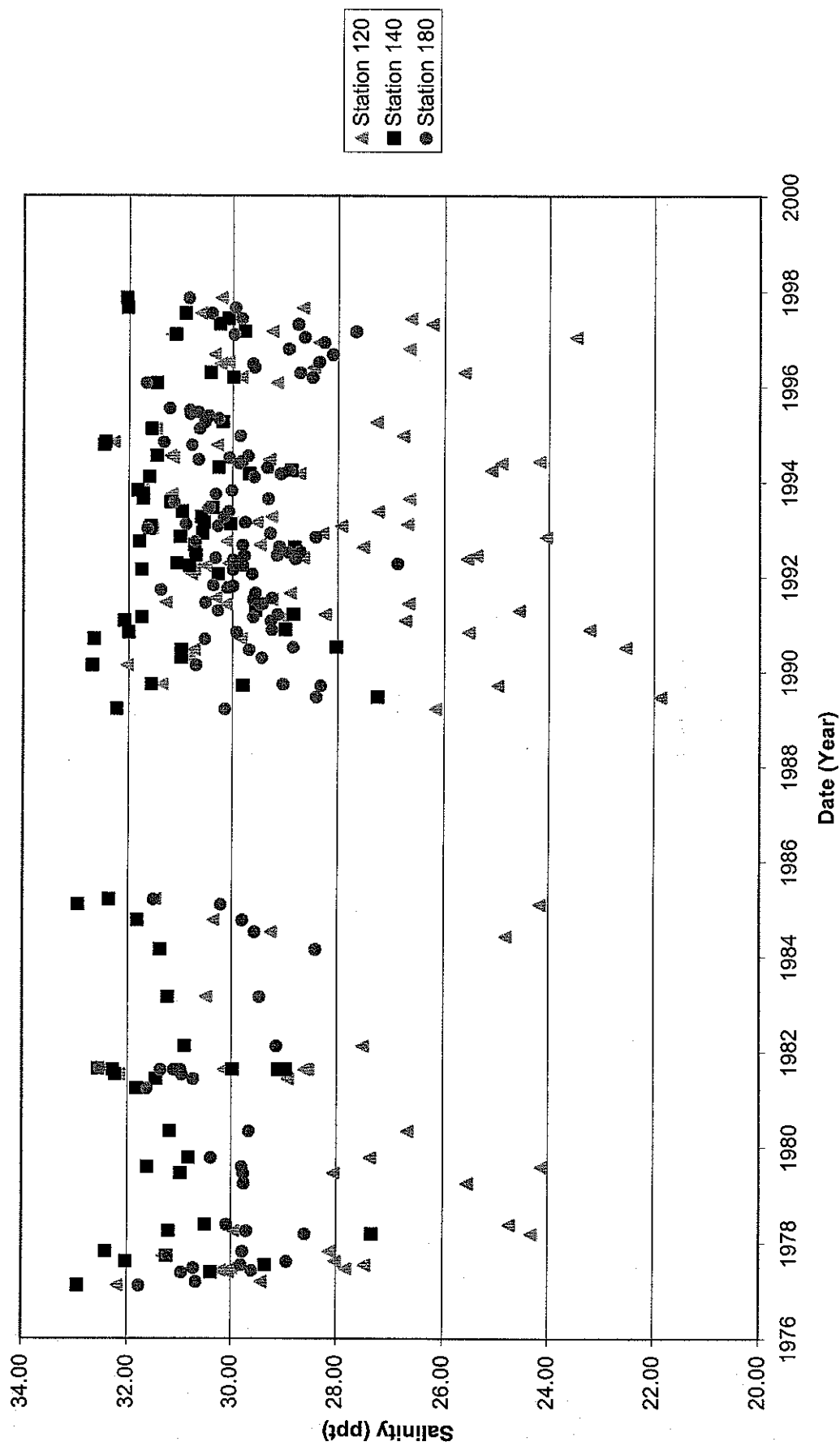


FIGURE 2.14

Moriches Bay Measured Salinity Distributions

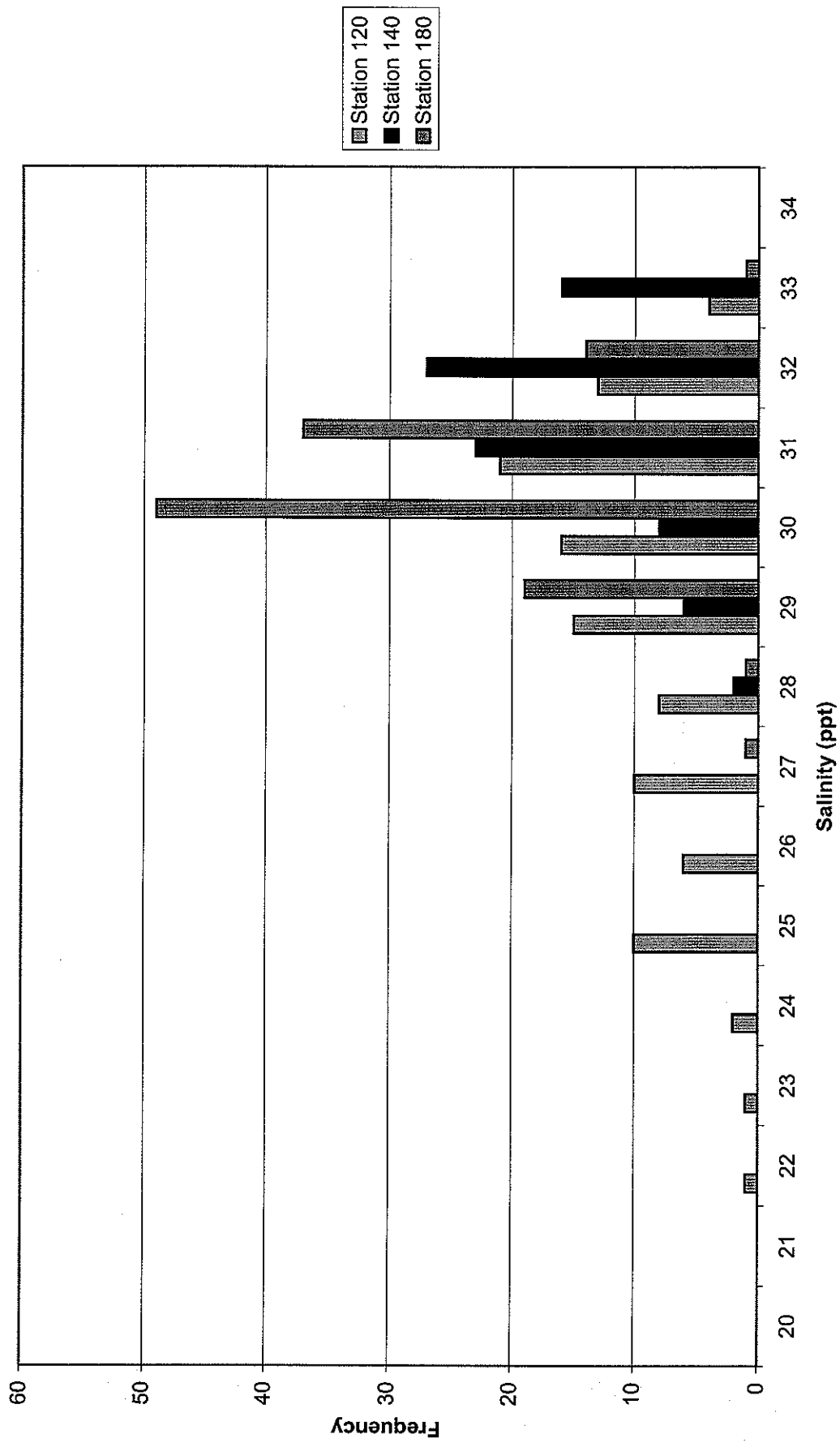


FIGURE 2.15

Shinnecock Bay
Measured Salinity Data

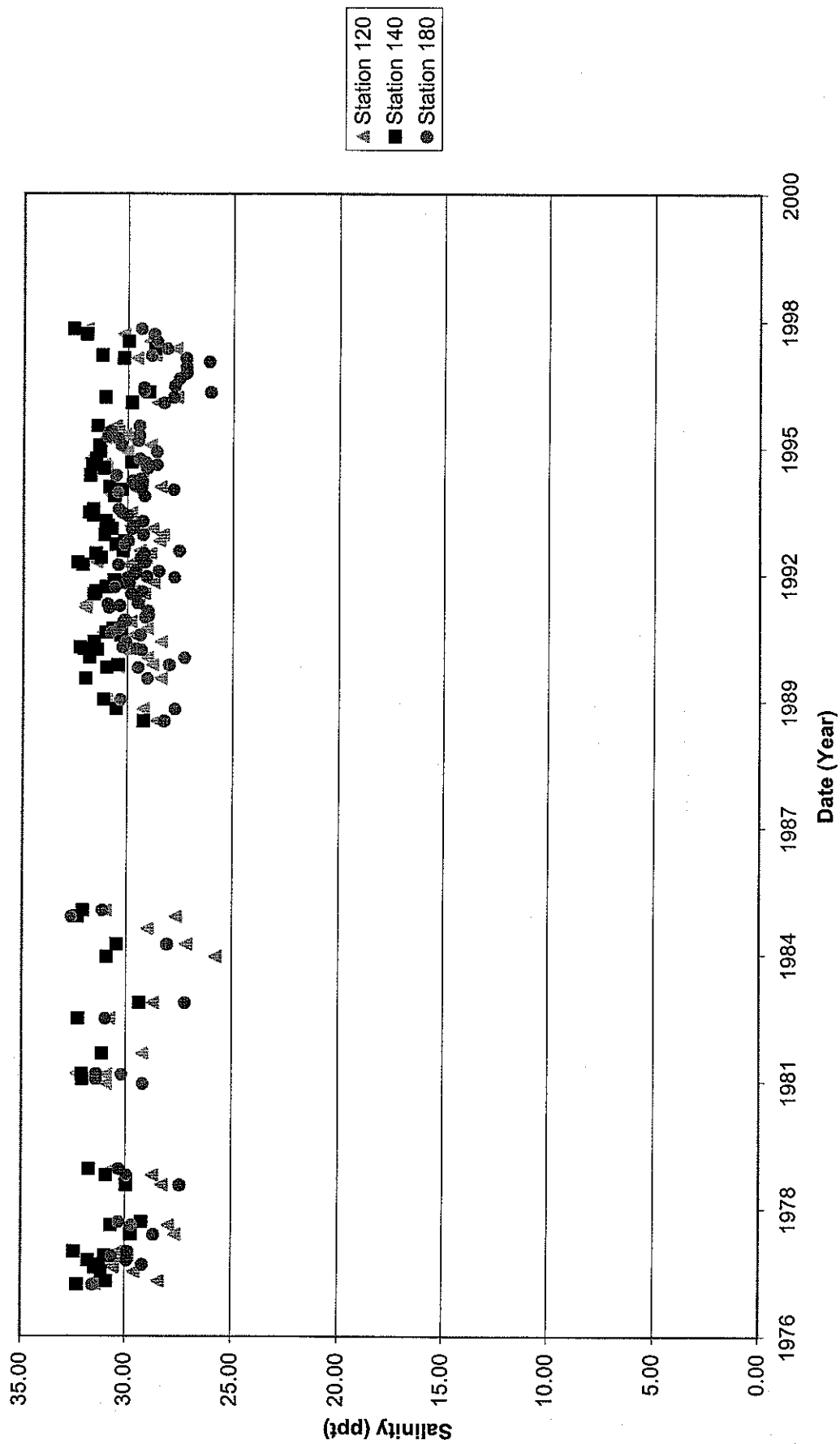


FIGURE 2.16

Shinnecock Bay Measured Salinity Distributions

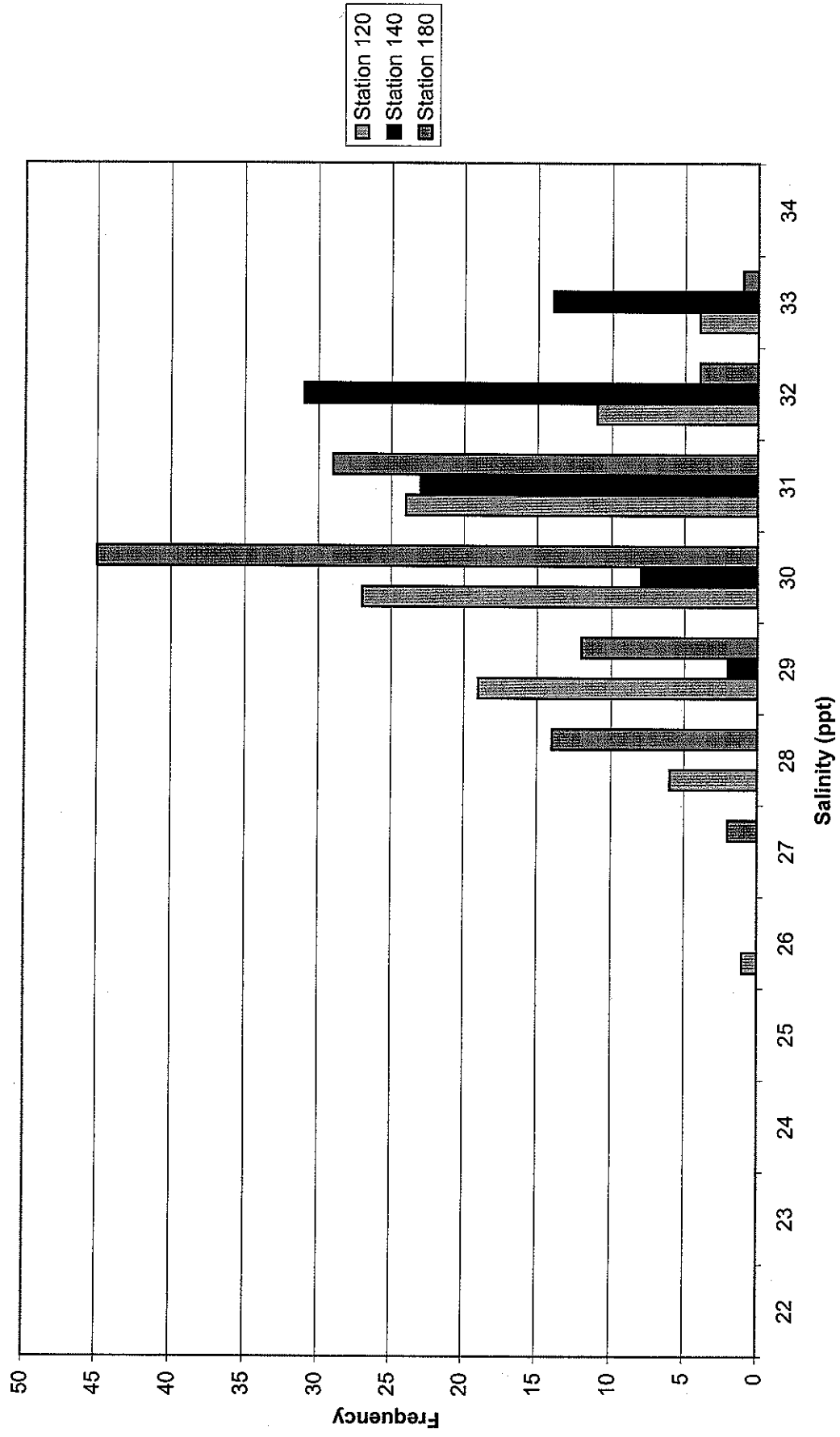


FIGURE 2.17

Great South Bay
Measured Temperature Data

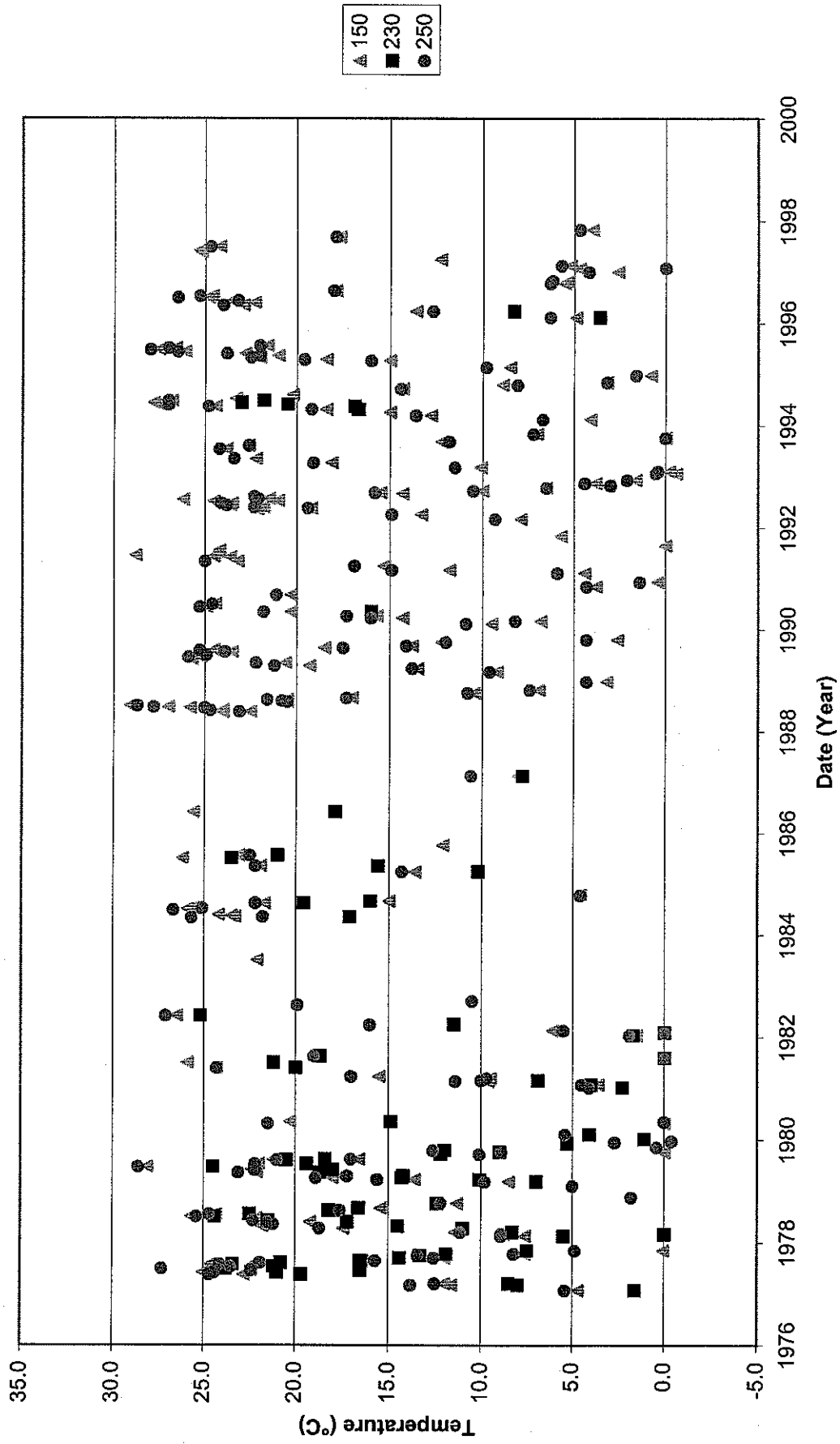


FIGURE 2.18

Great South Bay Measured Temperature Distributions

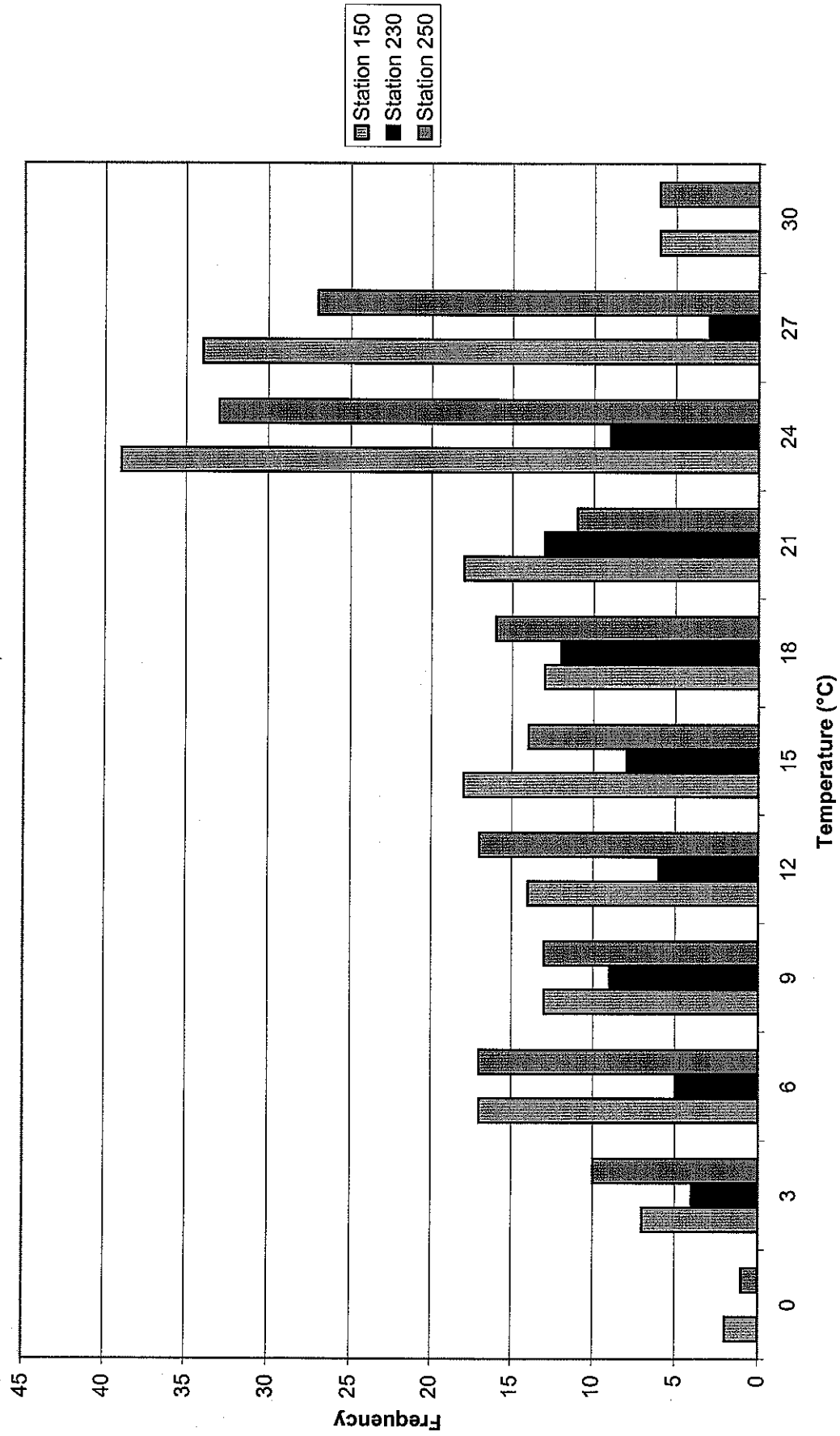


FIGURE 2.19

Moriches Bay Measured Temperature Data

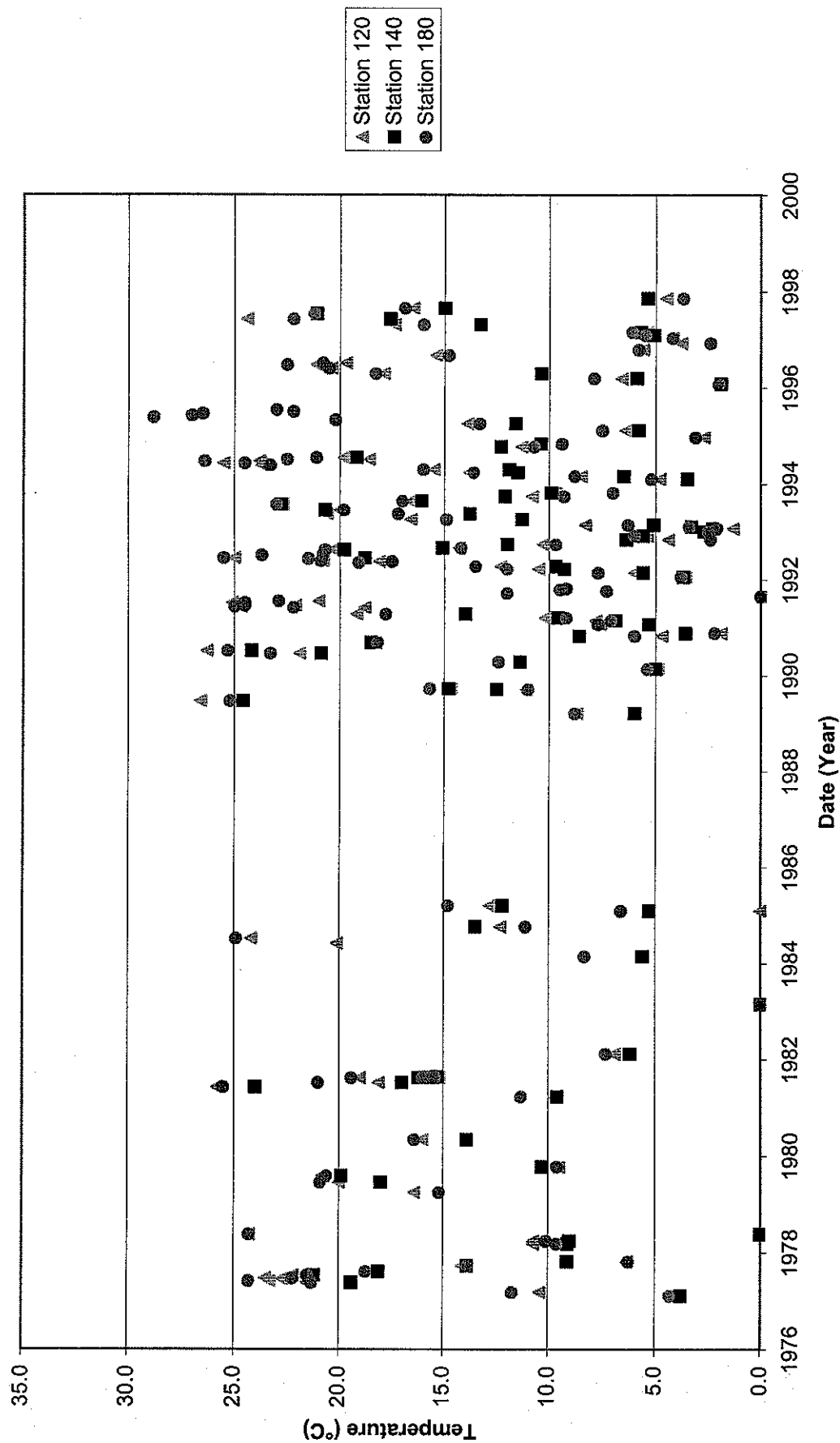


FIGURE 2.20

Moriches Bay Measured Temperature Distributions

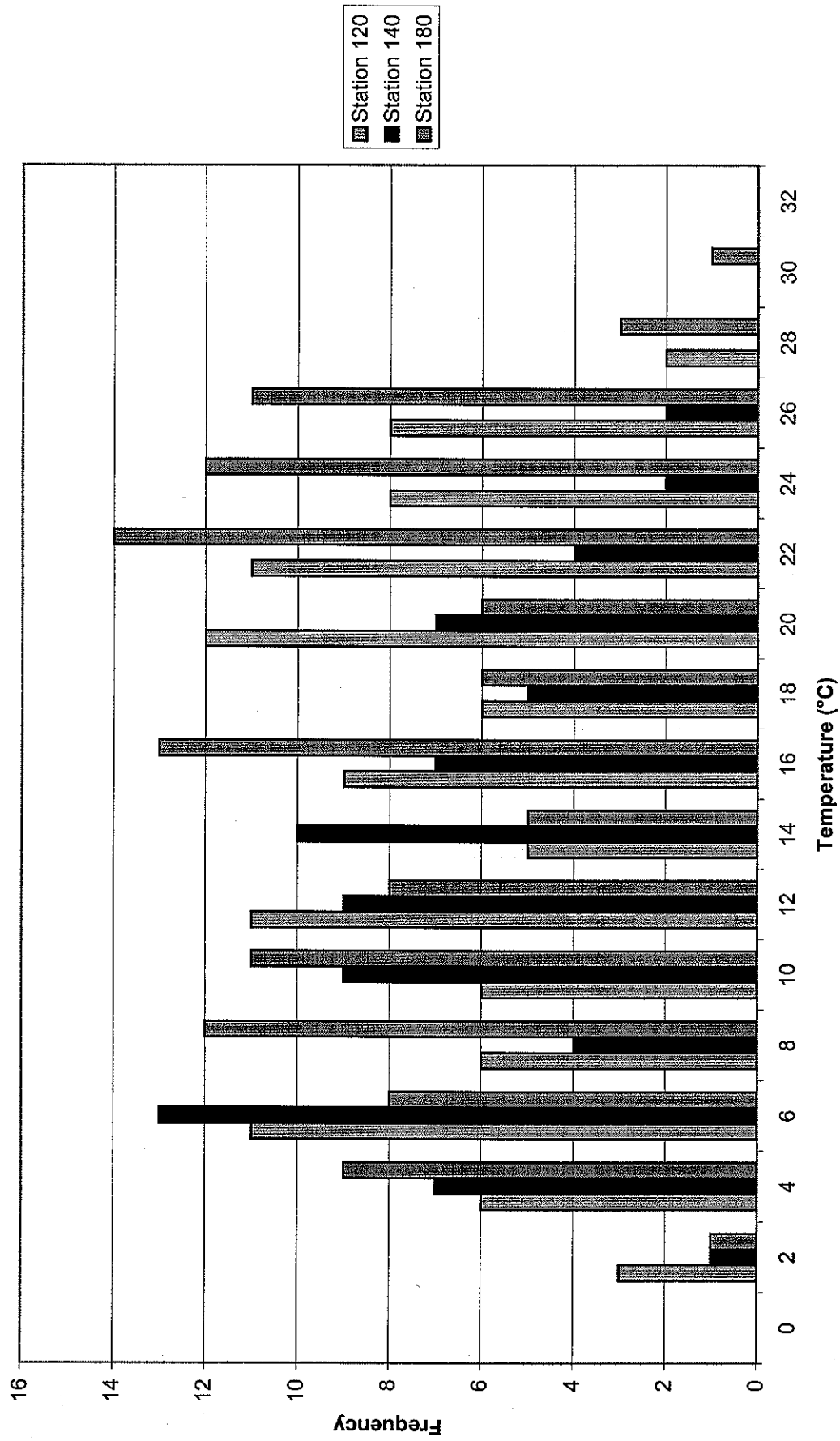


FIGURE 2.21

Shinnecock Bay
Measured Temperature Data

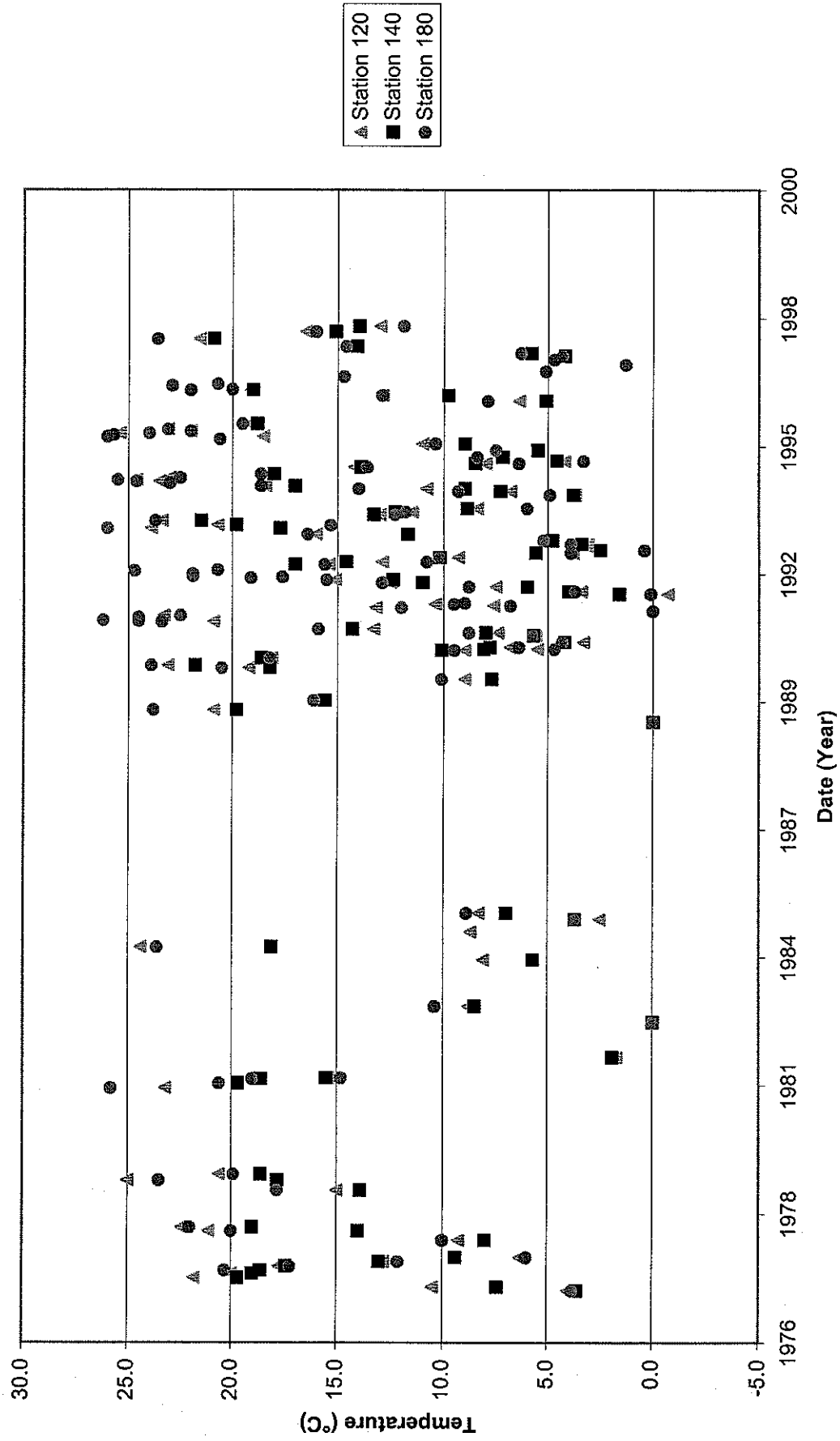


FIGURE 2.22

Shinnecock Bay Measured Temperature Distributions

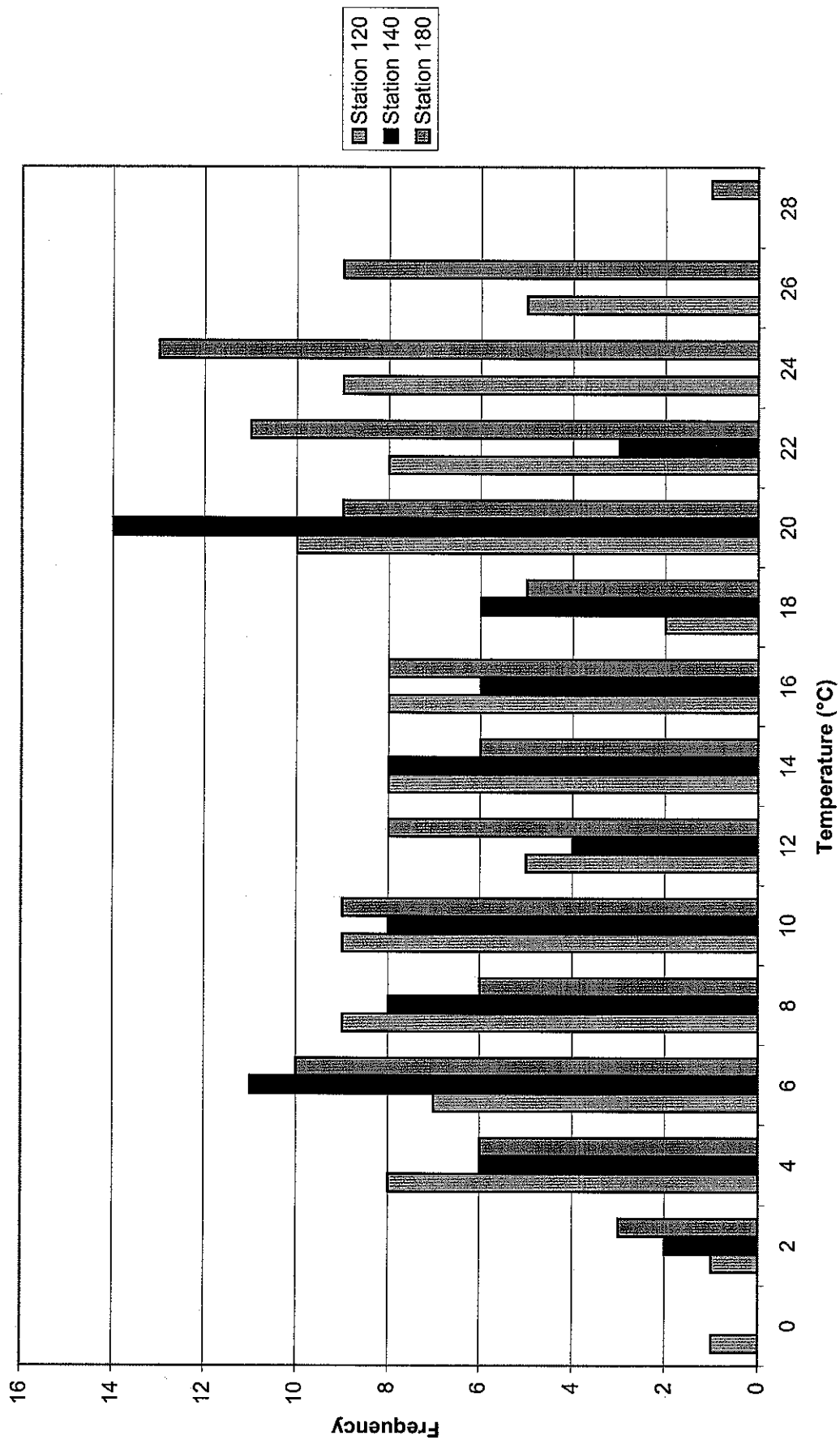


FIGURE 2.23

3. SIMULATION MODELS

3.1. General Description

Tidal hydrodynamics, salinity distributions, temperature distributions, and residence times within the Moriches Bay estuarial system were simulated using two numerical models. The first model, MIKE 21 HD, simulates tidal hydrodynamics. Results from the hydrodynamic model were then coupled with an advection/dispersion model, MIKE 21 AD, which simulates constituent transport. Both numerical models use the finite difference method to solve the appropriate governing equations for depth averaged unsteady flow.

3.2. Hydrodynamic Model (MIKE 21 HD)

The hydrodynamic model simulates two-dimensional flow in rivers and estuaries by solving the depth-averaged Navier Stokes equations for flow velocity and water depth. The equations account for friction losses, eddy viscosity, Coriolis forces and surface wind stresses. The general governing equations are:

$$\begin{aligned} \frac{\partial \zeta}{\partial t} + \frac{\partial p}{\partial x} + \frac{\partial q}{\partial y} &= 0 \\ \frac{\partial p}{\partial t} + \frac{\partial}{\partial x} \left(\frac{p^2}{h} \right) + \frac{\partial}{\partial y} \left(\frac{pq}{h} \right) + gh \frac{\partial \zeta}{\partial x} \\ &+ \frac{gp\sqrt{p^2 + q^2}}{C^2 \cdot h^2} - \frac{1}{p_w} \left[\frac{\partial}{\partial x} (h\tau_{xx}) - \frac{\partial}{\partial y} h\tau_{xy} \right] - \Omega q \\ &- fVV_x + \frac{h}{p_w} \frac{\partial}{\partial x} (p_a) = 0 \end{aligned}$$

$$\begin{aligned}
& \frac{\partial q}{\partial t} + \frac{\partial}{\partial y} \left(\frac{q^2}{h} \right) + \frac{\partial}{\partial x} \left(\frac{pq}{h} \right) + gh \frac{\partial \zeta}{\partial y} \\
& + \frac{gq \sqrt{p^2 + q^2}}{C^2 \cdot h^2} - \frac{1}{p_w} \left[\frac{\partial}{\partial x} (h \tau_{xy}) - \frac{\partial}{\partial y} (h \tau_{xy}) \right] - \Omega p \\
& - fVV_y + \frac{h}{p_w} \frac{\partial}{\partial y} (p_a) = 0
\end{aligned}$$

where:

$h(x, y, t)$ = water depth (ft)

$\zeta(x, y, t)$ = surface elevation (ft)

$p, q, (x, y, t)$ = flux densities in x - and y - directions ($\text{ft}^3/\text{s}/\text{ft}$) = (uh, vh) ;

(u, v) = depth averaged velocity in x - and y - directions

$C(x, y)$ = Chezy resistance ($\text{ft}^{1/2}/\text{s}$)

g = acceleration due to gravity (ft/s^2)

$f(V)$ = wind friction factor

$V, V_x, V_y, (x, y, t)$ = wind speed and components in x - and y - direction (ft/s)

$\Omega(x, y)$ = Coriolis parameter, latitude dependent (s^{-1})

$p_a(x, y, t)$ = atmospheric pressure ($\text{lb}/\text{ft}/\text{s}^2$)

p_w = density of water (lb/ft^3)

x, y = space coordinates (ft)

t = time (s)

$\tau_{xx}, \tau_{xy}, \tau_{yy}$ = components of effective shear stress

3.3. Advection-Dispersion Model (MIKE 21 AD)

The advection-dispersion model simulates two-dimensional depth-averaged constituent transport in rivers and estuaries. The model solves the governing equation of advection-dispersion (i.e., constituent transport of salt or tracer concentration in this case) using the velocities and water depths generated by the hydrodynamic model at each time step. The governing equation is:

$$\frac{\partial}{\partial t}(hC) + \frac{\partial}{\partial x}(uhC) + \frac{\partial}{\partial y}(vhC) = \frac{\partial}{\partial x}\left(h \cdot D_x \cdot \frac{\partial C}{\partial x}\right) + \frac{\partial}{\partial y}\left(h \cdot D_y \cdot \frac{\partial C}{\partial y}\right) - F \cdot h \cdot C + S$$

where:

C = compound concentration (arbitrary units)

u, v = horizontal velocity components in the x - and y - directions (ft/s)

h = water depth (ft)

D_x, D_y = dispersion coefficients in the x - and y - directions (ft²/s)

F = linear decay coefficient (1/s)

$S = Q_s \cdot (C_s - C)$

Q_s = source / sink discharge (ft³/s/ft²)

C_s = concentration of compound in the source / sink discharge

The primary limitation of the modeling system used in this investigation is that the equations are depth-averaged (i.e., two-dimensional in horizontal plane). Therefore, the vertical distributions of tidal currents and constituent concentration distributions are not modeled. Regardless, the model is judged to be an excellent representation of the well-mixed estuarial systems modeled in this study. Little additional accuracy would be gained from a three dimensional model although use of such a model would dramatically increase computation time and calibration efforts.

3.4. Residence Time Computations

Residence time is defined as the average length of time that water particles reside in a basin (Van de Kreeke, 1983). As indicated by the definition, the residence time is a measure of the renewal rate of embayment waters, and therefore has often been used as a relative measure of the water quality of a tidal embayment.

Considering an idealized, well-mixed control volume, V , and an exchange rate, Q , between the control volume and outside waters, the residence time of the control volume, under steady-state conditions can be written as:

$$T_r = \frac{V}{Q}$$

Now consider that the rate of loss of mass is due to "decay" according to the following general equation:

$$C(t) = C_0 \cdot e^{-Kt}$$

where:

$C(t)$ = tracer concentration at time t

C_0 = initial tracer concentration

K = decay coefficient

The mass balance for tracer concentration in the control volume can be written as:

$$V \frac{dC}{dt} = Q(C_e - C) - KVC$$

Where:

C_e = tracer concentration supplied to the control volume from the outside waters

Upon reaching steady-state (i.e. $dC/dt=0$) a steady state tracer concentration $C=C_s$ is achieved and represents the balance of mass lost to "decay" over time with that replaced by outside waters. The following equation can be derived from the above equations assuming steady state conditions:

$$\frac{V}{Q} = \frac{C_e - C_s}{KC_s}$$

Therefore, the residence time is given by:

$$T_r = \frac{V}{Q} = \frac{C_e - C_s}{KC_s}$$

Residence times have been computed for the present study according to the following procedure:

- Begin computations with an initial tracer concentration of 1.0 over the entire element mesh.
- Specify an equal decay coefficient, K , for each point of the mesh.
- Set a constant tracer coefficient of 1.0 at each model boundary (i.e. $C_e = 1$).
- Run the pollutant transport model until steady state conditions are achieved (i.e. C_s is determined over the entire mesh).
- Compute the residence time at each point using the above equation.

It should be noted that residence times computed using the above methodology represent the time it takes for water particles to leave any of the model boundaries. The residence times do not necessarily represent the time necessary for water particles to reach the ocean inasmuch as water particles can also exit via the lateral boundaries of the computational mesh.

4. NUMERICAL MESH GENERATION

4.1. General

The factors governing development of a finite-difference mesh are (1) the level of detail or resolution necessary to adequately represent the estuary and maintain numerical stability of the model and (2) the required extent or coverage of the mesh. MIKE21 is capable of accurately simulating tidal elevations/flows over a wide range of mesh resolutions. Accordingly, the bathymetric features of the estuary generally dictate mesh detail. However, model run times require consideration when developing a finite-difference mesh. Extremely fine meshes can result in inordinately long run times which may make calibration and/or production runs costly and difficult. In the present study, the level of detail required to accurately represent the study inlets determined the necessary resolution for the remainder of each mesh.

There are several factors that guide decisions regarding the aerial extent of the mesh. First, it is desirable to extend the mesh to areas that are sufficiently removed from the proposed areas of change so as to be unaffected by that change. Secondly, the outer regions of the mesh must be located along boundaries where conditions can be reasonably measured and described to the model. For example, it is more convenient to locate a boundary along a line crossing a well-defined channel than to locate a boundary across the middle of a large embayment, because flow conditions and/or tidal elevations are more easily stipulated for the well defined channel than in the open embayment.

4.2. Bathymetric Data

MIKE21 requires two types of data for mesh generation, namely: (1) bathymetric data, including horizontal coordinates and associated depths, and (2) shoreline coordinates defining land boundaries within the mesh. Shoreline and bathymetric data for Great South, Moriches and Shinnecock Bays were obtained from National Ocean Service/National Oceanic and

Atmospheric Administration (NOS/NOAA) nautical charts Nos. 12352 and 12353. Recent surveys were used for Moriches and Shinnecock Inlets. Recent surveys at Fire Island Inlet were incomplete. Shorelines adjacent to all inlets were based on 1995 topography. The resulting mesh geometries were checked relative to the nautical charts and alternations were made as deemed necessary to: (1) improve physical representation of the estuaries and (2) improve model stability in areas of large depth gradients.

The finite difference meshes created for Great South, Moriches and Shinnecock Bays are presented in Figures 4.1 to 4.3, respectively. The Great South Bay mesh (see Figure 4.1) includes 700 grid points (east to west) by 272 grid points (north to south). The grid covers approximately 415 square miles, including South Oyster Bay, Bellport Bay, and a portion of western Narrow Bay. The western boundary of Great South Bay was located between Biltmore Shores and Tobay Beach along the western end of South Oyster Bay in Nassau County. To the east, the Great South Bay grid extends to Smith Point at the confluence of Great South and Narrow Bays. The seaward extent of the finite difference mesh is located 6 to 8 miles offshore approximately along the 80-foot contour. The northern boundary was located inland in order to include the major tributaries connected to Great South Bay.

Figure 4.2 shows the finite difference mesh generated for Moriches Bay. Moriches Bay is represented by 600 grid points east to west and 360 grid points north to south, and covers approximately 100 square miles. All of Moriches Bay was included, extending east from Smith Point along Narrow Bay to the Quantuck Canal. The seaward boundary for Moriches Bay was located approximately along the 80-ft contour. The mesh was extended north to include all major tributaries to Moriches Bay.

The numerical grid for Shinnecock Bay is shown in Figure 4.3. This mesh includes 570 grid points (east to west) by 375 grid points (north to south), and covers about 75 square miles. The Quogue Canal defines the western limit of the mesh, which extends north to the Shinnecock Canal. The finite difference mesh extends east of Heady Creek, and south to the 80-ft contour.

4.3. Mesh Parameters

The spacing of the finite difference mesh influences the stability and accuracy of the hydrodynamic model. As stated previously, it is best when the boundary conditions are located in well-defined areas with boundary flows perpendicular to the mesh. To improve model stability in the present study, each mesh was aligned so that the offshore boundary was parallel to the shoreline (see Figures 4.1 to 4.3).

The Courant number serves as an empirical prediction of mesh quality and hydrodynamic model stability. The definition of the Courant number is as follows:

$$C_R = c \times \frac{\Delta t}{\Delta x}$$

$$c = \sqrt{g \times h}$$

Where:

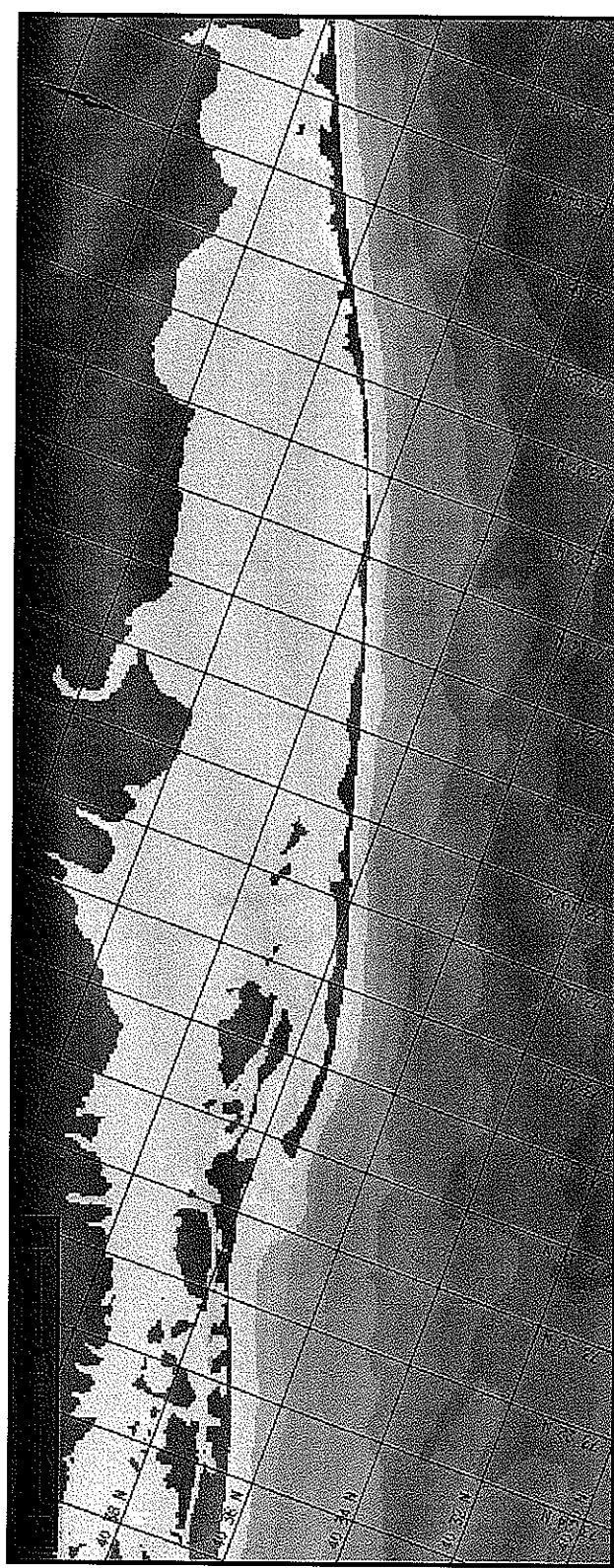
Δx = element side length (or grid spacing)

c = celerity

g = gravitational constant

h = water depth

A low Courant number generally indicates improved numerical stability. The suggested maximum Courant number is about 10 (Danish Hydraulic Institute, 1996). Inasmuch as the Courant number is inversely related to grid spacing, larger elements typically lead to improved stability. Larger elements, on the other hand, reduce bathymetric resolution. Grid resolution must, therefore, be assessed considering both geometric detail and numerical stability. Grid spacings of 75, 40, and 30 meters were selected for Great South, Moriches and Shinnecock Bays, respectively.

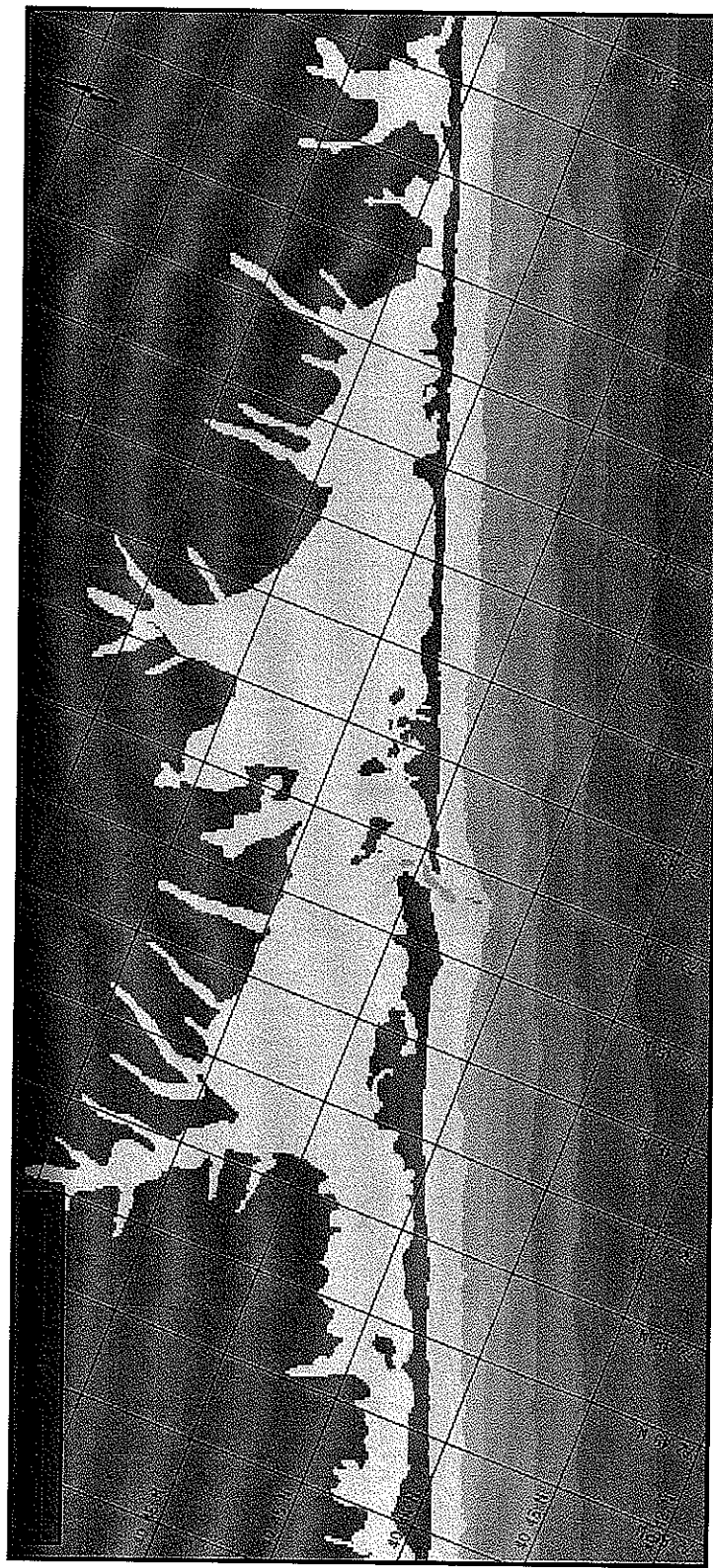


(ft)

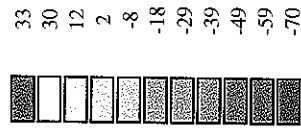
FIGURE 4.1
GREAT SOUTH BAY
FINITE DIFFERENCE MESH

FIRE ISLAND TO MONTAUK POINT
INLETS STUDY

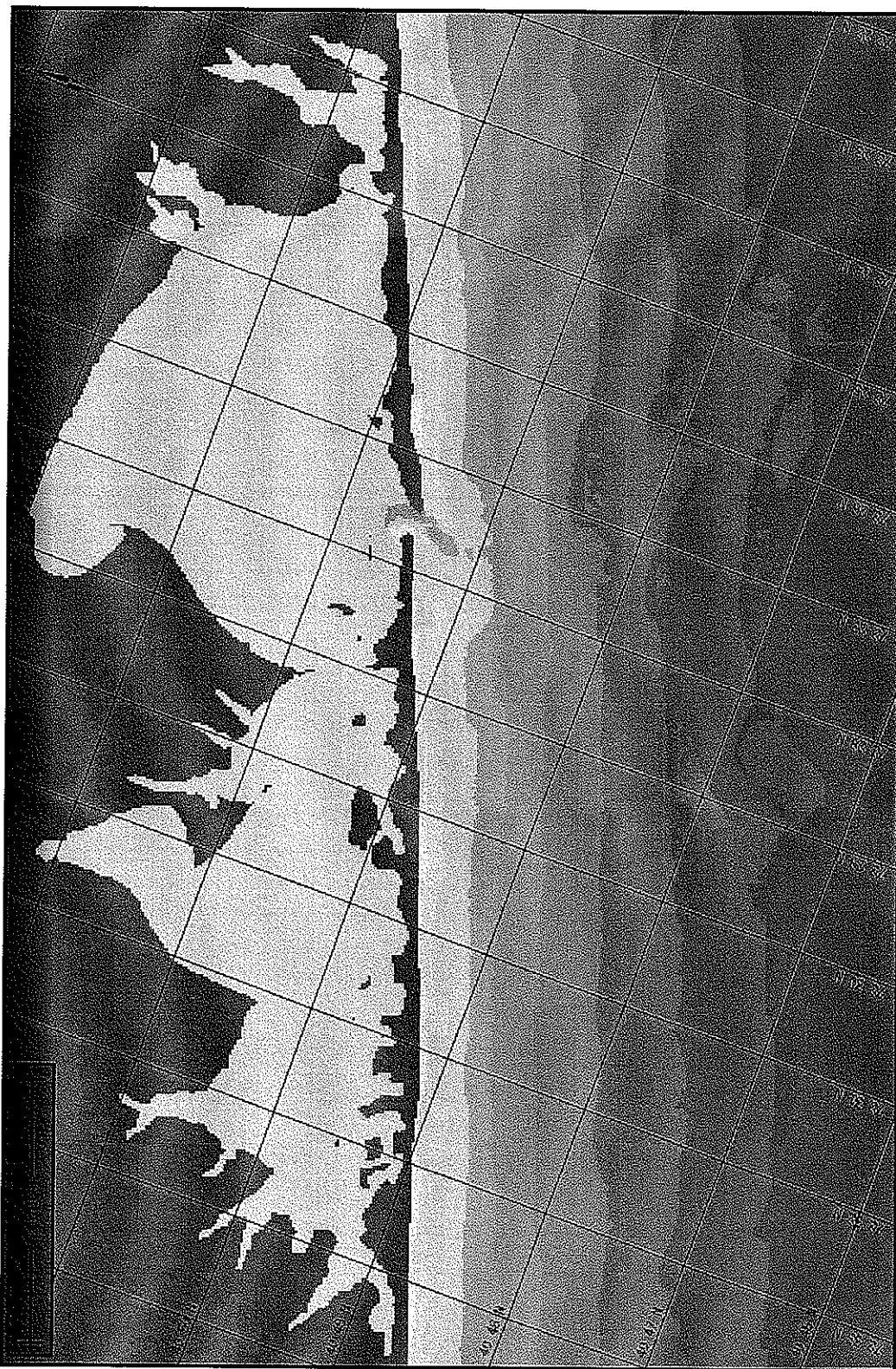
MOFFATT & NICHOL
ENGINEERS



Values



(ft)



5. MODEL CALIBRATION (EXISTING CONDITIONS)

5.1. General

The objective of the modeling effort is to determine the impact of barrier island breaches on tidal elevations, flushing rates, and salinity/temperature distributions within the bays. The problem requires the use of two models: 1) a hydrodynamic model, which computes the temporal and spatial distribution of water surface elevation and velocity; and 2) an advection-dispersion model, which computes the distributions of salinity and temperature. The hydrodynamic model considers the most important phenomena of the system, i.e., the rise and fall of the tide and variations in currents, before and after a breach. The currents from the hydrodynamic model are the driving force for the advective processes in the salinity/temperature model. The dispersive (diffusive) processes in the salinity/temperature model are computed from horizontal gradients and the dispersion coefficient. The dispersion coefficient is obtained during the model calibration process. The primary calibration parameters in the hydrodynamic model are the bottom frictional coefficient (Manning number) and the horizontal eddy viscosity.

As outlined below, there is sufficient elevation and current information available for determining boundary conditions and calibrating the hydrodynamic model. However, the available salinity and temperature data are of lower quality, consisting of single grab measurements at monthly (or longer) intervals. Furthermore, the freshwater input into the model, which includes surface and groundwater components, is difficult to quantify from existing records. Consequently, it was not possible to calibrate the dispersion coefficients in salinity and temperature to a high degree of accuracy. The approach taken was to establish boundary conditions and interior comparison points using average salinity and temperature values, and to adjust the dispersion coefficient to approximately match the average values. The impacts were then determined based on changes in these average values under different breach scenarios. This approach is reasonable for the purposes of this study, since changes in the salinity/temperature fields should be largely dependent on changes in the advective processes in the bays. Additional data sets which would

enable model comparisons to synoptic salinity data have been made available and will be incorporated into future modeling efforts.

Numerical models are typically calibrated with field measurements (e.g. measured tidal elevations, current velocities, salinities, water temperatures, etc.) in order to demonstrate that the model accurately reproduces the hydrodynamic system. The calibration process consists of adjusting model parameters so that model predictions match field observations as closely as possible. The model is considered properly calibrated when numerical results closely match field observations. Upon completion of satisfactory calibration, the model can be used to evaluate estuary hydrodynamics or the impacts of changes to the system (e.g. construction of training structures, island breaching or dredging).

Model calibration is best achieved by means of a set of simultaneous measurements along the model boundaries and throughout the modeled estuary. Data important to the present study include hydrodynamics, flow velocities (or discharge), temperature, and salinity. Wind effects, though important in many systems were ignored in the present study based on both (1) analyses by Pritchard (1981), who indicated wind-induced currents in Moriches Bay are an order of magnitude less than tidally-driven currents, and (2) previous modeling experience in the project area (Moffatt & Nichol, 1994).

5.2. Tidal Hydrodynamics

Since tidal elevation measurements were limited, MIKE 21 HD was calibrated for Great South, Moriches and Shinnecock Bays using predicted tidal elevation data based on NOAA tidal constituents. Discharge boundary conditions were also tested during model calibration at lateral boundaries of Great South Bay (South Oyster Bay at Biltmore Shores and Narrow Bay), Moriches Bay (Narrow Bay and Quantuck/Quogue Canals), and Shinnecock Bay (Quantuck/Quogue Canals) to determine the influence of various discharge conditions on model results. The selected discharge boundary conditions represent those parameters that best

reproduced tidal elevations within each estuary. Boundary condition locations for Great South, Moriches, and Shinnecock Bays are presented in Figures 5.1 to 5.3, respectively.

5.2.1. Model Parameters

The most dominant hydrodynamic model calibration parameters in MIKE 21 HD are eddy viscosity and bottom roughness (Manning's number), which affect lateral mixing and bottom friction in the hydrodynamic system, respectively. Different combinations of parameters were tested as part of the calibration process. Selected eddy viscosities and Manning's numbers correspond to those values that yield the best agreement between NOAA predicted and MIKE 21 HD simulated tides.

5.2.2. Calibration Results

Hydrodynamic model calibration for Great South, Moriches, and Shinnecock Bays was performed for and discussed in detail in **Interim Submission 9B: Inlet Dynamics - Without-Project Future Conditions** (USACE, 1999). The results of the hydrodynamic model calibration are summarized below.

The period selected for model calibration corresponds to the period used in **Interim Submission 9B: Inlet Dynamics - Without-Project Future Conditions** (USACE, 1999) for the hydrodynamic modeling, spanning 72 hours from 24 to 27 December 1989 and representing approximate mean tidal conditions for each estuary. Measured data for calibration at Great South, Moriches, and Shinnecock Bays were generally unavailable, and the use of available data was complicated by datum uncertainties (Note: measured data for Great South, Moriches, and Shinnecock Bays became available after calibration was completed and will be incorporated into future report revisions). Therefore, tidal boundary conditions were specified based on published NOAA tidal constituents. Great South and Shinnecock Bays were modeled with 30 second time steps and Moriches Bay required a 20 second time step for solution stability.

Great South Bay. Tidal flow enters Great South Bay through Fire Island Inlet, Narrow Bay and South Oyster Bay. The average modeled tide range at the Fire Island Breakwater for the calibration period was approximately 3.9 feet. This range is close to the mean tidal range of 4.1 feet (NOAA, 1996) at the Fire Island Breakwater. Manning's numbers were estimated for various water depths with higher friction values in shallow water and, conversely, lower values in deeper water. Model results were somewhat insensitive to changes in eddy viscosity. The MIKE 21 default eddy viscosity, $43 \text{ ft}^2/\text{s}$, was used throughout the mesh with ocean and inlet values modified to improve calibration results.

Moriches Bay. Moriches Bay tides are controlled by flows entering via Moriches Inlet, Narrow Bay, and Quogue Canal. Sensitivity analyses confirmed that Moriches Bay is relatively insensitive to a range of discharges at Quogue Canal. Therefore, the eastern boundary condition was represented by a no flow boundary condition. The average modeled tidal range at the inlet is approximately 3.2 feet, which closely matches the published (NOAA, 1996) mean tide range of 3.5 feet. Analyses also revealed that variations in Manning's numbers and eddy viscosities had minor impacts on calibration results for Moriches Bay. Accordingly, the model-default bottom friction, i.e. Manning's number, and eddy viscosity coefficients were used throughout the mesh with the coefficients in the bay refined to improve results during calibration.

Shinnecock Bay. The offshore (Ocean) and Quogue Canal boundary conditions in the Shinnecock Bay mesh were comprised of a time series of tidal elevations, whereas a zero flow boundary conditions was applied at the Shinnecock Canal. The average modeled tidal range at the inlet is approximately 2.6 feet, which is slightly lower than the 2.9-ft mean tide range published by NOAA (1996) for Shinnecock Inlet. Model calibration parameters used for Shinnecock Bay are similar to those used for Moriches Bay. MIKE 21 HD default values were used throughout the mesh with modified eddy viscosity in the bay to improve the calibration results. Selected values are similar to results determined in USACE (1998). Model results compare well with predicted tidal elevations and amplitudes. Correlation between predicted and modeled tide elevations is 99 to 100% with a standard error of less than one inch.

5.3. Advection/Dispersion

The MIKE 21 AD advection/dispersion model was calibrated in a manner similar to the hydrodynamic model. Model parameters were adjusted until the modeled water quality distributions throughout the estuarial system reproduced average measured values.

5.3.1. Model Parameters

In the case of the advection/dispersion model, the dispersion coefficients in the X and Y directions were adjusted to calibrate the model. Selection of the dispersion coefficients was based on comparing average measured and average modeled concentrations at locations throughout the bays and adjusting the dispersion coefficient accordingly to improve agreement between the two sets of concentrations. Calibrated dispersion coefficients are presented in Table 5.1.

Location	TABLE 5.1 DISPERSION COEFFICIENTS	
	X (ft ² /sec)	Y (ft ² /sec)
Great South Bay	540	540
Moriches Bay	129	129
Shinnecock Bay	183	183

For model stability reasons, the following upper limit, derived from the stability criteria for a pure diffusive case, was placed on the dispersion coefficients:

$$(D_x / \Delta x^2 + D_y / \Delta y^2) \cdot dt < 0.5$$

where:

D_x = Diffusion in X direction (m²/s)

D_y = Diffusion in Y direction (m²/s)

Δx = Grid spacing in X direction (m)

Δy = Grid spacing in Y direction (m)

dt = time step (s)

As is demonstrated in the above equation, stability of the advection/dispersion model is dependent on the time step used. To improve stability, time steps were reduced to 10 seconds for each model.

5.3.2. Salinity Boundary Conditions

Salinity, i.e. advection/dispersion, boundary conditions must be specified at the same locations as the hydrodynamic model boundary conditions. The Department of Health Services 1977 to 1997 salinity data were used to calibrate the advection/dispersion model. Because each set of data for each date in the record was collected over several hours, the data shows the effect of the tide changing phase. To reduce the effects of tidal phase and seasonal changes, the salinity data was averaged and this average salinity was used to calibrate the model. Additionally, the salinity data were filtered to remove incomplete data sets thereby avoiding biasing the data.

Great South Bay. Average salinities in Great South Bay range from 24.3 ppt in Bellport Bay to 30.9 ppt at the inlet. Average values at each measurement station are listed in Tables 2.3 and 2.4.

Model boundary conditions were determined from measurement stations at locations corresponding to the boundary locations. The offshore boundary was set to the local ocean salinity of 33 ppt. The eastern boundary, corresponding to station 100 (see Figure 2.8) in Narrow Bay equals 25.5 ppt and the western boundary was set to a range of values varying from 30.6 ppt near station 260 in the south to 29.6 ppt at station 270 near Biltmore.

Fresh water was introduced into Great South Bay at the rivers and creeks corresponding to the monitoring data collected by USGS. No additional fresh water data was available. Additional

effects of fresh water inflow into Great South Bay were incorporated into lateral boundary conditions. Salinity at the modeled sources was set to zero.

Moriches Bay. Average salinity in Moriches Bay ranged from 26.5 ppt at station 110 (see Figure 2.9) near the Forge River to 31.0 ppt at station 140 near Moriches Inlet. Average values at each measurement station are listed in Table 2.5.

Salinity at the ocean boundary was set to 33 ppt (local ocean salinity). At the eastern and western boundaries, salinity was derived from corresponding measurement stations as 27.4 ppt (corresponding to station 200), and 27.0 ppt (corresponding to station 100), respectively.

Freshwater source data was unavailable for sources in Moriches Bay and was not included in this study. Modeled salinity in Moriches Bay was controlled via salinity at the lateral boundaries of the modeled region.

Shinnecock Bay. Shinnecock Bay average salinity ranged from 27.9 ppt at station 100 (see Figure 2.10) near Shinnecock Canal to 31.1 ppt at station 140 near Shinnecock Inlet. Average values at each measurement station are listed in Table 2.6.

Salinity boundary conditions were set to 33 ppt at the ocean boundary (local ocean salinity) and 28.0 ppt at the western boundary (Quogue Canal near station 190).

As was the case for Moriches Bay, freshwater source data was unavailable for sources in Shinnecock Bay and was not included in this study. Modeled salinity in Shinnecock Bay was dependent upon salinity at the lateral boundaries.

5.3.3. Salinity Calibration Results

Advection/dispersion model calibration results are shown for each measurement station (shown in Figures 2.8 to 2.10) and compare measured values to modeled values. Modeled salinity values

were averaged over the final 5 tidal cycles (~62 hours) of the simulation and were compared to average measured values. The standard deviation of the measured salinity, shown in Tables 2.3 to 2.6, is plotted with the average values, providing a range of potential results.

Great South Bay. Advection/Dispersion modeling shows that salinity in Great South Bay is influenced by freshwater inflow from the streams and rivers feeding the bay. Calibration results shown in Figure 5.4 indicate that average modeled values compare well with average measured values. The calibration results show that modeled salinity at measurement stations 160, 190, and 240 is higher than measured values due to undervalued fresh water inflow in these areas. Modeled salinity at stations 170, 180, 200, and 230 was also higher than expected due to excessive ocean water entering the bay through the inlet.

Modeled values typically fall within one standard deviation of the measured values. The standard error of the values equals 0.96 ppt. Figures 5.5 and 5.6 show salinity at peak ebb and flood tides respectively.

Moriches Bay. Comparisons between the average simulated and average measured salinity, shown in Figure 5.7 for various locations throughout Moriches Bay, show generally good agreement for the entire bay system. It is noted, however, that the simulated salinity at station 110 was significantly higher (2.4 ppt) than measured values, possibly due to unaccounted for freshwater inflow from the Forge River. Predicted salinity was slightly higher than measured salinity for many of the remaining stations (120, 130, 140, 150, 160, and 170) indicating that additional, unaccounted for fresh water is entering the bay, possibly through groundwater seepage and additional surface sources. Differences between modeled and measured salinity were as much as 2.4 ppt with a standard error of 0.7 ppt. Peak ebb and flood tide salinity contours are shown in Figures 5.8 and 5.9, respectively.

Shinnecock Bay. Average modeled salinity in Shinnecock Bay compared well with average measured values as shown in Figure 5.10. It is noted, however, that the simulated salinity was higher than measured salinity at stations in the eastern basin of Shinnecock Bay (stations 100, 120, 130, and 150) as well as at the inlet (station 140) due to influences from Shinnecock Canal

which was not modeled in this study. Predicted salinity was less than measured salinity in the western basin of Shinnecock Bay (stations 160, 170, 180, and 190) indicating that insufficient ocean water is mixing with the bay water in the western basin. This can also be attributed to changes in flow patterns at and near the inlet due to the absence of Shinnecock Canal in the model. Peak differences between measured and modeled values were as high as 1.3 ppt with a standard error of 0.8 ppt. Figures 5.11 and 5.12 show salinity in Shinnecock Bay at peak ebb and peak flood, respectively.

5.3.4. Temperature Boundary Conditions

Temperature data boundary conditions must be specified at the same mesh boundaries used in the hydrodynamic model. As previously mentioned, temperature data are available at various locations in each bay for a period extending from 1977 through 1997. As with the salinity data, the temperature data shows the effect of the tide changing phase and was averaged to reduce the effects of tidal phase and seasonal changes. Additionally, the temperature data were filtered to remove incomplete data sets, thereby avoiding biasing the data.

Great South Bay. Average temperatures in Great South Bay range from 15.1 °C at the inlet to 16.5 °C near Babylon and Bellport. Model boundary conditions were determined from measurement stations at locations corresponding to the boundary locations. The offshore boundary was set to the local ocean temperature of 14.0 °C. The eastern boundary of the model at Narrow Bay equals 15.6 °C which corresponds to station 100 and the western boundary was set to a range of values varying from 16.0 °C near station 260 in the south to 16.3 °C at station 270 near Biltmore.

Fresh water sources into Great South Bay were also calibrated to produce the correct temperature at the corresponding measurement stations. Temperatures at the modeled sources were set to values corresponding to the location of the source in the model. The freshwater sources and their respective temperatures at the model boundary are listed in Table 5.2.

TABLE 5.2
GREAT SOUTH BAY SOURCE TEMPERATURE

Source	Temperature °C
Carlls River	16.5
Carmans River	15.8
Champlin Creek	16.5
Connetquot River	16.3
Massapequa	16.2
Patchogue River	15.7
Penataquit Creek	16.3
Sampawams	16.5
Santapogue	16.5
Swan River	15.7

Moriches Bay. Average temperatures measured in Moriches Bay ranged from 13.2 °C at station 110 near the Forge River to 11.6 °C at station 140 at Moriches Inlet. Temperature boundary conditions values were set in a manner similar to the salinity boundary conditions where the boundary values were extracted from measurement stations in close proximity to the model boundaries. Temperature at the ocean boundary was set to 11.0 °C, at the eastern boundary corresponding to station 200 in Quantuck Bay temperature was set to 13.3 °C, and at the western boundary corresponding to station 100 in Narrow Bay temperature was set to 13.1 °C.

Shinnecock Bay. Average temperatures measured in Shinnecock Bay ranged between 12.6 °C at station 190 near Quogue Canal to 11.3 °C at station 140 near Shinnecock Inlet. The temperature at the model boundary was set to 11 °C in the ocean and 12.6 °C at the western boundary.

5.3.5. Temperature Calibration Results

Advection/dispersion model calibration results are shown for each measurement station (shown in Figures 2.8 to 2.10) and compare measured values to modeled values. As was the case with salinity, modeled temperature values were averaged over the final 5 tidal cycles (~62 hours) of the simulation and were compared to average measured values. The standard deviation of the measured temperature, shown in Tables 2.7 to 2.9, is plotted with the average values, providing a range of potential differences in model results.

Great South Bay. Temperature calibration results shown in Figure 5.13 indicate that modeled temperatures compare well with measured temperatures. Modeled values fall within one standard deviation of the measured values. Modeled temperature at stations 170, 180, 200, and 230 was lower than expected due to excessive ocean water entering the bay through the inlet. Temperature distributions at peak ebb and peak flood are shown in Figures 5.14 and 5.15, respectively.

Moriches Bay. Moriches Bay calibration results for temperature are shown in Figure 5.16. Modeled and measured temperature comparisons at measurement locations throughout Moriches Bay show excellent agreement for the entire bay system. Differences between measured and modeled temperatures were less than 0.4 °C with a standard error of 0.2 °C for all of the measurement stations. Figures 5.17 and 5.18 show temperature distributions in Moriches Bay at peak ebb and peak flood tides, respectively.

Shinnecock Bay. Temperature calibration results for Shinnecock Bay, shown in Figure 5.19, indicate excellent agreement between measured and modeled values throughout the entire bay system. Computed differences in calibration results were less than 0.2 °C at each station with a standard error of 0.15 °C for all of the stations. Temperature calibration for Shinnecock Bay appears to be unaffected by the absence of Shinnecock Canal. Temperature distributions in Shinnecock Bay are shown in Figure 5.20 and 5.21 for peak ebb and peak flood tides, respectively.

5.3.6. Residence Time

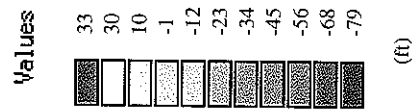
The method used to compute residence times is based on the method described in Section 3.4. Note that particles leaving a bay via lateral boundaries are considered to have left the system and their residence time is determined as the time to reach these boundaries. Calibrated diffusion coefficients from salinity and temperature modeling were kept constant. The model was run for 440 hours for Great South Bay and 315 hours for Moriches and Shinnecock Bays to allow the constituents to reach equilibrium.

Great South Bay. Tracer concentration decay curves are shown in Figure 5.22 for locations corresponding to measurement stations 150, 230, and 250. The curves show that the tracer concentration, while tidally varying, has reached a dynamic equilibrium. Figure 5.23 shows the time averaged residence time throughout Great South Bay. Peak residence times occur in the eastern basin of Great South Bay with times longer than 20 days.

Moriches Bay. Representative decay curves of tracer concentration within the eastern basin (180), the western basin (120) and the inlet entrance (140) are shown in Figure 5.24. The figure shows that all three curves reach steady-state tracer concentrations although considerable oscillations of tracer concentration occur close to the inlet entrance area. The contours of residence time for the entire bay are presented in Figure 5.25. The predicted residence times reach 3 to 5 days within the western basin. Maximum residence times greater than 10 days occur within the eastern basin. That the residence times within the eastern basin are high relative to the western basin is consistent with the relatively low flow exchange between Moriches and Shinnecock bay at the eastern boundary of the computational mesh.

Shinnecock Bay. Tracer concentration decay curves are shown in Figure 5.26 for locations corresponding to measurement stations 120 in the eastern basin, 140 near the inlet, and 180 in the western basin. Residence time contours for Shinnecock Bay are shown in Figure 5.27. Residence times in the eastern basin and western basin are on the order of 3 to 7 days.

Biltmore Shores Boundary



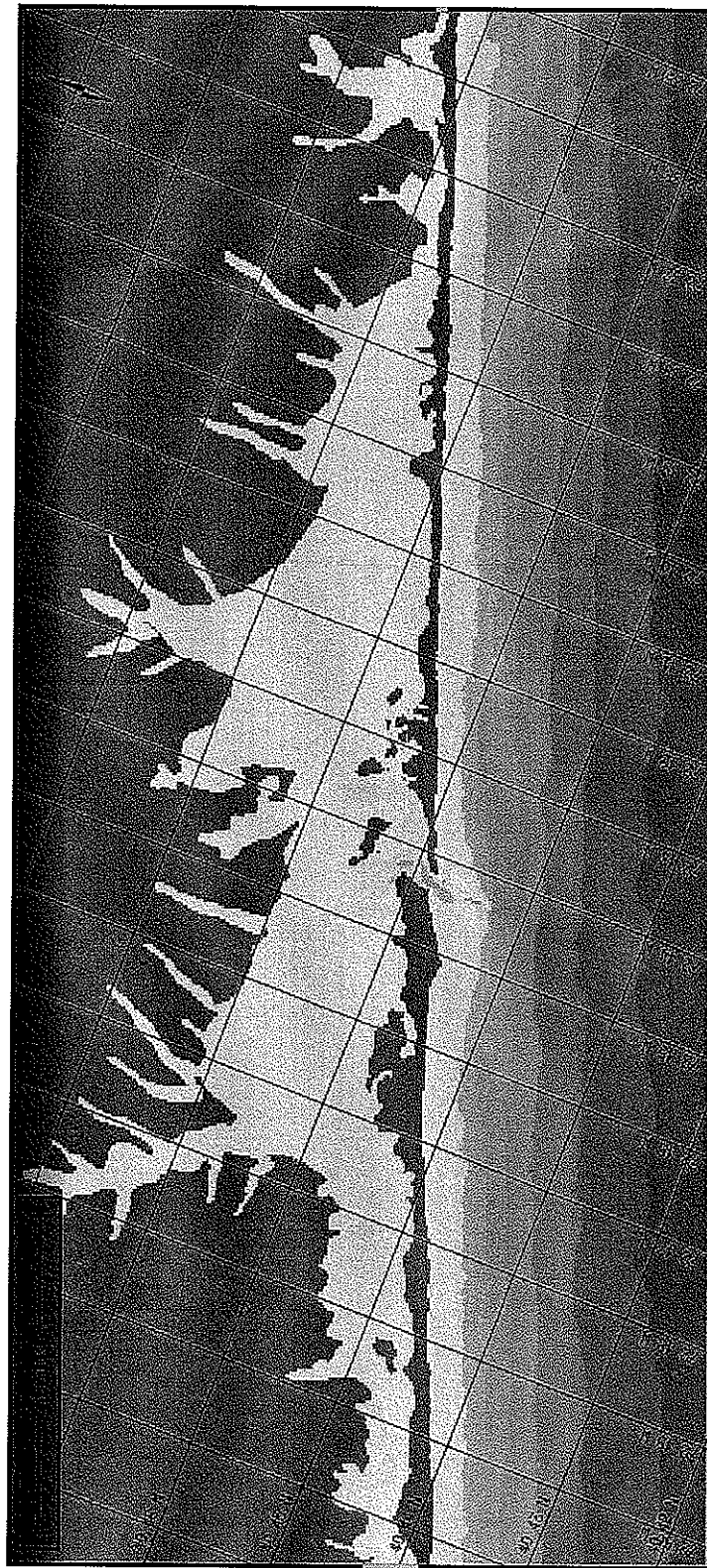
Ocean Boundary

Narrow Bay Boundary



FIRE ISLAND TO MONTAUK POINT
INLETS STUDY

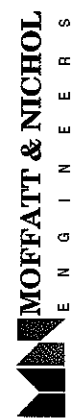
FIGURE 5.1
GREAT SOUTH BAY
INPUT BOUNDARIES



Narrow Bay Boundary

Ocean Boundary

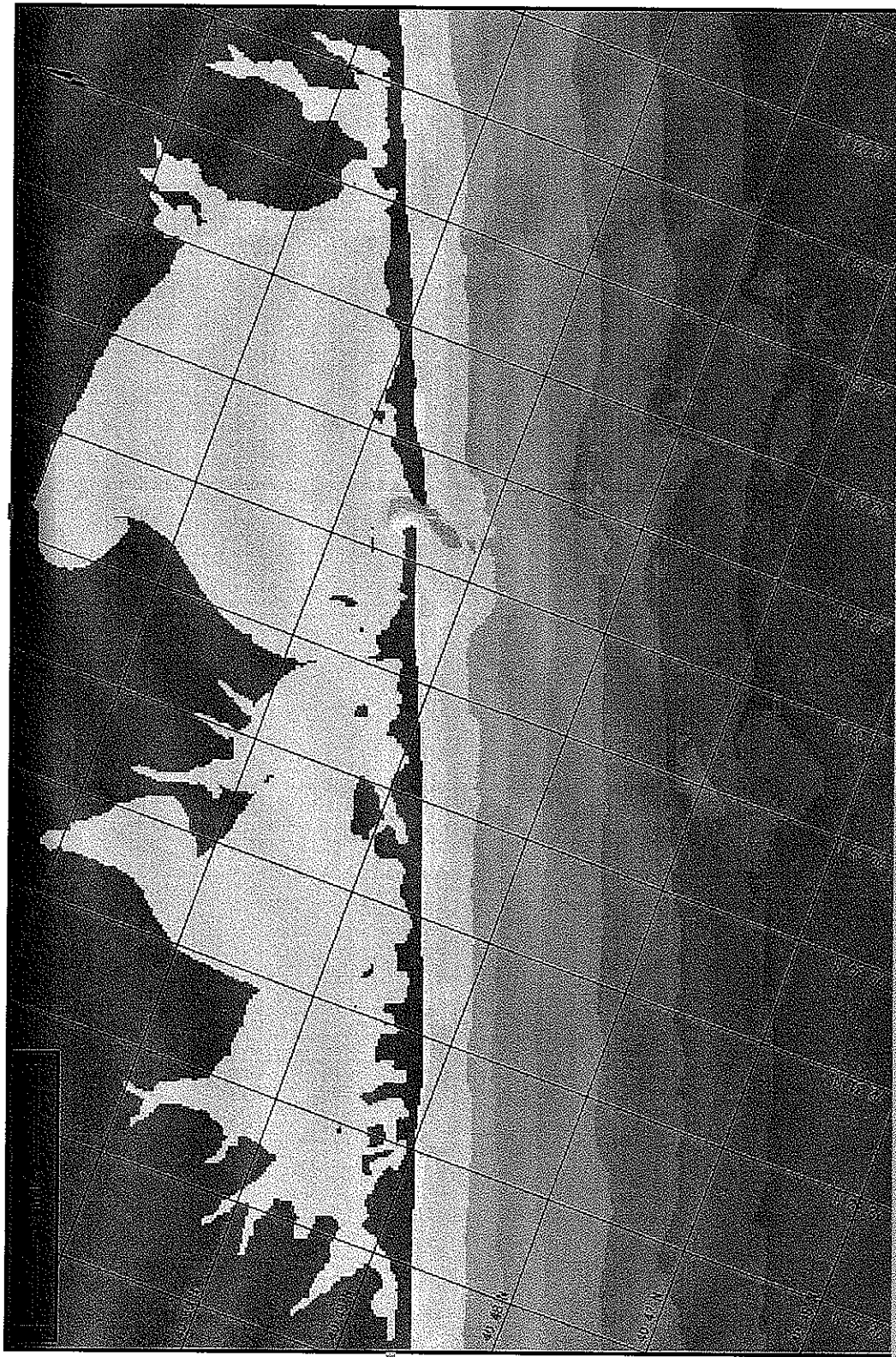
Quantuck Canal



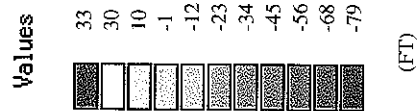
FIRE ISLAND TO MONTAUK POINT
INLETS STUDY

FIGURE 5.2
MORICHES BAY
INPUT BOUNDARIES

Shinnecock Canal



Ocean Boundary



Quantuck Canal

FIGURE 5.3
SHINNECOCK BAY
INPUT BOUNDARIES

FIRE ISLAND TO MONTAUK POINT
INLETS STUDY

MOFFATT & NICHOL
ENGINEERS

Great South Bay Modeled Salinity Calibration Average Measured vs. Average Modeled

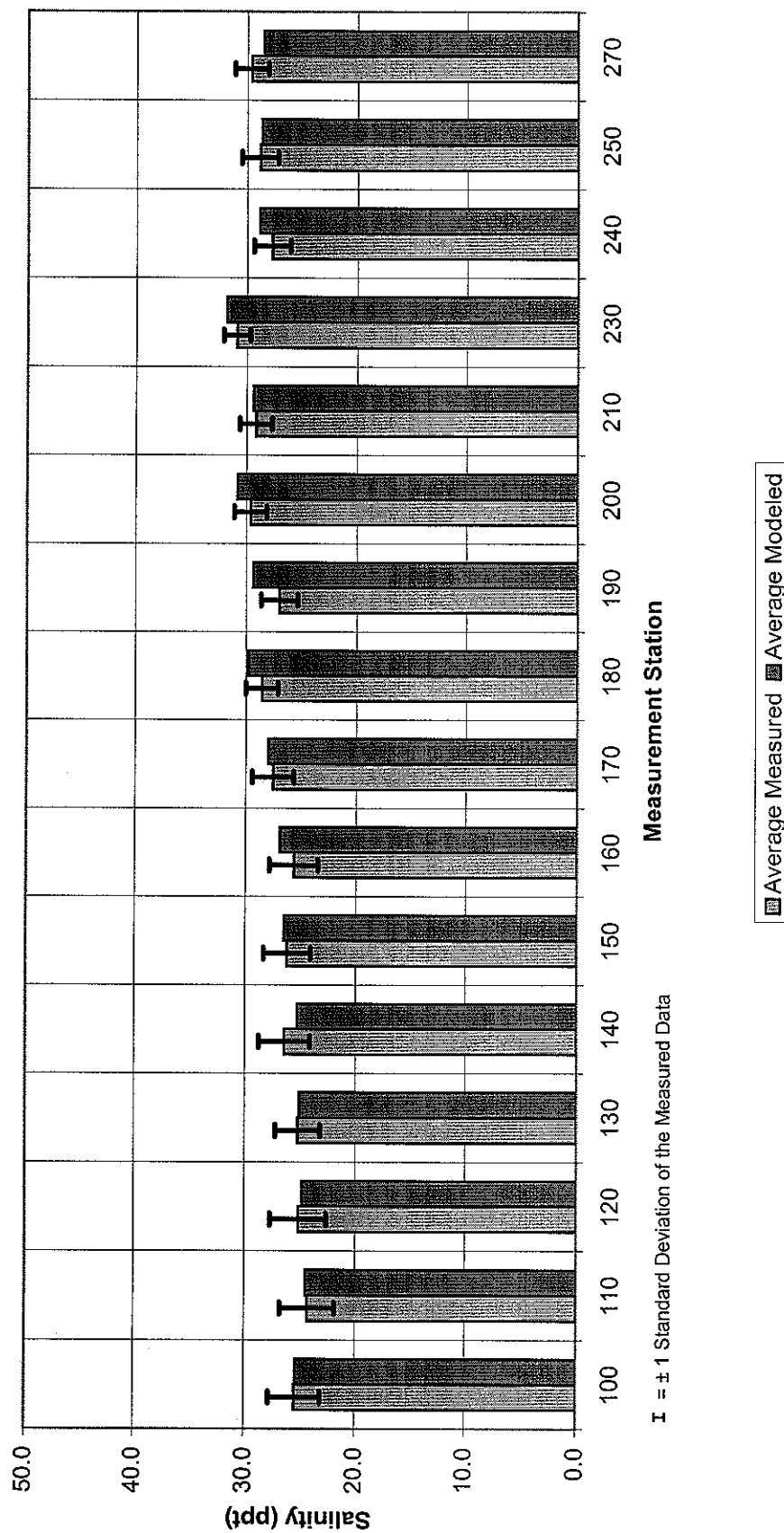


FIGURE 5.4

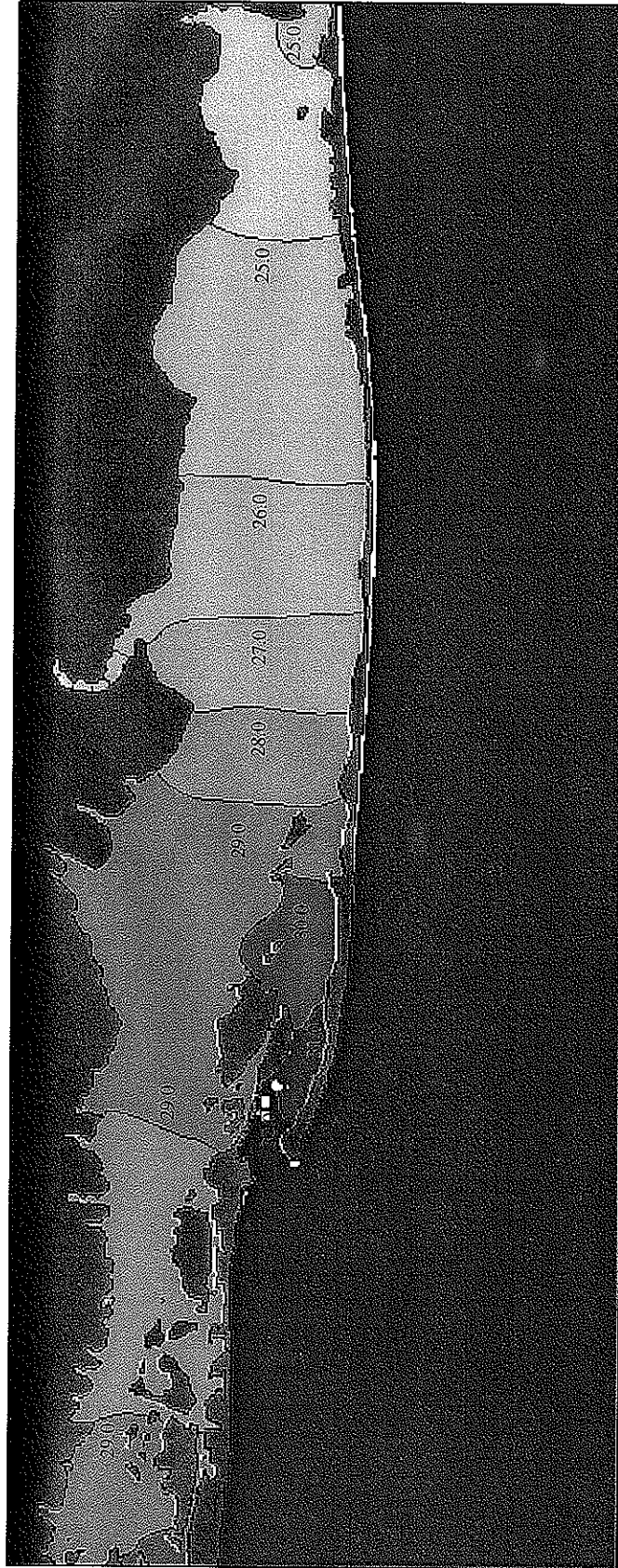
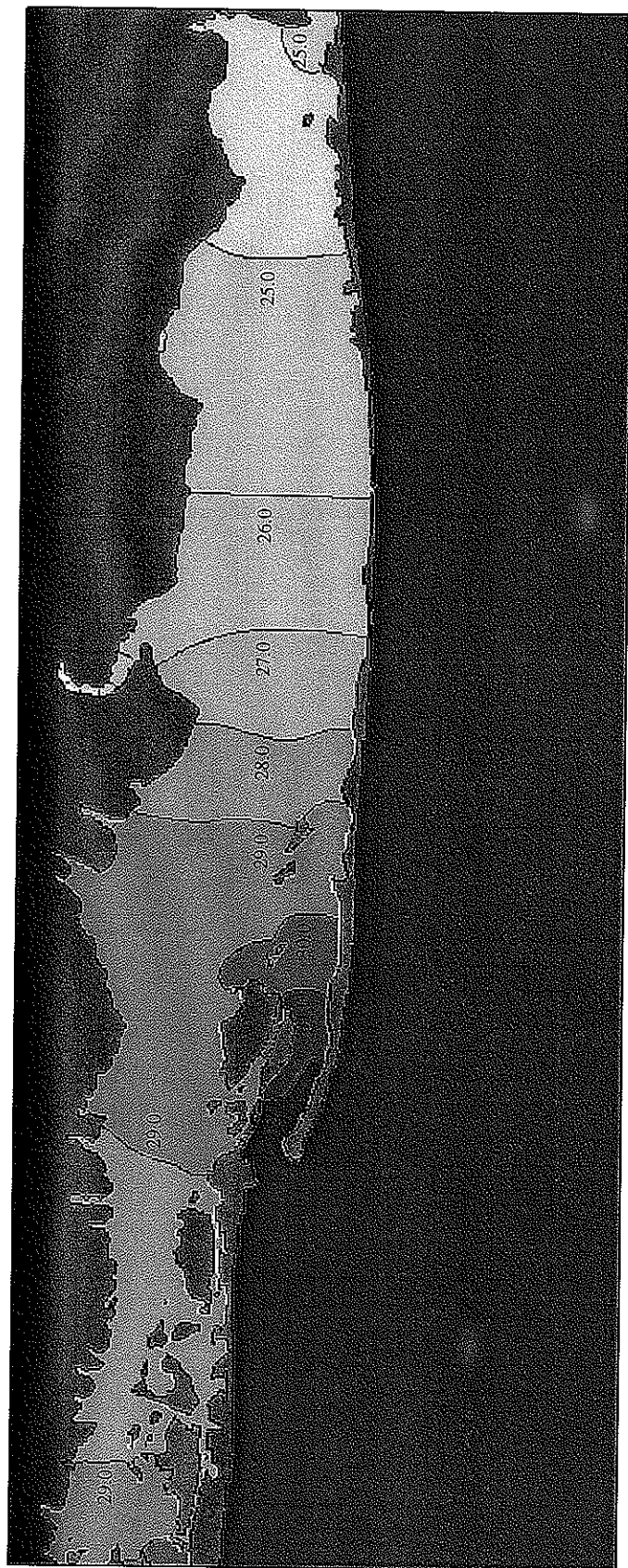


FIGURE 5.5
GREAT SOUTH BAY
EXISTING CONDITIONS
PEAK EBB SALINITY (PPT)

FIRE ISLAND TO MONTAUK POINT
INLETS STUDY

MOFFATT & NICHOL
ENGINEERS



Moriches Bay Modeled Salinity Calibration **Average Measured vs. Average Modeled**

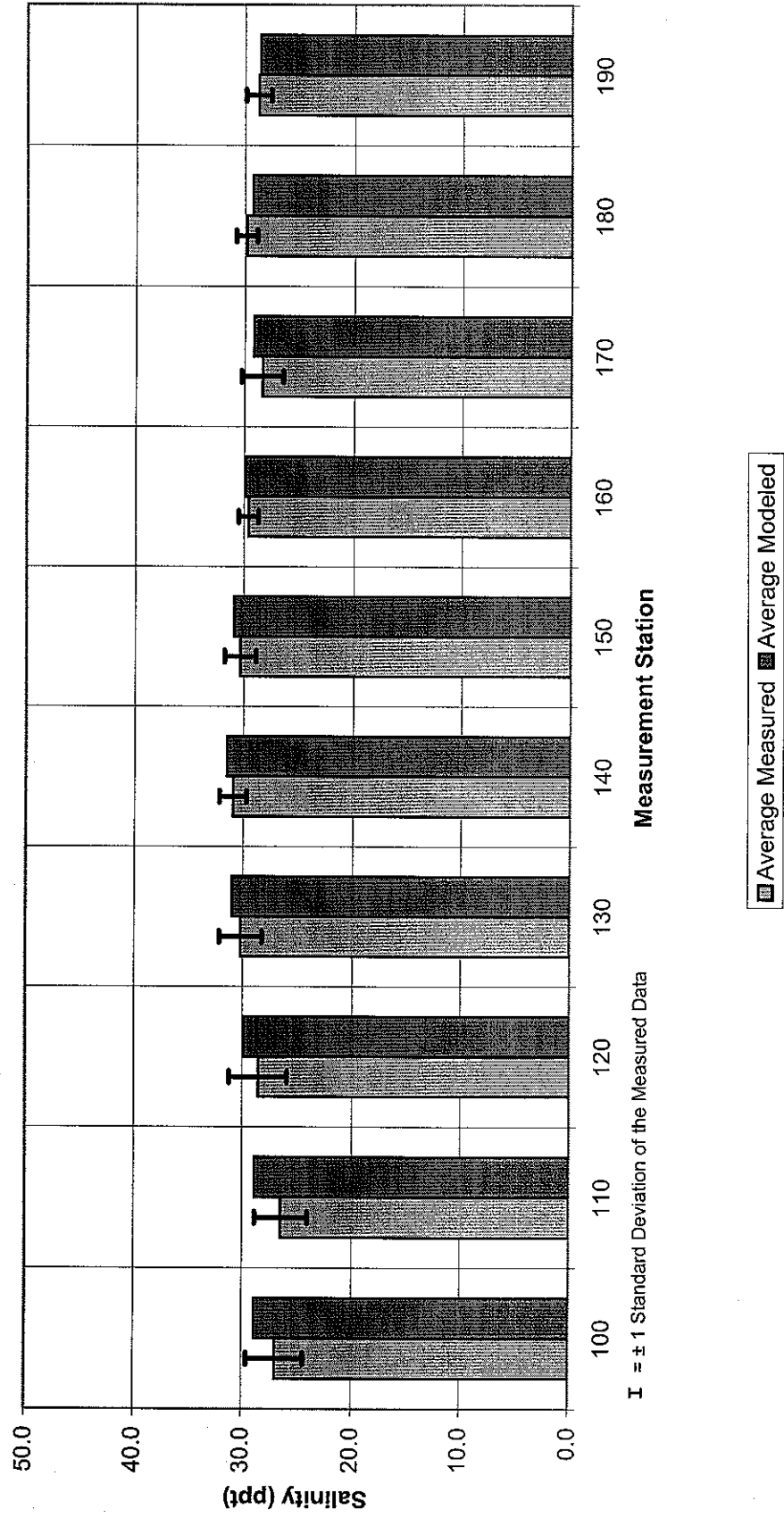


FIGURE 5.7

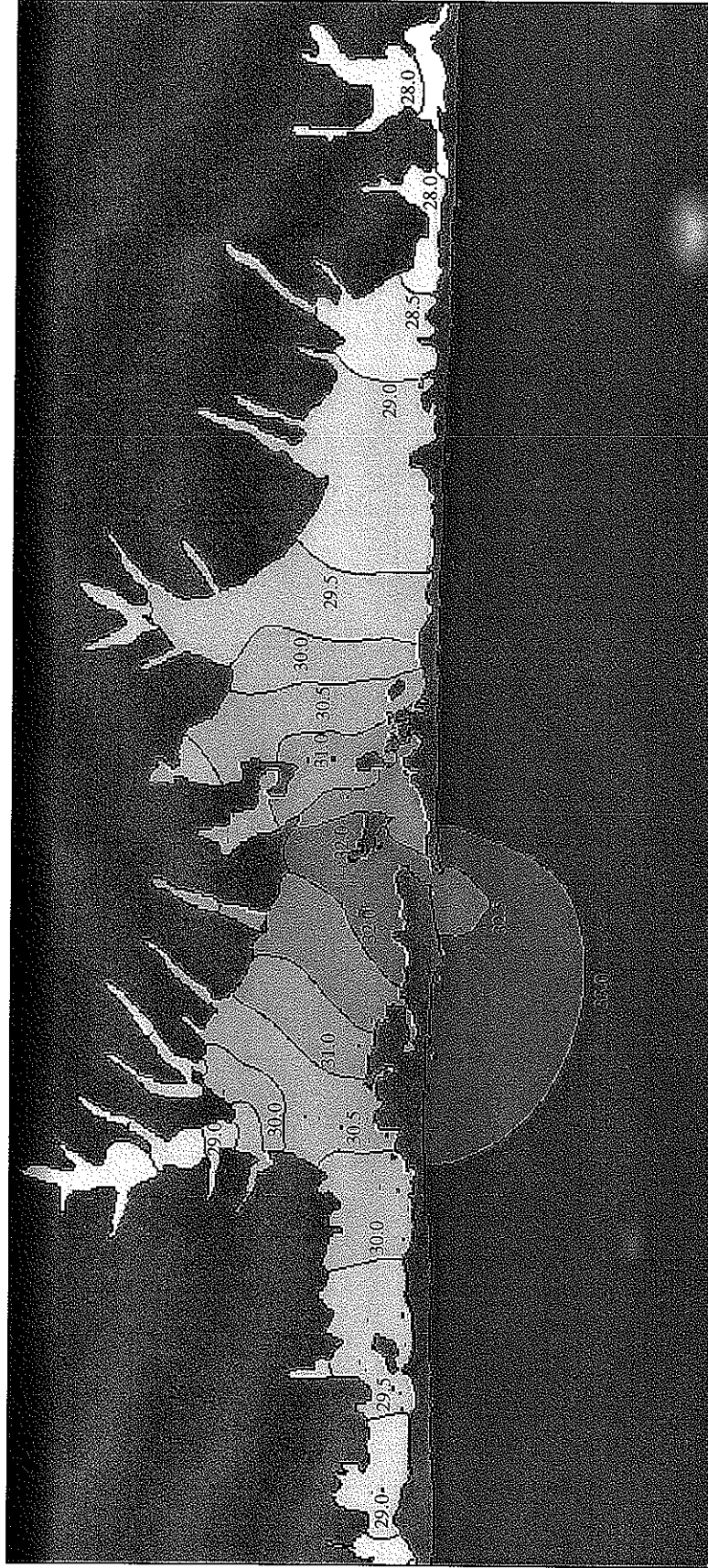


FIGURE 5.8
MORICHES BAY
EXISTING CONDITIONS
PEAK EBB SALINITY (PPT)

FIRE ISLAND TO MONTAUK POINT
INLETS STUDY

MOFFATT & NICHOL
ENGINEERS

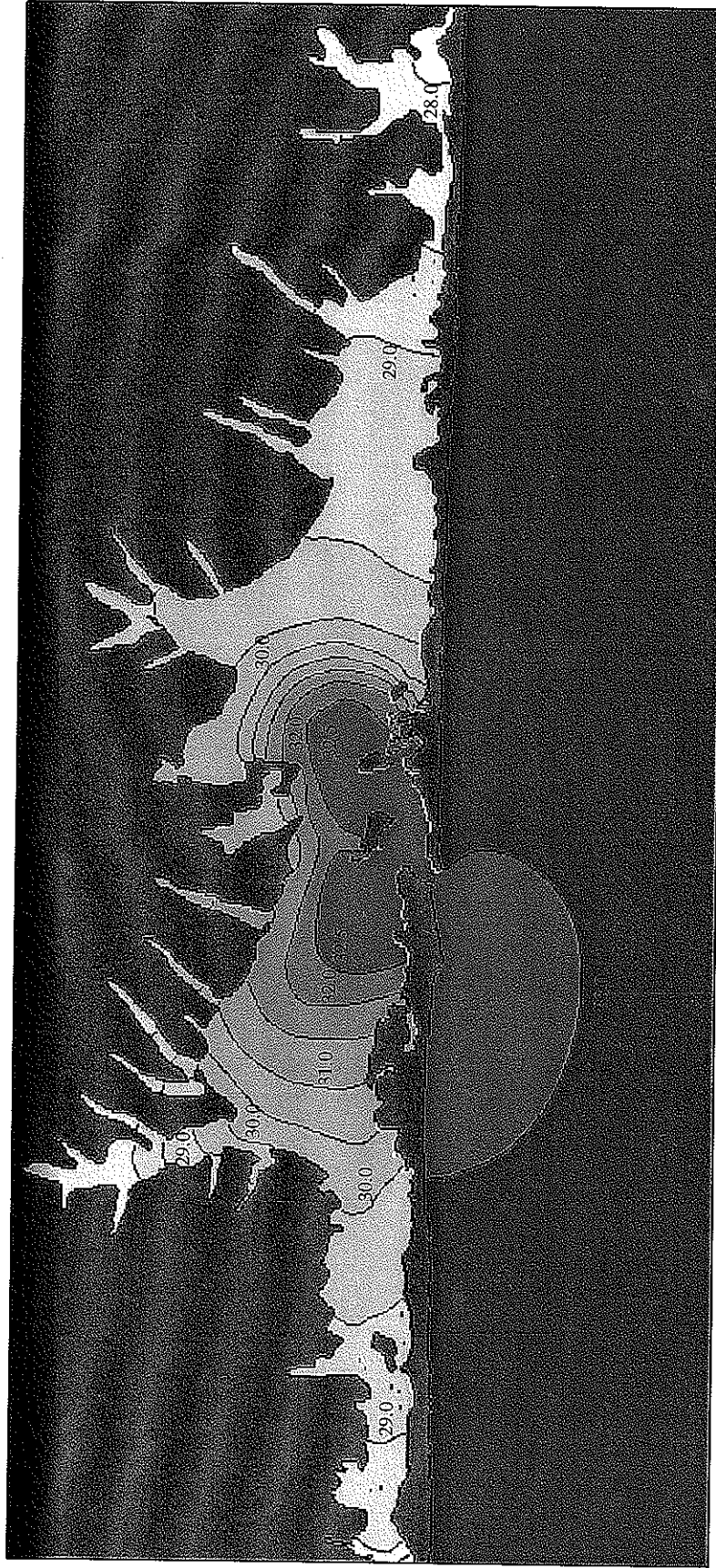


FIGURE 5.9
MORICHES BAY
EXISTING CONDITIONS
PEAK FLOOD SALINITY (PPT)

FIRE ISLAND TO MONTAUK POINT
INLETS STUDY

MOFFATT & NICHOL
ENGINEERS

Shinnecock Bay Modeled Salinity Calibration Average Measured vs. Average Modeled

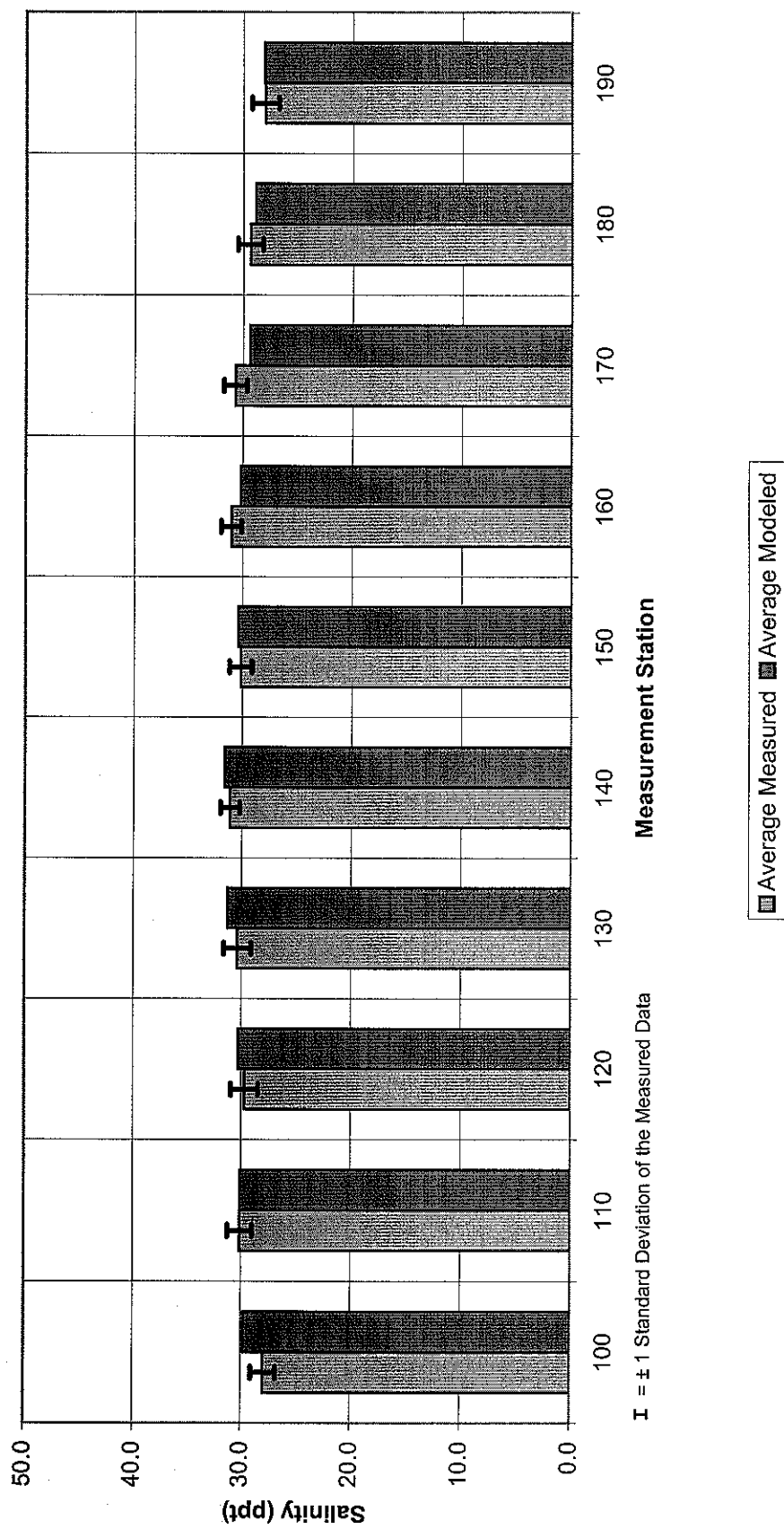


FIGURE 5.10

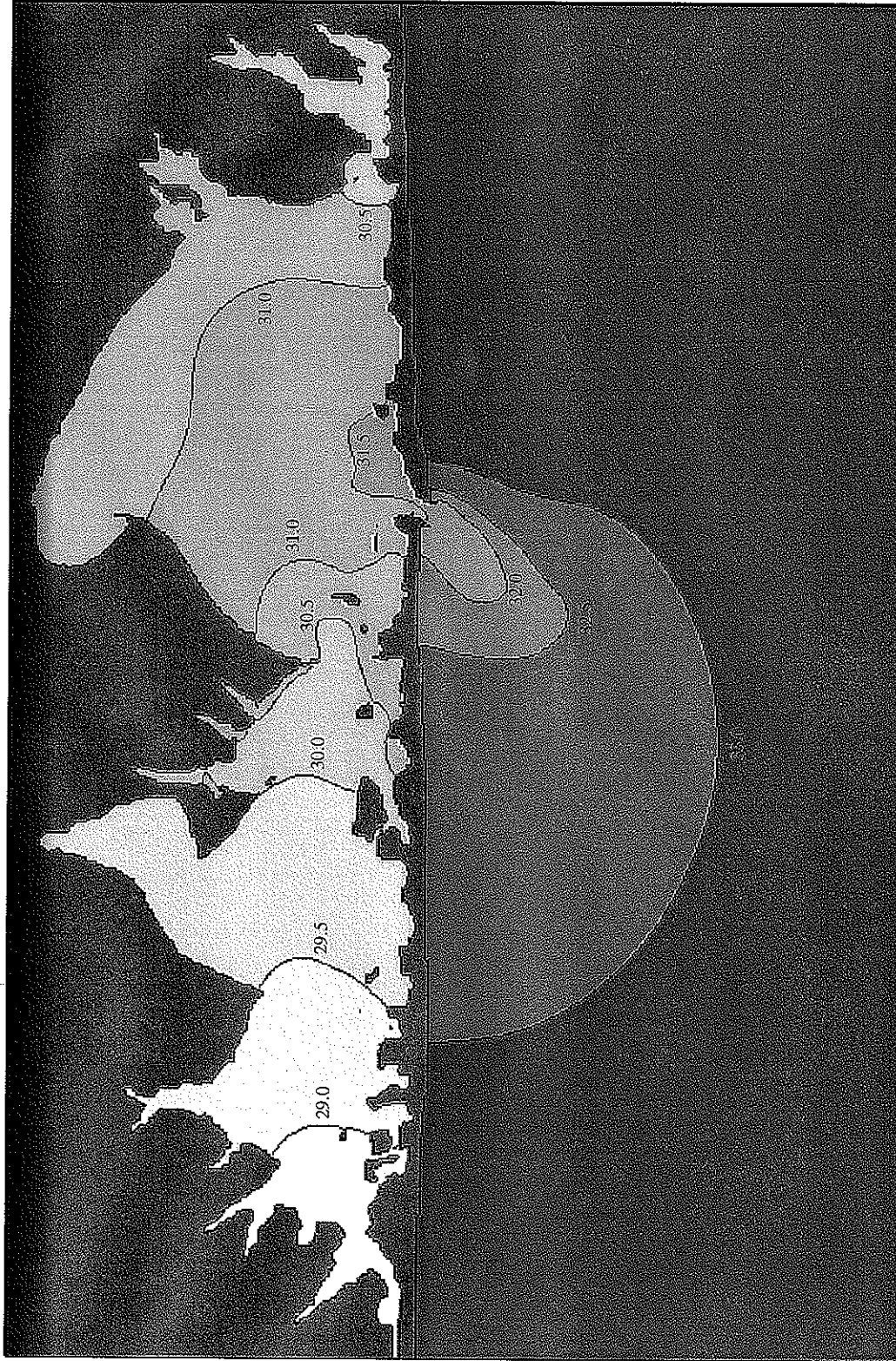
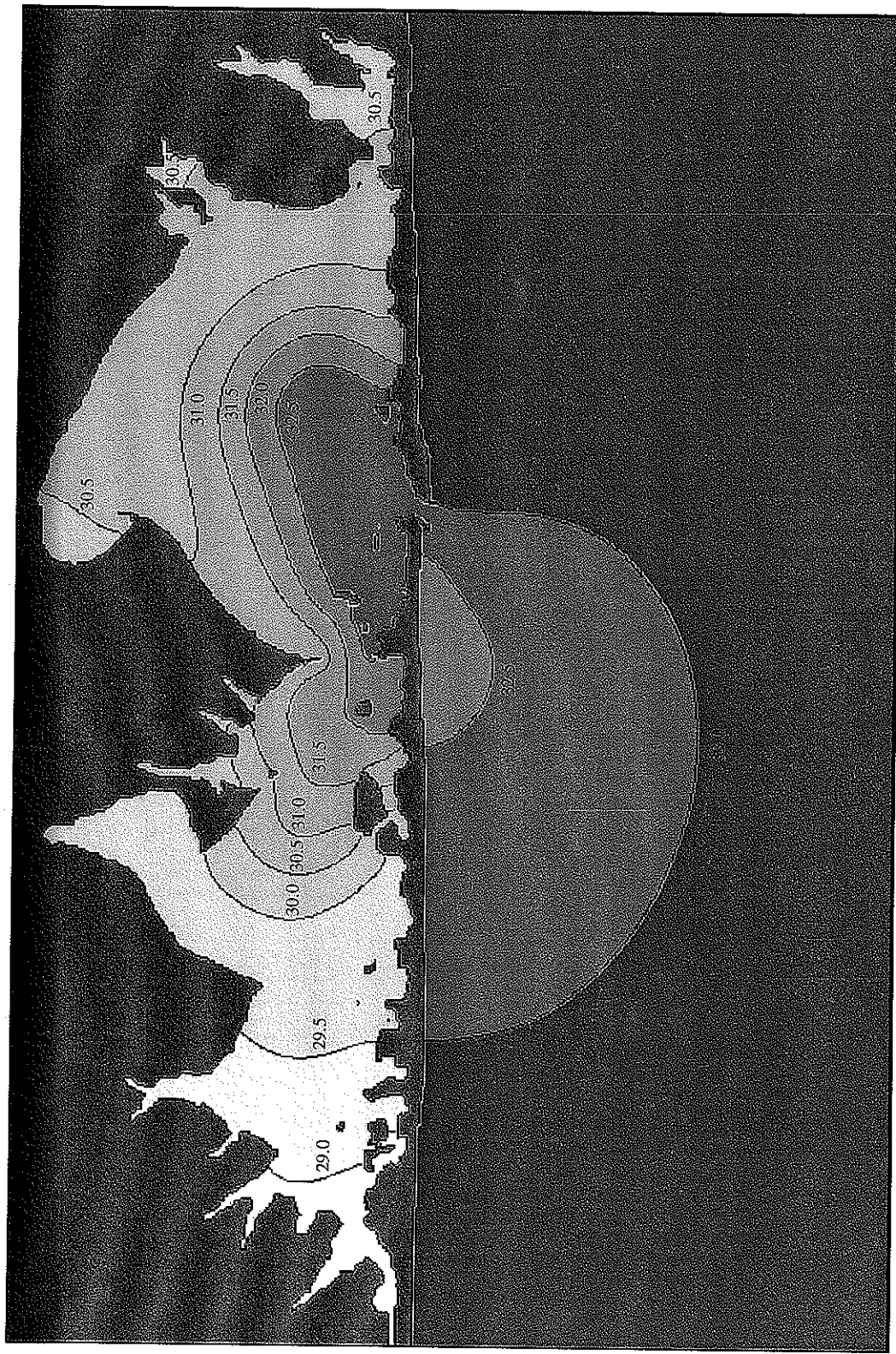


FIGURE 5.11
SHINNECOCK BAY
EXISTING CONDITIONS
PEAK EBB SALINITY (PPT)

FIRE ISLAND TO MONTAUK POINT
INLETS STUDY



Great South Bay Modeled Temperature Calibration Average Measured vs. Average Modeled

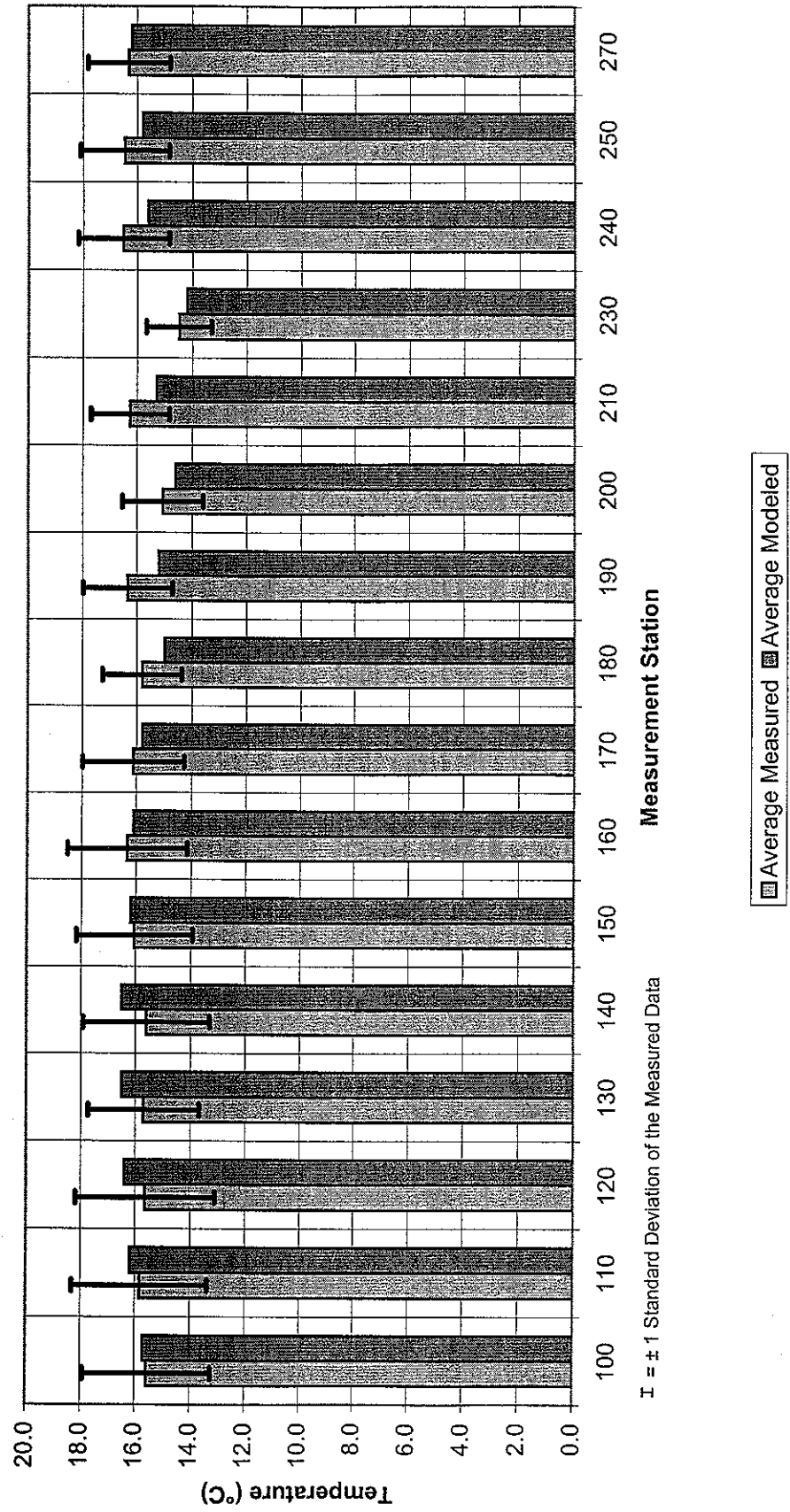


FIGURE 5.13

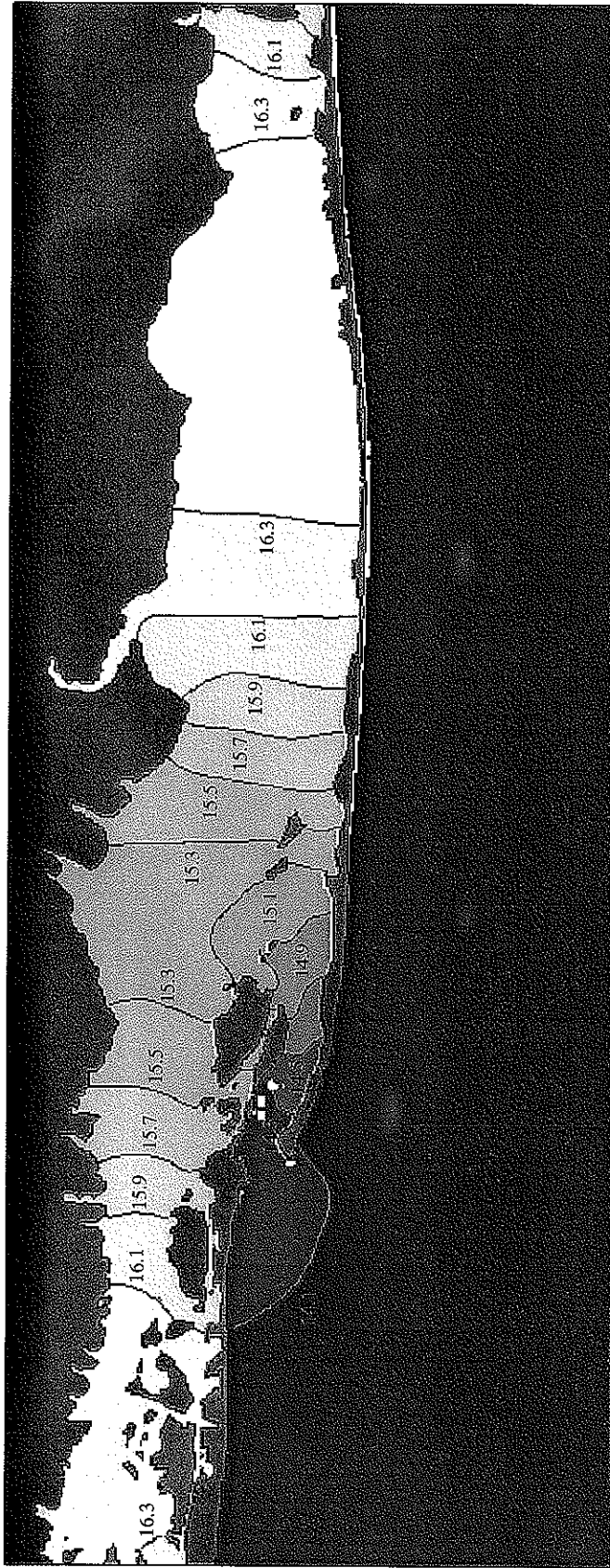


FIGURE 5.14
GREAT SOUTH BAY
EXISTING CONDITIONS
PEAK EBB TEMPERATURE (°C)

FIRE ISLAND TO MONTAUK POINT
INLETS STUDY

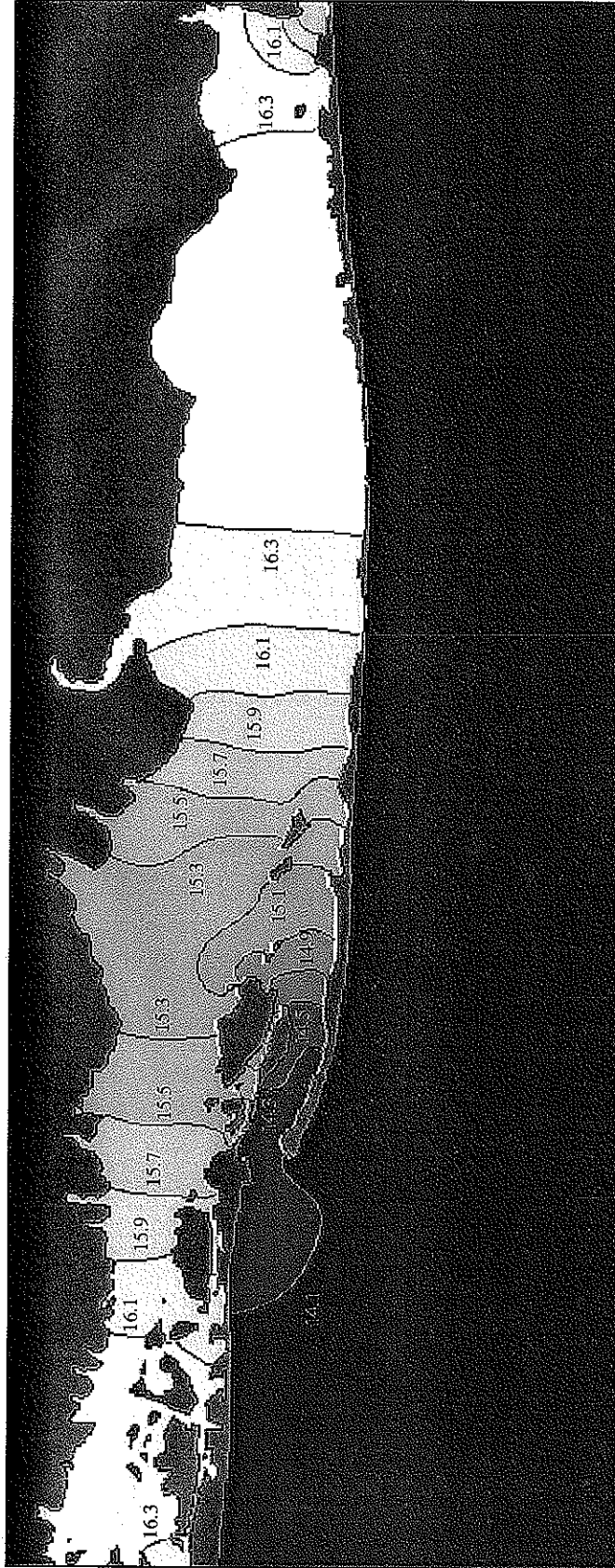


FIGURE 5.15
GREAT SOUTH BAY
EXISTING CONDITIONS
PEAK FLOOD TEMPERATURE (°C)

FIRE ISLAND TO MONTAUK POINT
INLETS STUDY

MOFFATT & NICHOL
ENGINEERS

Moriches Bay Modeled Temperature Calibration **Average Measured vs. Average Modeled**

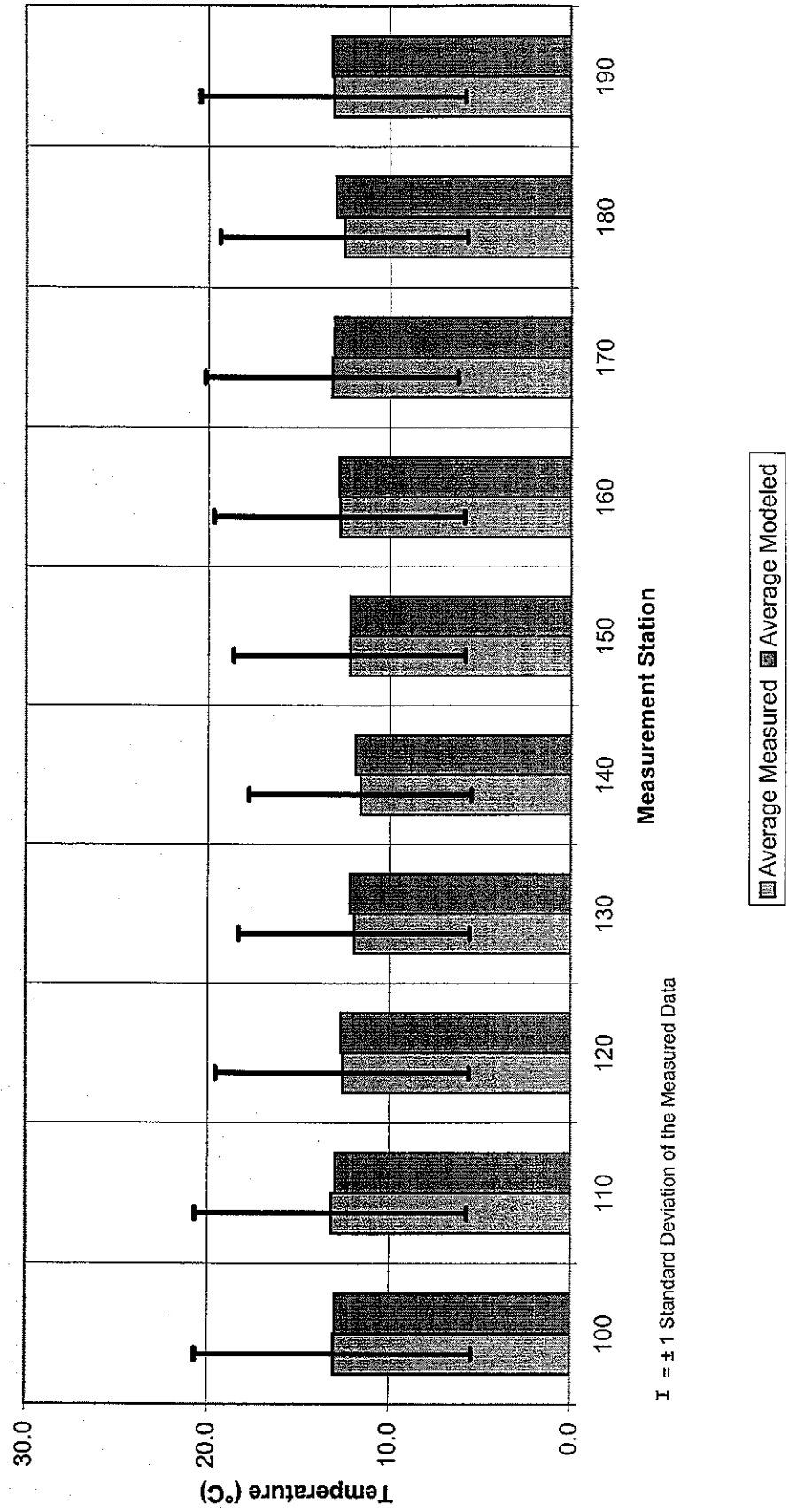


FIGURE 5.16

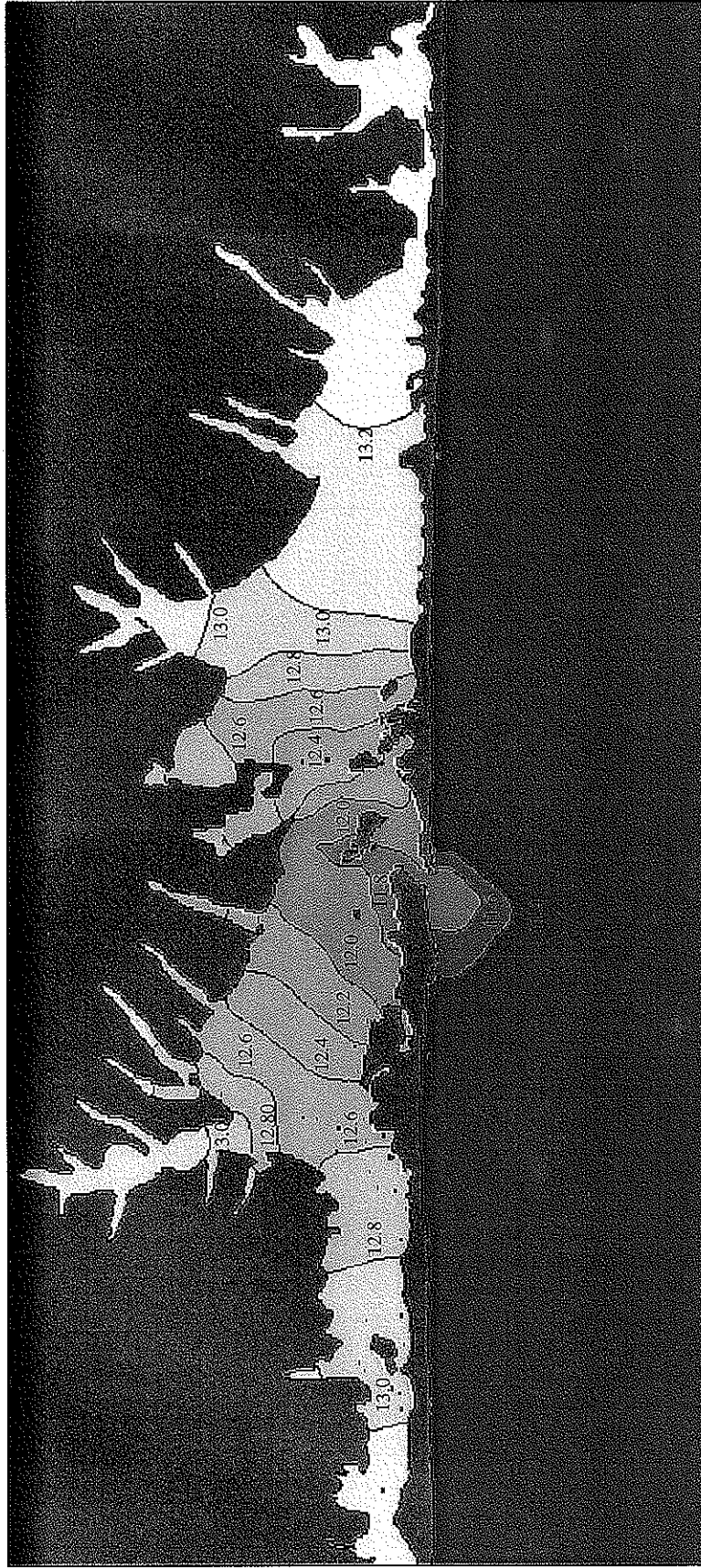


FIGURE 5.17
MORICHES BAY
EXISTING CONDITIONS
PEAK EBB TEMPERATURE (°C)

FIRE ISLAND TO MONTAUK POINT
INLETS STUDY

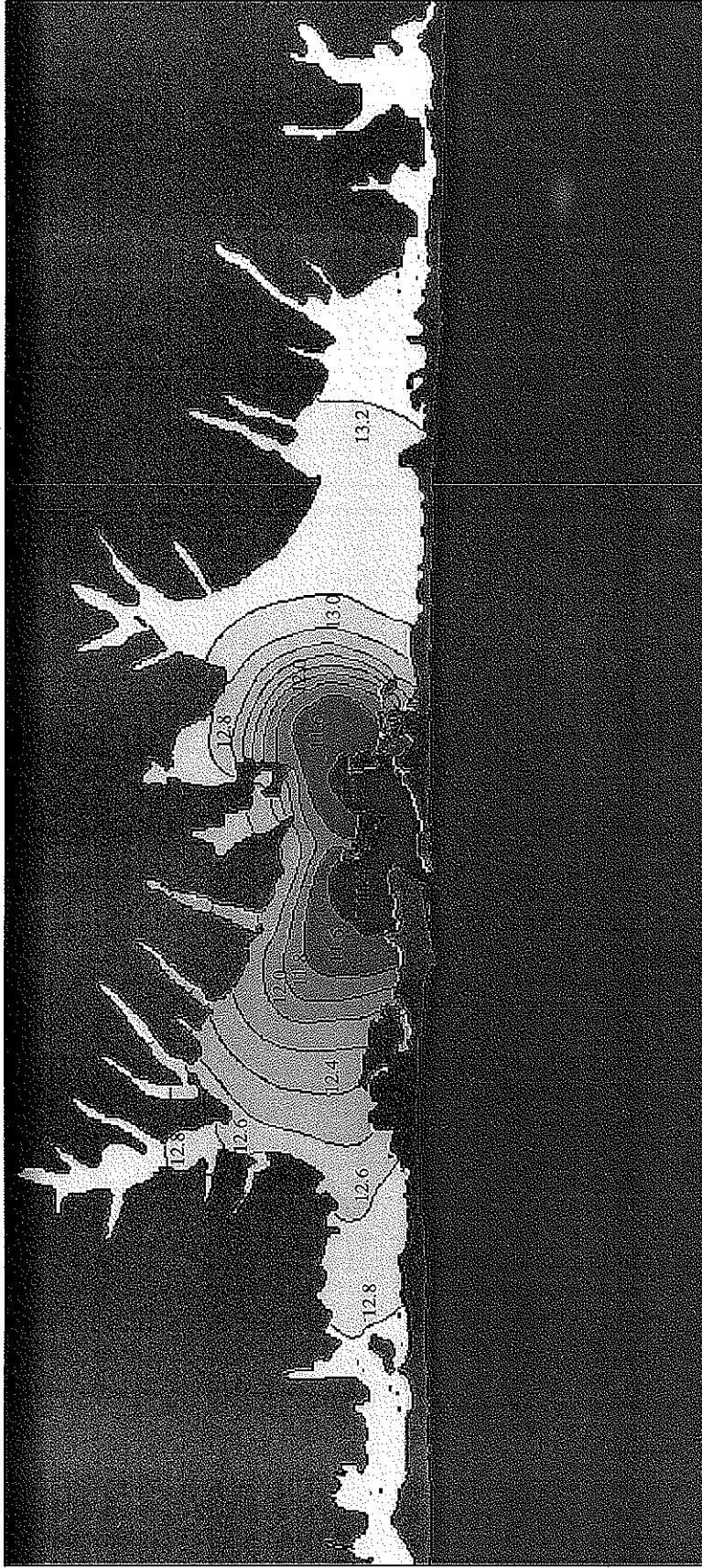


FIGURE 5.18
MORICHES BAY
EXISTING CONDITIONS
PEAK FLOOD TEMPERATURE (°C)

FIRE ISLAND TO MONTAUK POINT
INLETS STUDY

MOFFATT & NICHOL
ENGINEERS

Shinnecock Bay Modeled Temperature Calibration **Average Measured vs. Average Modeled**

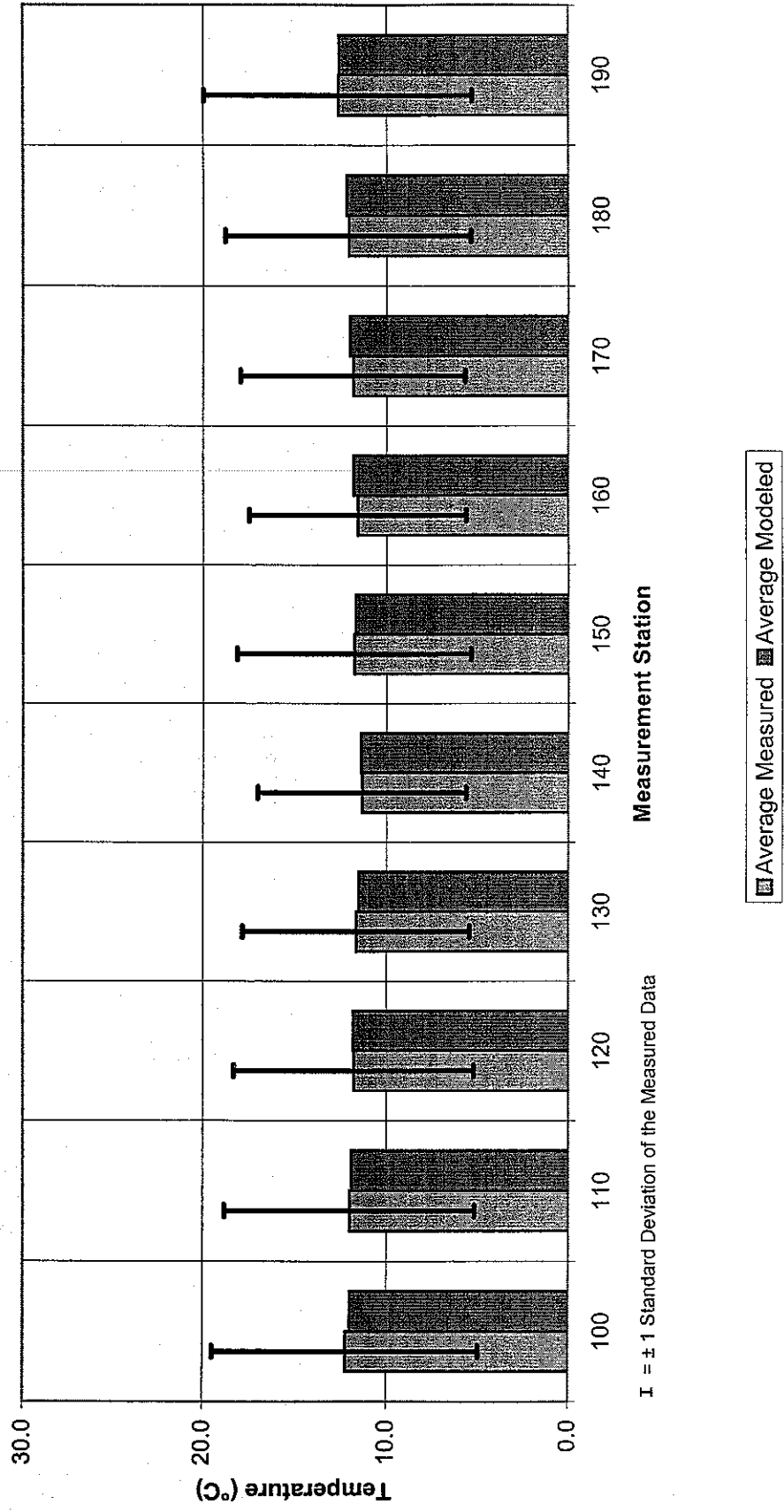


FIGURE 5.19

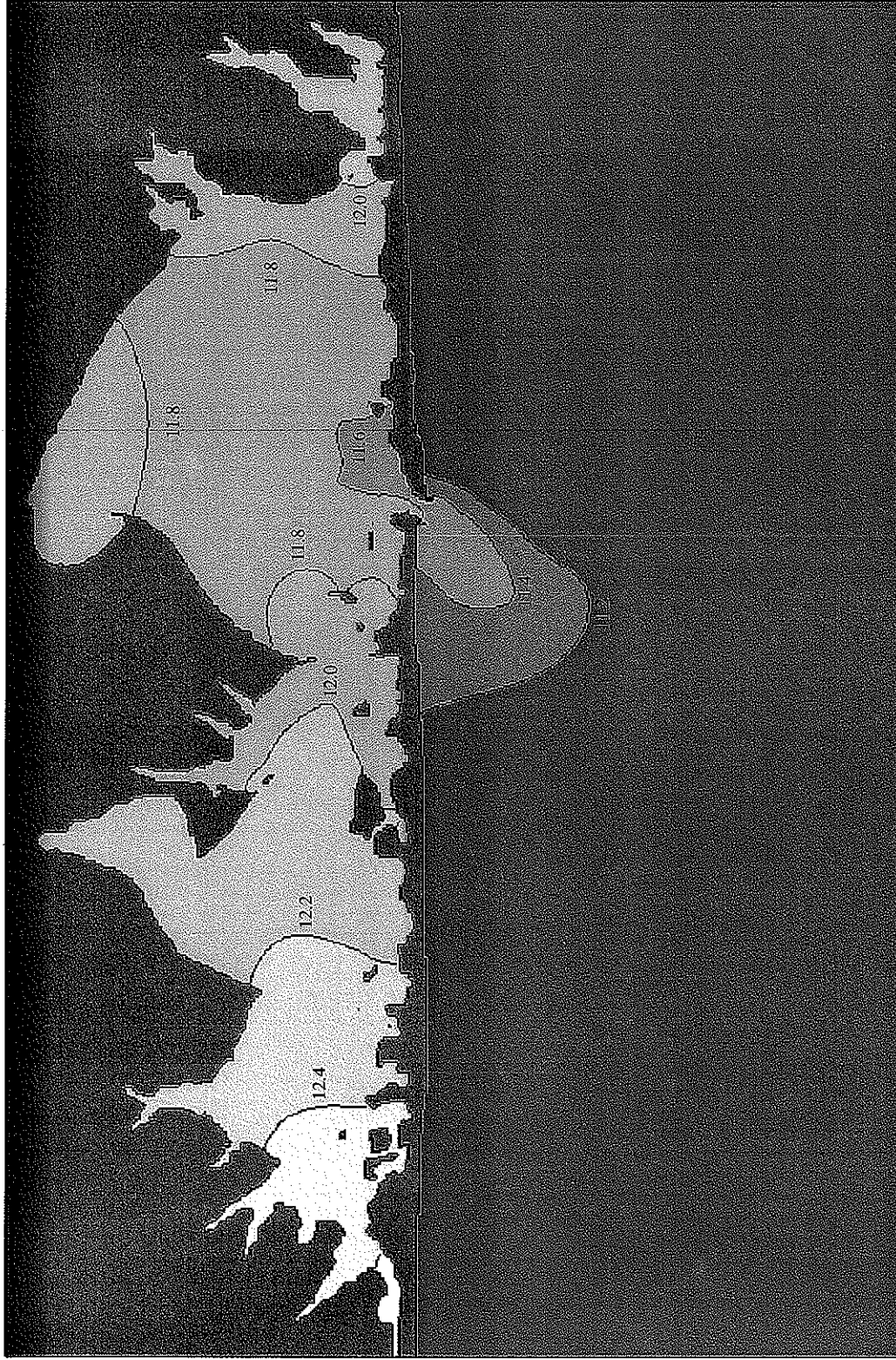


FIGURE 5.20
SHINNECOCK BAY
EXISTING CONDITIONS
PEAK EBB TEMPERATURE (°C)

FIRE ISLAND TO MONTAUK POINT
INLETS STUDY



FIGURE 5.21
SHINNECOCK BAY
EXISTING CONDITIONS
PEAK FLOOD TEMPERATURE (°C)

FIRE ISLAND TO MONTAUK POINT INLETS STUDY

Great South Bay Existing Condition Residence Time Stability Curves

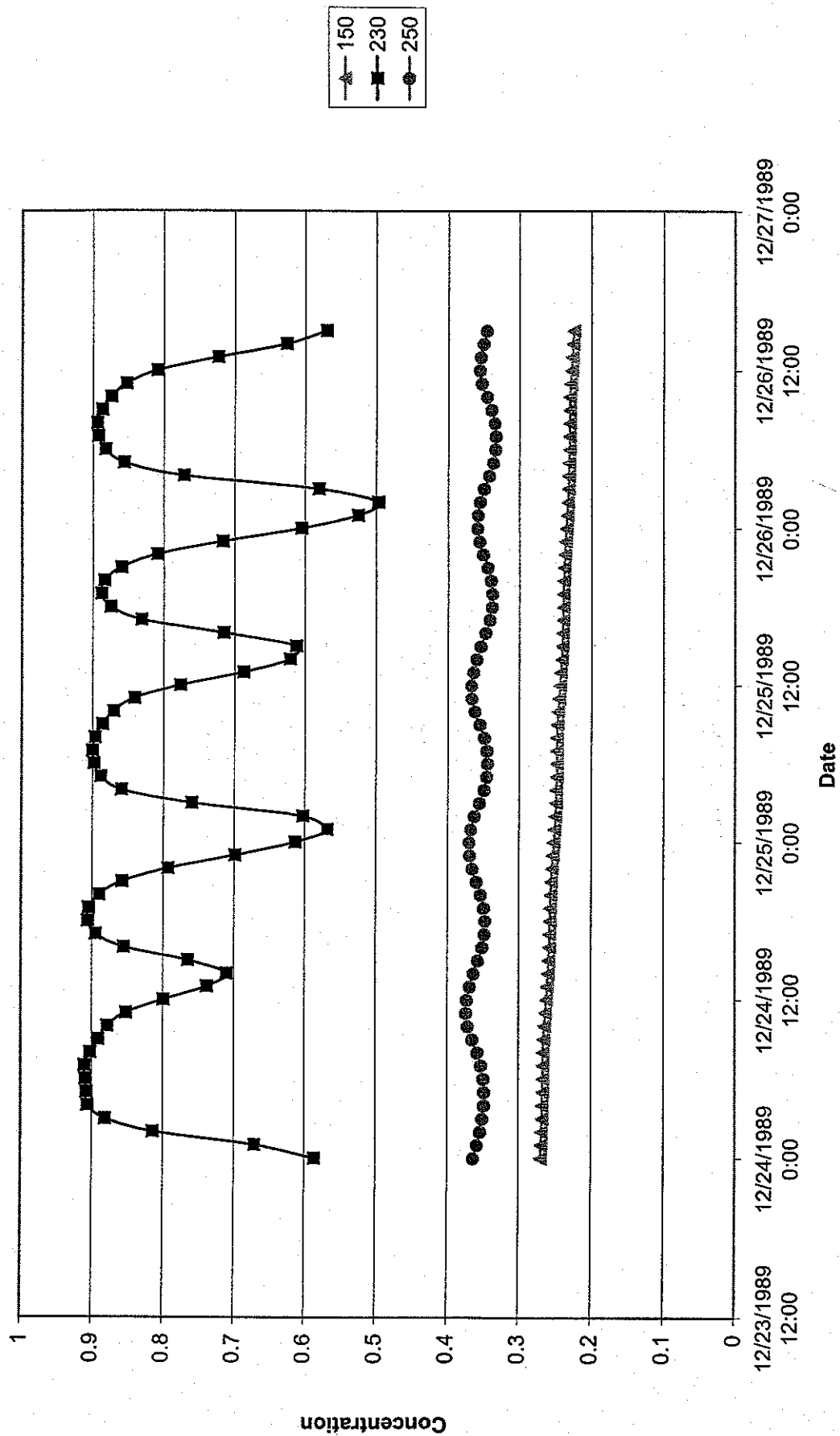


FIGURE 5.22



Moriches Bay Existing Condition Residence Time Stability Curves

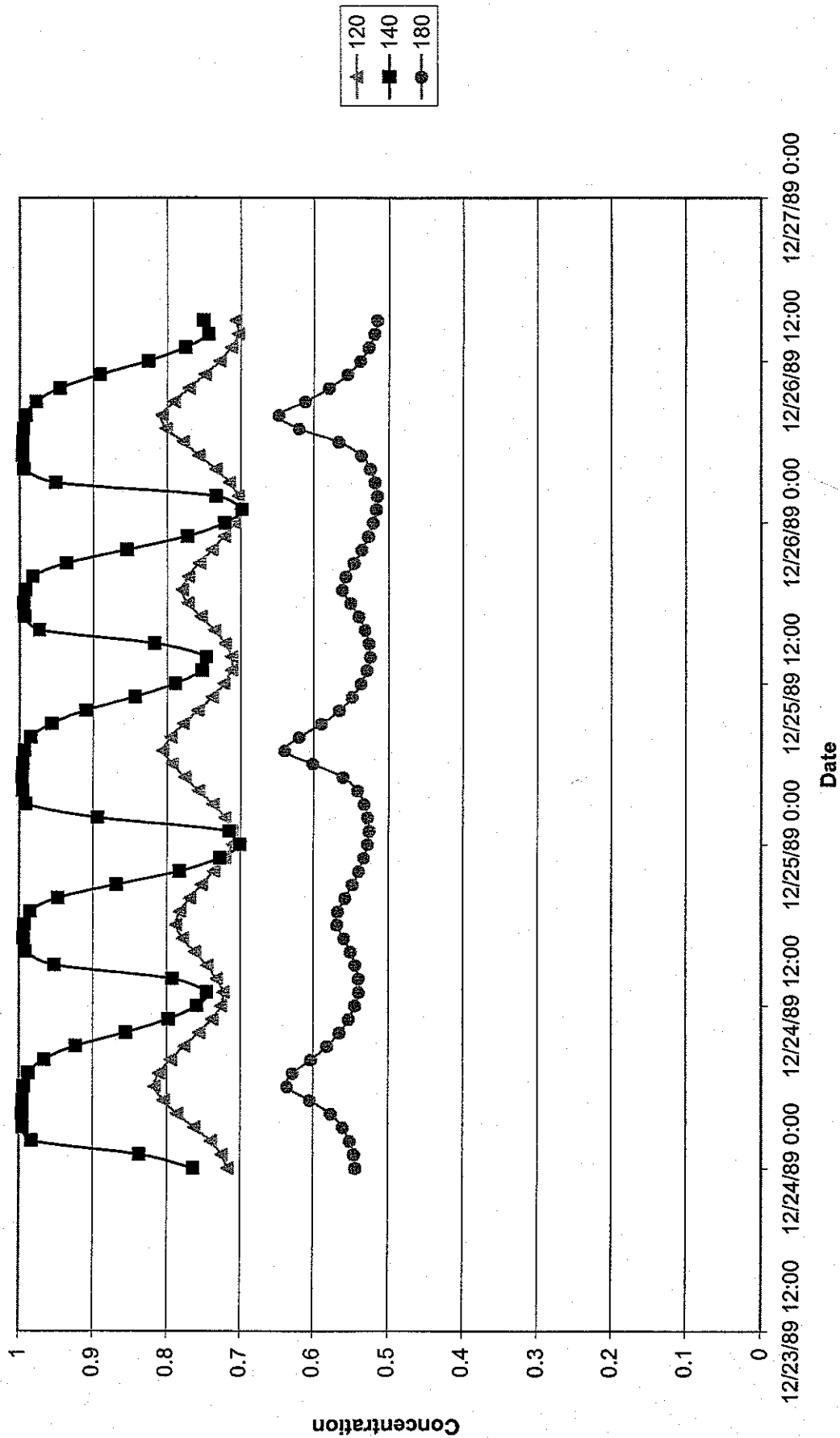


FIGURE 5.24



FIGURE 5.25
MORICHES BAY
EXISTING CONDITIONS
RESIDENCE TIME (DAY)

FIRE ISLAND TO MONTAUK POINT
INLETS STUDY

MOFFATT & NICHOL
ENGINEERS

Shinnecock Bay Existing Condition Residence Time Stability Curves

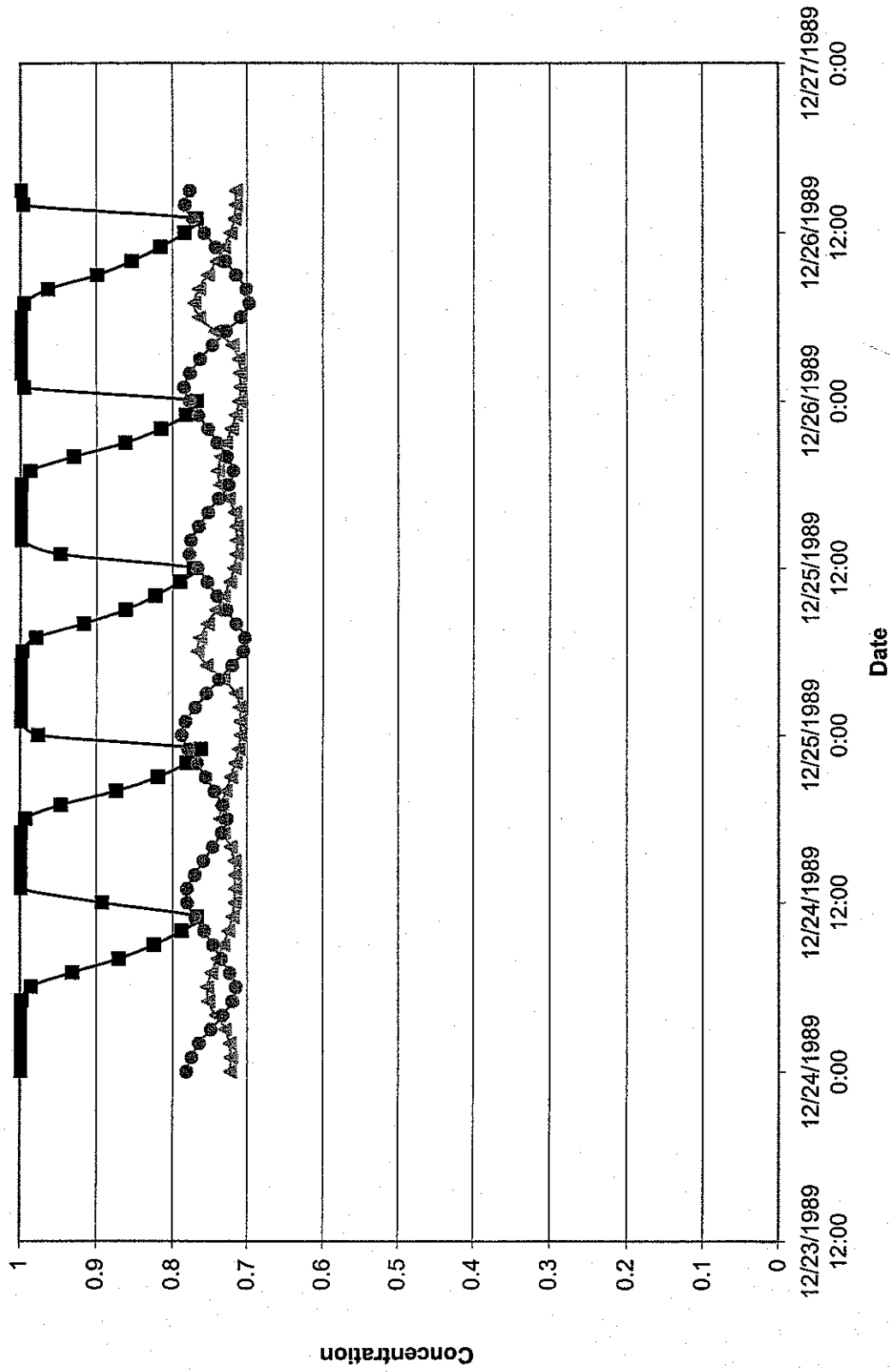


FIGURE 5.26



FIGURE 5.27
SHINNECOCK BAY
EXISTING CONDITIONS
RESIDENCE TIME (DAY)

FIRE ISLAND TO MONTAUK POINT
INLETS STUDY

MOFFATT & NICHOL
ENGINEERS

6. IMPACTS OF BARRIER ISLAND BREACHING

6.1. General

The calibrated tidal hydrodynamic model (USACE, 1999) and advection/dispersion model were used to evaluate the impacts of breaches on salinity, temperature and residence times throughout Great South, Moriches, and Shinnecock Bays under normal tide conditions. Boundary conditions used for calibration purposes were also used for breach conditions.

6.2. Breach Characteristics

The selected breaches for future without-project conditions are discussed in detail in USACE (1999) and are summarized below. A single breach location was selected for each bay, based on USACE (1996) updated to reflect recent construction (i.e. Westhampton Interim) and reported erosion hotspots (i.e. west of Shinnecock Inlet). Figures 6.1 to 6.4 summarize potential breach locations. The model was applied to the location in each bay judged to be most vulnerable to breaching. Each breach was modeled with cross-sections corresponding to three-month and nine-month closure periods.

6.2.1. Breach Locations

Great South Bay. Locations along Fire Island that were judged to have at least a moderate likelihood of breach formation included Old Inlet, Atlantique, Water Island and Barrett Beach (USACE 1996). Old Inlet is backed by shallow bay waters and historic records indicate that a breach at this location is unlikely. The Atlantique area has experienced significant storm erosion during recent years, but the barrier in this area is relatively wide with widths from 800 to 1,000 feet. The Water Island and Barrett Beach location was judged vulnerable to permanent inlet formation. This area is characterized by large dunes with low swales, barrier widths less than

300 feet, and recently severe bluff recession. A breach at Water Island/Barrett Beach would have significant impacts on Fire Island Inlet, as it is further removed from the inlet. Consequently, a breach near Water Island and Barrett Beach was selected. Figure 6.5 shows the finite-difference model mesh for Great South Bay including the breach.

Moriches Bay. Locations vulnerable to breaching along Moriches Bay include Pikes Beach and a narrow barrier island segment east of Pattersquash Island. Recent construction of the Westhampton Interim Project reduces the likelihood of a breach immediately east of Moriches Inlet. Immediately west of Moriches Inlet, accretion predominates for a distance of approximately two miles. The likelihood of a permanent breach further west is low, as water depths in Narrow Bay may be inadequate to support breach growth. The selected breach location for Moriches Bay was at Pikes Beach (see Figure 6.6).

Shinnecock Bay. The shoreline 3,000 feet west of Shinnecock Inlet was estimated in USACE (1996) to have a moderate potential for barrier island breaching. Recent severe erosion in this area has, however, increased the likelihood of a breach. Previous analyses indicate that breaches have a greater impact on existing inlets when the breach is removed from the inlet vicinity (Moffatt and Nichol, 1994). Nonetheless, the high likelihood of a breach immediately west of Shinnecock Inlet makes it necessary to examine the consequences of a breach at this location. The breach location for Shinnecock Bay is reflected in the finite-difference mesh shown in Figures 6.7.

6.2.2. Breach Sizes

Impacts to study area tidal inlets are dependent upon the interval from breach formation to closure. During this interval, it is anticipated that tidal flows through the existing inlet are reduced with a concomitant increase in shoaling while the breach is open. As the breach enlarges, impacts to the bay and existing inlet increase. Breach impacts were examined for two scenarios, namely: (1) Breach Contingency Plan with a closure period of three months, and (2) Westhampton breach closure period of nine months. The former scenario reflects a rapid

response to breach formation, a smaller breach opening and reduced impacts to existing inlets. The latter scenario examines the effects of slower response to breach formation. Breach cross-sectional areas relative to time for Great South, Moriches and Shinnecock Bays are summarized in Table 6.1 and correspond to locations described previously. Existing inlet cross-sectional areas were not changed for modeled breach scenarios.

TABLE 6.1 BARRIER ISLAND BREACH CHARACTERISTICS			
Estuary	Breach Cross-Sectional Area (ft ²)		Breach Location
	3 Months	9 Months	
Great South Bay	15,800	29,200	Water Island/Barrett Beach
Moriches Bay	9,500	14,900	Pikes Beach
Shinnecock Bay	10,100	15,900	West of Shinnecock Inlet

6.3. Breach Case 1 (3-Month Breach)

Breach Case 1 corresponds to a breach with dimensions similar to a breach that has been open for three months (three-month breach). Existing condition bathymetry for each bay was modified to include a breach with dimensions equivalent to a three-month breach. The calibrated models were run using the breach-modified bathymetry to simulate the effects of a breach on hydrodynamics and water quality. **Interim Submission 9B: Inlet Dynamics - Without-Project Future Conditions** (USACE, 1999) describes the effects of the three-month breach on hydrodynamics. The effects of the breach on water quality, described in the following sections, reflect breach-induced changes in the hydrodynamics.

6.3.1. Salinity

Great South Bay. Advection/Dispersion modeling results for the three-month breach case, shown in Figure 6.8, indicate that salinity is increased in the eastern basin close to the breach and decreased slightly in locations remote from the breach. When compared to existing conditions,

average salinity is increased at stations 120, 130, 140, and 150 directly by the influx of additional ocean water through the breach. Increases range from a maximum of approximately 1.6 ppt closest to the inlet to 0.7 ppt in Patchogue Bay. Stations further west in Great South Bay have smaller increases in salinity. Near the existing inlet and further west beyond the inlet salinity decreases by 0.1 to 0.3 ppt during breach conditions. Decreases in the western sections of the bay can be attributed to a reduction in flow through the existing inlet, which decreases circulation in western sections of the bay. In the extreme western sections of the bay, salinity is dominated by flow from Hempstead Bay (stations 250, 260, and 270) and experience little change as a result of the breach. Salinity in the center of Great South Bay decreases 0.1 to 0.3 ppt due to changes in circulation patterns at the inlet.

Figures 6.9 and 6.10 show salinity in Great South Bay at peak ebb and peak flood tide conditions, respectively, while Figures 6.11 and 6.12 graphically depict the relative difference in salinity between existing conditions and the three-month breach case. Positive values indicate areas where existing salinity values are higher than salinity values for the three-month breach case.

Moriches Bay. The impacts of a breach at Pikes Beach on salinity in Moriches Bay are summarized in Figure 6.13 (see Figure 2.10 for station locations). Salinities at stations 150, 170, and 190 in the eastern basin close to the breach increase 0.2 to 0.3 ppt relative to existing conditions. Salinities at stations near the existing inlet (stations 100, 110, and 140) are unchanged from existing conditions. At stations 120 and 130 in the western basin, salinity increases 0.1 ppt as a result of a redirection of flow from the existing inlet into the western basin. Finally, salinity at station 180, located close to the breach, increases by 1.7 ppt. Salinities within the eastern basin are increased as ocean waters more readily reach the eastern basin through the breach.

Salinity contour plots are presented in Figures 6.14 and 6.15 for peak ebb and peak flood tides, respectively. Figures 6.16 and 6.17 show the relative change in salinity from existing conditions to the 3-month breach conditions for peak ebb and peak flood tides, respectively.

Shinnecock Bay. Salinity in eastern Shinnecock Bay is significantly impacted by a breach immediately west of Shinnecock Inlet. Comparisons of existing condition salinity versus with-breach salinity are shown in Figure 6.18 for each measurement station (see Figure 2.11). Analysis of these results shows that salinity is increased by 0.7 to 0.8 ppt at stations 100, 110, and 120 and by 0.3 to 0.5 ppt at stations 130, 140, 150, and 160 three months after a breach occurs. These increases can be attributed to additional ocean water entering the bay via the breach. The effects on salinity are less pronounced at stations 130, 140, 150, and 160 as these stations are closer to the inlet and, therefore, closer to ocean salinity under existing conditions. Salinity in the far western basin of Shinnecock Bay is reduced during a breach. Analysis of the results presented in Figure 6.18 for station 180 shows that salinity decreases by 0.4 ppt during a breach. This reduction can be attributed to a shift in the flow of saline waters toward the eastern basin, which allows fresher water into the bay through Quogue Canal at the western boundary.

Salinity contour plots at peak ebb tide and peak flood tide for the 3-month breach are shown in Figures 6.19 and 6.20, respectively. The difference between existing conditions and the 3-month breach conditions are shown in Figure 6.21 for peak ebb tide and Figure 6.22 for peak flood tide.

6.3.2. Temperature

Great South Bay. Advection/Dispersion modeling indicates that temperature in Great South Bay is relatively unchanged by breaching. Figure 6.23 shows average existing condition temperatures compared to average temperature for the three-month breach case. Average temperature decreases in the vicinity of the breach are on the order of 0.5°C. Temperatures throughout the rest of Great South Bay increased slightly by less than 0.1°C. Average temperatures in the bay are shown in Figures 6.24 and 6.25 for peak ebb and peak flood tide conditions, respectively, with the relative difference in average temperatures between existing conditions and the three-month breach case shown in Figure 6.26 and 6.27 for peak ebb and peak flood tides, respectively.

Moriches Bay. The impacts of a breach at Pikes Beach on temperature distributions in Moriches Bay are summarized in Figure 6.28. Temperature contour plots for peak ebb tide and peak flood tide are shown in Figures 6.29 and 6.30, respectively. Analysis of the results shows that temperatures are essentially unchanged for the three-month breach case except for areas immediately in front of the breach which decrease up to 0.8 °C due to the additional ocean water entering the bay via the breach. Figures 6.31 and 6.32 show contours of the difference in temperature between existing conditions and the 3-month breach for peak ebb tide and peak flood tide, respectively.

Shinnecock Bay. The effects of a breach west of Shinnecock Inlet on temperature in Shinnecock Bay are minimal. Figure 6.33 shows comparisons of existing conditions and with-breach temperatures. There is a minor increase in temperature at stations 170 and 180 due to the inlet forcing flow to the eastern basin resulting in less ocean water and more water from the Quogue Canal in the western basin. Contours of temperature difference between existing conditions and the with-breach case are shown in Figure 6.36 for peak ebb tide and 6.37 for peak flood tide.

6.3.3. Residence Times

Great South Bay. Figure 6.38 shows the residence time for Great South Bay for the three-month breach case. Residence times were significantly impacted by a breach in eastern Great South Bay with reductions in residence times on the order of 3 to 4 weeks. High local reductions in residence times are expected as the breach was located in an area with high residence times under existing conditions. Residence times in western Great South Bay increased 4 to 6 days as the breach affected circulation patterns and reduced flow via the existing inlet. Figure 6.39 shows the change in residence time for the three-month breach case relative to existing conditions.

Moriches Bay. Residence time throughout Moriches Bay is shown in Figure 6.40 for the three-month breach case. Relative changes in residence time compared to existing conditions are

shown in Figure 6.41. Residence times in Moriches Bay decreased with a breach at Pikes Beach with changes on the order of 0.5 to 0.8 days. Decreases in residence time close to the breach were approximately 8 days as the breach was located in an area with high residence times under existing conditions. Residence times close to the bay entrances (i.e. the inlet and lateral boundaries) decrease minimally.

Shinnecock Bay. Shinnecock Bay residence time is shown in Figure 6.42 for the three-month breach case. The three-month breach case is compared to existing conditions in Figure 6.43 which shows the relative difference in residence time. Residence time decreases throughout the bay on the order of 0.5 to 1.5 days except in the extreme eastern and western basins where residence time actually increases by 0.3 to 0.9 days. Residence time decreased significantly close to the breach. A breach in the western basin, where residence time is on the order of 7 days, would be expected to show a much higher impact on local residence times.

6.4. Breach Case 2 (9-Month Breach)

Breach Case 2 corresponds to a breach with dimensions similar to a breach that has been open for nine months (nine-month breach). Existing condition bathymetry for each bay was modified to include a breach with dimensions equivalent to a nine-month breach. The calibrated models were run using the breach-modified bathymetry to simulate the effects of a breach with these dimensions on hydrodynamics and water quality. **Interim Submission 9B: Inlet Dynamics - Without-Project Future Conditions** (USACE, 1999) describes the effects of the nine-month breach on hydrodynamics.

6.4.1. Salinity

Great South Bay. Modeling results show very little difference in the effects of a three- or nine-month breach on bay salinity. Average modeled salinity at each measurement station is shown in Figure 6.23 for existing conditions, the three-month breach, and the nine-month breach. Figures 6.44 and 6.45 show salinity at peak ebb and peak flood tides, respectively. Figures 6.46 and

6.47 show the relative change in salinity throughout the bay for peak ebb and peak flood tides, respectively.

Moriches Bay. The impacts of a nine-month breach on salinity distributions are similar to those of a three-month breach and are summarized in Figure 6.13. Salinity at stations 180 and 190 in the eastern basin of Moriches Bay increased 0.3 and 0.1 ppt, respectively, relative to the three-month breach due to increased flow of ocean water via the larger breach. Salinity at stations 120 and 130 in the western basin decreased 0.1 ppt. Salinity contour plots showing salinity at peak ebb tide and peak flood tide are presented in Figure 6.48 and 6.49, respectively. Figures 6.50 and 6.51 show plots of the difference in salinity between existing conditions and the nine-month breach.

Shinnecock Bay. Salinity in Shinnecock Bay nine months after a breach is very similar to salinity three months after a breach. Figure 6.17 shows that salinity at the measurement stations is the same for both cases. Salinity contour plots showing salinity at peak ebb tide and peak flood tide are presented in Figure 6.52 and 6.53, respectively. Figures 6.54 and 6.55 show plots of the difference in salinity between existing conditions and the nine-month breach.

6.4.2. Temperature

Great South Bay. Modeled average temperature in Great South Bay is shown in Figure 6.23 at each measurement station for existing conditions, the three-month breach case, and the nine-month breach case. These results indicate that there is very little additional impact from the nine-month breach as results are nearly identical to those of the three-month breach. Figures 6.56 and 6.57 show the temperature throughout the bay at peak ebb and peak flood tides, respectively. The relative difference in temperature between existing conditions and the nine-month breach case is shown in Figure 6.58 for peak ebb tide and Figure 6.59 for peak flood tide conditions.

Moriches Bay. The three month and nine month breach impacts on Moriches Bay are similar. Temperature contour plots showing temperature at peak ebb tide and peak flood tide are presented in Figure 6.60 and 6.61, respectively. Figures 6.62 and 6.63 show plots of the difference in temperature between existing conditions and the nine-month breach.

Shinnecock Bay. In Shinnecock Bay, the effects on temperature of a breach open for nine months are very similar to the effects of a breach open for three months. Comparisons of temperature at each measurement station, shown in Figure 6.26, indicate no difference between the three- and nine-month breach cases. Temperature contour plots showing temperature at peak ebb tide and peak flood tide are presented in Figure 6.64 and 6.65, respectively. Figures 6.66 and 6.67 show plots of the difference in temperature between existing conditions and the nine-month breach.

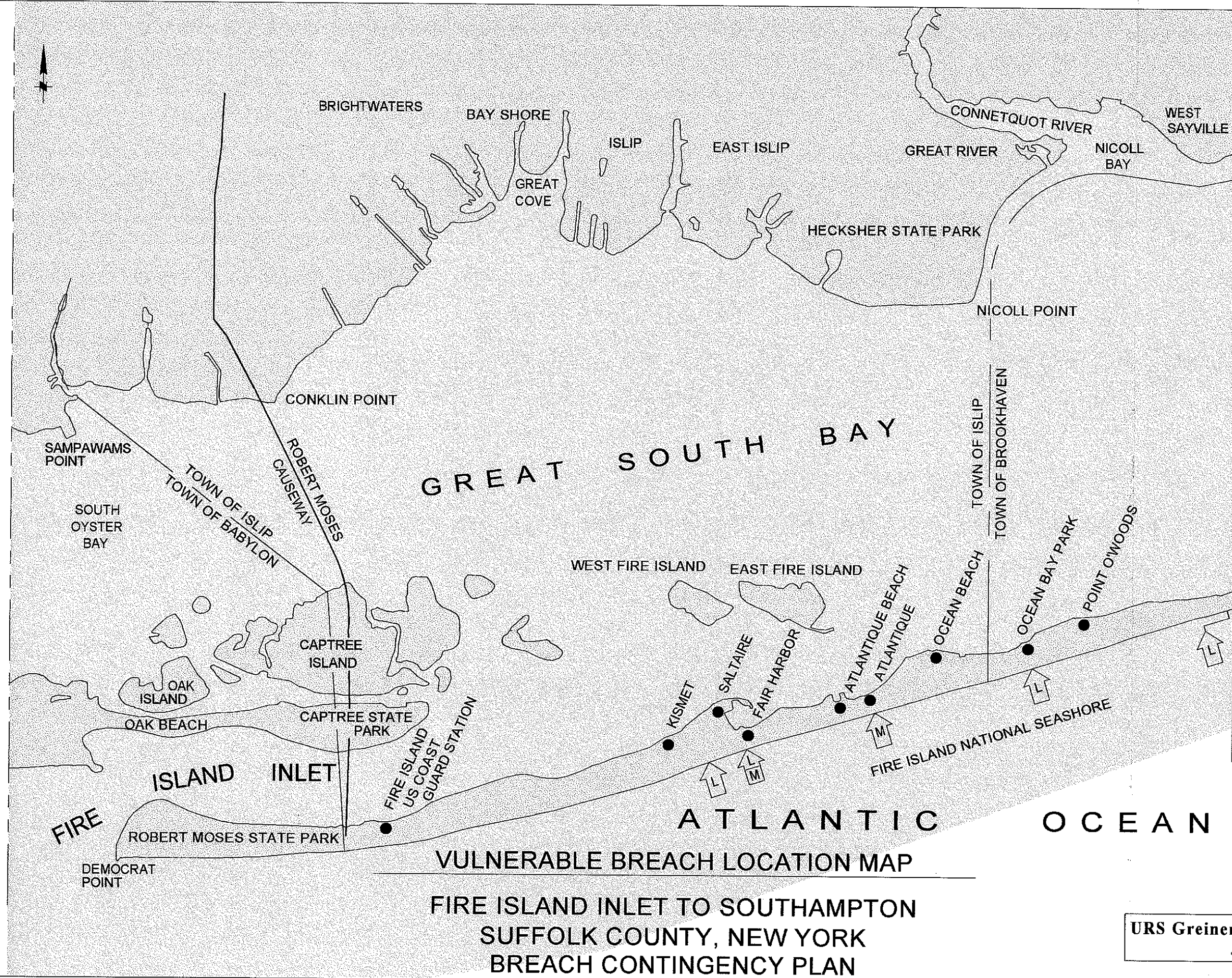
6.4.3. Residence Time

Great South Bay. Figure 6.68 shows the residence time throughout Great South Bay for the nine-month breach case. Residence times are decreased an additional 3 days close to the breach and 0.5 to 1 day in other areas of the bay relative to the three-month breach. The impacts of the nine-month breach can be attributed to high existing condition residence times and the location of the breach in the eastern basin. The relative changes in residence time for the nine-month breach compared to existing conditions is shown in Figure 6.69.

Moriches Bay. Residence times throughout Moriches Bay are shown in Figure 6.70 with the relative change in residence time between the nine-month breach and existing conditions shown in Figure 6.71. Results indicate that residence times decrease further for the nine-month breach case. Residence times in the vicinity of the nine-month breach are 0.7 days less than for the three-month breach. Residence time decrease by less than 0.1 days in areas further removed from the breach.

Shinnecock Bay. Shinnecock Bay residence times are shown in Figure 6.72 and the relative change in residence time due to the nine-month breach is shown in Figure 6.73. Residence times in the western basin were further lowered on the order of 0.2 days compared to the three-month breach. Residence times in the western basin increase 0.1 to 0.2 days relative to the three-month breach.

\\3892-07\DWG\FIMP-6-1.DWG



MATCHLINE E

LEGEND

- ASSESSMENT OF BREACH VULNERABILITY
- ↑ L LOW
 - ↑ M MODERATE
 - ↑ H HIGH

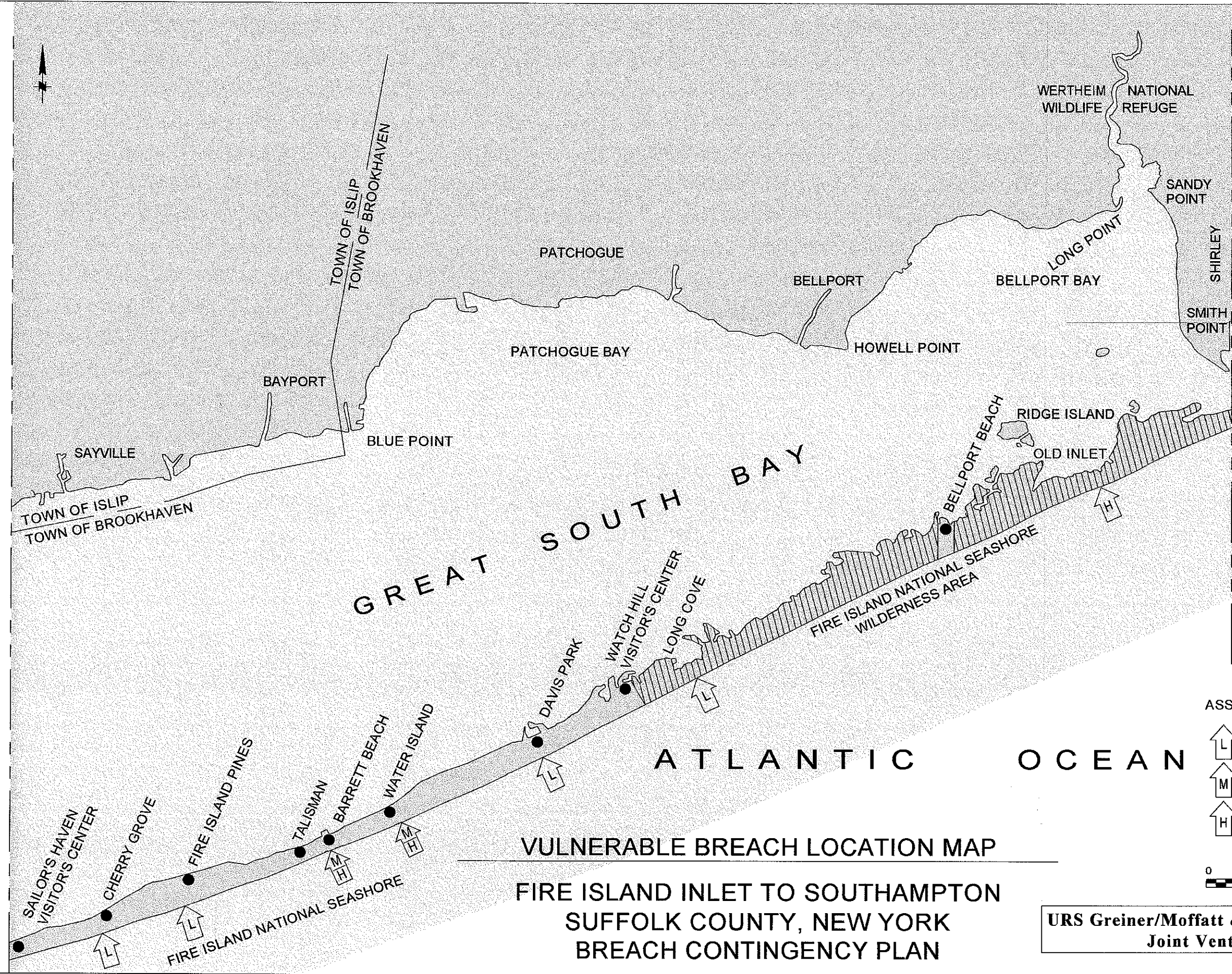
0 2500 5000 7500
SCALE: 1:5000

URS Greiner/Moffatt & Nichol Engineers
Joint Venture

FIGURE 6.1

13892-071DWG\FIMP-6-2.DWG

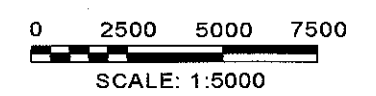
MATCHLINE E



MATCHLINE D

LEGEND

- ASSESSMENT OF BREACH VULNERABILITY
- ↑ L LOW
 - ↑ M MODERATE
 - ↑ H HIGH



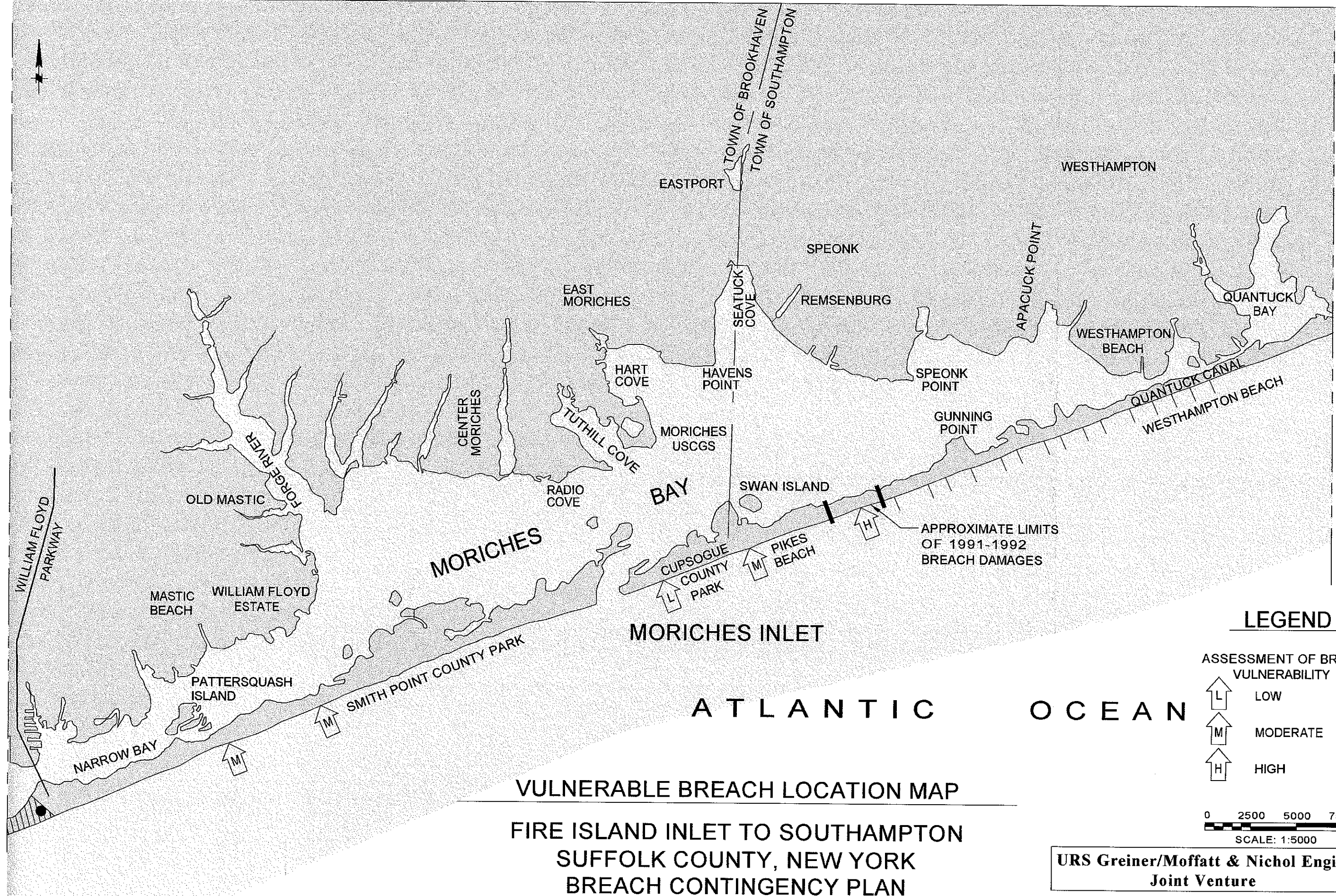
VULNERABLE BREACH LOCATION MAP
FIRE ISLAND INLET TO SOUTHAMPTON
SUFFOLK COUNTY, NEW YORK
BREACH CONTINGENCY PLAN

URS Greiner/Moffatt & Nichol Engineers
Joint Venture

FIGURE 6.2

13892-07\DWG\FIMP-6-3.DWG

MATCHLINE D



MATCHLINE C

FIGURE 6.3

13982-07\DWG\FIMP-6-4.DWG

MATCHLINE C

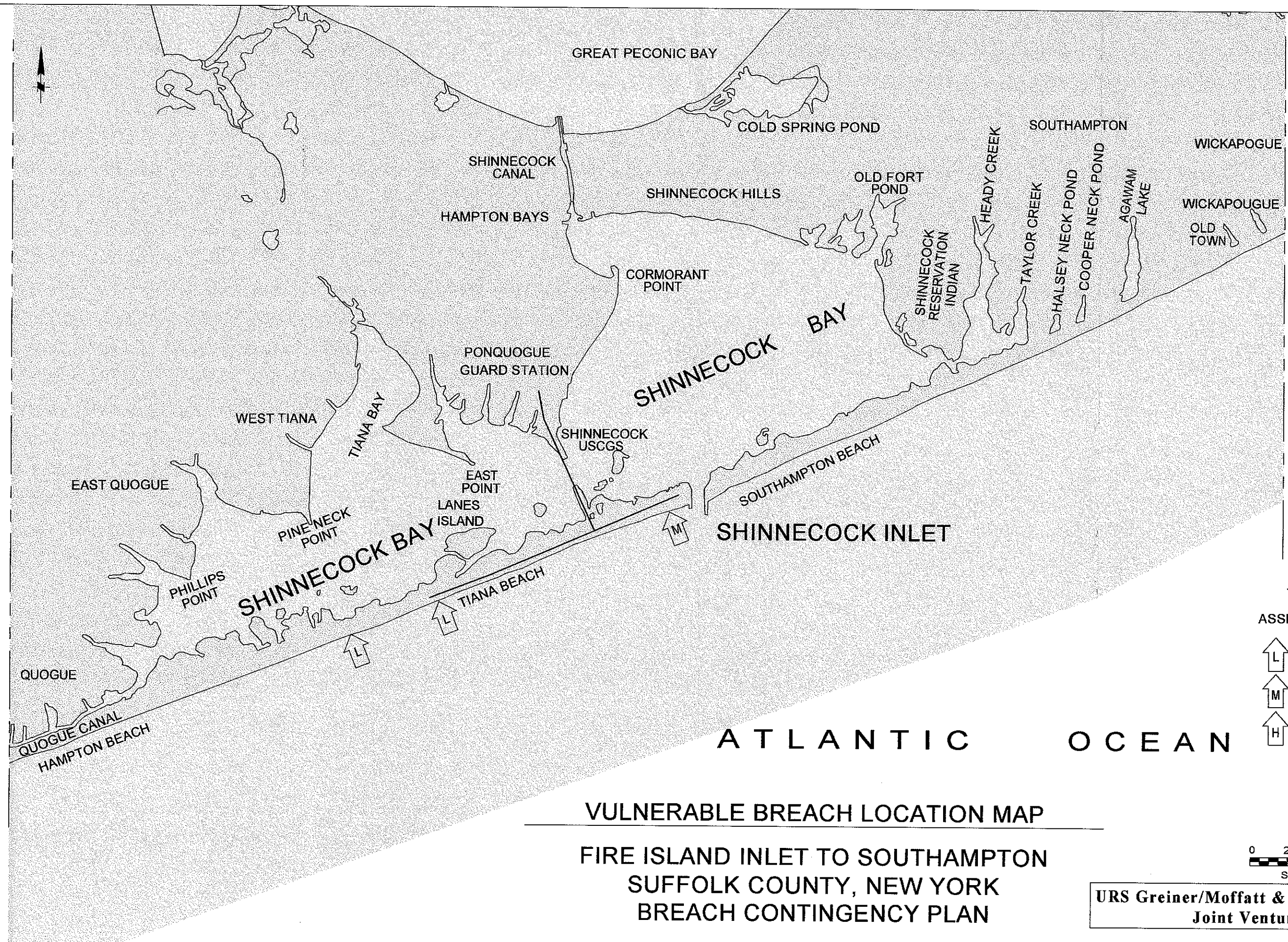


FIGURE 6.4

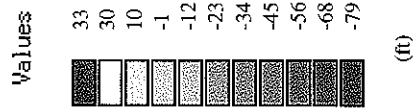


FIGURE 6.5
GREAT SOUTH BAY
BREACH MESH

FIRE ISLAND TO MONTAUK POINT
INLETS STUDY

MOFFATT & NICHOL
ENGINEERS

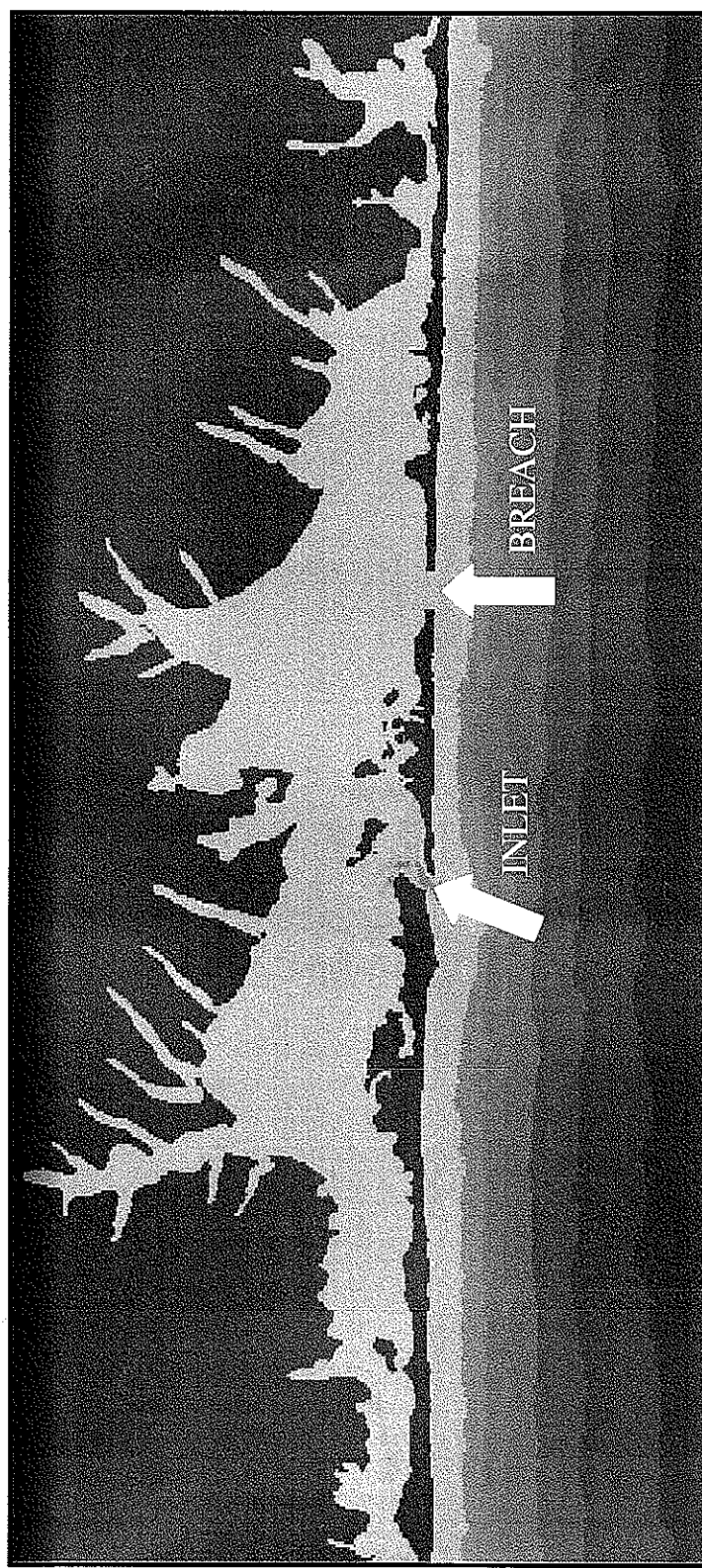


FIGURE 6.6
MORICHES BAY
BREACH MESH

FIRE ISLAND TO MONTAUK POINT
INLETS STUDY

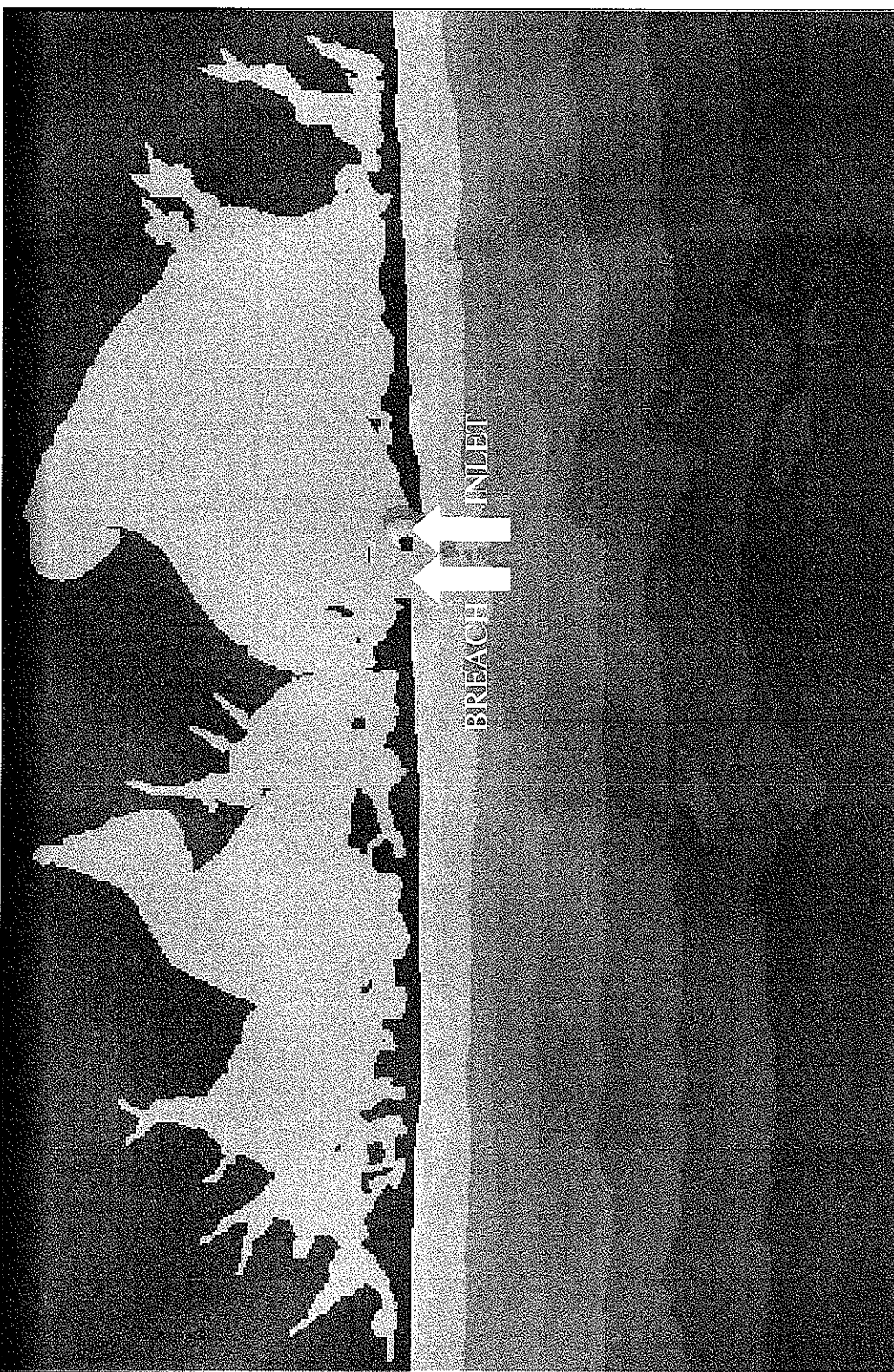


FIGURE 6.7
SHINNECOCK BAY
BREACH MESH

FIRE ISLAND TO MONTAUK POINT
INLETS STUDY

Great South Bay Salinity Modeling Results Existing Conditions vs. With-Breach Cases

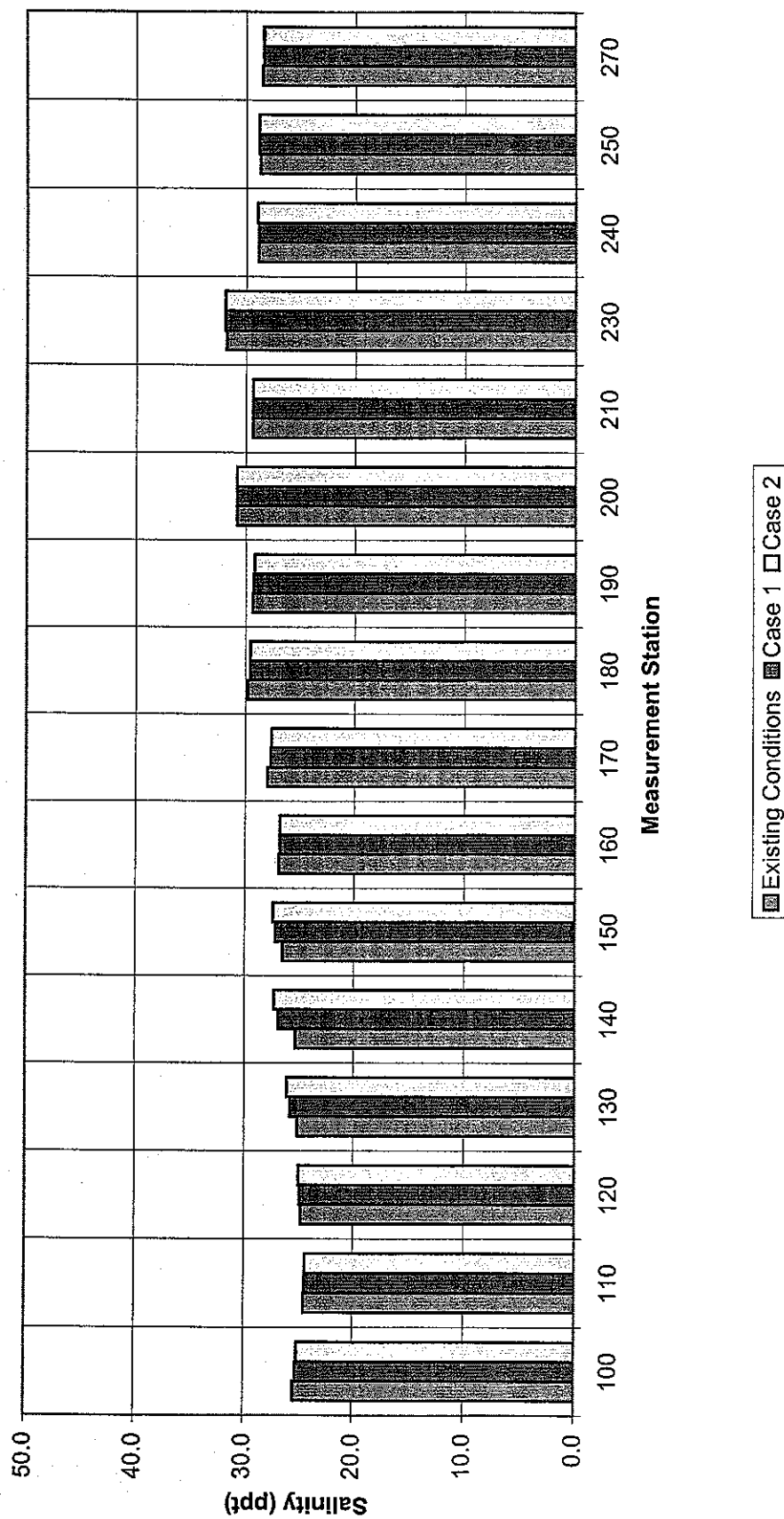


FIGURE 6.8

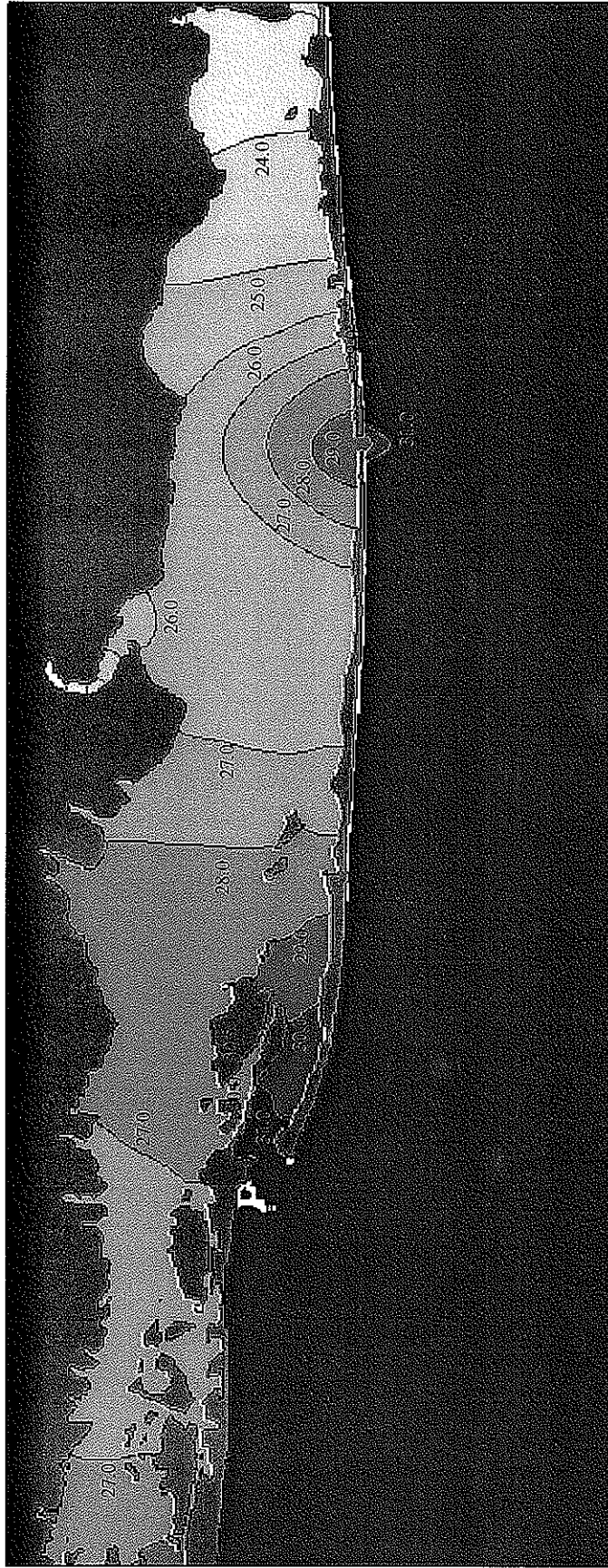


FIGURE 6.9
GREAT SOUTH BAY
3-MONTH BREACH
PEAK EBB SALINITY (PPT)

FIRE ISLAND TO MONTAUK POINT
INLETS STUDY

MOFFATT & NICHOL
ENGINEERS



FIGURE 6.10
GREAT SOUTH BAY
3-MONTH BREACH
PEAK FLOOD SALINITY (PPT)

FIRE ISLAND TO MONTAUK POINT
INLET'S STUDY

MOFFATT & NICHOL
ENGINEERS

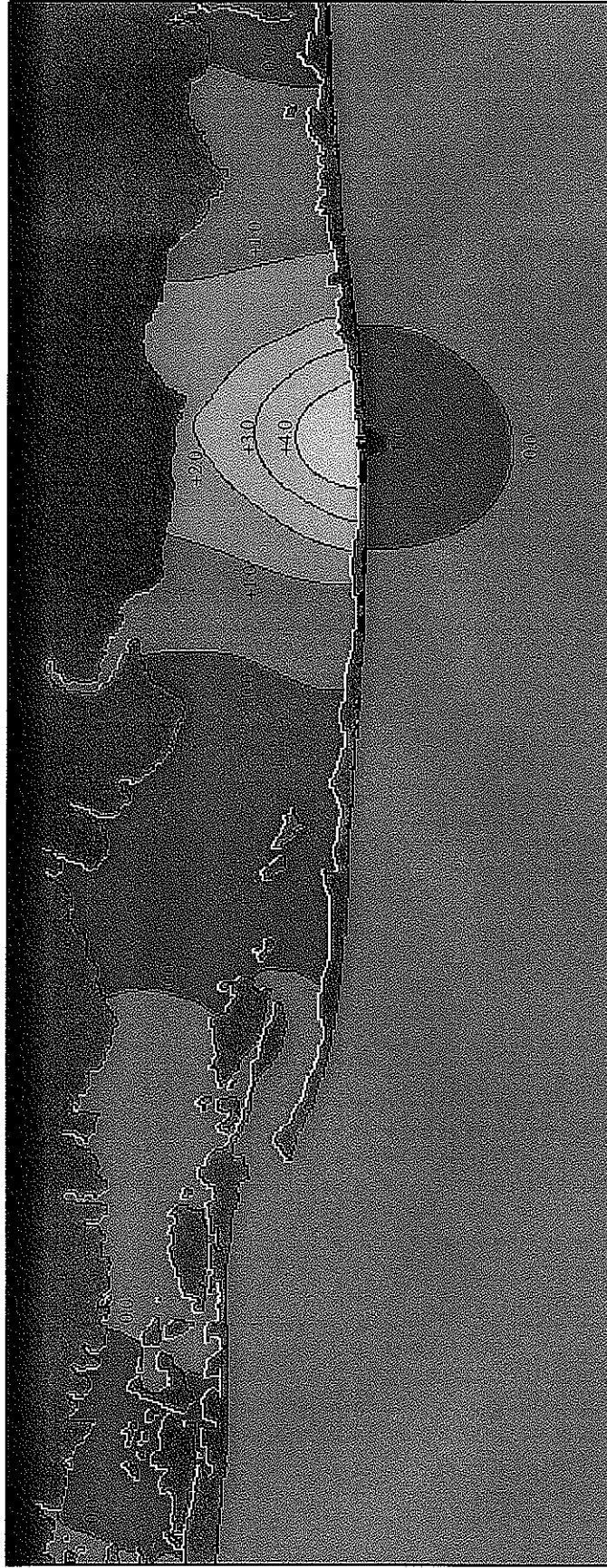


FIGURE 6.11
GREAT SOUTH BAY
EXISTING VS. 3-MONTH BREACH
PEAK EBB SALINITY (PPT)

FIRE ISLAND TO MONTAUK POINT
INLETS STUDY

MOFFATT & NICHOL
ENGINEERS

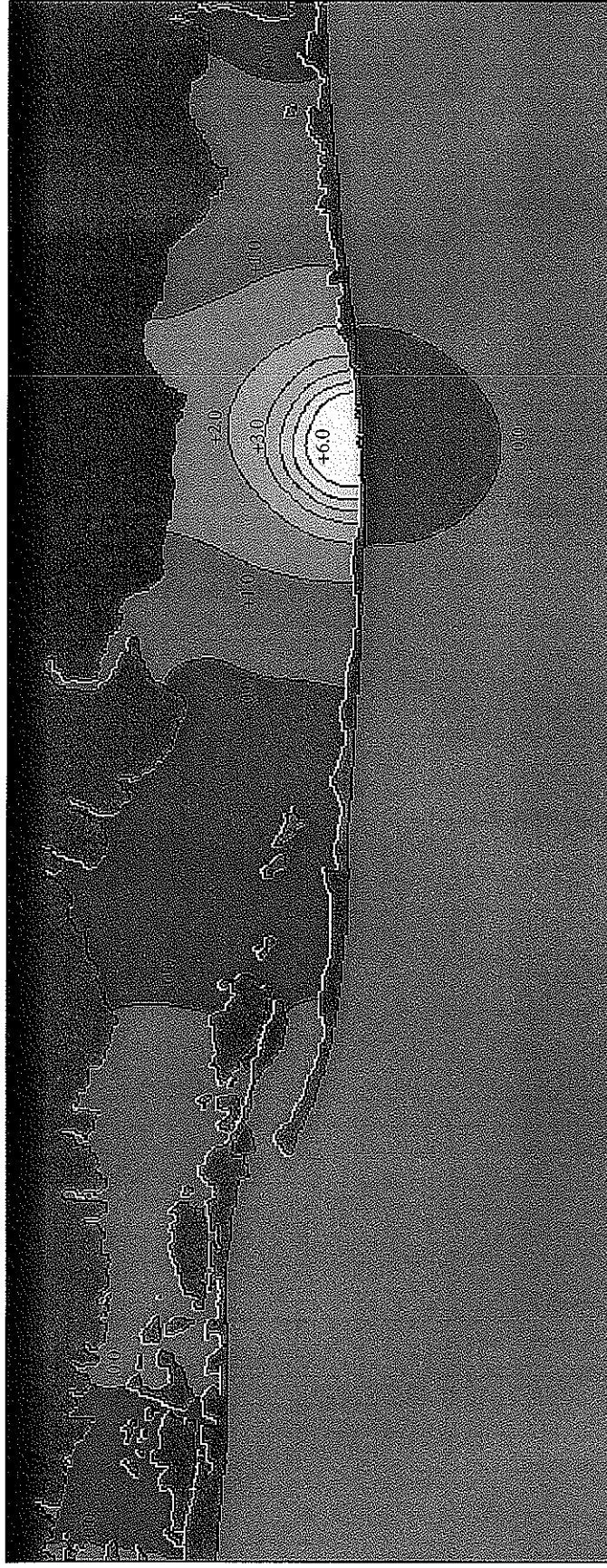


FIGURE 6.12
GREAT SOUTH BAY
EXISTING VS. 3-MONTH BREACH
PEAK FLOOD SALINITY (PPT)

FIRE ISLAND TO MONTAUK POINT
INLETS STUDY

MOFFATT & NICHOL
ENGINEERS

Moriches Bay Salinity Modeling Results **Existing Conditions vs. With-Breach Cases**

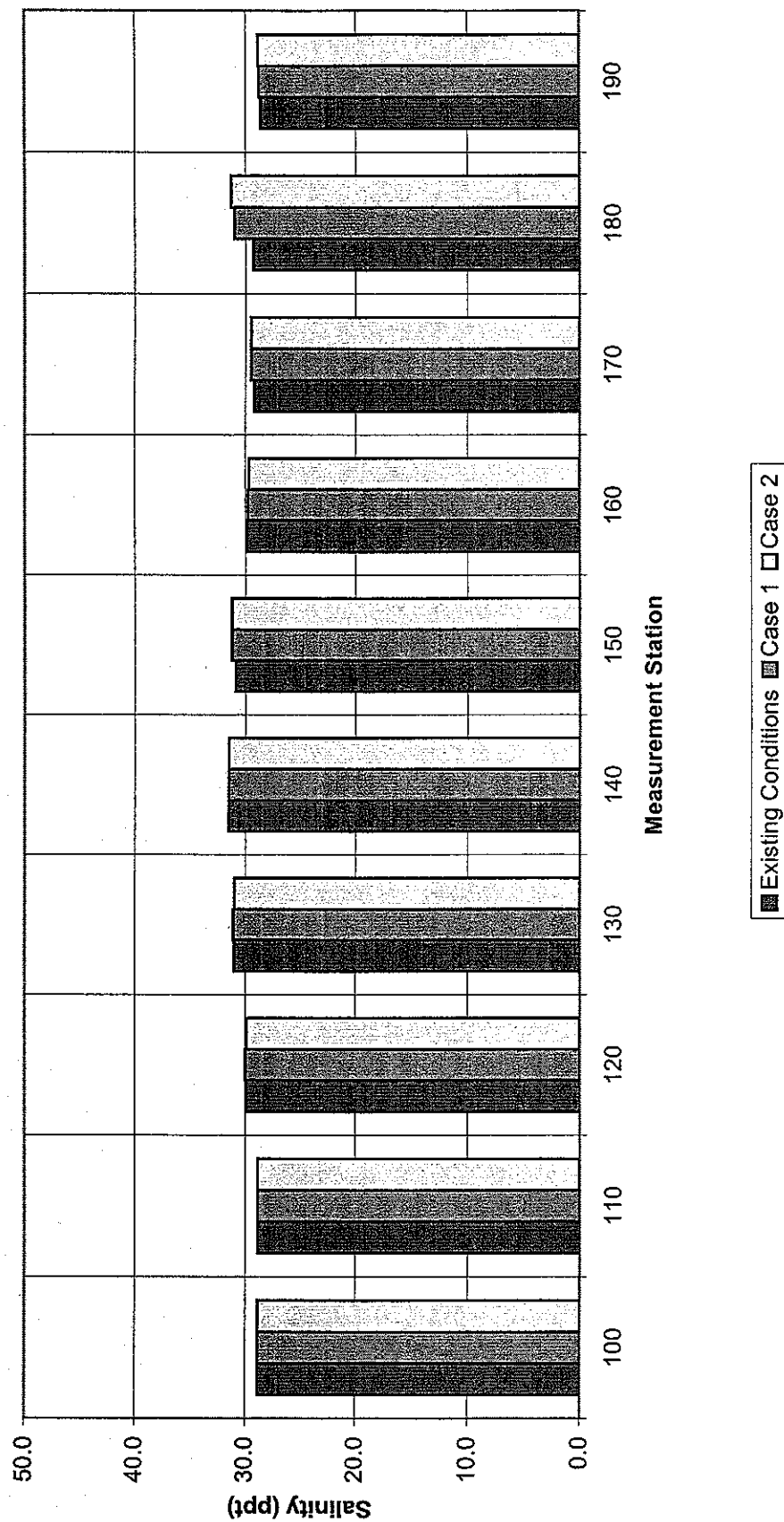


FIGURE 6.13

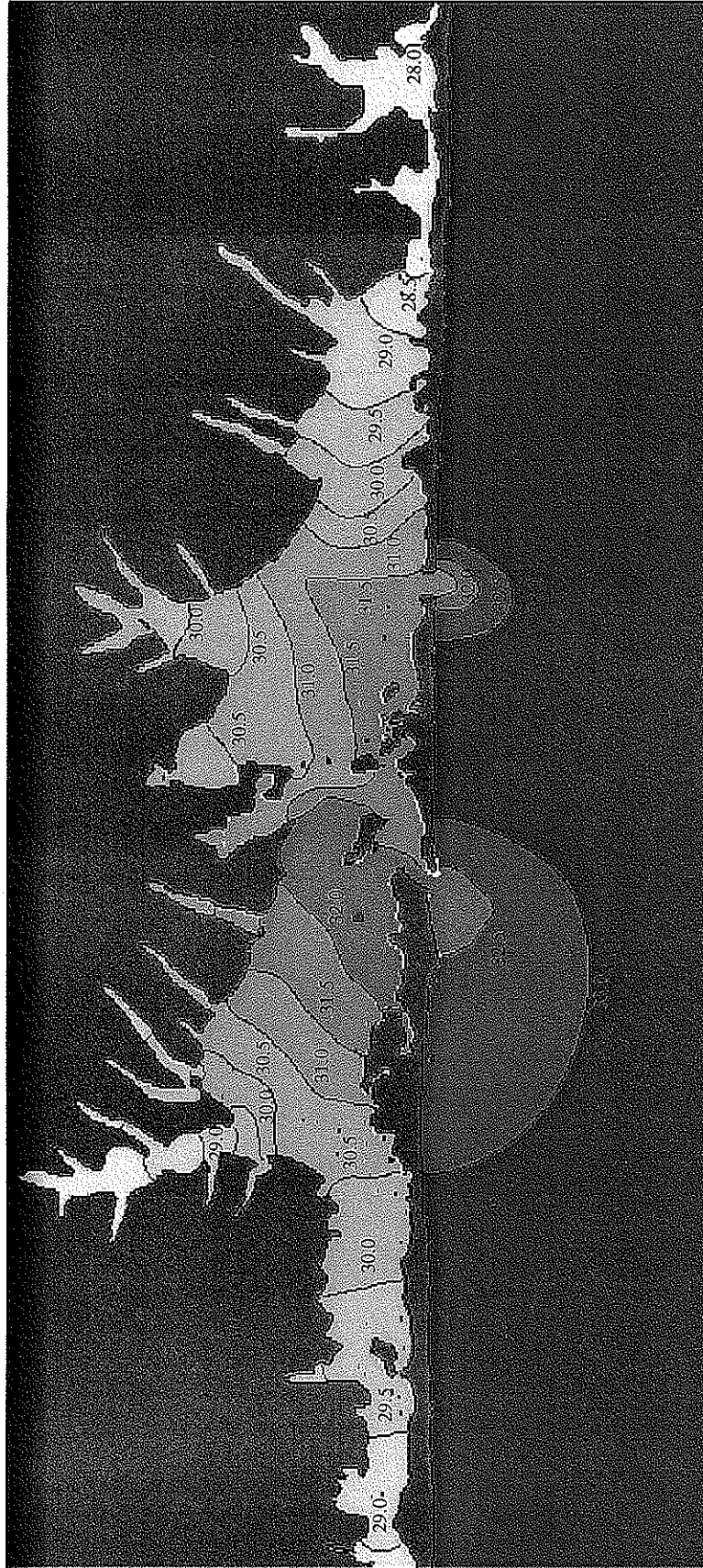


FIGURE 6.14
MORICHES BAY
3-MONTH BREACH
PEAK EBB SALINITY (PPT)

FIRE ISLAND TO MONTAUK POINT
INLETS STUDY

MOFFATT & NICHOL
ENGINEERS

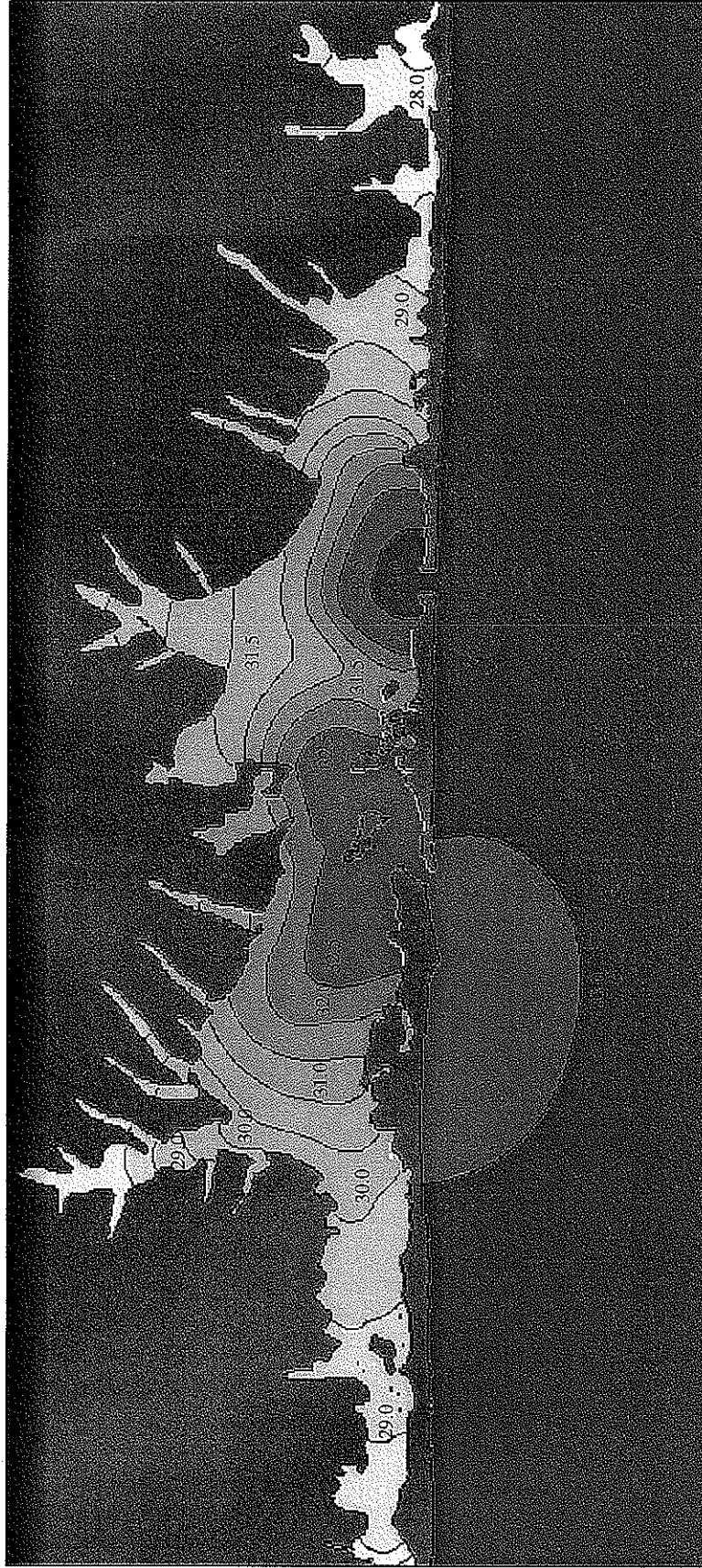


FIGURE 6.15
MORICHES BAY
3-MONTH BREACH
PEAK FLOOD SALINITY (PPT)

FIRE ISLAND TO MONTAUK POINT
INLETS STUDY

MOFFATT & NICHOL
ENGINEERS

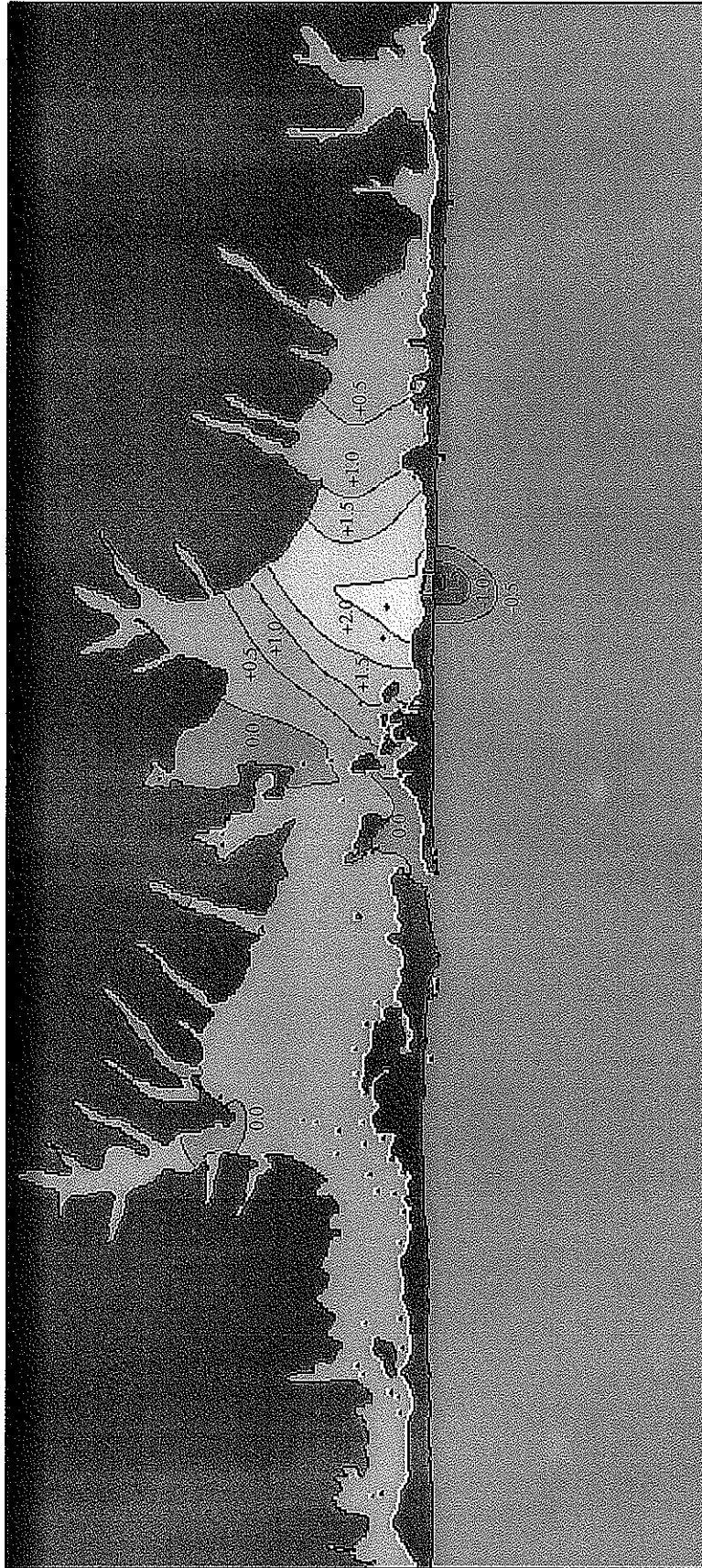


FIGURE 6.16
MORICHES BAY
EXISTING VS. 3-MONTH BREACH
PEAK EBB SALINITY (PPT)

FIRE ISLAND TO MONTAUK POINT
INLETS STUDY

MOFFATT & NICHOL
ENGINEERS

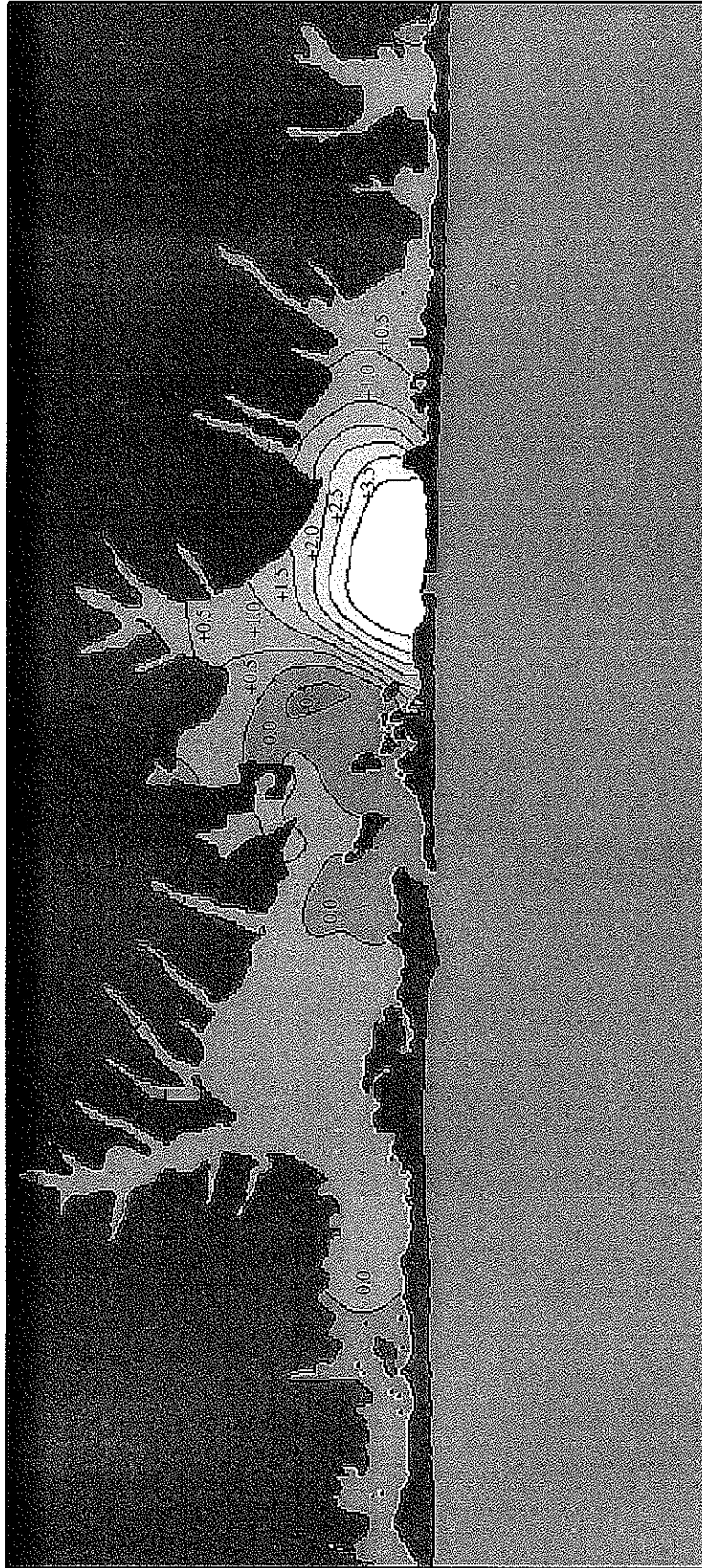


FIGURE 6.17
MORICHES BAY
EXISTING VS. 3-MONTH BREACH
PEAK FLOOD SALINITY (PPT)

FIRE ISLAND TO MONTAUK POINT
INLETS STUDY

MOFFATT & NICHOL
ENGINEERS

Shinnecock Bay Salinity Modeling Results **Existing Conditions vs. With-Breach Cases**

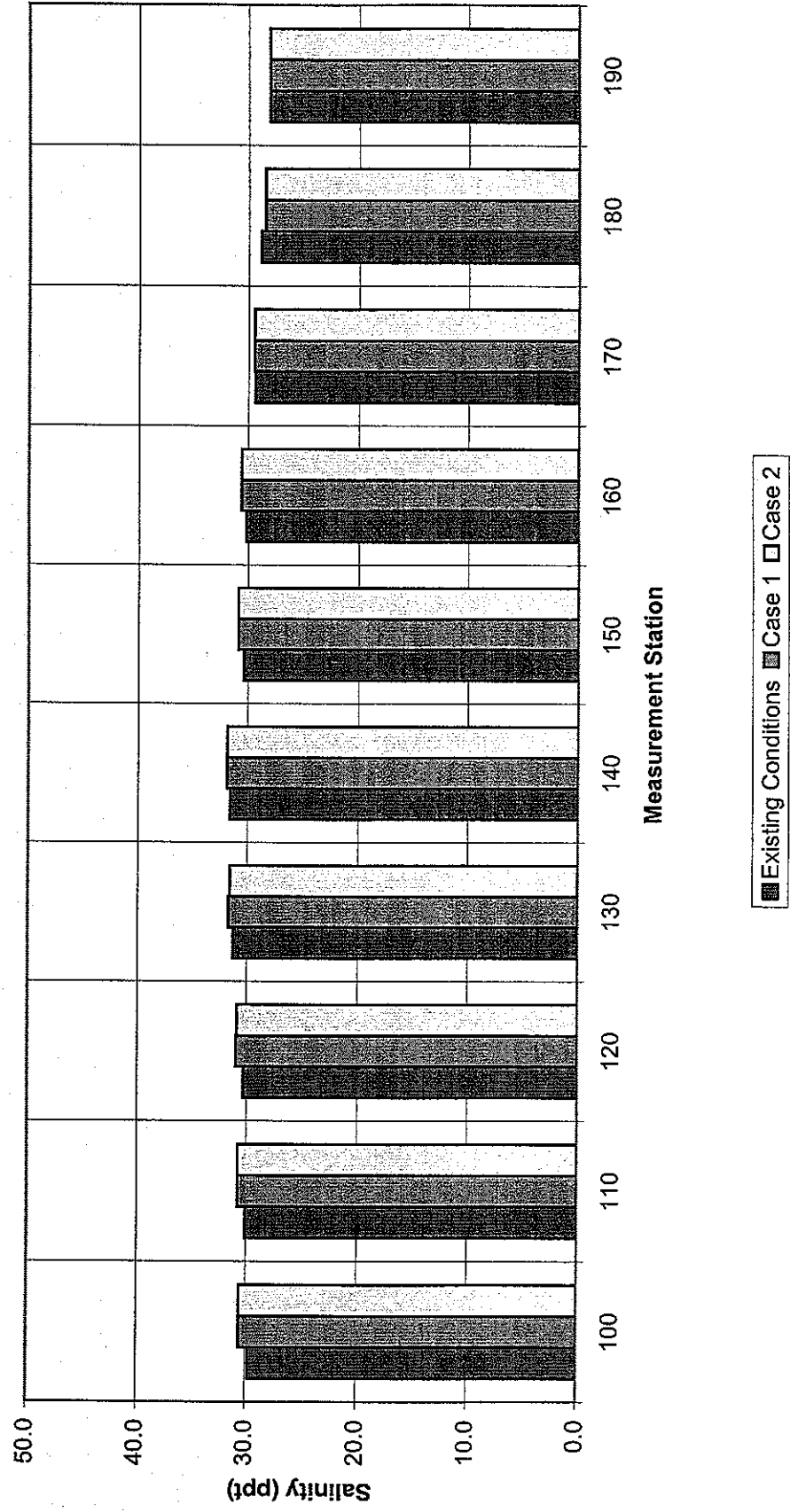


FIGURE 6.18

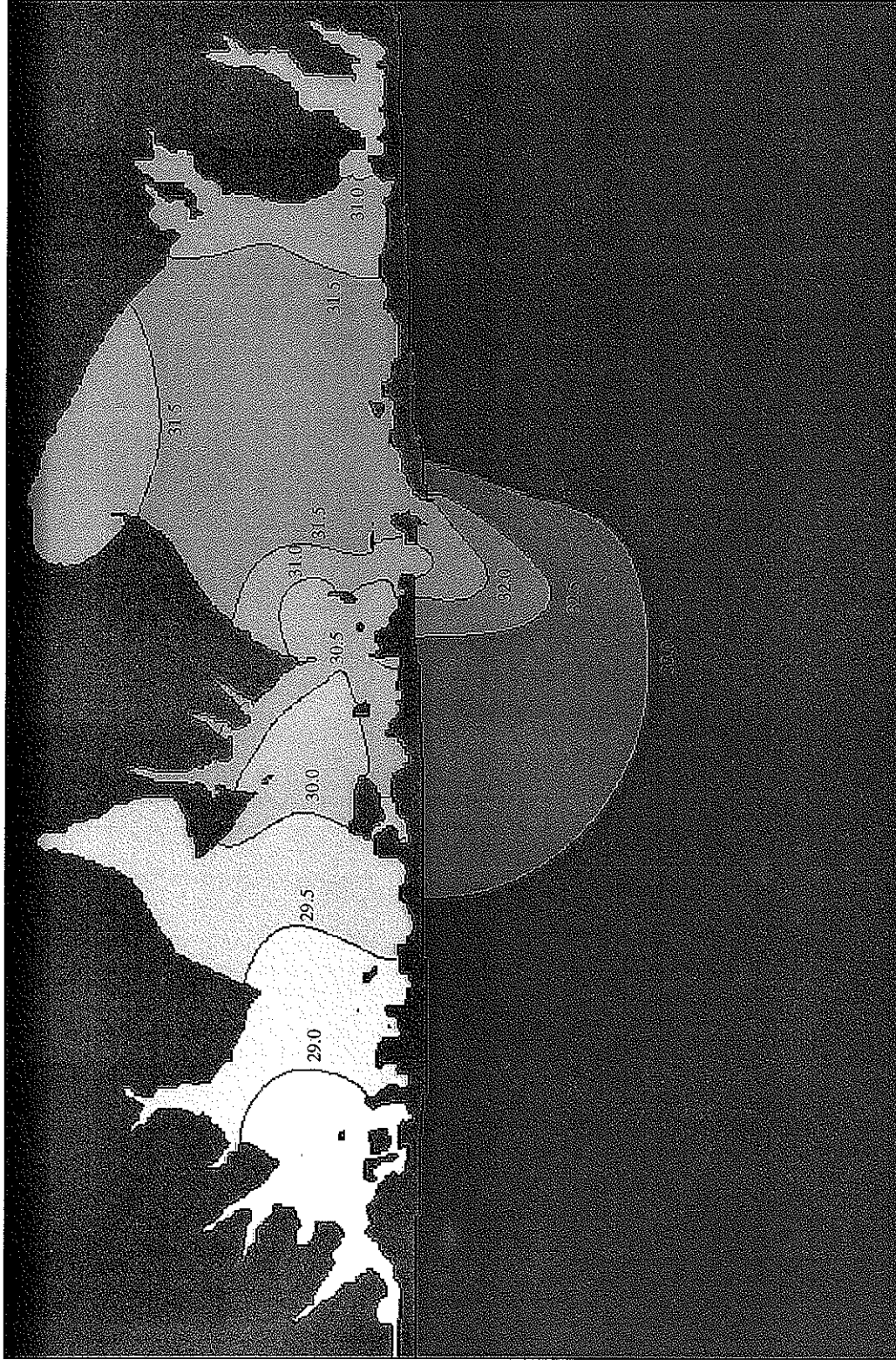


FIGURE 6.19
SHINNECOCK BAY
3-MONTH BREACH
PEAK EBB SALINITY (PPT)

FIRE ISLAND TO MONTAUK POINT
INLETS STUDY

MOFFATT & NICHOL
ENGINEERS

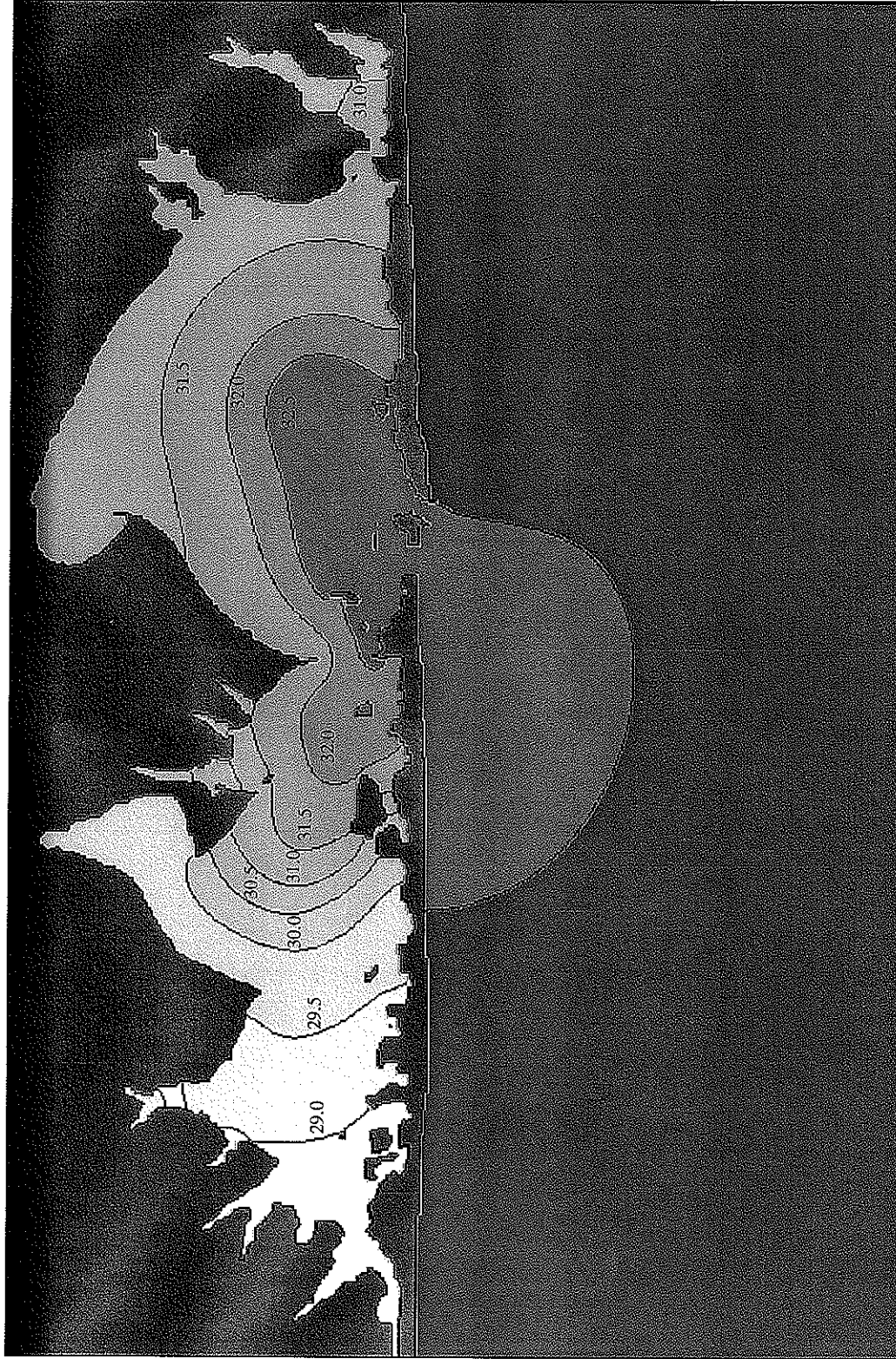


FIGURE 6.20
SHINNECOCK BAY
3-MONTH BREACH
PEAK FLOOD SALINITY (PPT)

FIRE ISLAND TO MONTAUK POINT
INLETS STUDY

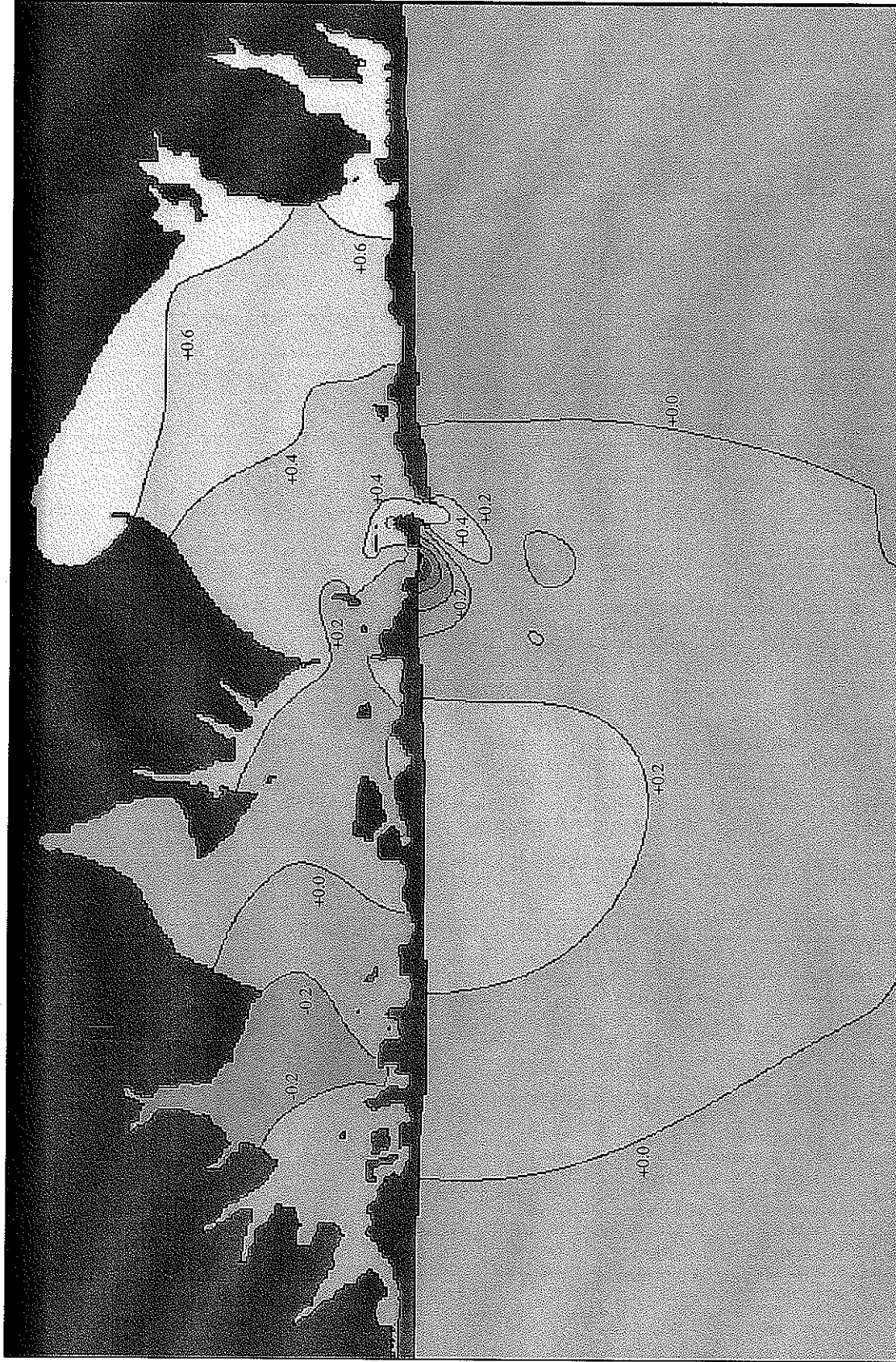


FIGURE 6.21
SHINNECOCK BAY
EXISTING VS. 3-MONTH BREACH
PEAK EBB SALINITY (PPT)

FIRE ISLAND TO MONTAUK POINT
INLETS STUDY

MOFFATT & NICHOL
ENGINEERS

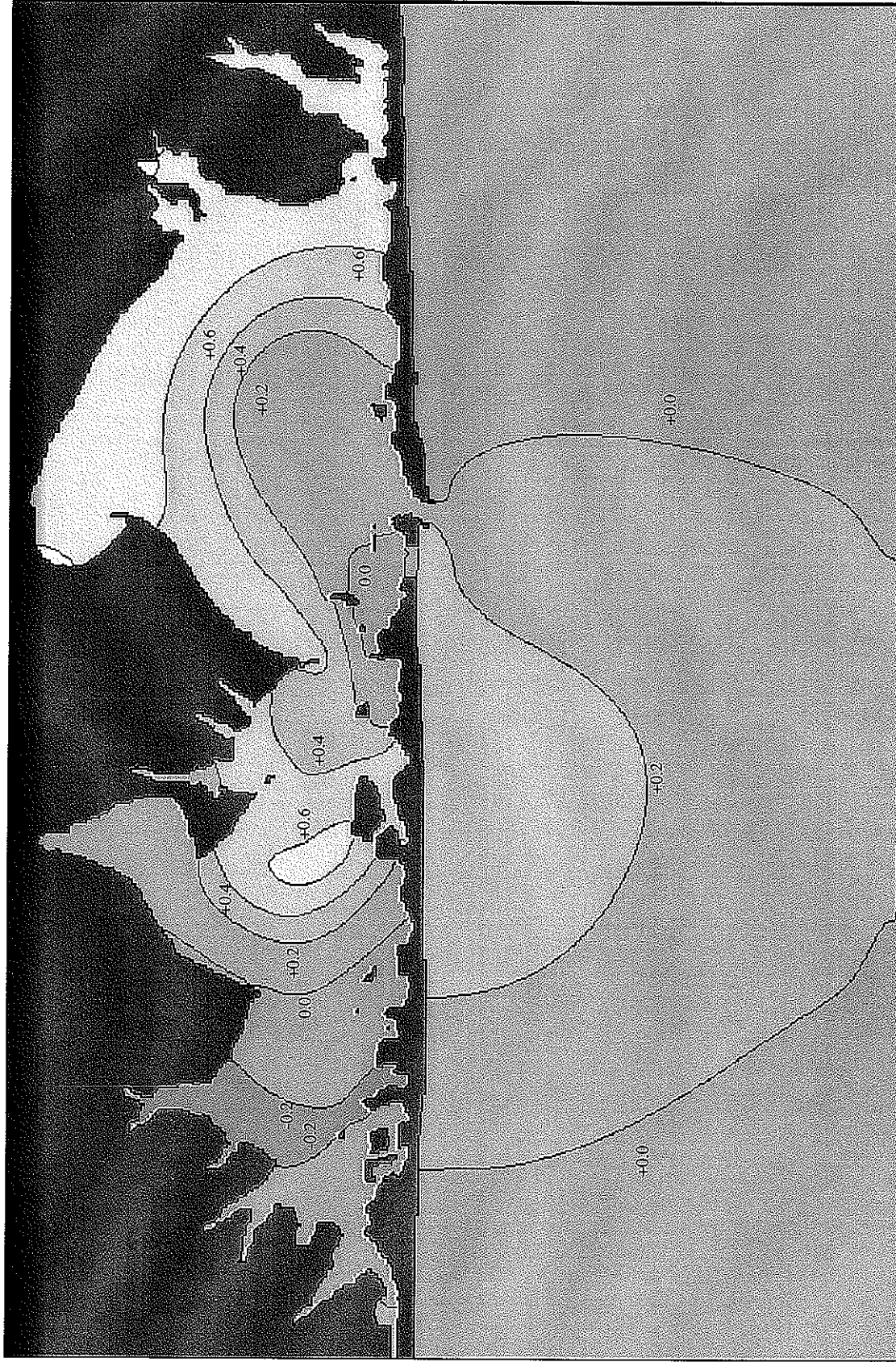


FIGURE 6.22
SHINNECOCK BAY
EXISTING VS. 3-MONTH BREACH
PEAK FLOOD SALINITY (PPT)

FIRE ISLAND TO MONTAUK POINT
INLETS STUDY

Great South Bay Temperature Modeling Results Existing Conditions vs. With-Breach Cases

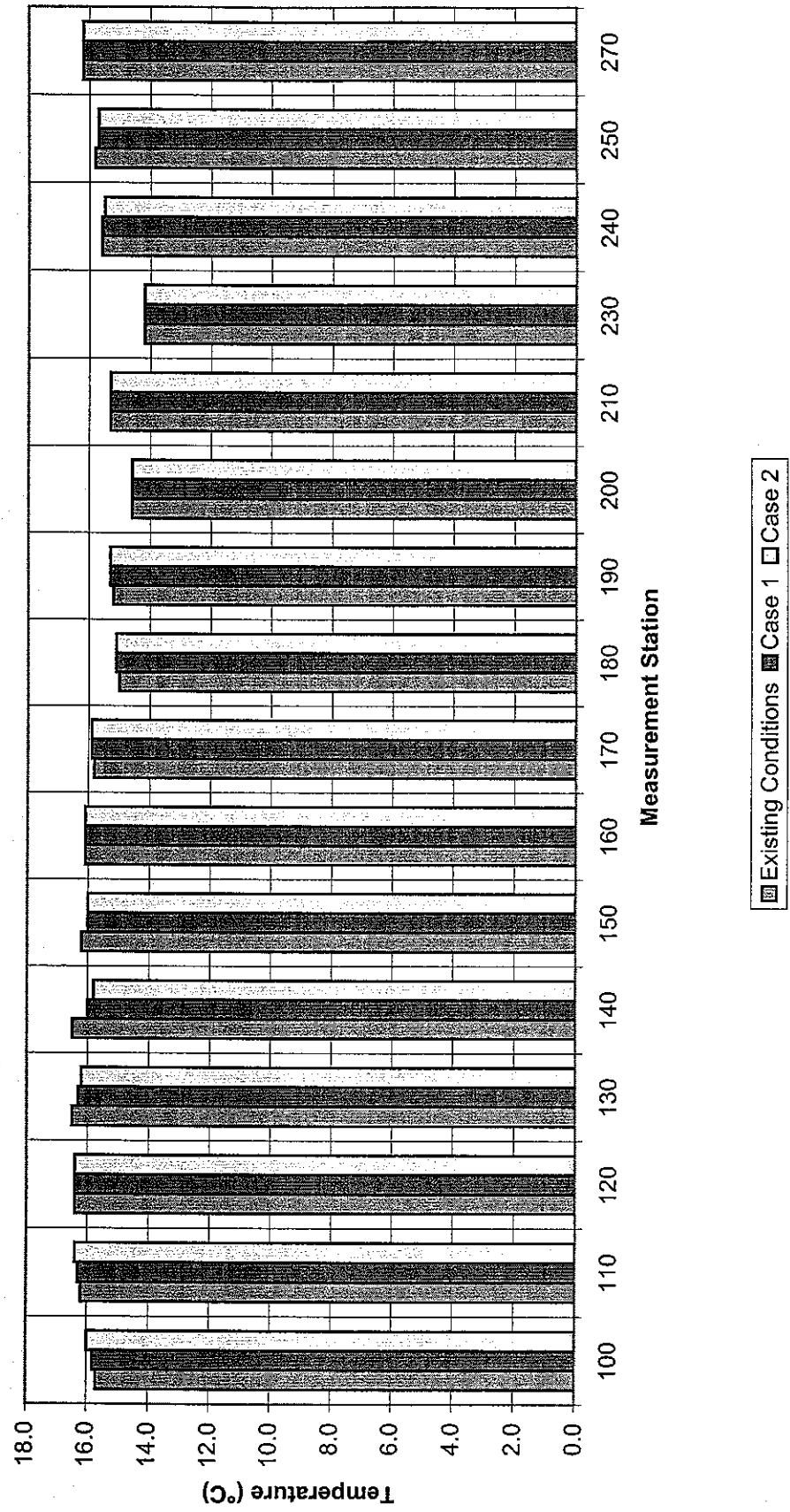


FIGURE 6.23

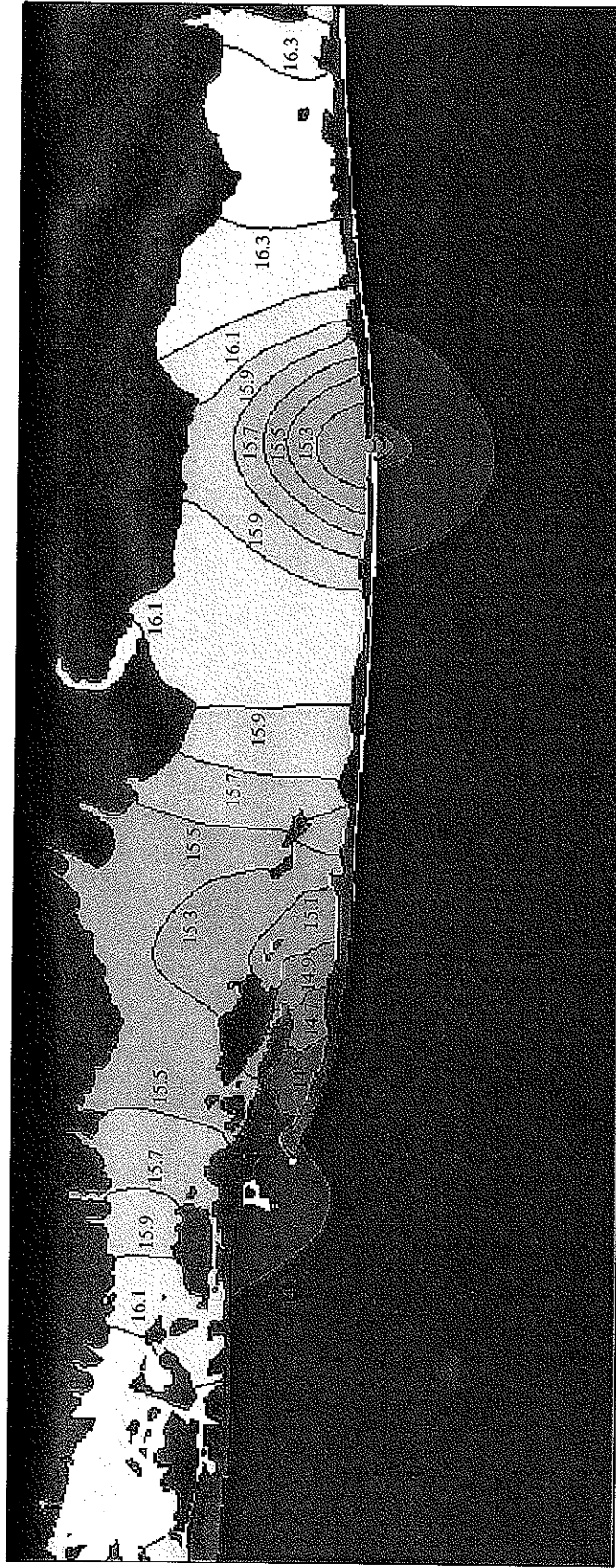


FIGURE 6.24
GREAT SOUTH BAY
3-MONTH BREACH
PEAK EBB TEMPERATURE (°C)

FIRE ISLAND TO MONTAUK POINT
INLETS STUDY

MOFFATT & NICHOL
ENGINEERS

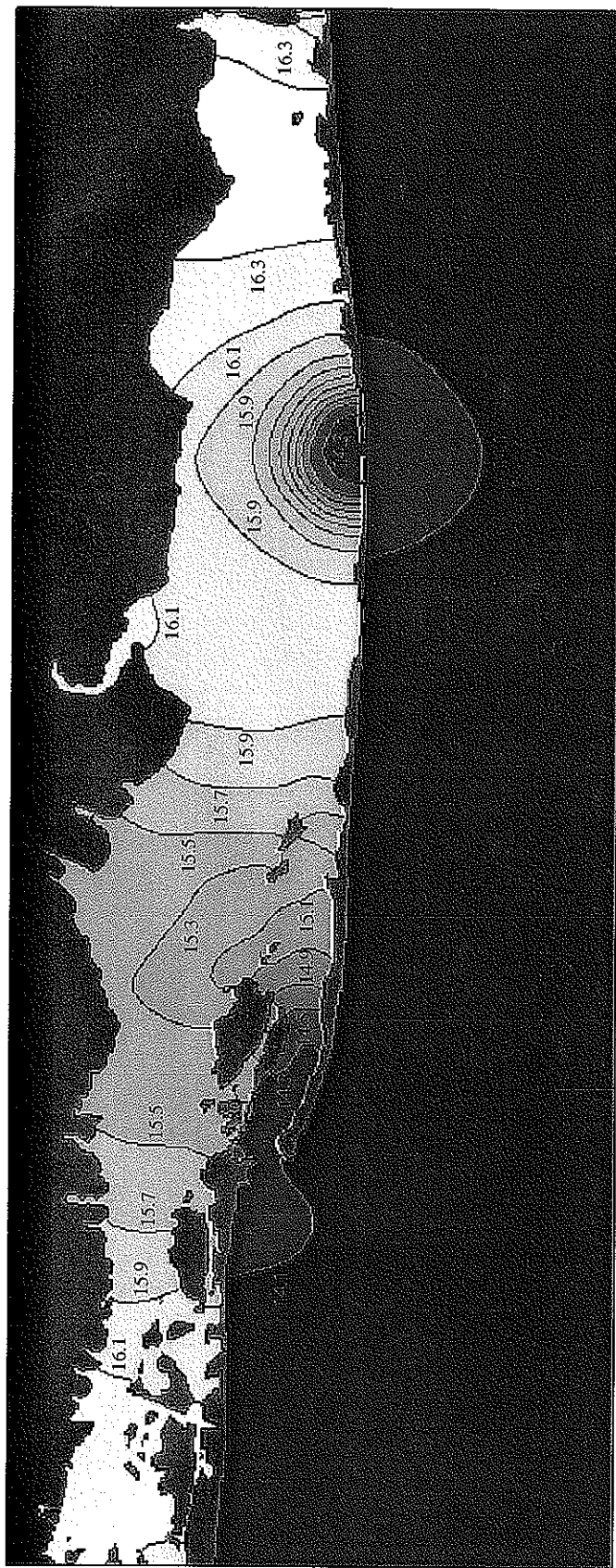


FIGURE 6.25
GREAT SOUTH BAY
3-MONTH BREACH
PEAK FLOOD TEMPERATURE (°C)

FIRE ISLAND TO MONTAUK POINT
INLETS STUDY

MOFFATT & NICHOL
ENGINEERS

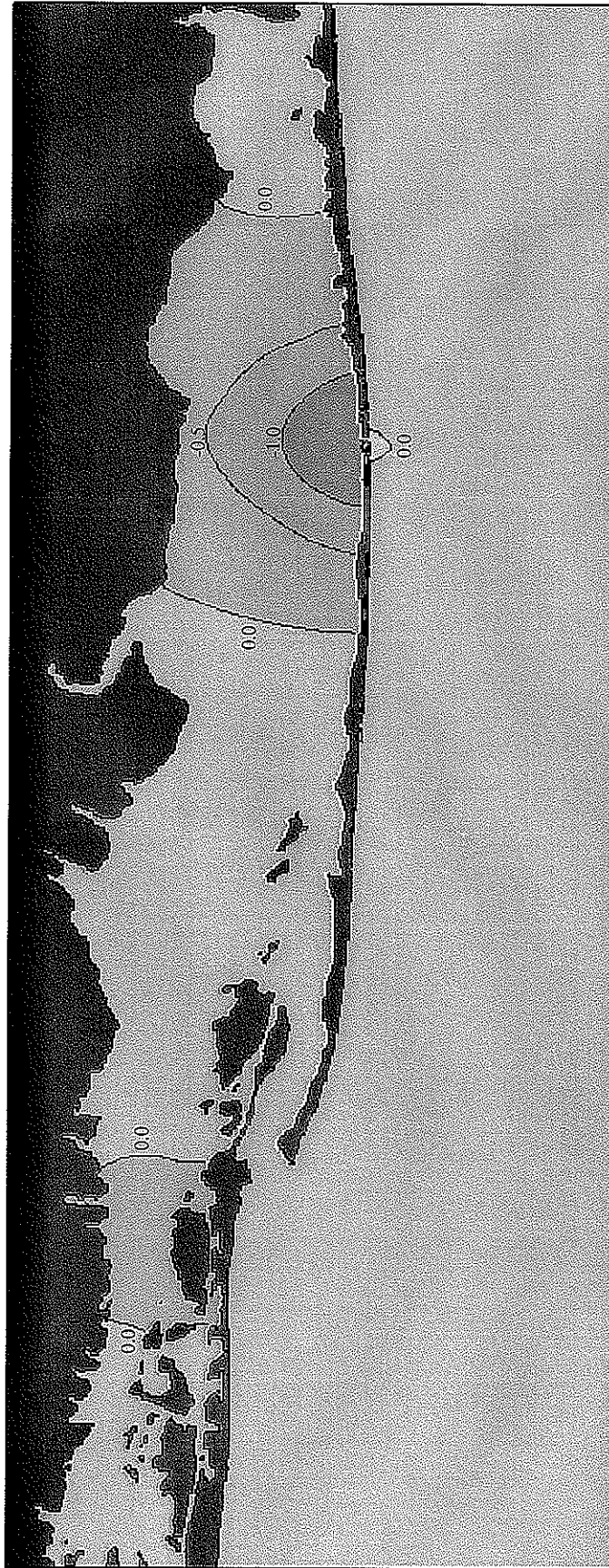


FIGURE 6.26
GREAT SOUTH BAY
EXISTING VS. 3-MONTH BREACH
PEAK EBB TEMPERATURE (°C)

FIRE ISLAND TO MONTAUK POINT
INLETS STUDY

MOFFATT & NICHOL
ENGINEERS

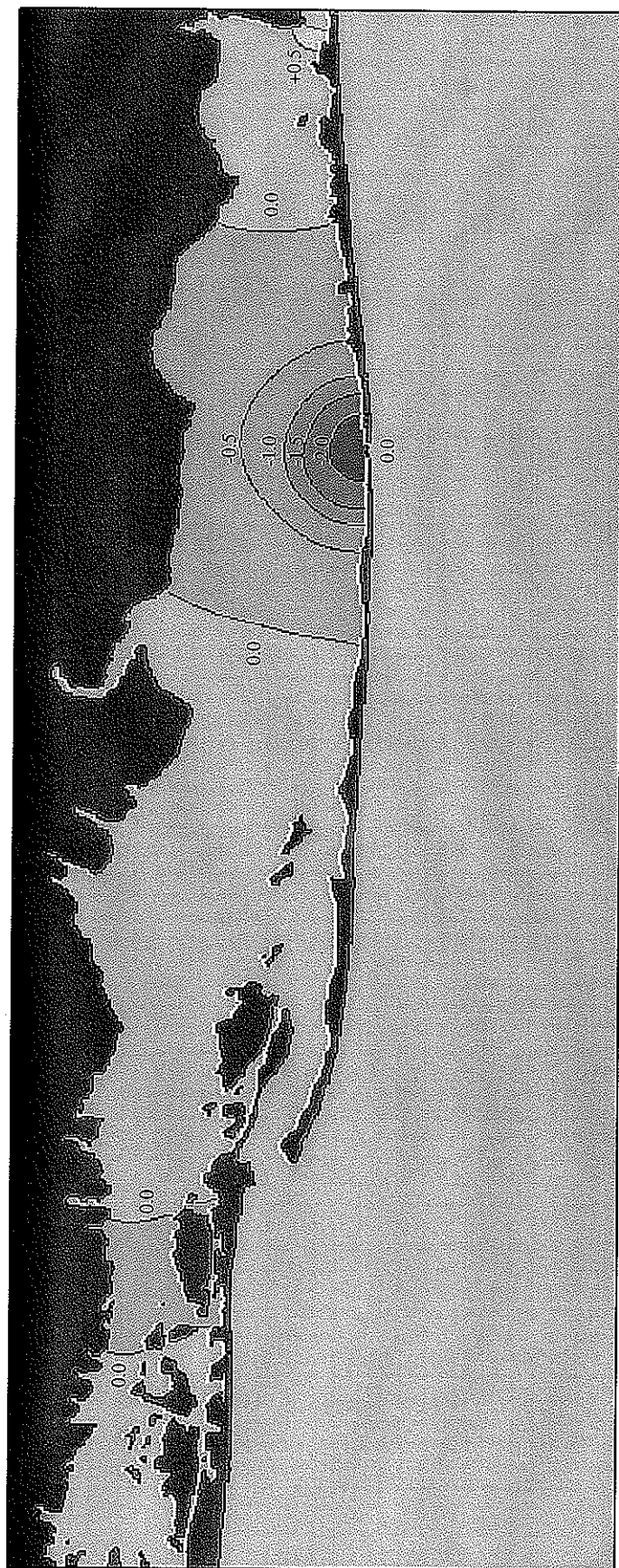


FIGURE 6.27
GREAT SOUTH BAY
EXISTING VS. 3-MONTH BREACH
PEAK FLOOD TEMPERATURE (°C)

FIRE ISLAND TO MONTAUK POINT
INLETS STUDY

MOFFATT & NICHOL
ENGINEERS

Moriches Bay Temperature Modeling Results **Existing Conditions vs. With-Breach Cases**

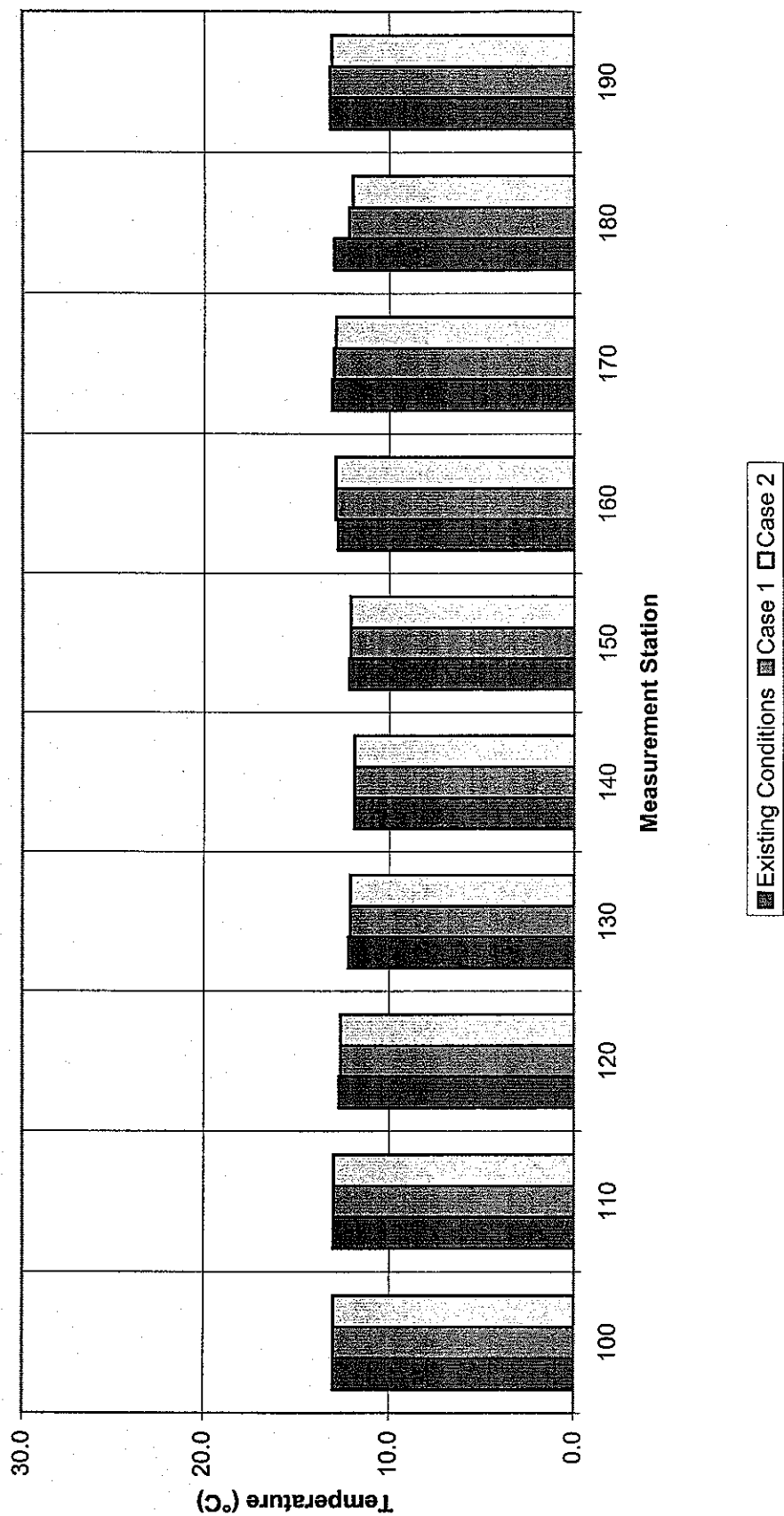


FIGURE 6.28

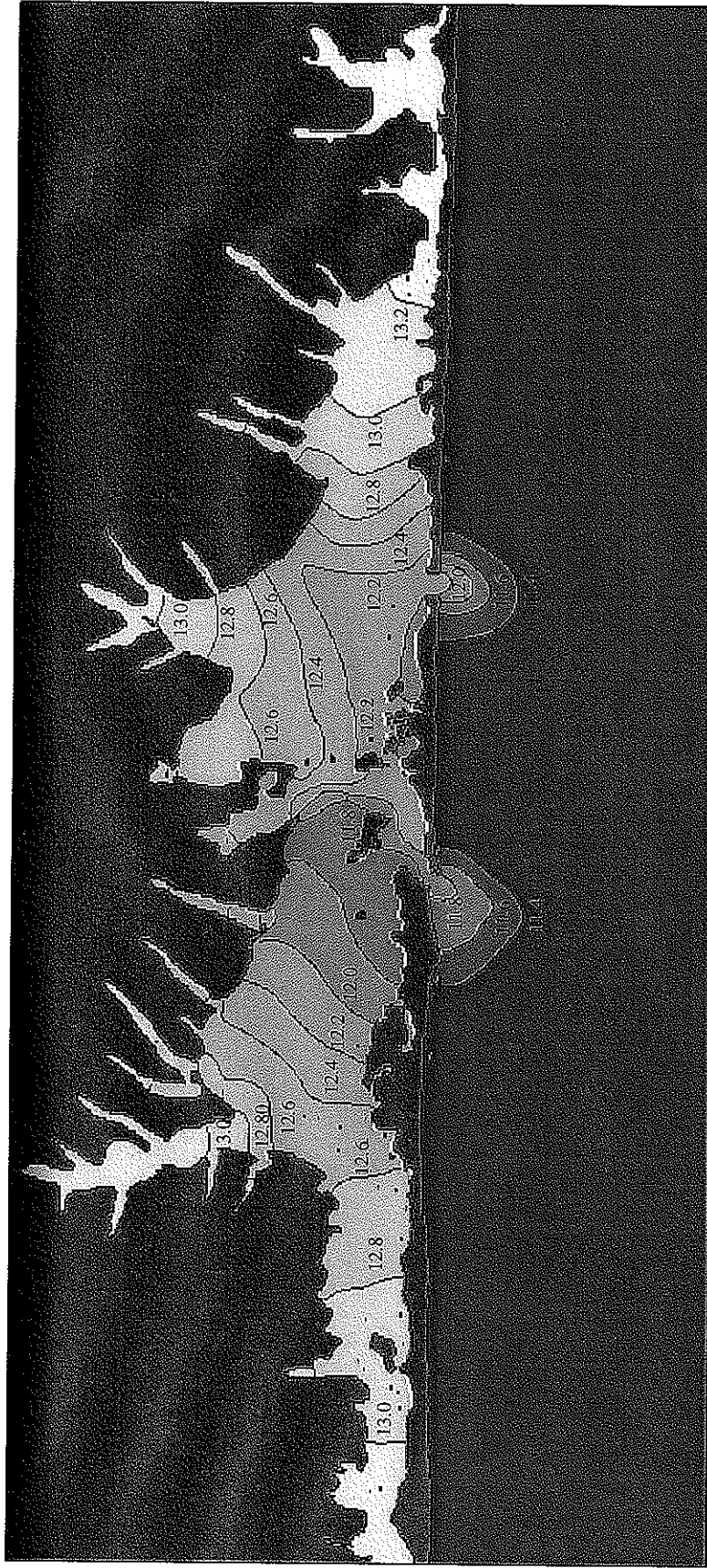


FIGURE 6.29
MORICHES BAY
3-MONTH BREACH
PEAK EBB TEMPERATURE (°C)

FIRE ISLAND TO MONTAUK POINT
INLETS STUDY

MOFFATT & NICHOL
ENGINEERS

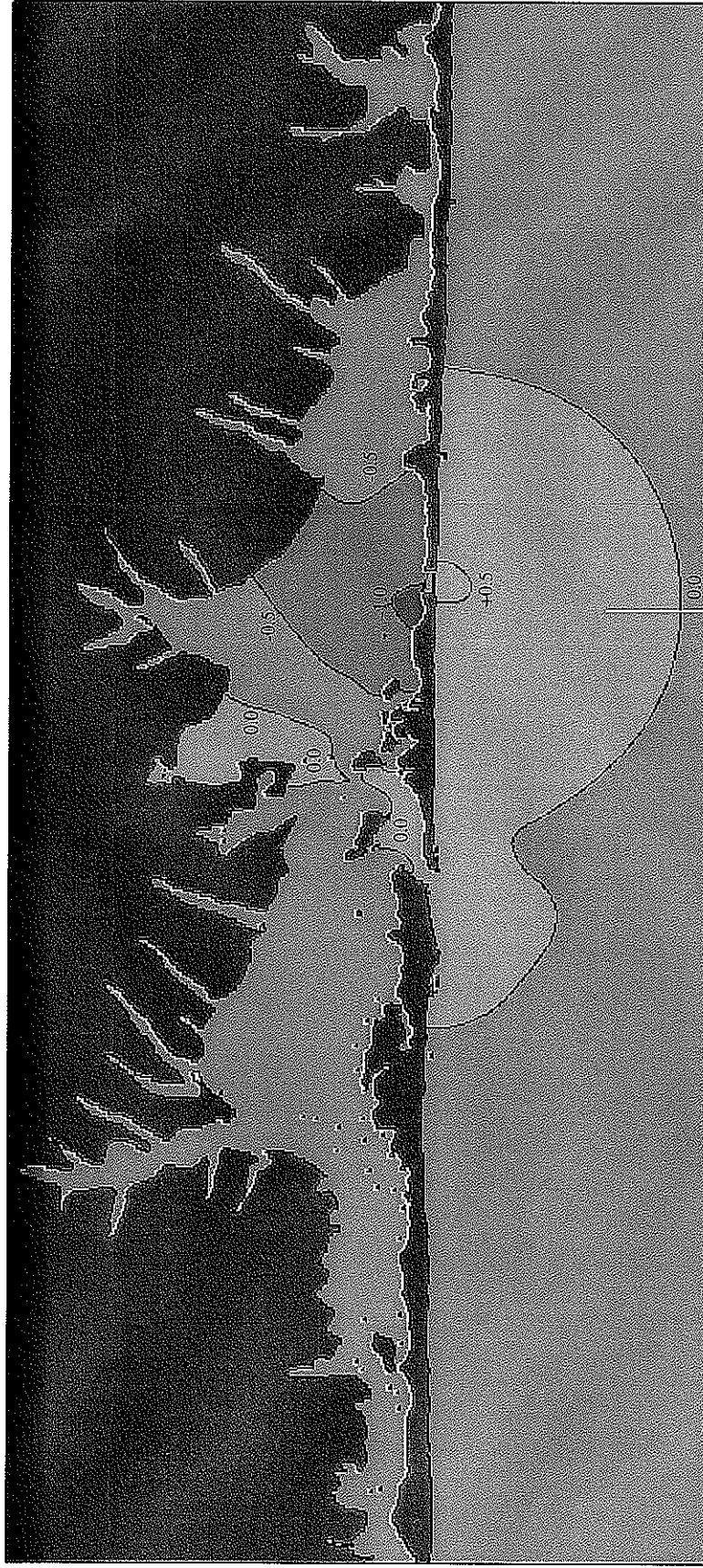


FIGURE 6.31
MORICHES BAY
EXISTING VS. 3-MONTH BREACH
PEAK EBB TEMPERATURE (°C)

FIRE ISLAND TO MONTAUK POINT
INLETS STUDY



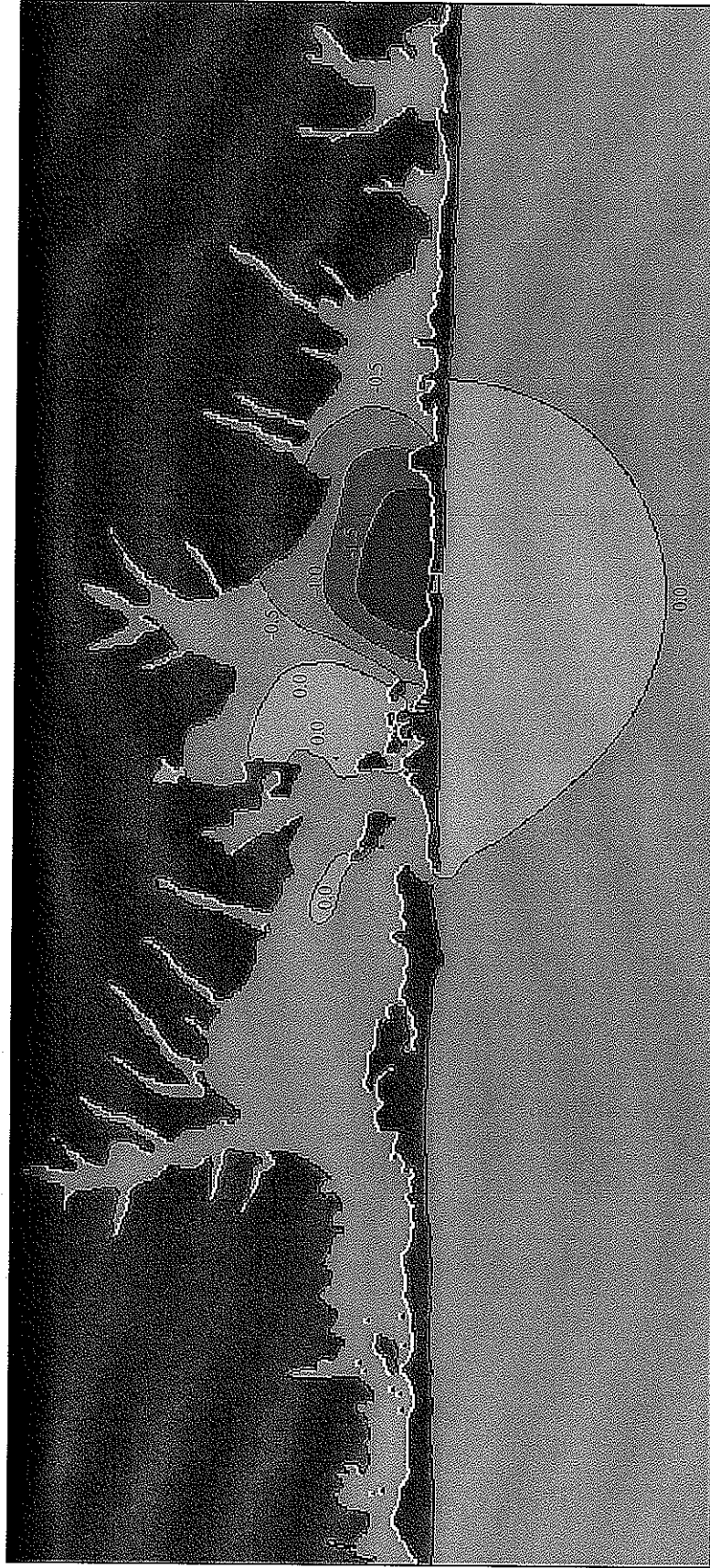


FIGURE 6.32
MORICHES BAY
EXISTING VS. 3-MONTH BREACH
PEAK FLOOD TEMPERATURE (°C)

FIRE ISLAND TO MONTAUK POINT
INLETS STUDY

MOFFATT & NICHOL
ENGINEERS

Shinnecock Bay Temperature Modeling Results **Existing Conditions vs. With-Breach Cases**

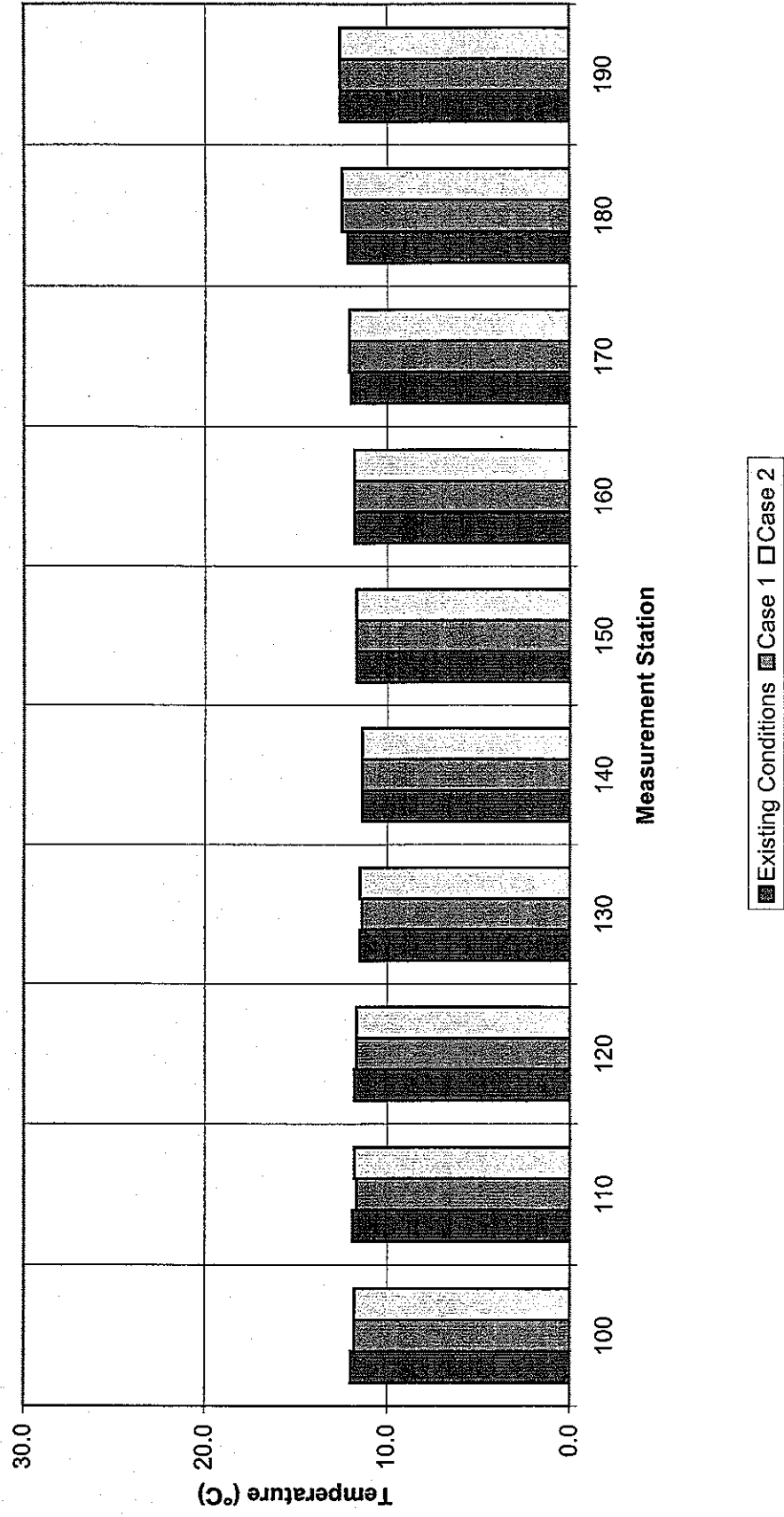


FIGURE 6.33

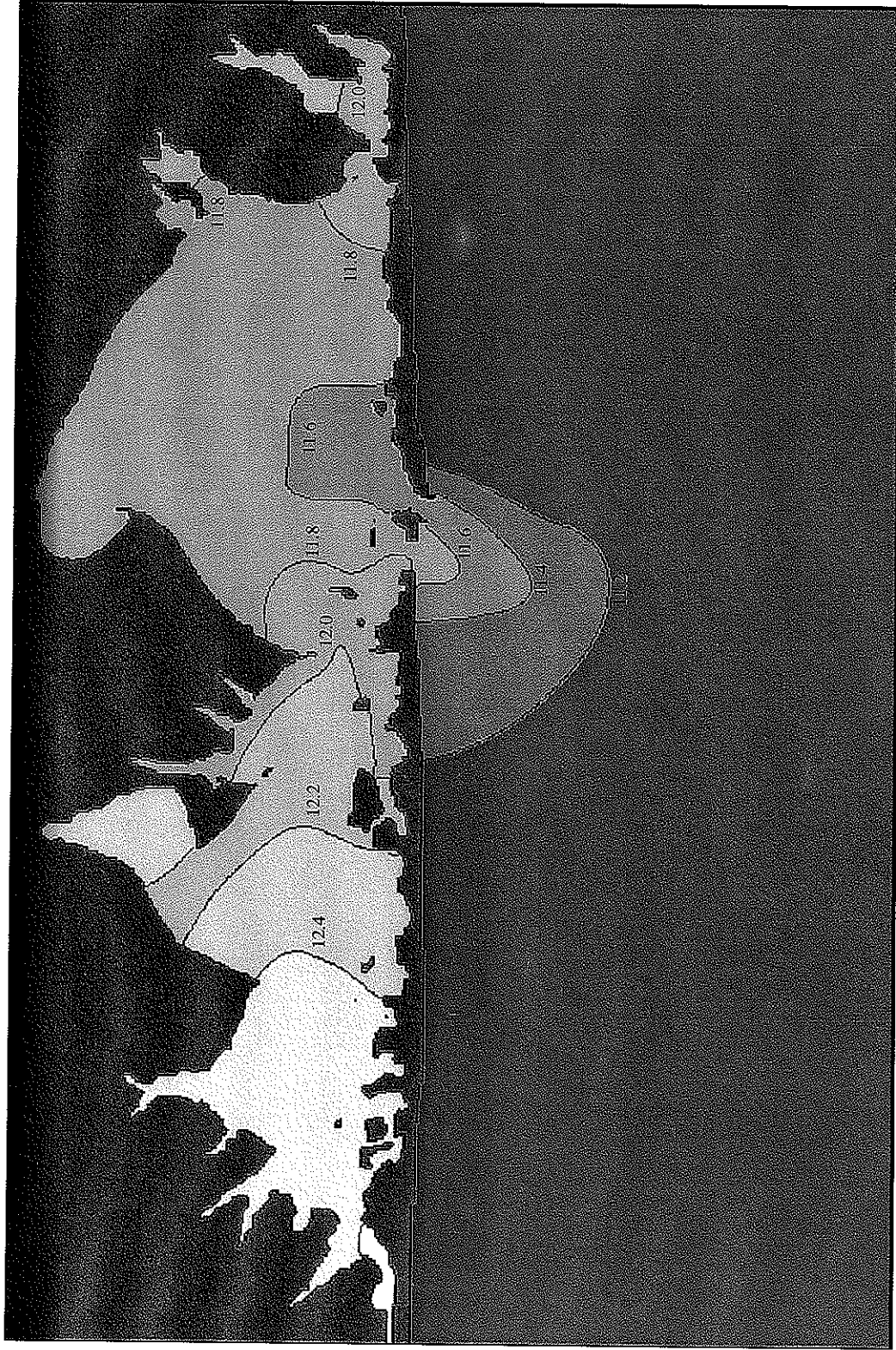


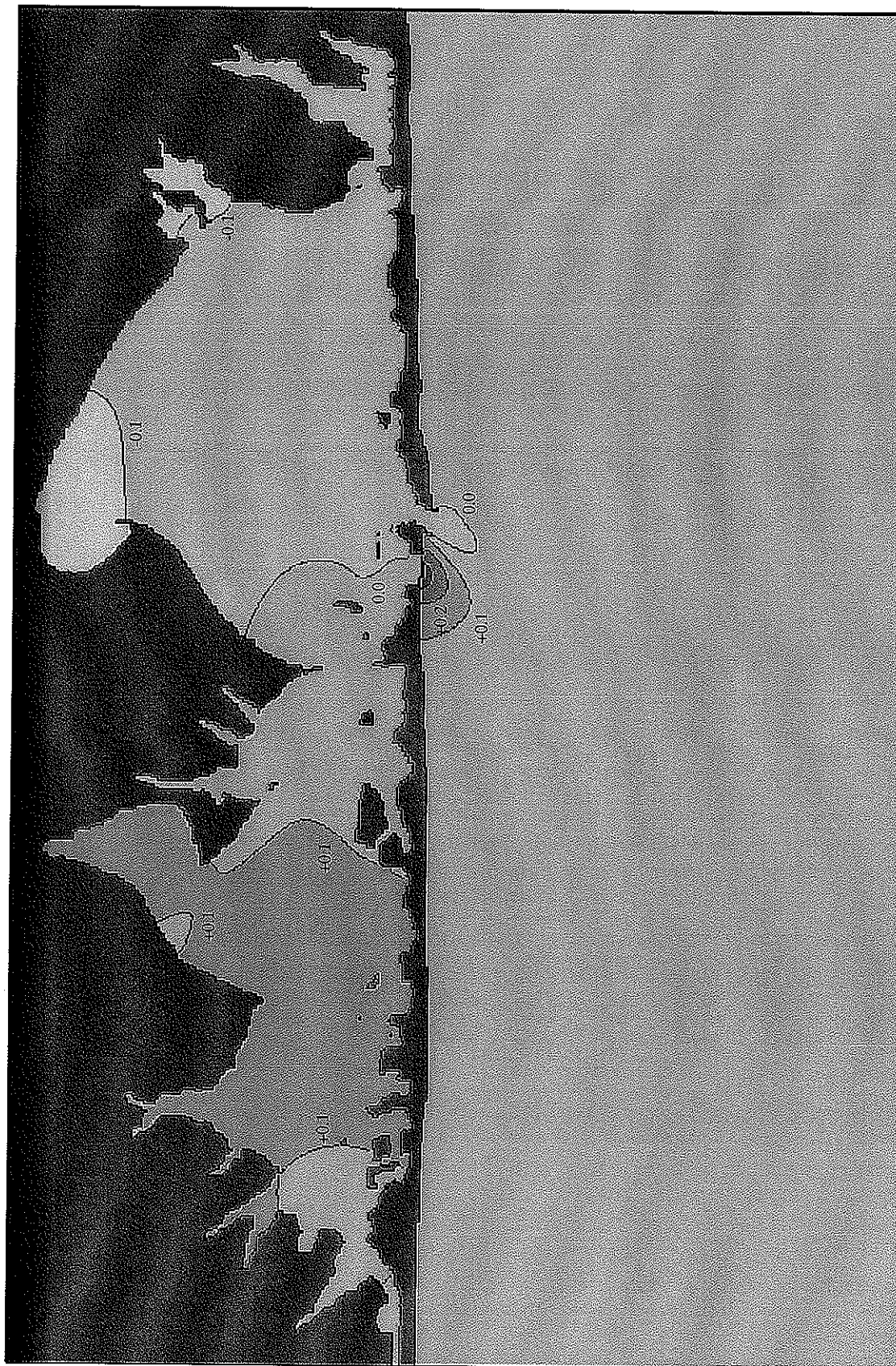
FIGURE 6.34
SHINNECOCK BAY
3-MONTH BREACH
PEAK EBB TEMPERATURE (°C)

FIRE ISLAND TO MONTAUK POINT
INLETS STUDY



FIGURE 6.35
SHINNECOCK BAY
3-MONTH BREACH
PEAK FLOOD TEMPERATURE (°C)

FIRE ISLAND TO MONTAUK POINT
INLETS STUDY



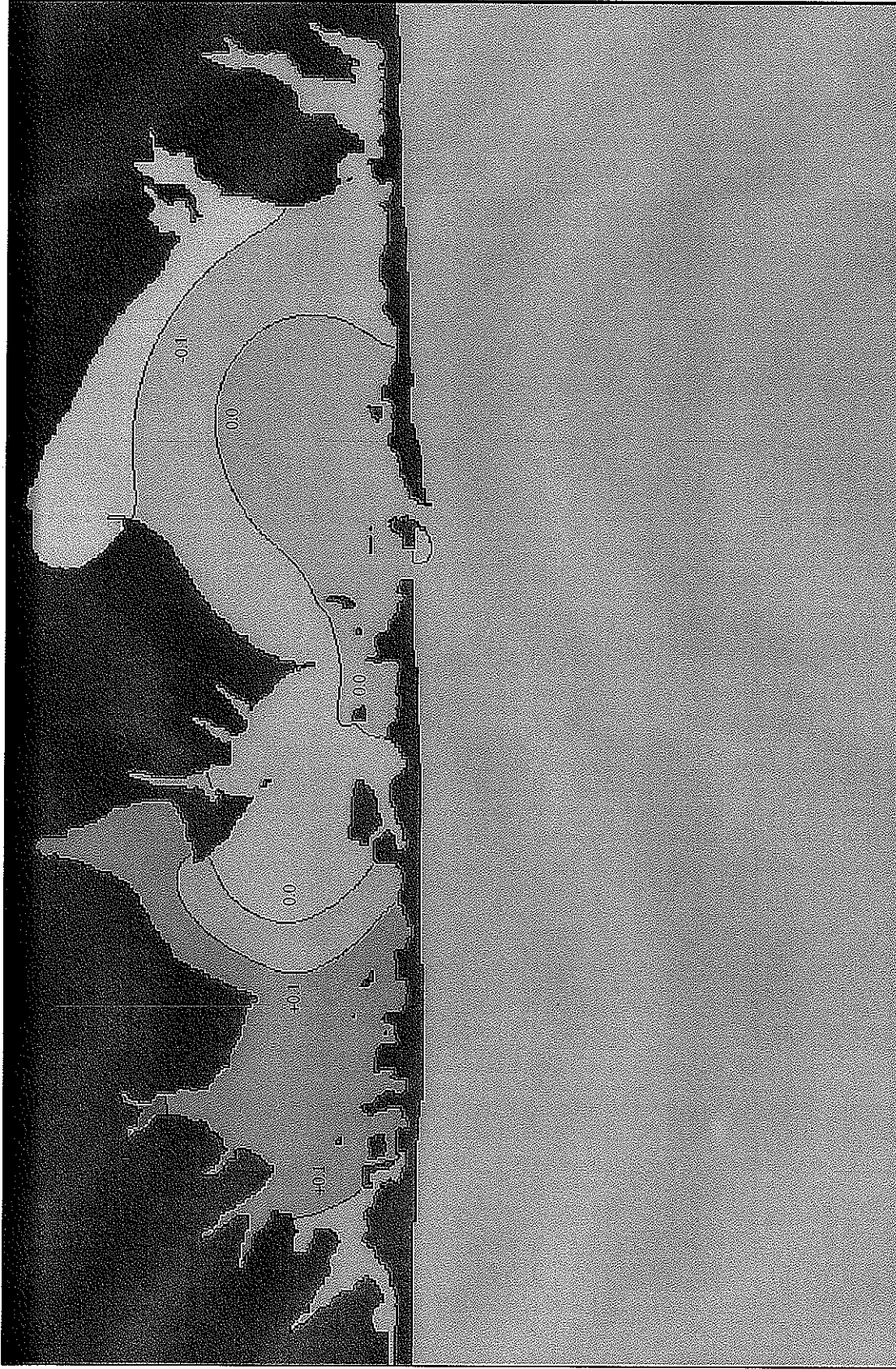



FIGURE 6.37
SHINNECOCK BAY
EXISTING VS. 3-MONTH BREACH
PEAK FLOOD TEMPERATURE (°C)

FIRE ISLAND TO MONTAUK POINT
INLETS STUDY



FIGURE 6.38
GREAT SOUTH BAY
3-MONTH BREACH
RESIDENCE TIME (DAY)

FIRE ISLAND TO MONTAUK POINT INLETS STUDY



MOFFATT & NICHOL
ENGINEERS



FIGURE 6.39
GREAT SOUTH BAY
EXISTING VS. 3-MONTH BREACH
RESIDENCE TIME (DAY)

FIRE ISLAND TO MONTAUK POINT
INLETS STUDY

MOFFATT & NICHOL
ENGINEERS



FIGURE 6.40
MORICHES BAY
3-MONTH BREACH
RESIDENCE TIME (DAY)

FIRE ISLAND TO MONTAUK POINT
INLETS STUDY

MOFFATT & NICHOL
ENGINEERS



FIGURE 6.41
MORICHES BAY
EXISTING VS. 3-MONTH BREACH
RESIDENCE TIME (DAY)

FIRE ISLAND TO MONTAUK POINT
INLETS STUDY

MOFFATT & NICHOL
ENGINEERS



FIGURE 6.42
SHINNECOCK BAY
3-MONTH BREACH
RESIDENCE TIME (DAY)

FIRE ISLAND TO MONTAUK POINT
INLETS STUDY

MOFFATT & NICHOL
ENGINEERS

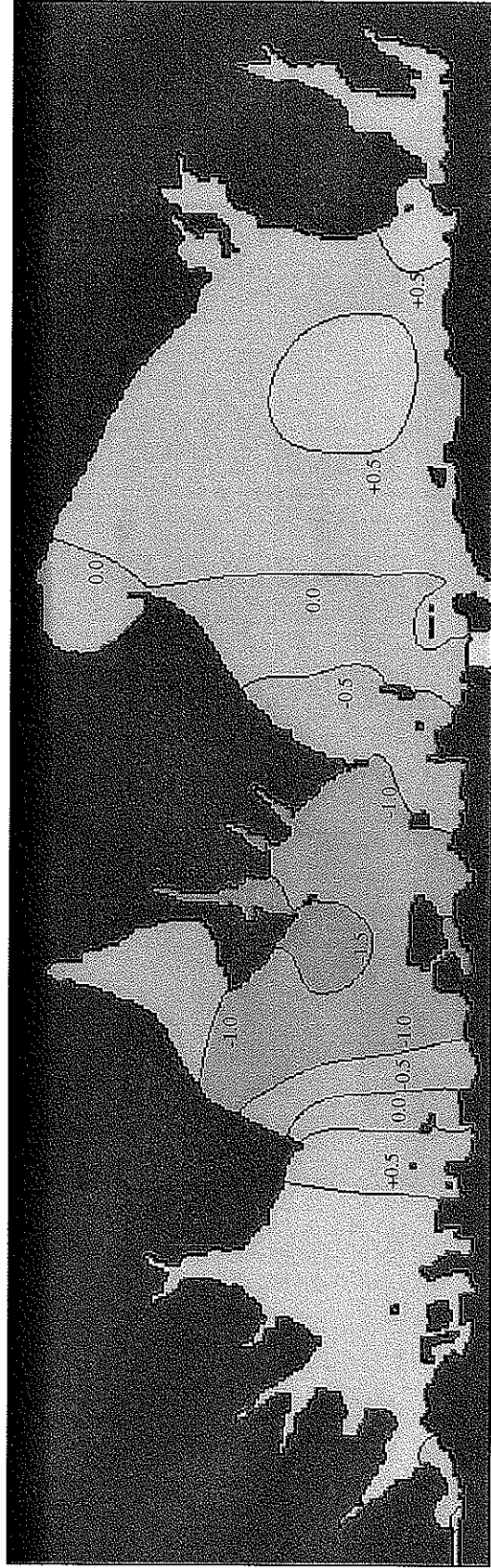


FIGURE 6.43
SHINNECOCK BAY
EXISTING VS. 3-MONTH BREACH
RESIDENCE TIME (DAY)

FIRE ISLAND TO MONTAUK POINT
INLETS STUDY

MOFFATT & NICHOL
ENGINEERS

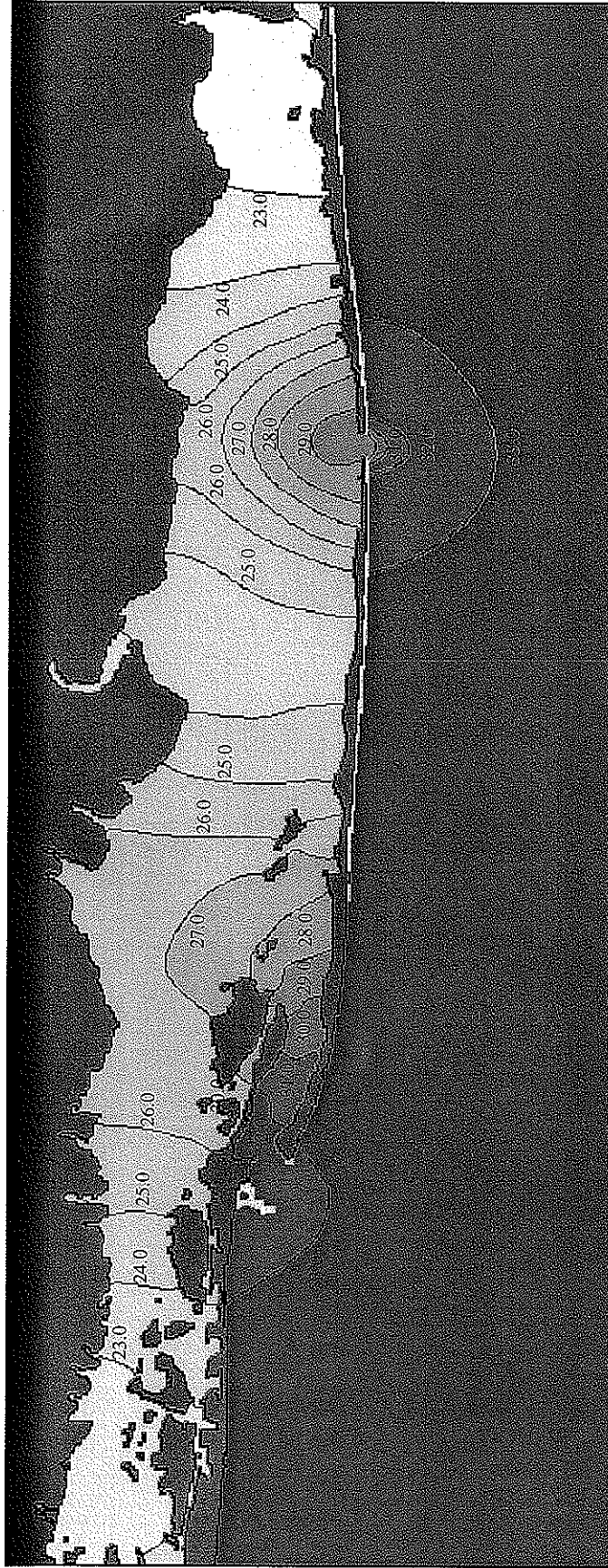


FIGURE 6.44
GREAT SOUTH BAY
9-MONTH BREACH
PEAK EBB SALINITY (PPT)

FIRE ISLAND TO MONTAUK POINT
INLETS STUDY



FIGURE 6.45
GREAT SOUTH BAY
9-MONTH BREACH
PEAK FLOOD SALINITY (PPT)

FIRE ISLAND TO MONTAUK POINT
INLETS STUDY

MOFFATT & NICHOL
ENGINEERS

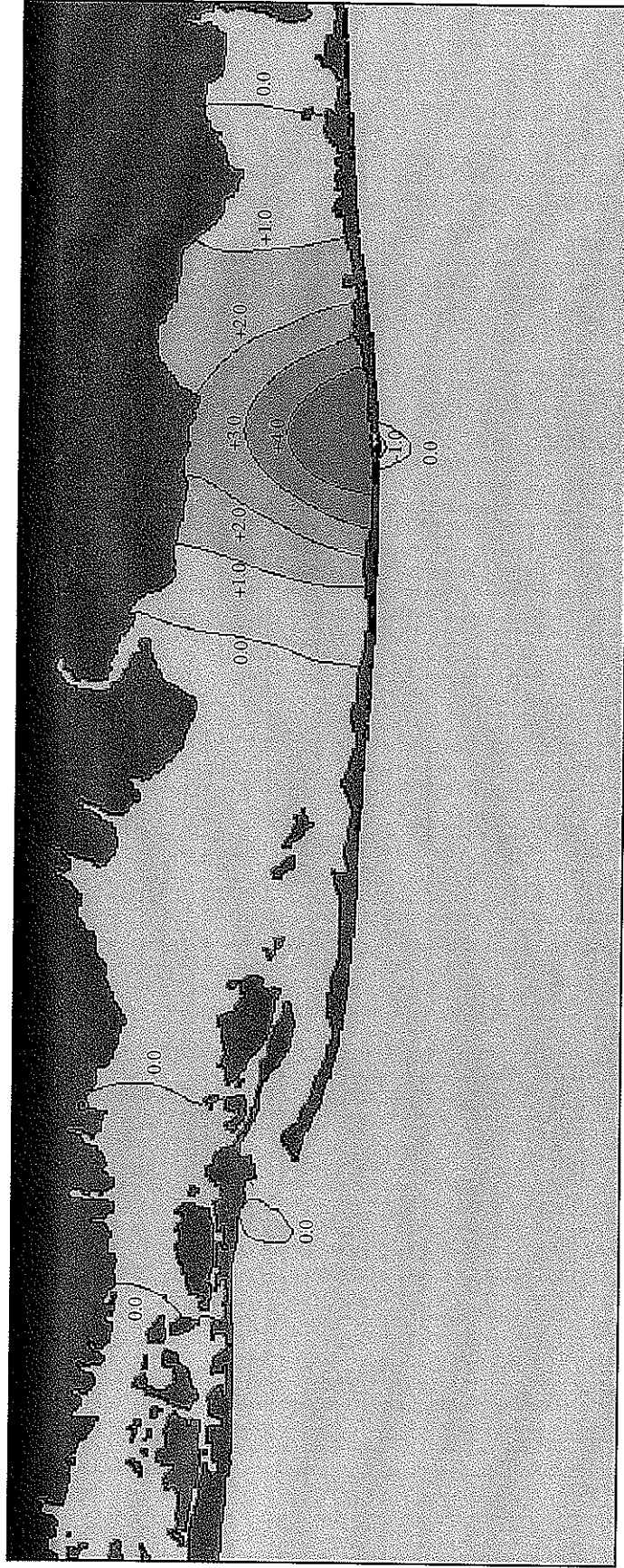


FIGURE 6.46
GREAT SOUTH BAY
EXISTING VS. 9-MONTH BREACH
PEAK EBB SALINITY (PPT)

FIRE ISLAND TO MONTAUK POINT
INLETS STUDY

MOFFATT & NICHOL
ENGINEERS

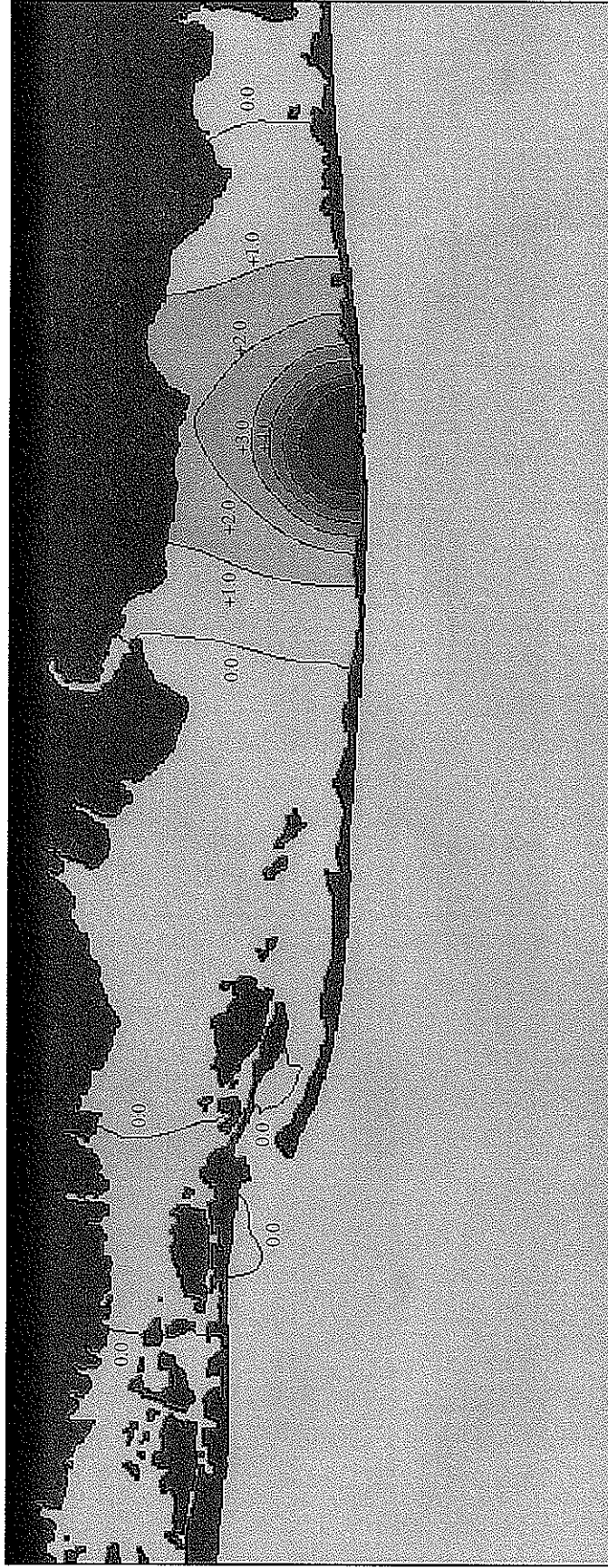


FIGURE 6.47
GREAT SOUTH BAY
EXISTING VS. 9-MONTH BREACH
PEAK FLOOD SALINITY (PPT)

FIRE ISLAND TO MONTAUK POINT
INLETS STUDY

MOFFATT & NICHOL
ENGINEERS

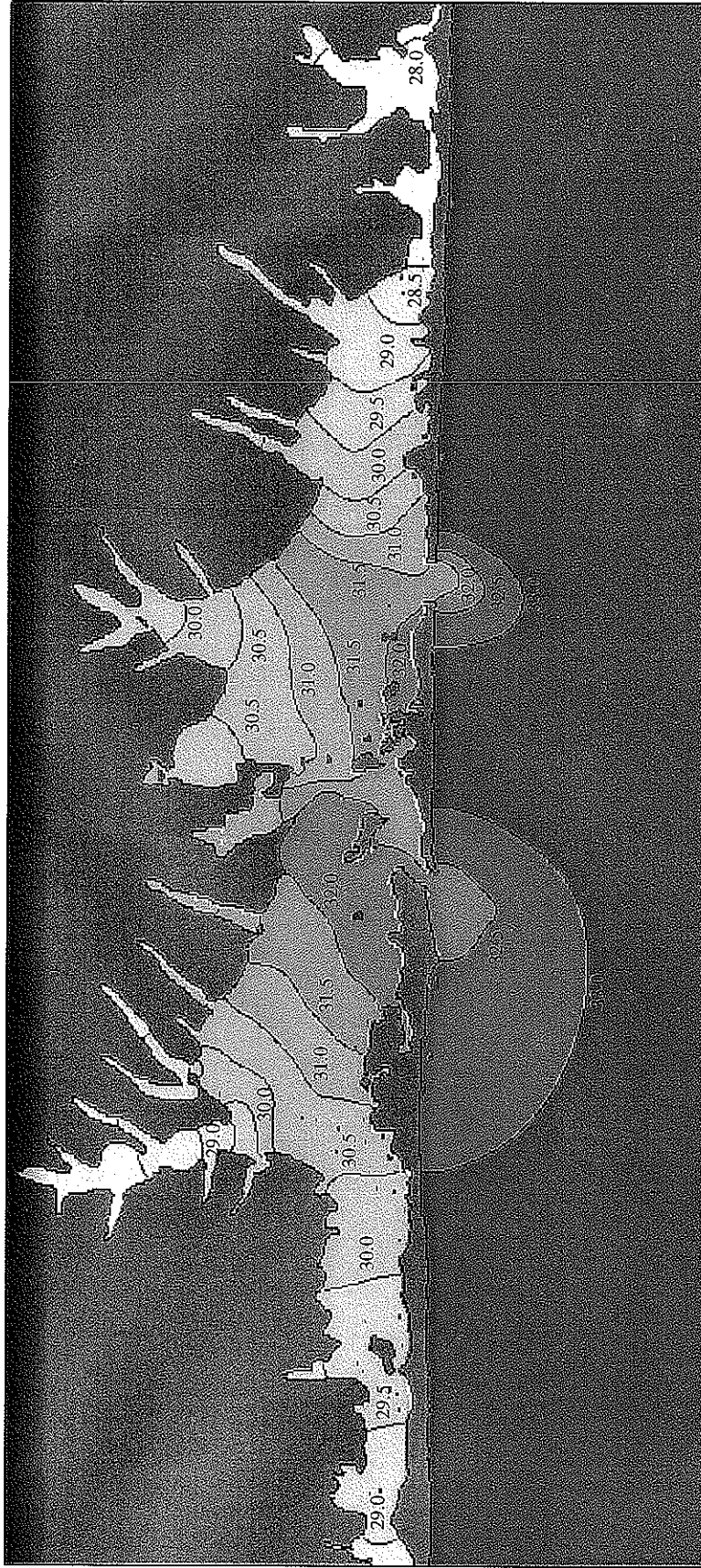


FIGURE 6.48
MORICHES BAY
9-MONTH BREACH
PEAK EBB SALINITY (PPT)

FIRE ISLAND TO MONTAUK POINT
INLETS STUDY

MOFFATT & NICHOL
ENGINEERS

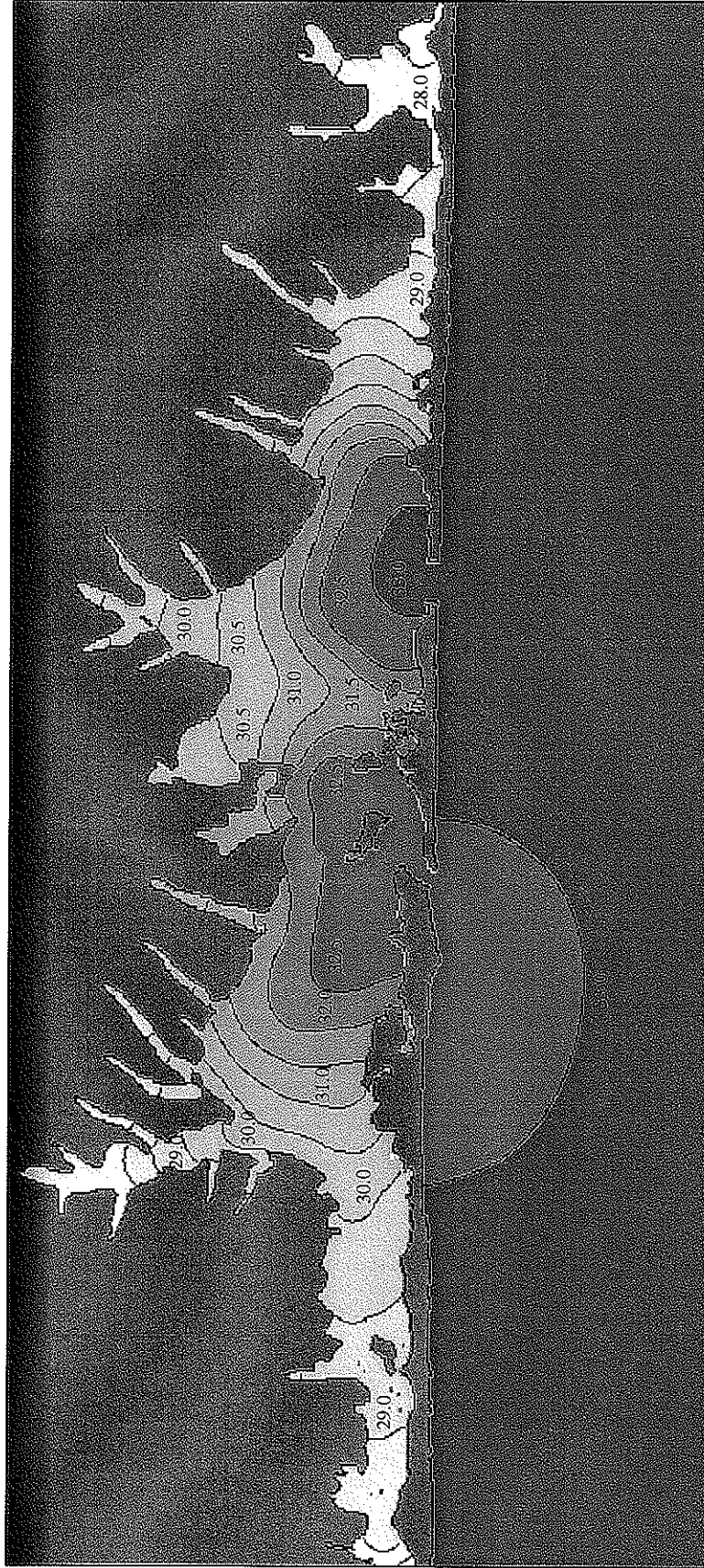


FIGURE 6.49
MORICHES BAY
9-MONTH BREACH
PEAK FLOOD SALINITY (PPT)

FIRE ISLAND TO MONTAUK POINT
INLETS STUDY

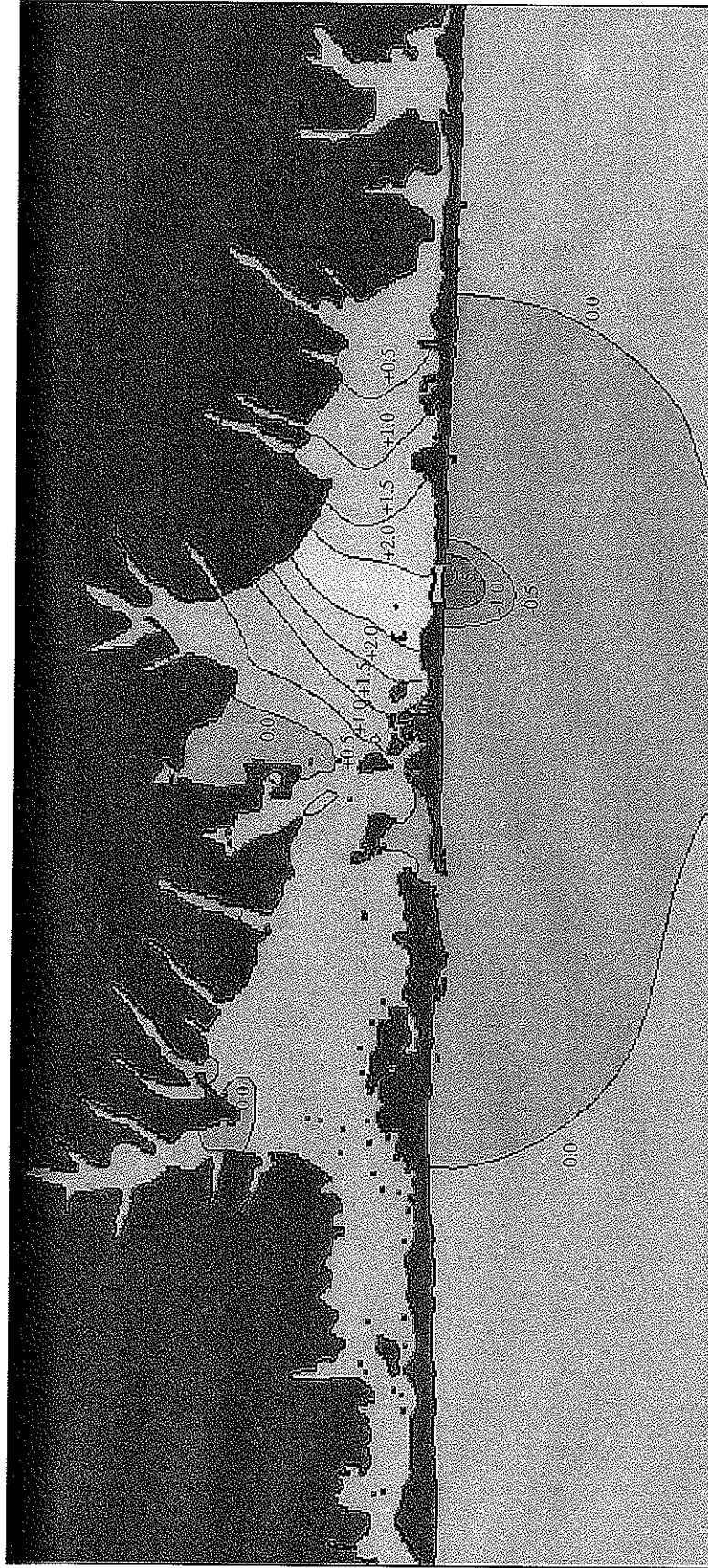


FIGURE 6.50
MORICHES BAY
EXISTING VS. 9-MONTH BREACH
PEAK EBB SALINITY (PPT)

FIRE ISLAND TO MONTAUK POINT
INLETS STUDY

MOFFATT & NICHOL
ENGINEERS

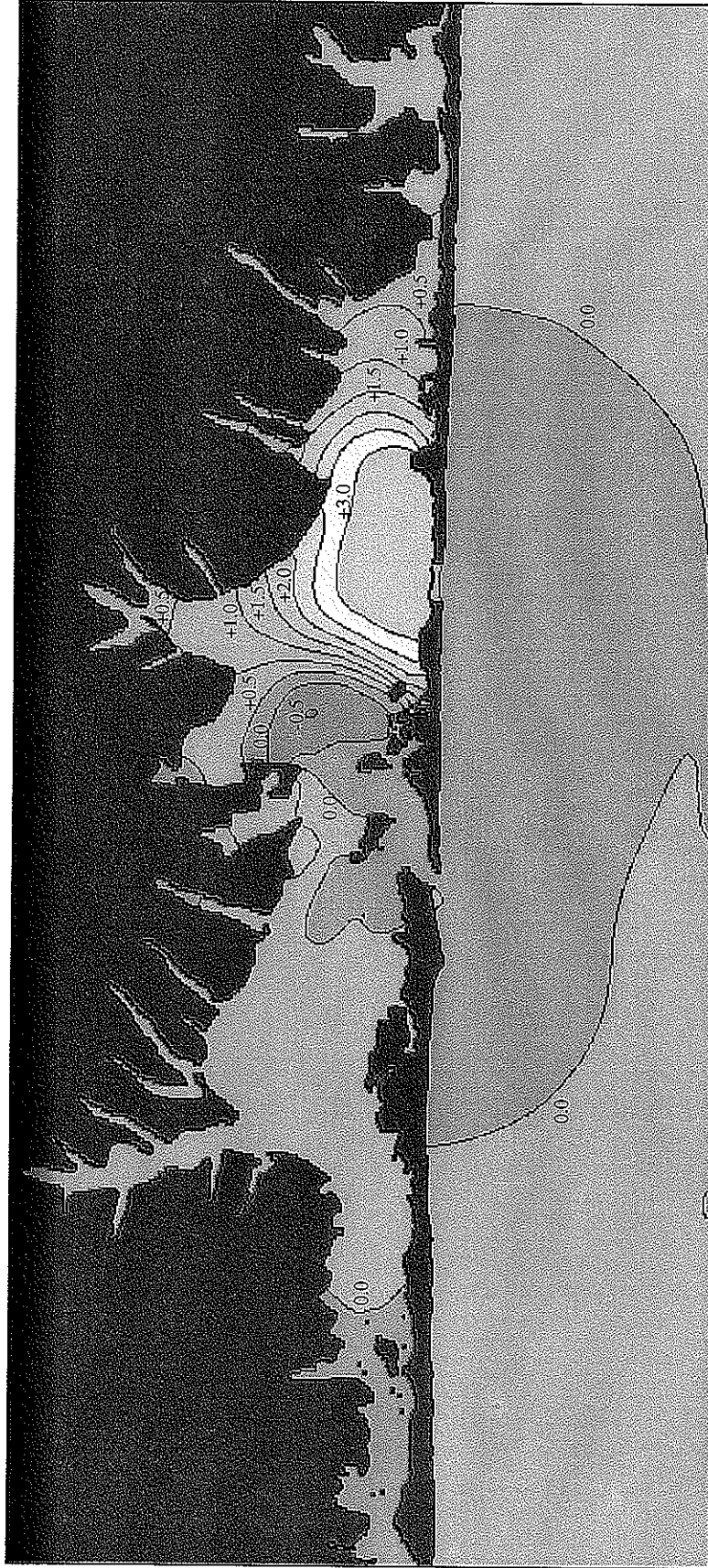


FIGURE 6.51
MORICHES BAY
EXISTING VS. 9-MONTH BREACH
PEAK FLOOD SALINITY (PPT)

FIRE ISLAND TO MONTAUK POINT
INLETS STUDY

MOFFATT & NICHOL
ENGINEERS

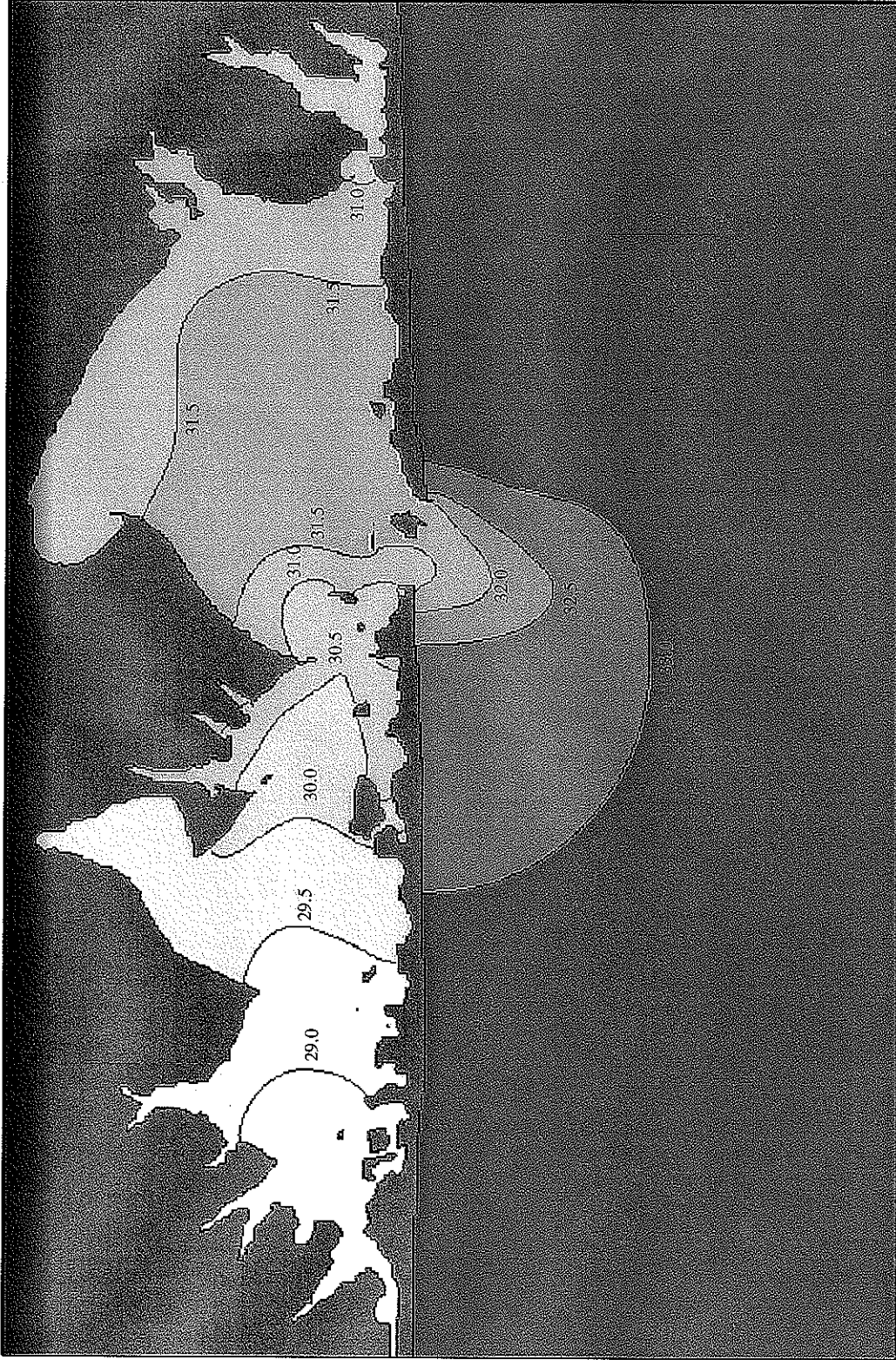
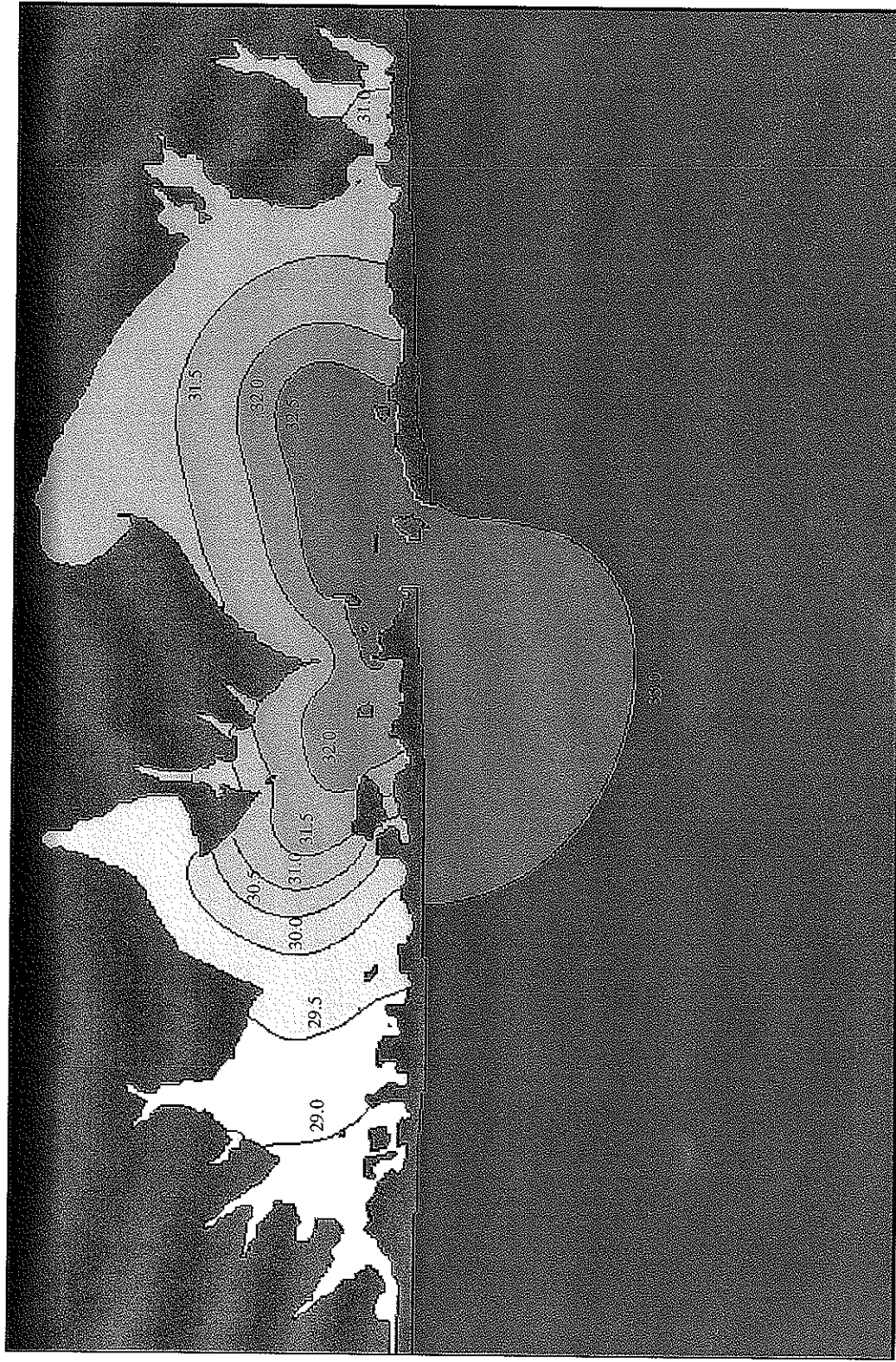


FIGURE 6.52
SHINNECOCK BAY
9-MONTH BREACH
PEAK EBB SALINITY (PPT)

FIRE ISLAND TO MONTAUK POINT
INLETS STUDY



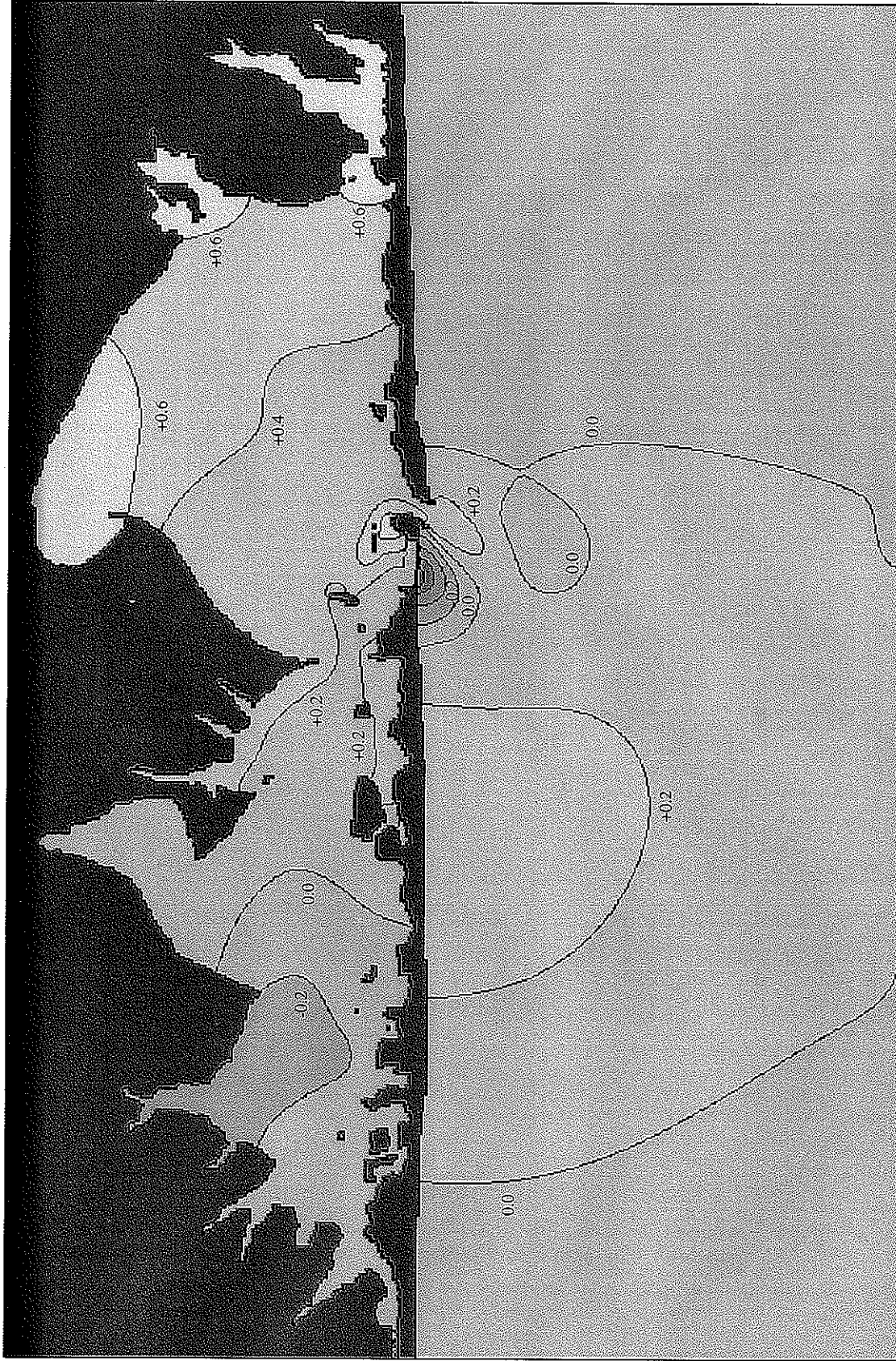


FIGURE 6.54
SHINNECOCK BAY
EXISTING VS. 9-MONTH BREACH
PEAK EBB SALINITY (PPT)

FIRE ISLAND TO MONTAUK POINT
INLETS STUDY

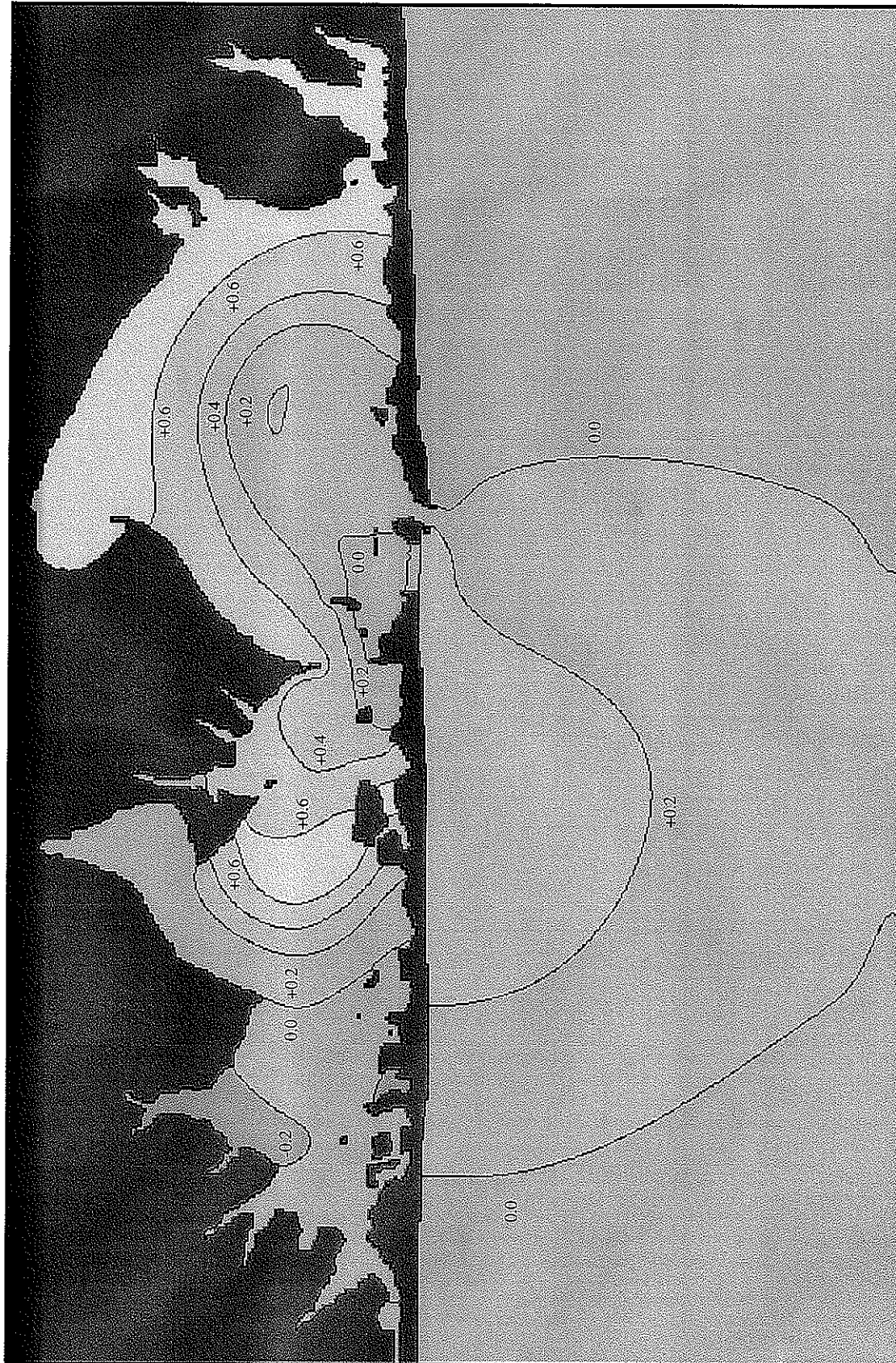


FIGURE 6.55
SHINNECOCK BAY
EXISTING VS. 9-MONTH BREACH
PEAK FLOOD SALINITY (PPT)

FIRE ISLAND TO MONTAUK POINT
INLETS STUDY

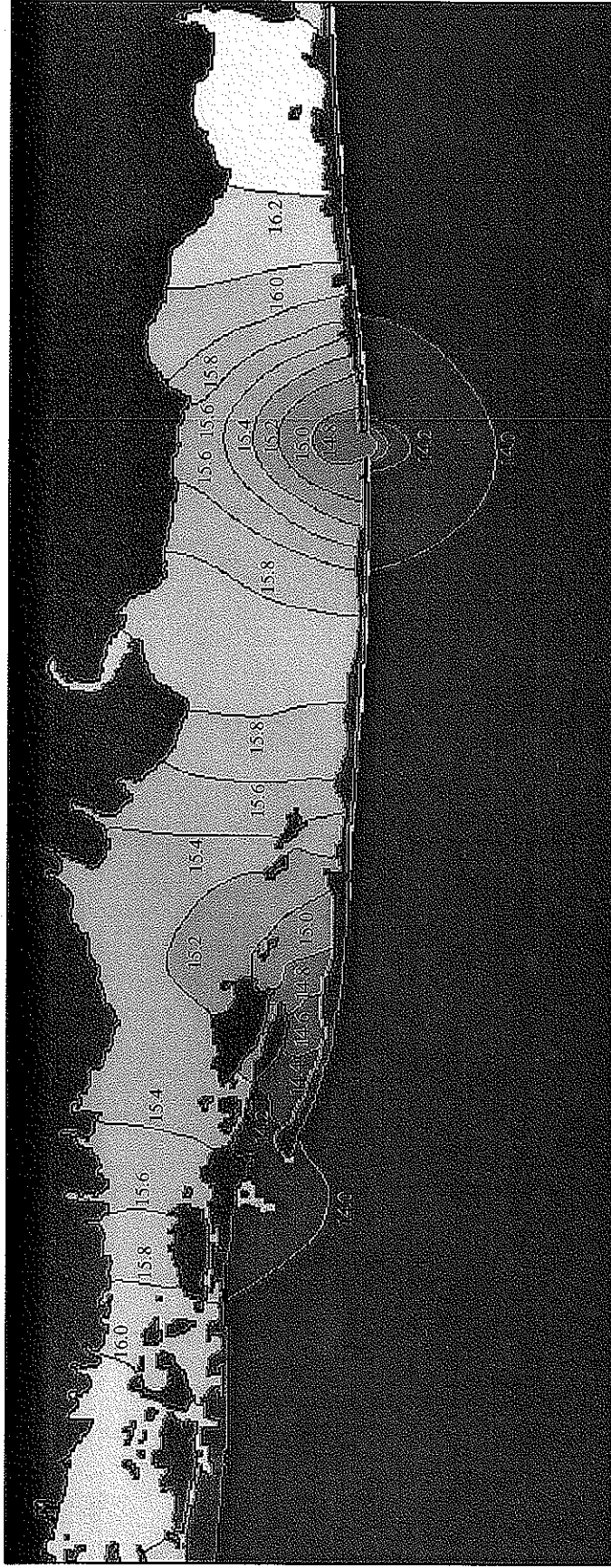


FIGURE 6.56
GREAT SOUTH BAY
9-MONTH BREACH
PEAK EBB TEMPERATURE (°C)

FIRE ISLAND TO MONTAUK POINT
INLETS STUDY

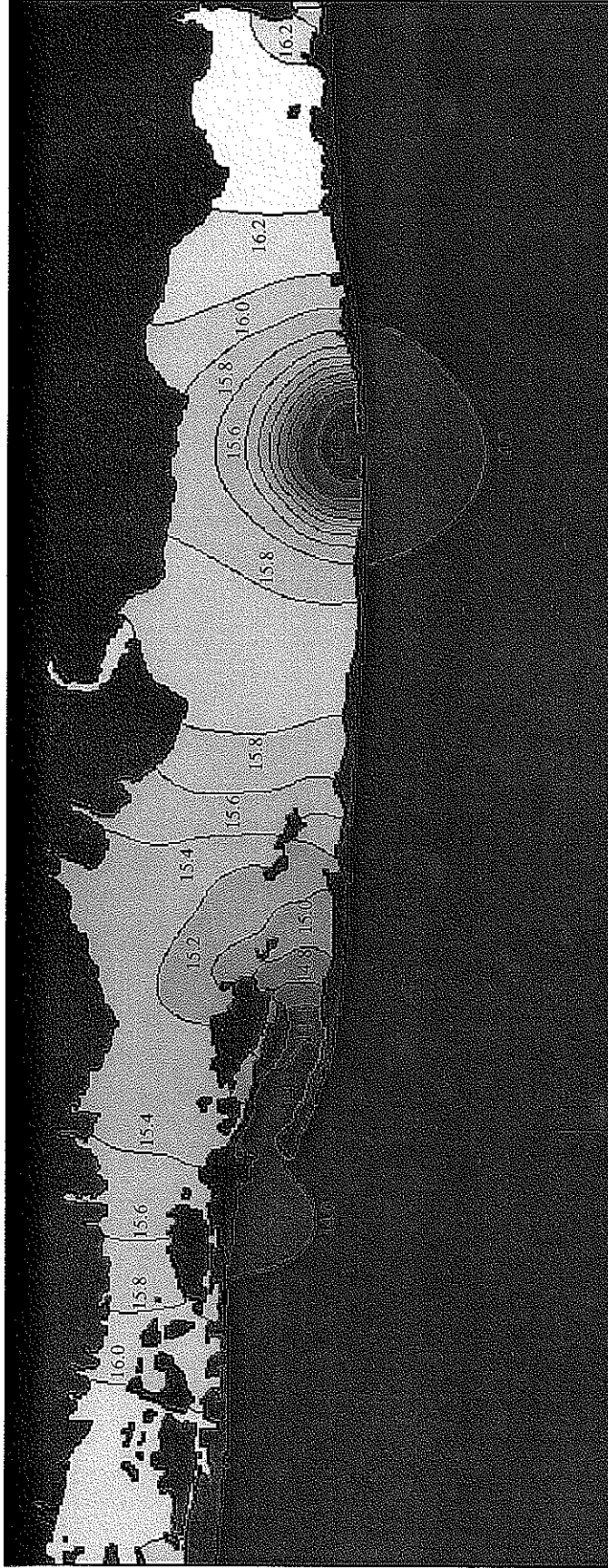


FIGURE 6.57
GREAT SOUTH BAY
9-MONTH BREACH
PEAK FLOOD TEMPERATURE (°C)

FIRE ISLAND TO MONTAUK POINT
INLETS STUDY

MOFFATT & NICHOL
ENGINEERS

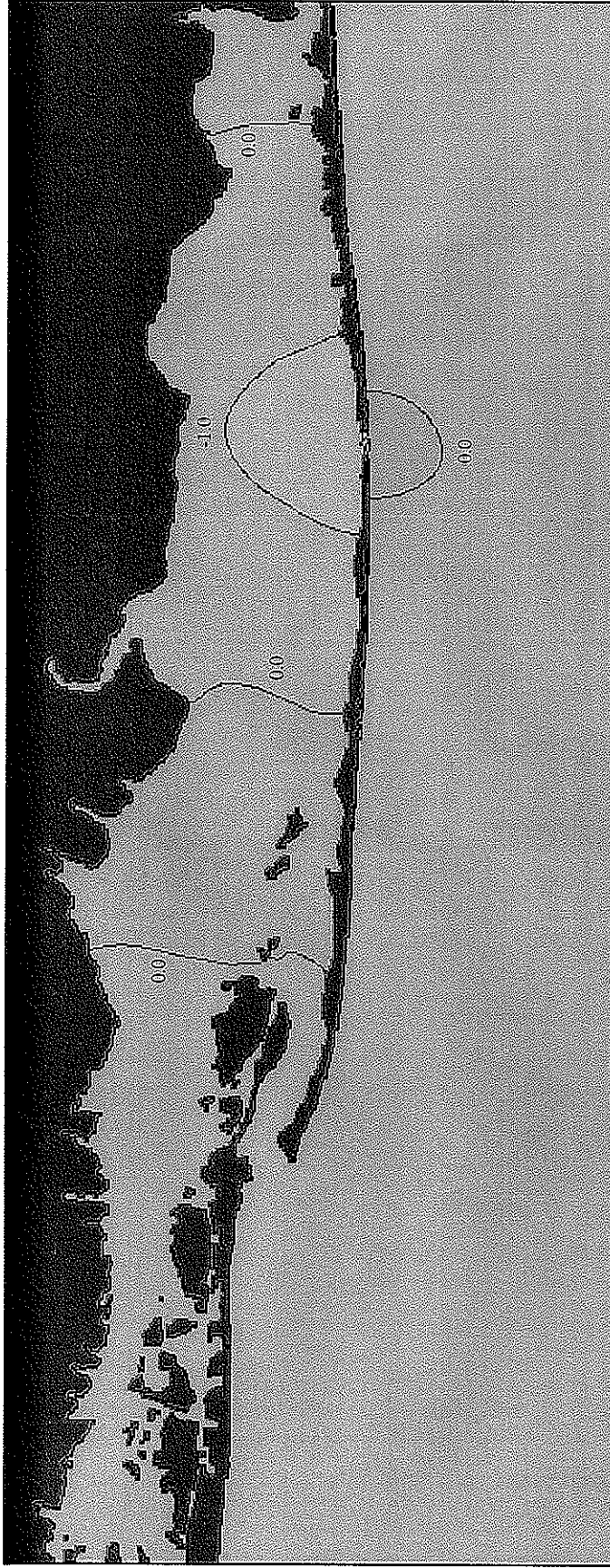
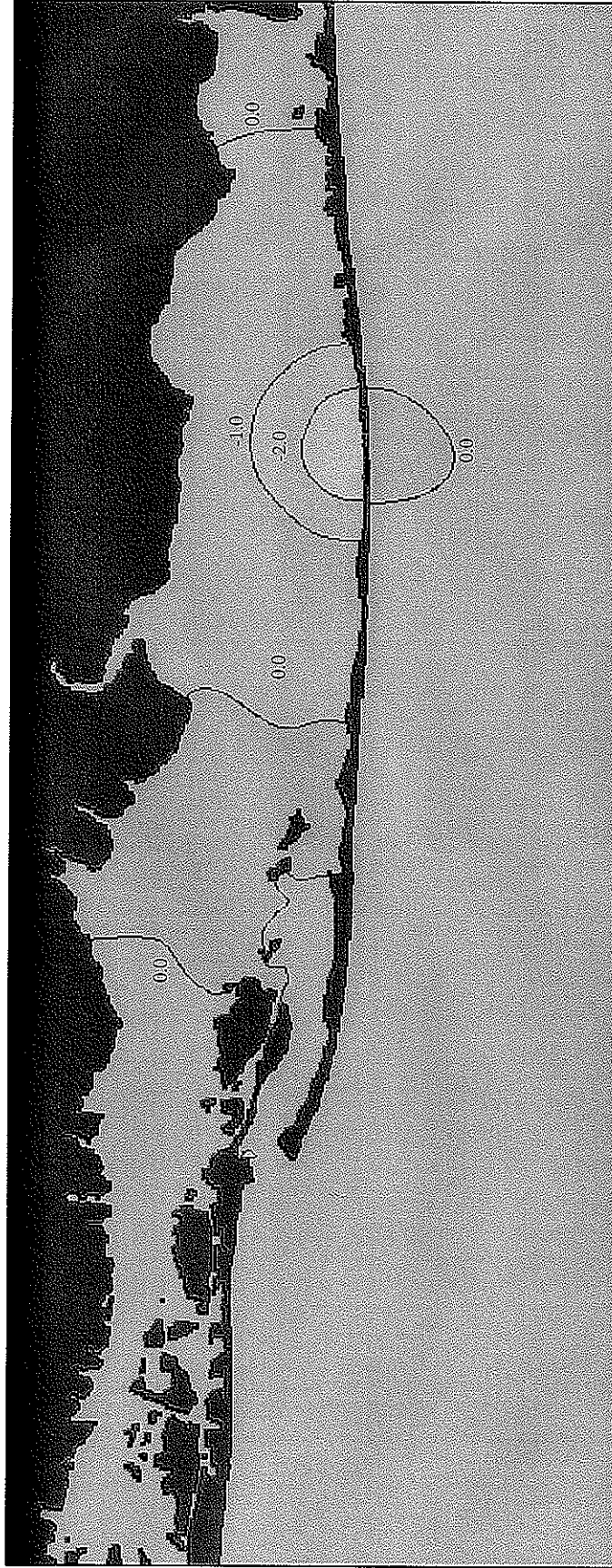


FIGURE 6.58
GREAT SOUTH BAY
EXISTING VS. 9-MONTH BREACH
PEAK EBB TEMPERATURE (°C)

FIRE ISLAND TO MONTAUK POINT
INLETS STUDY

MOFFATT & NICHOL
ENGINEERS



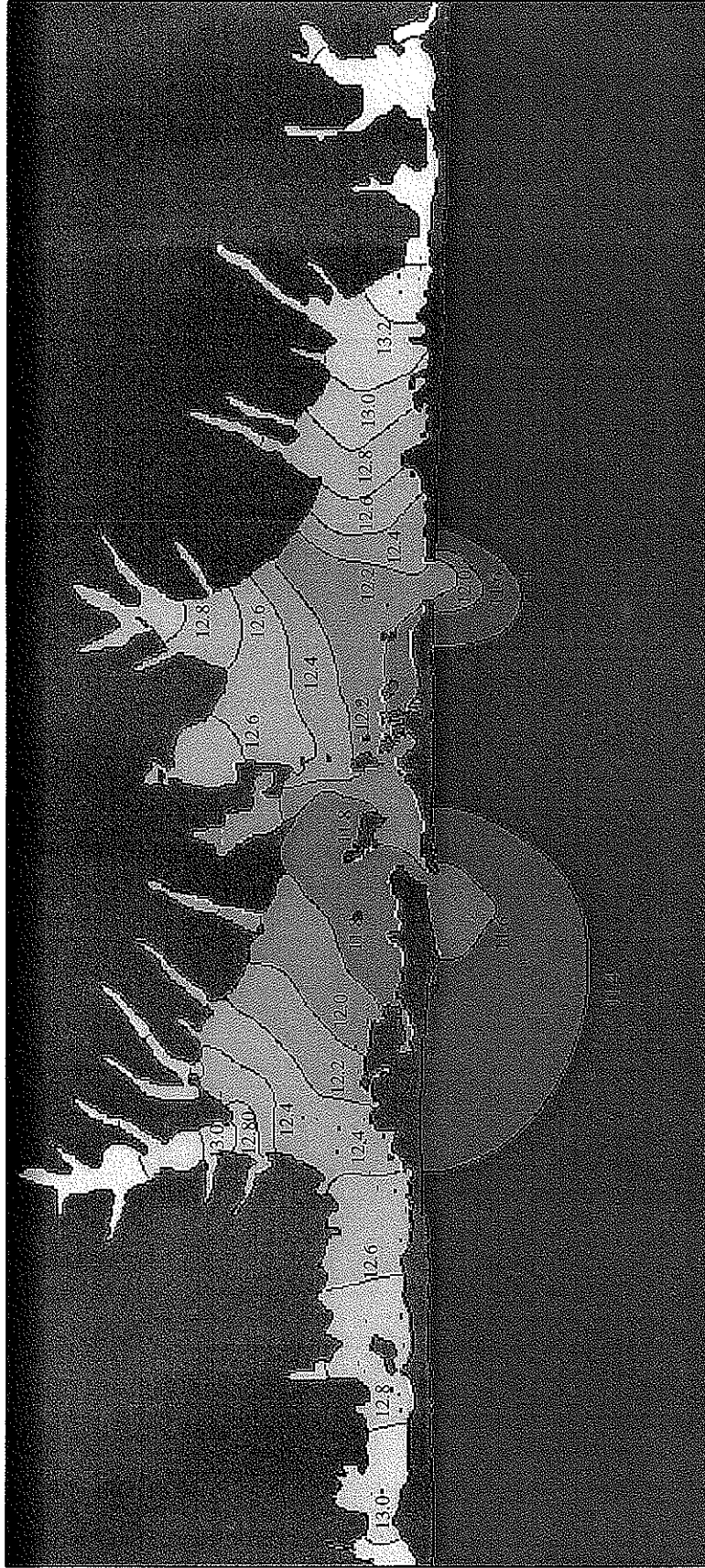
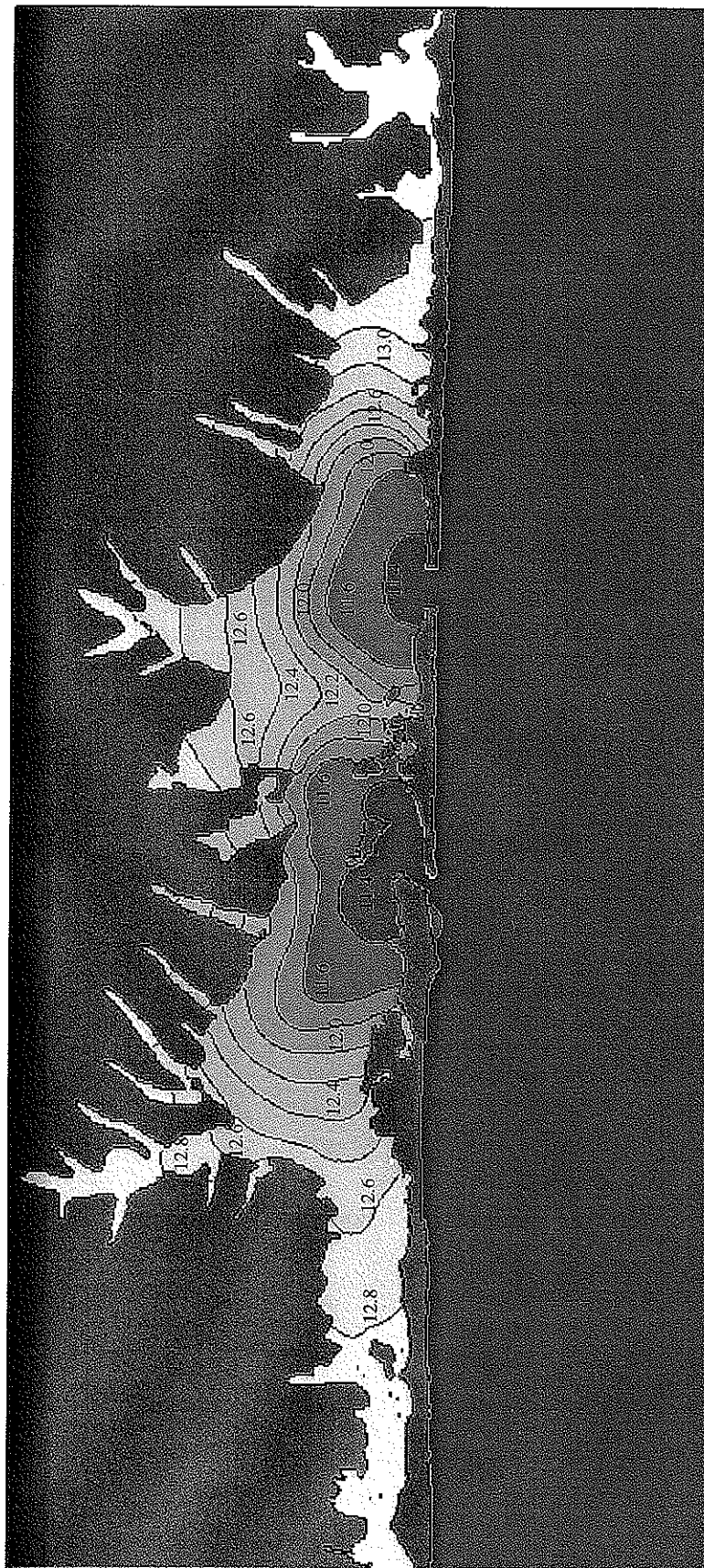


FIGURE 6.60
MORICHES BAY
9-MONTH BREACH
PEAK EBB TEMPERATURE (°C)

FIRE ISLAND TO MONTAUK POINT
INLETS STUDY



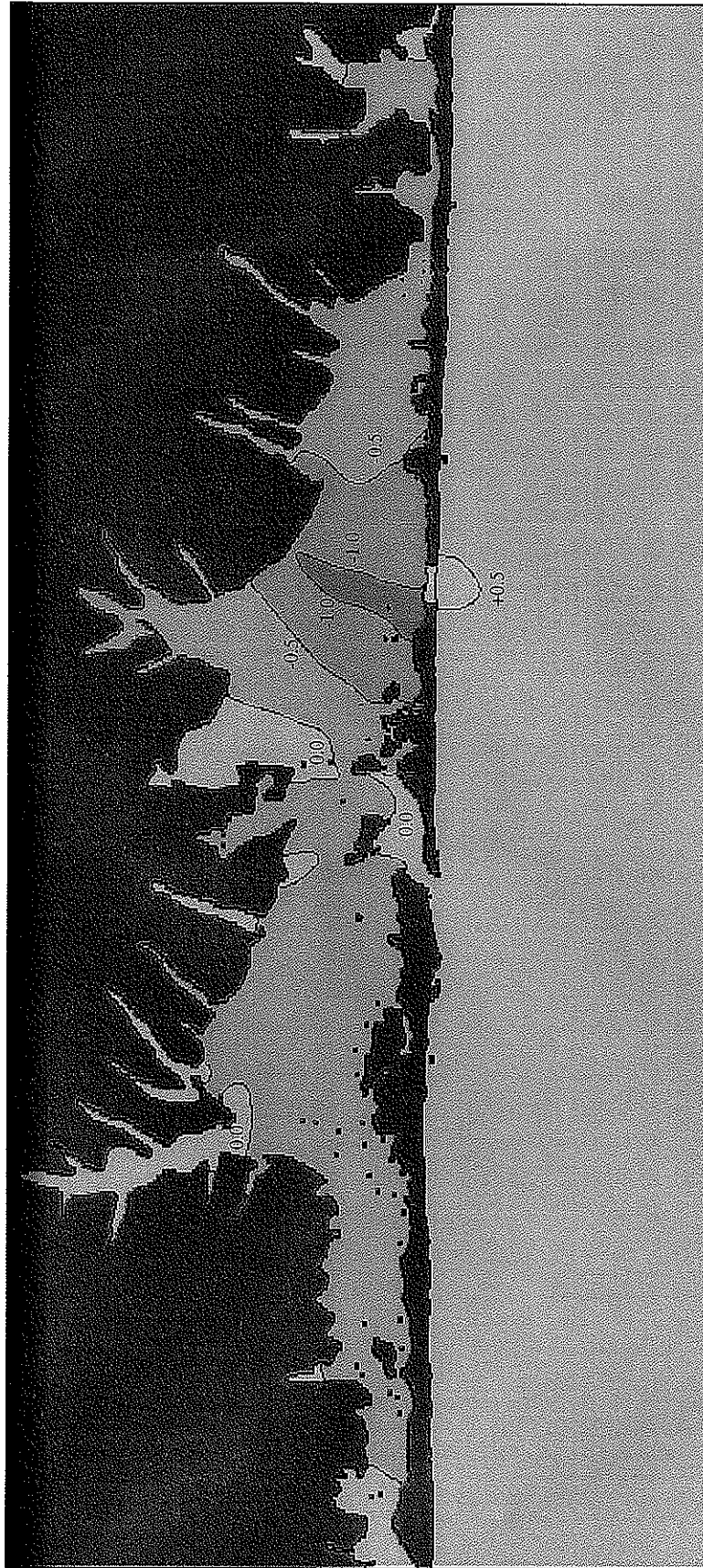


FIGURE 6.62
MORICHES BAY
EXISTING VS. 9-MONTH BREACH
PEAK EBB TEMPERATURE (°C)

FIRE ISLAND TO MONTAUK POINT
INLETS STUDY

MOFFATT & NICHOL
ENGINEERS

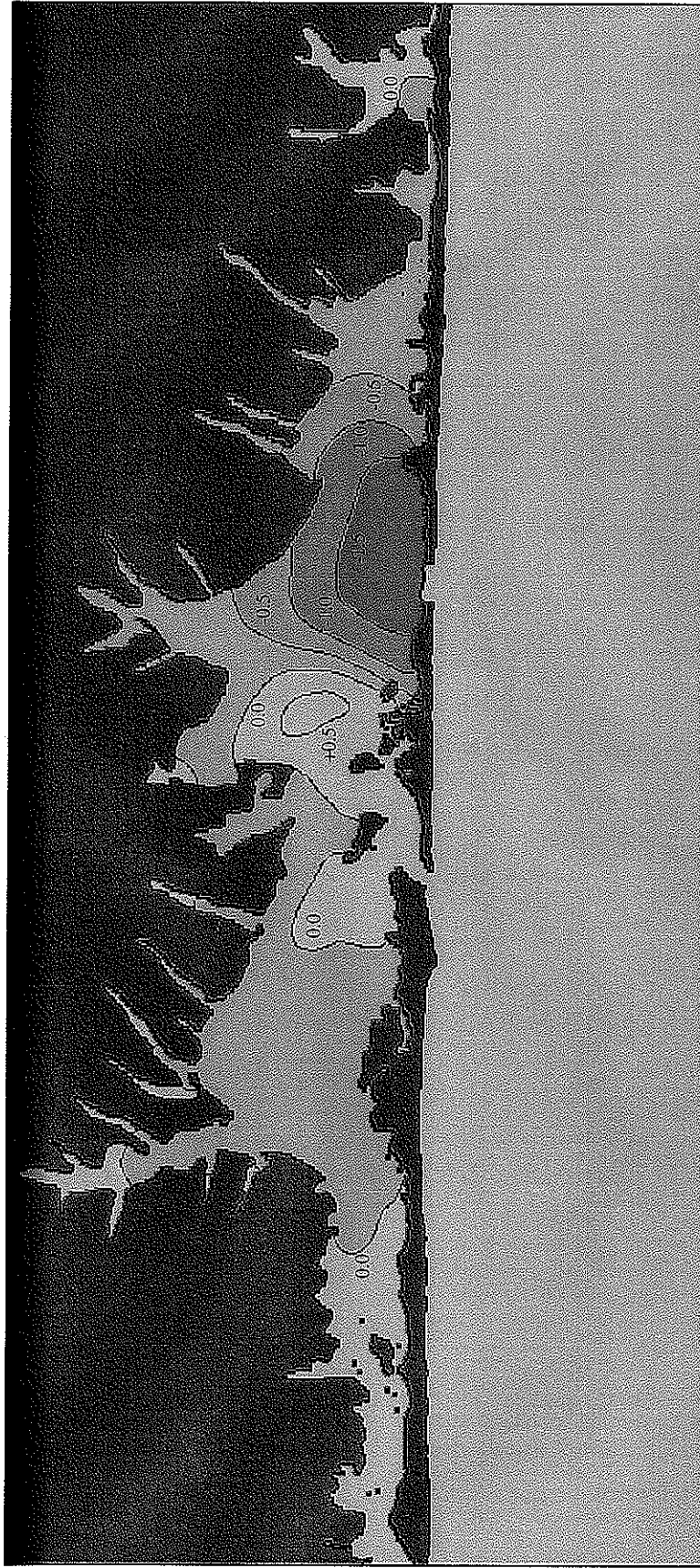


FIGURE 6.63
MORICHES BAY
EXISTING VS. 9-MONTH BREACH
PEAK FLOOD TEMPERATURE (°C)

FIRE ISLAND TO MONTAUK POINT
INLETS STUDY

MOFFATT & NICHOL
ENGINEERS

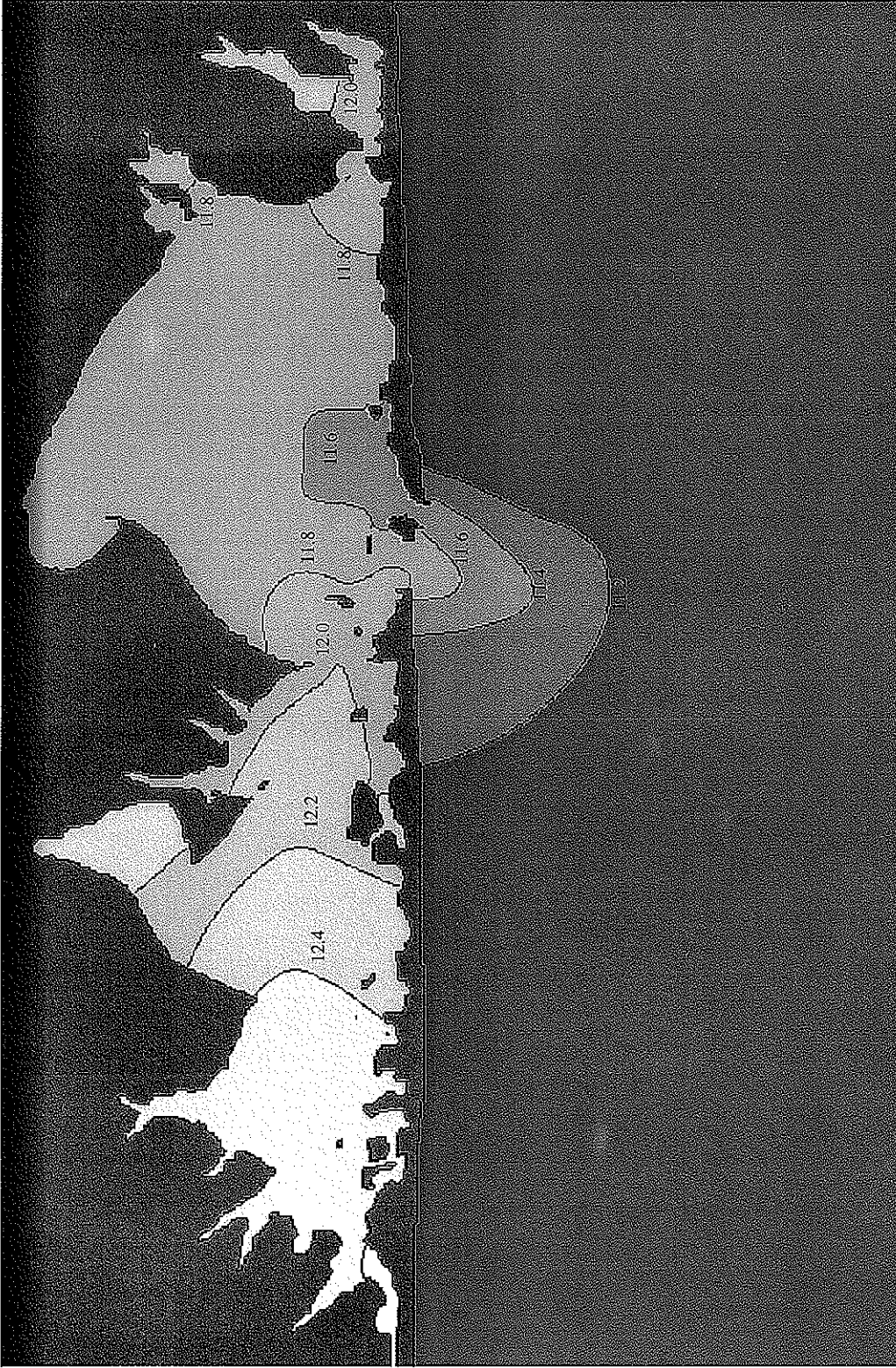


FIGURE 6.64
SHINNECOCK BAY
9-MONTH BREACH
PEAK EBB TEMPERATURE (°C)

FIRE ISLAND TO MONTAUK POINT
INLETS STUDY

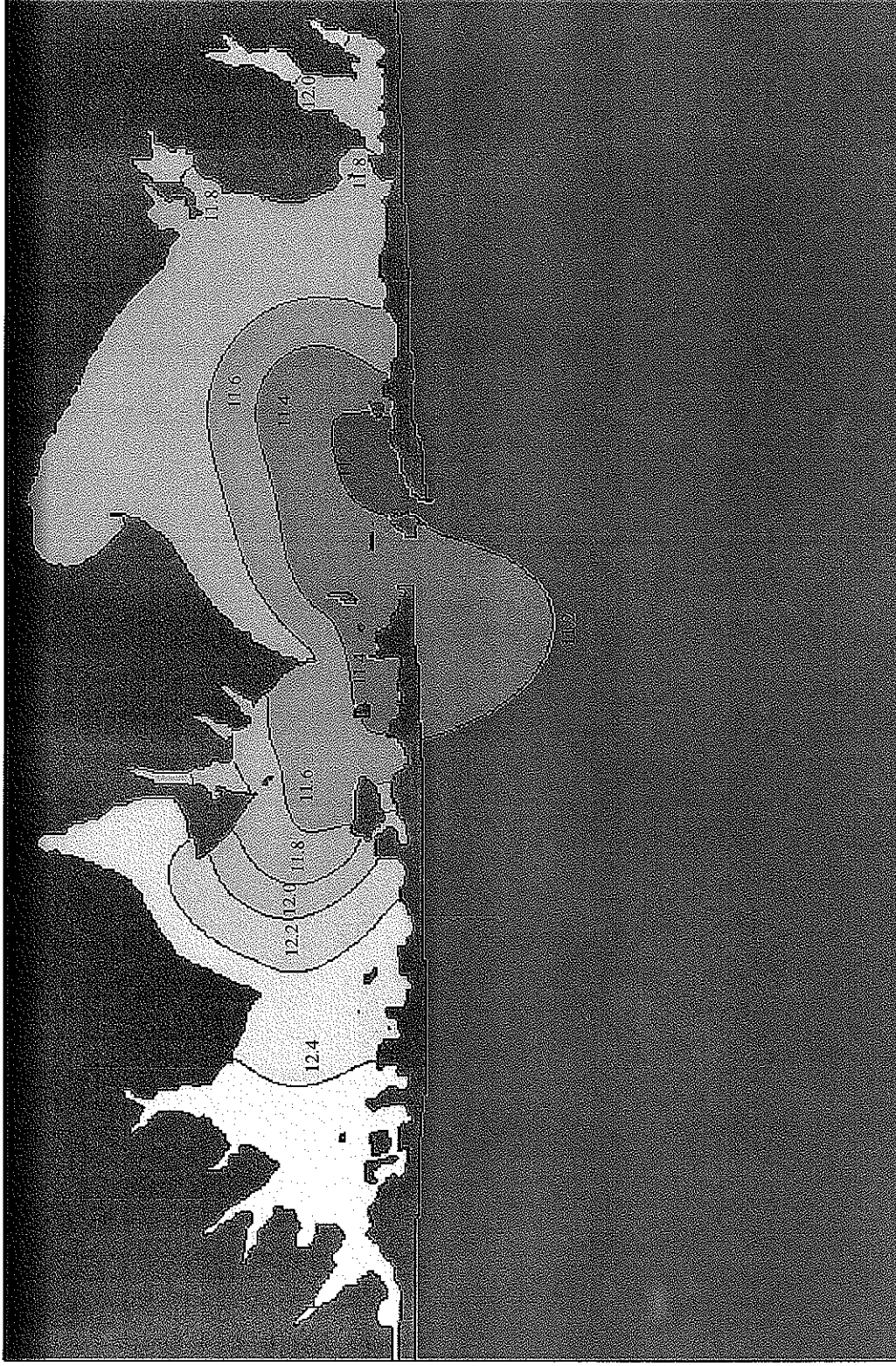


FIGURE 6.65
SHINNECOCK BAY
9-MONTH BREACH
PEAK FLOOD TEMPERATURE (°C)

FIRE ISLAND TO MONTAUK POINT
INLETS STUDY

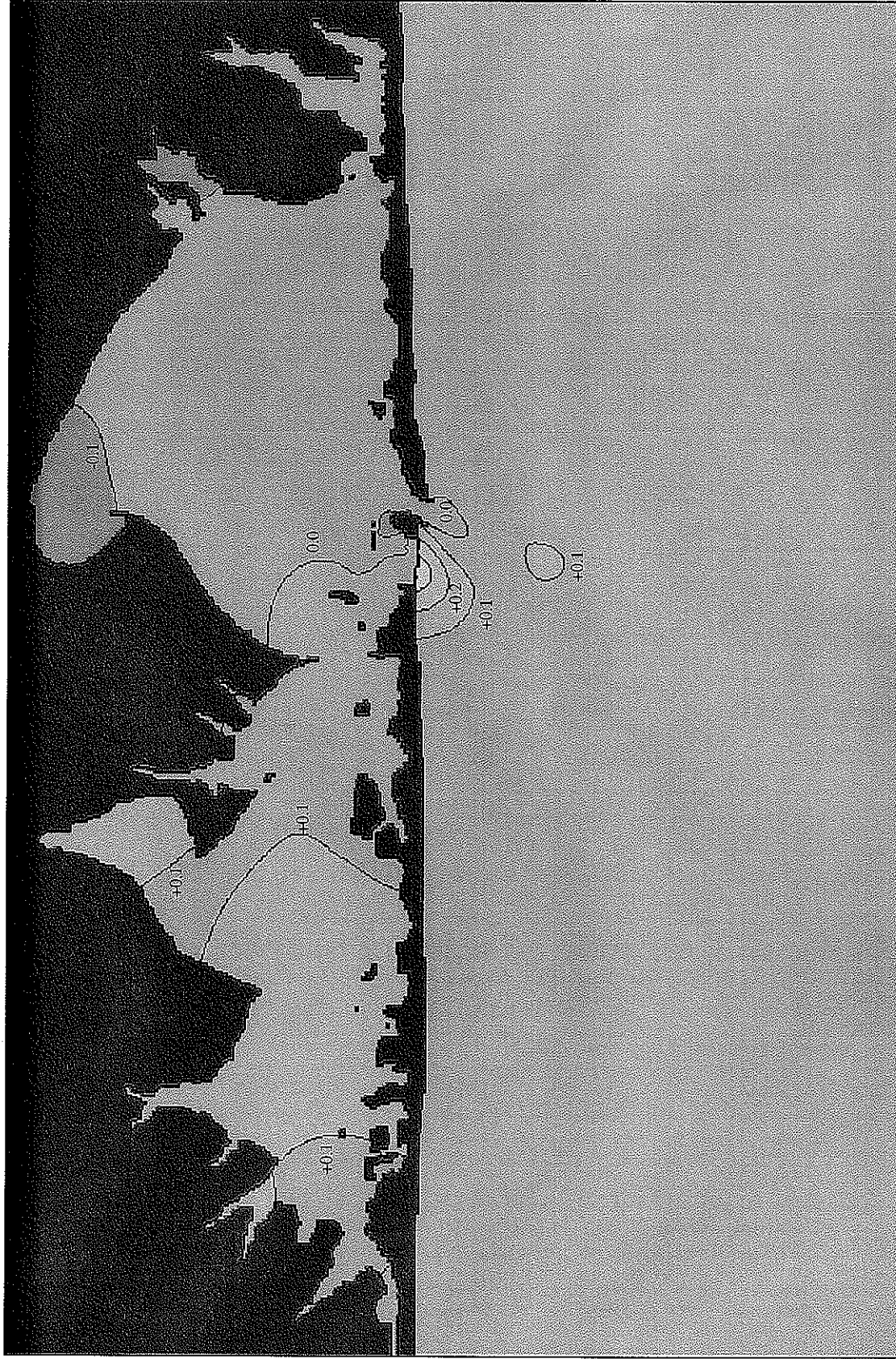


FIGURE 6.66
SHINNECOCK BAY
EXISTING VS. 9-MONTH BREACH
PEAK EBB TEMPERATURE (°C)

FIRE ISLAND TO MONTAUK POINT
INLETS STUDY

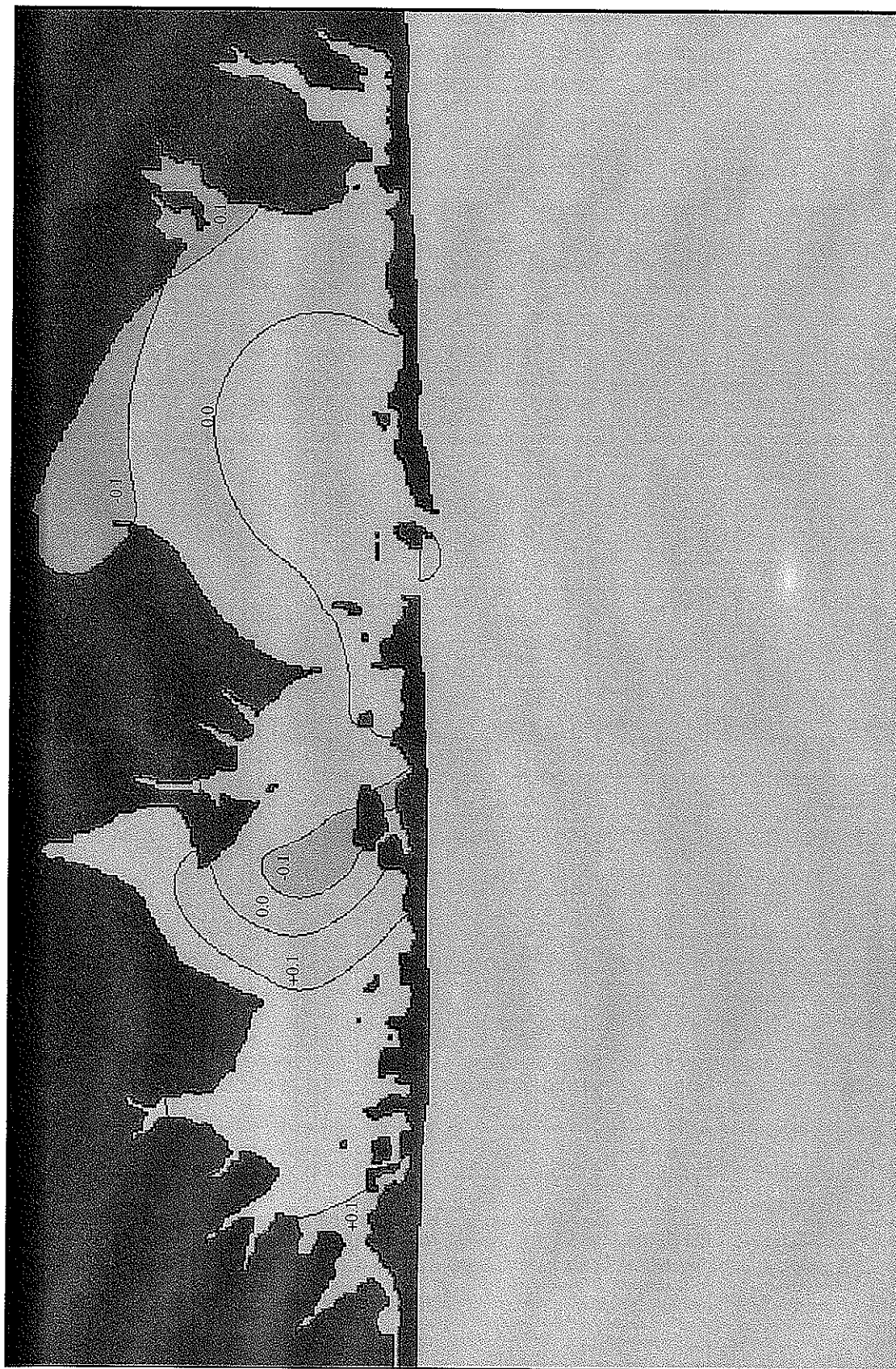


FIGURE 6.67
SHINNECOCK BAY
EXISTING VS. 9-MONTH BREACH
PEAK FLOOD TEMPERATURE (°C)

FIRE ISLAND TO MONTAUK POINT
INLETS STUDY



FIGURE 6.68
GREAT SOUTH BAY
9-MONTH BREACH
RESIDENCE TIME (DAY)

FIRE ISLAND TO MONTAUK POINT
INLETS STUDY

MOFFATT & NICHOL
ENGINEERS







FIGURE 6.71
MORICHES BAY
EXISTING VS. 9-MONTH BREACH
RESIDENCE TIME (DAY)

FIRE ISLAND TO MONTAUK POINT
INLETS STUDY

MOFFATT & NICHOL
ENGINEERS



FIGURE 6.72
SHINNECOCK BAY
9-MONTH BREACH
RESIDENCE TIME (DAY)

FIRE ISLAND TO MONTAUK POINT
INLETS STUDY

MOFFATT & NICHOL
ENGINEERS



FIGURE 6.73
SHINNECOCK BAY
EXISTING VS. 9-MONTH BREACH
RESIDENCE TIME (DAY)

FIRE ISLAND TO MONTAUK POINT
INLETS STUDY

MOFFATT & NICHOL
ENGINEERS

7. FINDINGS AND CONCLUSIONS

7.1. General

This report presented future without-project conditions at Great South, Moriches, and Shinnecock Bays, specifically salinity, temperature, and residence time. The results in this report follow *Interim Submission No. 9A, Inlet Dynamics - Existing Conditions* (February, 1999) and *Interim Submission No. 9B, Inlet Dynamics - Without-Project Future Conditions* (March, 1999). Advection/dispersion modeling was performed using the MIKE 21 finite difference model to simulate inlet and estuarial salinity, temperature and residence time response to the presence of barrier island breaches.

7.2. Model Calibration

Analyses show that the advection/dispersion model was successfully calibrated for each inlet/bay system. Calibration results are summarized as follows:

- Average modeled salinity was within 2 ppt of average measured values for each station in each bay;
- Average modeled temperature was within 1°C of average measured values for each station in each bay.

7.3. Future Without-Project Inlet/Bay Water Quality

Breach scenarios for each inlet/bay system were investigated as the future without-project condition using the calibrated advection/dispersion model. Breaches with dimensions typical of breaches open for three months and nine months were modeled to reflect the differences between closure operations at Westhampton Beach in 1993 and operations proposed as part of the Breach

Contingency Plan (USACE, 1996). Future without-project modeling results are summarized in the following sections.

7.3.1. Future Without-Project Inlet/Bay Salinity

Generally, impacts of the barrier island breaches on salinity in Great South, Moriches, and Shinnecock Bays were localized to the areas near the breaches and existing inlets.

Great South Bay.

- Salinity in the vicinity of the breach in Great South Bay increased 1.6 and 2.0 ppt for the three-month and nine-month cases, respectively;
- Salinity changed ± 0.1 ppt in areas further removed from the breach; and
- Salinity in the vicinity of the existing inlet decreased on the order of 0.5 ppt.

Moriches Bay.

- Moriches Bay salinity changes were highest near the breach; specifically, salinity increased near the breach by 1.7 and 2.0 ppt for the three- and nine-month breach cases, respectively;
- Changes to salinity distant from the breach location were on the order of ± 0.1 to 0.3 ppt; and
- There was no significant difference between three- and nine-month salinities.

Shinnecock Bay.

- Shinnecock Bay salinity changes were highest in the eastern basin with increases of over 0.6 ppt;
- Salinity increases in the western basin were typically less than 0.4 ppt; and
- There was no significant difference between three- and nine-month salinities.

7.3.2. *Future Without-Project Inlet/Bay Temperature*

As was the case with salinity, impacts of the barrier island breaches on temperature in Great South, Moriches, and Shinnecock Bays were near the breaches and existing inlets.

Great South Bay.

- Temperature in the vicinity of the breach in Great South Bay decreased 0.5 and 0.7°C for the three-month and nine-month cases, respectively;
- Temperature changed $\pm 0.1^\circ\text{C}$ in areas further removed from the breach; and
- Salinity inland from the inlet increased slightly as flow into the bay via the inlet was reduced due to the breach.

Moriches Bay.

- Temperatures in Moriches Bay were largely unaffected by the breaches except for the area directly inland from the breach;
- Temperature decreased at the breach by 0.8 and 1.0°C for the three- and nine-month breach cases, respectively;
- Changes to temperature in Moriches Bay in areas other than the breach location were on the order of $\pm 0.1^\circ\text{C}$; and
- There was no significant difference in impact due to the modeled six-month breach closure delay.

Shinnecock Bay.

- Temperatures in the eastern basin of Shinnecock Bay were slightly depressed while temperatures in the western basin were slightly increased;
- Temperatures in the eastern basin decreased less than 0.2°C;
- Temperature increases in the western basin were less than 0.3 ppt; and
- There was no significant difference in impact due to the modeled six-month breach closure delay.

7.3.3. Future Without-Project Inlet/Bay Residence Time

Residence time results reflect the changes in circulation caused by the breaches. These results also demonstrate the impact of breach location has on circulation. For example, residence time will change significantly when the breach occurs in an area of low bay circulation, but will show modest changes near an existing inlet.

Great South Bay.

- Residence times were significantly impacted by a breach in eastern Great South Bay with reductions in residence times on the order of 3 to 4 weeks.
- Residence times in western Great South Bay increased 4 to 6 days as the breach affected circulation patterns and reduced flow through the existing inlet.
- The reductions in residence times for the three-month and nine-month breaches are approximately 3 days close to the breach and 0.5 to 1 day in other areas of the bay.

Moriches Bay.

- A breach at Pikes Beach reduces residence times in Moriches Bay by 0.5 to 0.8 days;
- Decreases in residence time close to the breach are on the order of 8 days; while
- Residence times close to the bay entrances (i.e., the inlet and lateral boundaries) decrease only 0.5 days.

Shinnecock Bay.

- Residence time decreases throughout the bay (0.5 to 1.5 days) except in the extreme eastern and western basins where residence time increases by 0.3 to 0.9 days;
- As with the other bays, the residence time decreased the most near the breach; and
- A breach in the western basin, where residence time is on the order of 7 days, would be expected to show a much higher impact on local residence times.

8. REFERENCES

Bocamazo, L. M., 1994. Personal Communication.

Chu, Y. and Nersesian, G. K., 1992. Scour Hole Development and Stabilization at Shinnecock and Moriches Inlets, New York. Proc. Coastal Engineering Practice'92, ASCE, pp571-582.

Cialone, A. M., 1994. Inundation Modeling. Draft Report. Coastal Engineering Research Center, US Army Engineer Waterway Experiment Station, Vicksburg, MS.

DiLorenzo, J. L., 1986. The Overtide and Filtering Response of Inlet/Bay Systems. Ph.D. Dissertation. Marine Sciences Research Center, State Univ. of New York at Stony Brook.

Leatherman S. P. and Allen, J. R., 1985. Geomorphologic Analysis of South Shore of Long Island Barriers, New York. Final Report. Prepared for US Army Corps of Engineers, New York District, New York, New York.

Mehta, A. J., 1990. Coastal Processes. Class Notes, University of Florida.

Nersesian, G. K., Kraus N. C. and Carson F. C., 1992. Functioning of Groins at Westhampton Beach, Long Island, New York. Proceedings of 23rd International Coastal Engineering Conference'92, Venice, Italy.

Norton, W. R., King, I. P. and Orlob, G. T., 1973. A Finite Element Model For Lower Granite Reservoir. Prepared for the Walla Walla District, US Army Corps of Engineers, Walla Walla, WA.

Pritchard, D. W. and DiLorenzo, J. L., 1981. Computed Current Velocities in Moriches Inlet and Moriches Bay. Final Report. Marine Science Research Center, State University of New York, NY

Pritchard, D. W., 1983. Salinity Measurements in Moriches Bay. Final Report. Marine Science Research Center, State University of New York, NY

US Army Corps of Engineers, 1963. General Design Memorandum No.1 - Beach Erosion & Hurricane Project, Moriches to Shinnecock Reach, Long Island, NY US Army Engineer District, New York, New York.

US Army Corps of Engineers, 1994. Decision Document - Interim Plan For Storm Damage Protection, Moriches to Shinnecock Reach, Long Island, NY US Army Engineer District, New York, New York.

Van de Kreeke, J., 1983. Residence Time: Applications Small Boat Basins. ASCE Journal of Waterway, Port, Coastal and Ocean Engineering, Vol. 109, No. 4.

Van de Kreeke, J., 1984. Stability of Multiple Inlets. Proceedings of 19th International Coastal Engineering Conference '84, Houston, Texas.